Investigating the Lytic Transglycosylases of *Burkholderia pseudomallei*

Thesis Submitted for the Degree of

Doctor of Philosophy

at the University of Leicester

by

Christopher Jenkins

Department of Infection, Immunity and Inflammation

University of Leicester

September 2017

Abstract

Peptidoglycan is a mesh like structure that is an integral part of the bacterial cell wall. Comprised of glycan chains interconnected with short peptide chains, it is responsible for protecting the bacteria from hydrostatic pressures as well as providing a scaffold for many cell wall spanning structures. Tight regulation of the synthesis, maintenance and turnover of peptidoglycan is essential to maintaining integrity of bacteria. One family of enzymes involved in the regulated cleavage of peptidoglycan are lytic transglycosylases (Ltgs). These proteins are highly conserved in bacteria and function in the restructuring of peptidoglycan during growth and division but also in the insertion of large macromolecular structures including secretion systems and flagella. One class of Ltgs, called resuscitation-promoting factors (Rpf) have also been implicated in resuscitation of dormant *Actinobacteria*.

Burkholderia pseudomallei is the causative agent of melioidosis, a tropical disease prevalent particularly in South East Asia and Northern Australia which claims the lives of an estimated 89,000 people per year. Based on sequence homology to Ltgs of *E. coli,* we have identified 5 putative Ltgs (LtgA-E) encoded by genes on chromosome 1 of *Burkholderia pseudomallei* strain K96243. This study aimed to understand the role of these proteins in *B. pseudomallei* biology and investigate their capacity as drug targets. Using a range of approaches I have shown the muralytic activity of four of these Ltgs. The X-ray crystal structure of LtgE was solved and the catalytic site identified using site directed mutagenesis. In complementary studies single and multiple deletion mutants of *B. pseudomallei* have been generated. Excision of single or multiple *ltg* genes from *B. pseudomallei* resulted in mutants with severely altered cellular morphology (increased cell length and defects in cell division), motility and reduced biofilm formation. Δ*ltgEBDC* had a small increase in susceptibility to carbenicillin, doxycycline and ceftazidime. Δ*ltgB*, Δ*ltgD*, *ΔltgE* were all attenuated in the BALB/c mice model of melioidosis.

In addition, I began to develop a model for the generation of non culturable *Burkholderia*. Incubation in NaCl concentrations >2.5% (w/v) for 7 days resulted in a complete loss of culturability on solid media. Live/dead staining however, revealed a

substantial population of seemingly viable bacteria. Attempts to resuscitate these into actively growing cells however were unsuccessful.

Given the role in virulence, the assays available and optimised for use with *B. pseudomallei* Ltgs and the X-ray crystal structure of LtgE, it would appear that Ltgs are good candidates for novel drug targets and that the tools are now in place for high throughput screening of Ltg inhibitors.

Acknowledgements

I would first like to thank my supervisors Dr Galina Mukamolova and Dr Eduard Galyov for sharing their expertise and supporting me through the last four years. Their enthusiasm and genuine desire to help me throughout my studies and further myself has been invaluable and I believe I will benefit from their advice for years to come.

I would also like to say thank you to Dstl for their collaboration, and in particular Dr Sarah Harding for her advice and guidance throughout this PhD. Sarah has invested a lot of time in providing feedback and in arranging experiments for my PhD at Dstl, for which I'm very grateful.

Thank you to the huge number of people who have been more than willing to help me with various aspects of this project including Obolbek Turapov, Russell Wallis, Natalie Allcock, Natalie Lazar Adler, Depesh Pankhania, Kay Barnes, Mark Richards and of course all members of Lab 213b. To Joss and Somie, I really appreciate your hard work and the contributions you made and I wish both of you all the luck for the future.

To my family and friends, I'm sure most of you still don't really understand what I've been doing for the last four years but I appreciate your 'interest', your encouragement and your support!

Finally to Darren - you've been with me more than anyone throughout this entire process, listening to me moan about failed experiments and deadlines but also getting drunk with me celebrating the highlights and breakthroughs. Thank you for your…I was going to say patience but well… tolerance, I'm almost there!

Contents

List of tables

List of Figures

List of abbreviations

%	Percent
+/-	Plus or minus
°C	Degrees centigrade
aa	Amino acid
Amp	Ampicillin
AT	Autotransporters
Bp	Base pair(s)
cDNA	Complementary DNA
CFU	Colony forming unit
dH_2O	Distilled water
DMSO	Dimethyl sulfoxide
DNA	Deoxyribonucleic acid
dNTP	Deoxynucleotide
DTT	Dithiothreitol
g	Gram
gDNA	Genomic DNA
GI	Genomic island
IAA	2-Iodoacetamide
IPTG	Isopropyl β-D-1-thiogalactopyranoside
Kan	Kanamycin
l	Litre
LA	Luria agar
LB	Luria broth
log	Logarithmic
LPS	lipopolysaccharide
Ltg	Lytic transglycosylase
M	Molar
M9	Minimal glucose M9 media
Mbp	Megabase pairs
ml	milliliter
MLD	Median lethal dose
Mlt	Membrane bound lytic transglycosylase
mM	millimolar
mm	millimeter
NaCl	Sodium chloride
NAG	*N*-Acetylglucosamine acid
NAM	*N*-Acetylmuramic acid
NC	Non-culturable
NO	Nitric oxide
OD	Optical density
OD_{600}	Optical density reading at 600nm
PBS	Phosphate buffered saline
PCR	Polymerase chain reaction
PG	Peptidoglycan
RNA	Ribonucleic acid

Rpf	Resuscitation promoting factor
RP-HPLC	Reverse phase high pressure liquid chromatography
rpm	Revolutions per minute
RT-PCR	Reverse transcriptase-polymerase chain reaction
SDS-PAGE	Sodium dodecyl sulfate-polyacrylamide gel electrophoresis
Slt	Soluble lytic transglycosylase
T3SS	Type three secretion system
T6SS	Type six secretion system
V	Volts
v/v	Volume to volume
w/v	Weight to volume
xg	Multiplied by gravity
YT	Yeast tryptone
µ	Micro
µF	Microfarad
Ω	Ohm

Chapter 1

Introduction

1.1. The *Burkholderia* genus

The *Burkholderia* genus was first proposed by Eiko Yabuuchi in 1992 into which he proposed the transfer of seven Pseudomonas species. These species included; *Pseudomonas cepacia*, *Pseudomonas mallei* and *Pseudomonas pseudomallei*. This decision was based upon physiological, biochemical and morphological differences between other Pseudomonas species as well as 16S rRNA sequencing (1).

The *Burkholderia* genus is now comprised of 117 species and can be found in a variety of ecological niches including soils, sea water, hospital environments, human and animal hosts and in plant rhizospheres (2, 3). The range of environments and locations is indicative of the diversity of these species and trying to understand mechanisms by which one genus can survive in a range of environments is extremely complex. Many of these species are soil dwelling and form non-infectious relationships with plants, regarded as virtually harmless in terms of human, animal and plant infections. There are however exceptions, such as *Burkholderia pseudomallei*, *Burkholderia mallei* and members of the *Burkholderia cepacia* complex (Bcc). The Bcc comprises of 20 species that naturally occur in the environment including *Burkholderia anthina*, *Burkholderia cepacia*, *Burkholderia cenocepacia*, *Burkholderia multivorans*, *Burkholderia stabilis*, *Burkholderia ubonensis* and *Burkholderia vietnamiensis*. These organisms, particularly *B. multivorans* and *B. cenocepacia* can cause severe nosocomial infections, particularly in patients with cystic fibrosis or reduced immune systems. Other members of Bcc can also colonise plant rhizospheres, including maise and onions (4) as well as cause plant diseases in onions and bananas (5). A partial phylogenetic tree of the *Bukholderia* genus based upon 16S rRNA sequences can be seen in Figure 1 (2).

Three members of the *Burkholderia* genus that have been the focus of much research are the highly pathogenic strains *B. pseudomallei* and *B. mallei* which cause somewhat similar infections and the much less virulent strain and model organism *B. thailandensis*. These three species have been defined as the *Burkholderia pseudomallei* complex/group (Bpc) (3). Despite high similarity between their genomes these species can be differentiated by a number of phenotypes including arabinose assimilation (4), latex agglutination (5) and PCR (3, 6-8).

B. mallei is a Gram negative, non-motile bacterium which causes a severe disease known as glanders in horses and similar species but has also been known to infect humans. It is an obligate pathogen and is incapable of persistence in the environment. *B. mallei* is considered to be a clone of *B. pseudomallei* due to its highly similar but drastically reduced genome compared to *B. pseudomallei* with two chromosomes of 3.3 and 2.2Mbp (compared to 4.07 and 3.17 Mbp of *B. pseudomallei*), which lacks or has variants of 1200 *B. pseudomallei* genes. It is thought that *B. mallei* evolved from *B. pseudomallei* after genes required for environmental survival were lost by an ancestral strain within a mammalian host (17, 18). Further loss of gene clusters has been noted between *B. mallei* strains leading to varying levels of virulence (19).

Burkholderia thailandensis is a closely related species with high genetic similarity to *B. pseudomallei* (7) but is much less pathogenic in animal models (8, 9). Given this, it is often used as a model organism, particularly in institutions lacking containment level 3 laboratories. The reduced virulence of this species is thought to be due to its lack of the type 3 secretion system 3 (13) and capsular polysaccharide (14). Although a capsulated strain has been *B. thailandensis* has been isolated. The presence of this capsule however was not sufficient to increase the virulence in animal models compared to non-capsulated strains (15). *B. thailandensis* has also been shown to have reduced replication in human macrophages (16).

B. pseudomallei is a Gram negative, motile, non-spore forming saprophyte and the causative agent of the disease melioidosis (6) which is further described below.

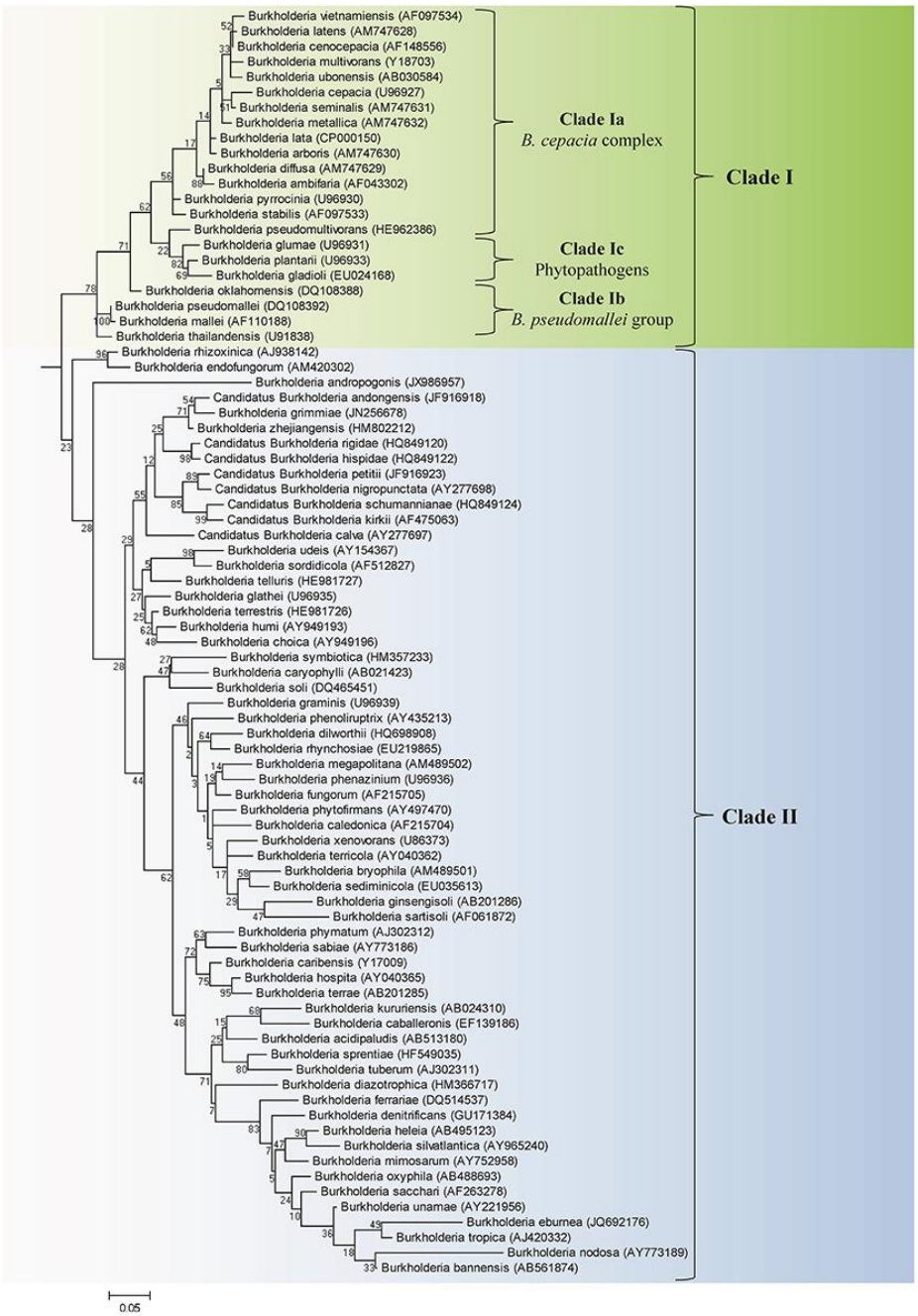

Figure 1: Phylogeny tree of the *Burkholderia* genus based on 16S rRNA gene sequences

22 of the 97 members, highlighted in green, are pathogenic organisms (clade I), which include the *Bukholderia cepacia* complex and the *Burkholderia psudomallei* group. The remaining members of clade I are plant pathogens. The majority of the remaining genus, highlighted in the blue area, are non-pathogenic, environmental species and form clade II. The tree was rooted using four species from the genera *Cupriadivus* and *Ralstonia*. Accession numbers are shown in brackets next to each species. Figure modified from (2).

1.2. Melioidosis

1.2.1. Epidemiology

Melioidosis is an emerging disease becoming of significant prominence in the last 50 years. It was not until the beginning of the 20th century when a patient from Burma was identified as having a 'glanders-like' disease that melioidosis was first described by Alfred Whitmore and C.S. Krishnaswami (9, 10). While the post-mortem initially suggested the patient died of glanders as a result of infection by *B. mallei*, medical officers were sceptical to their conclusions as the 40 year old patient had been recently released from prison and had no contact with *B. mallei* infected horses. It was not until they observed the more rapid growth, that the bacterium was motile (unlike *B. mallei*) and a lack of scrotal inflammation when infecting guinea pigs (a symptom of glanders) that they proposed that they were dealing with a new disease caused by a similar but distinct bacterial species (10).

Over the following decades melioidosis has become much more familiar globally, thanks to increased awareness and better diagnostic facilities in endemic areas. Melioidosis is highly endemic in Australia's Northern territory and South East Asia, particularly Thailand, Singapore, Laos, Cambodia and Malaysia (11). For example in one of the most endemic regions of the world, North East Thailand, there are estimated to be over 2000 cases of melioidosis annually with a fatality rate of approximately 42% (12). However, due to ever increasing global travel, higher population densities, improved diagnostic capability and severe weather events (such as the 2004 Indian Ocean tsunami) the number and distribution of melioidosis cases globally is increasing rapidly (Figure 22) (13-15). A recent publication by Limmathurotsakul et al. (2016) mapped and predicted using models based on global human and animal cases of melioidosis, that the global burden of melioidosis is much greater than previously thought. They estimate that there are 165,000 cases of melioidosis per annum, resulting in 89,000 deaths per year (11).

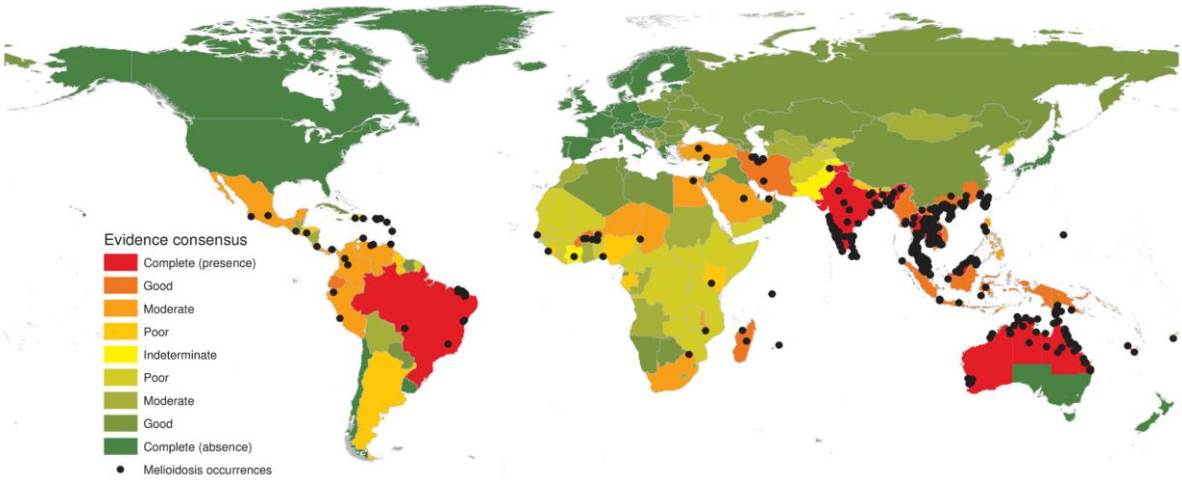

Figure 2 Global spread of *B. pseudomallei* and reported cased of melioidosis from 1910-2014

Evidence based occurrence of *B. pseudomallei* is shown by colour coding countries. Green indicates no recorded evidence of *B. pseudomallei*. Red indicates high evidence consensus for the presence of *B. pseudomallei*. Black dots indicate positive melioidosis cases. Figure from (11).

B. pseudomallei is typically found in tropical and subtropical areas of the world. With increased reporting of cases it is now known that melioidosis is endemic to 45 countries including those located in Latin America and the Caribbean (most notably Brazil, Haiti and the Dominican Republic), the Middle East and Africa. It is also likely to be endemic in another 34 countries that are known to have *B. pseudomallei* present, particularly in countries of sub-Saharan Africa (11). Limmathurotsakul et al. predict that globally, 3 billion people are living in areas likely to have *B. pseudomallei* (11).

1.2.2. Presentation of disease

Infection typically occurs through subcutaneous inoculation through an open wound, often on the bare feet of rice field workers in South East Asia (16). Given the high temperatures of endemic areas coupled with the desire to work at pace, workers often negate the use of protective footwear. Seasonal events including high rains which wash *B. pseudomallei* to the surface and high winds increasing aerosolisation result in increased infection rates (17, 18). While it is possible to become infected through ingestion this is more common to grazing animals (16). The infectious dose in humans in unknown, however a study using mice revealed an intravenous, LD_{50}, of between 10^3 and 10^5 CFU (19).

It is not yet clear why the onset of the disease can vary, but it can be anywhere between 24 hours to many decades following exposure. Melioidosis became of greater interest following the Vietnam War as US veterans began showing symptoms of the disease, sometimes many years after the initial exposure, particularly helicopter crew members exposed to aerated bacteria from dry soils disturbed by the rotor blades (20, 21). This resulted in melioidosis being referred to as the 'Vietnam time bomb'. However this is not always the case, with one study showing that 25% of recurrent infections are as a result of re-infection rather than relapse of the same strain (22). Clinically it has been shown that by the age of 4, 80% of children in high risk areas, such as Northern Thailand, have antibodies against *B. pseudomallei* (23). It is currently unclear exactly when and why dormant *Burkholderia* resuscitate into an infectious form in the human host.

Depending on the route of infection the presenting symptoms can vary. Cases from inoculation frequently result in fever, joint ache, soft tissue infection and abscesses in

many organs including, spleen, prostate, liver, lung, brain. Infection through inhalation typically results in fever, pneumonia followed by the spread and formation of abscesses in organs mentioned above. In the most severe cases bacteraemia followed by septicaemia is a severe risk and is often the cause of mortality. The severity of infection can depend on a number of factors including the route of inoculation, the dose and the existence of pre-existing conditions. Such pre-existing conditions include diabetes, liver disease and cystic fibrosis, as such people with these conditions are deemed to have a much higher risk of developing an infection with *B. pseudomallei* (13, 24).

1.2.3. Persister cells

Persister cells are a subpopulation of dormant bacteria that are able to survive antibiotic exposure at levels often >100x MIC (25). These cells have been shown to be genetically identical to antibiotic sensitive bacteria in the population (have not acquired resistance through mutation) but instead are phenotypically tolerant (26). Upon removal of the antibiotic pressure these bacteria are then able to resume growth but the population of persisters within the culture does not increase. It is thought that persister cells may be a contributing factor in latent disease.

Burkholderia species, including *B. pseudomallei* have been shown to form persister cells. These cells form between 0.02-0.26% of the population when treated for 24 hours at 10x MIC levofloxacin. The percentage of persister cells in a population can vary significantly depending on the antibiotic used with trimethoprim having a larger population than cells treated with doxycycline for example (27). It has been recently observed that finafloxacin, a fluoroquinolone, is effective at treating persister cells however finafloxacin is not currently licensed for use in the treatment of melioidosis (28). It has also been shown that *B. pseudomallei* is able to form persister cells in response to an anaerobic environment, an environment typically found during melioidosis infection. It was shown that exposure to an anaerobic environment could lead to 0.1% of the population being capable of persistence and surviving antibiotic therapies against aerobically grown *B. pseudomallei* (ceftazidime and co-trimoxazole) and drugs targeting anaerobic bacteria specifically metronidazole and tinidazole) (29). The cause of persister cell formation in *B. pseudomallei* in unknown but deletion of the

toxin gene *hicA* which forms part of a toxin:antitoxin system resulted in increased persister cell formation when exposed to ciprofloxacin. Using structural analysis it was suggested that that HicA has RNAase activity (30).

Persister cells are not necessarily the only cause of latent infection, particularly patients that do not develop symptomatic disease for years after exposure and have never received antibiotic treatment for melioidosis. These bacteria may be in a non culturable state, induced by a number of factors that can resuscitate into actively growing bacteria capable of causing latent infection. Non culturable forms of *Burkholderia* are explored in greater detail in chapter 6.

1.2.4. Diagnosis

Given the high mortality rate of melioidosis, early diagnosis is essential to the success of treatment, furthermore, failure to diagnose correctly can severely influence the disease outcome. There are a number of issues with diagnosis. For example, given the similarity of symptoms to many pulmonary infections, particularly tuberculosis, it is often misdiagnosed. As with most diagnoses, the gold standard is to identify the organism by culturing from bodily fluids. However, given the short time in which *B. pseudomallei* can cause septicaemia and death, the time it takes to culture bacteria is often too long particularly when culturing from fluids containing multiple organisms i.e. from typically non-sterile sites such as pus and sputum. Samples are typically taken from the throat, sputum, rectum, wounds, blood or abscesses and *B. pseudomallei* is often dismissed as contamination (31).

There are attempts to identify barriers and to increase the awareness of melioidosis through the formation of focus groups, leaflet and audio/visual campaigns (32) and devising simple experiments to confirm *B. pseudomallei* infection such as culturing of *B. pseudomallei* on Ashdowns media. Ashdown agar contains gentamicin and the dyes crystal violet and neutral red which *B. pseudomallei* are intrinsically resistant to (33).

The most common methods for diagnosis are to detect antibodies in a biological sample by indirect haemagglutination (IHA), however this is often unreliable particularly in endemic areas due to the presence of *B. pseudomallei* specific antibody in healthy individuals. Less than 50% of culture positive samples are deemed IHA

positive, with many results being subjective and highly dependent on the parameters imposed such as the titre of the test (34). Two bacterial identification kits are also available; API20NE and API20E (35).

A fast developing and exciting diagnosis tool is a lateral flow device that incorporates a capsular polysaccharide-specific monoclonal antibody which has a 98% positive identification rate (against 77 *B. pseudomallei* strains) and showed that 97% of closely related species did not result in a positive result (36) . When tested on clinical samples the lateral flow device proved more effective at diagnosing *B. pseudomallei* than IHA and PCR based methods (37). Other methods include MALDI-TOF (38), PCR (6) and sequencing of gene targets (39).

One of the main issues with diagnosis is that they can involve relatively complex and potentially expensive procedures which may not be feasible in remote areas of South East Asia where the disease can be most prevalent, however with increased development of devices such as a lateral flow device alongside increased training it is hoped that speed to diagnosis can be reduced and as a consequence so will fatalities.

1.2.5. Treatments and vaccines

Treatment of melioidosis can be problematic. This is due, in part, to the intrinsic resistance of *B. pseudomallei* to many antibiotics including penicillins, cephalosporins, rifamycins, and aminoglycosides (40, 41). The intracellular nature of *B. pseudomallei* infection also poses difficulty in treatment. The Centre for Disease Control and Prevention recommends a two phase treatment regime. The first consists of initial intravenous antimicrobial therapy for 10-14 days (ceftazidime or meropenem). The second phase is an eradication phase consisting of 12-20 week period of oral antimicrobial therapy (trimethoprim-sulfamethoxazole and/or doxycycline) twice daily (42, 43). Treatment can be an expensive and impractical option in endemic areas. An alternative is the production of a cost effective vaccine. Given that *B. pseudomallei* is a potential biothreat there has been increased interest in the development of a vaccine by a number of agencies including governments. Whist there are no currently licensed vaccines against *B. pseudomallei,* progress is being made. There are a number of potential live attenuated strains but given the high mortality risk, the risk of reversion is thought to be too great. If the host immune system is compromised sufficiently and

thus the risk of latent infection is higher than with subunit or inactivated whole cell vaccines for example. Other options include sub unit, DNA and dendritic cell vaccines (44). Examples of subunit vaccines include using LPS and capsular polysaccharide which provided at best a 50% survival rate and an increase in mean time to death from 11 to 17.6 days (45). Coupling of a capsular polysaccharide (2-O-acetyl-6-deoxy-β-d-manno-heptopyranose) to tetanus toxin domain was suitable for increasing the lethal dose of K96243 by over 100 fold as well as increasing median survival time and improving clearance of bacteria in surviving mice (46). Endotoxin free outer membrane protein, OmpW, was capable of providing protective immunity in BALB/c and C57BL/6 mice (47). Both these subunit vaccines are potentially much safer than the live attenuated alternatives which pose the risk of reversion to virulence. One such candidate is the *purM* mutant which was cleared from the lung, liver, and spleen in BALB/c mice and was avirulent in Syrian hamster models (48). Another mutant unable to grow in the absence of diaminopimelate (a derivative of lysine) was avirulent in BALB/c mice and was unable to form MNGC (49).

Killed whole cell *B. pseudomallei* vaccines have been shown to have some protection against melioidosis and glanders under laboratory conditions. BALB/c mice injected with heat inactivated, *B. pseudomallei*, *B. thailandensis* or *B. mallei* could result in up to 80% survival rate when subsequently treated with *B. pseudomallei* at 100 times the median lethal dose (MLD) (50). Alternatively cells can be killed with paraformaldehyde which has been shown in some cases to provide protection where heat inactivation could not (51). Inactivated whole cell vaccines however may not be able to produce a high enough immune response to result in immunity but are cheap and expose the host to a wide range of antigens.

1.2.6. Biothreat agent

There are a number of events in which biological material has been used to cause harm to other individuals. Perhaps the most prominent was the distribution of letters containing anthrax spores sent to media outlets and politicians in the US in 2001. This incident led to the death of 5 people, infection of another 17 with antibiotic treatment prescribed to of tens of thousands of potentially infected individuals (52). There has subsequently been increased research and resources committed to the development of medical countermeasures against biological agents. *B. pseudomallei* has a number of features that contribute to it being such a potential agent. These include but are not limited to, a high mortality rate, its ability to be aerosolised, no current vaccine and its intrinsic resistance to many antibiotics (53). As such it is classed a category B select agent in the US and therefore has associated restrictions imposed including security, transport, access and limitations on genetic manipulation (53) .

1.3. Animal and *Galleria* models of melioidosis

The evaluation of *B. pseudomallei* mutant pathogenicity, antibiotic therapy or vaccine efficacy often requires the use of animal models of infection. Dependent on the type of infection (acute, chronic or latent) or the route of infection there are a range of small animal models that can be used. These typically involve the use of mice such as BALB/c and C57BL6, with choice of mouse being dependent on the type of infection to be established. BALB/c mice are typically more sensitive to melioidosis compared to C57BL6 mice which have been shown to be 10^4 fold more resistant to *B. pseudomallei* infection. Moreover BALB/c mice are much more susceptible to intraperitoneal (IP) challenge compared to C57BL6 mice (54). As a result C57BL6 mice are more likely to form chronic infection between 5-10 weeks post challenge whereas BALB/c mice are more prone to acute infection. The differences between types of infection by these two mouse strains are due to differences in immune response and immune bias. BALB/c mice have a predominantly T helper 2 (TH2) biased response, more typically associated with the clearance of parasitic infections, whereas C57BL6 mice have a TH1 biased response more typically associated with the clearance of intracellular pathogens (55). BALB/c mice are typically more docile compared to C57BL6 mice

which are generally more aggressive. Other small animal models, although these are less commonly used, include the Syrian hamster and diabetic rat. Both have increased susceptibility to melioidosis (compared to mice models) and tend to result in acute infection resulting in death within 7 days. Many of the virulence factors described in the Chapter 1.5 were identified using small animal models, predominantly BALB/c models of infection to show the effect of mutation of genes encoding virulence factors on the pathogenicity of *B. pseudomallei*.

A more accurate representation of melioidosis infection in humans is to use non-human primates (NHP). However, there are much greater ethical considerations with this type of model compared to small animal models, particularly the harm-benefit assessment. In addition there is increased legislation, infrastructure, training requirements and cost, which often make this model of infection unsuitable/unavailable to many research organisations. As a result, there is currently only a small amount of research into non-human primates as models of melioidosis. However an existing and developing include the marmoset model (*Callithrix jacchus*) which has been shown to follow very closely human infection of *B. pseudomallei* (56). Marmosets are highly susceptible to *B. pseudomallei* infection with a median lethal dose (LD_{50}) of less than 10 colony forming units (CFU) by the aerosol route. The disease also shows wide spread bacterial dissemination, bacteraemia, fever, liver failure and abscess formation (57). This model has also progressed into looking at the effect of different *B. pseudomallei* strains on disease presentation. Two clinical isolates (HBPUB10303a and HBPUB10134a) and two lab strains (K96243 and 1026b) were evaluated and while there was moderately increased virulence in the clinical strains the authors note that lab strains are suitable for the melioidosis model and the strain used does not affect the model outcome (57). The development of a rhesus macaque aerosol model for *B. mallei* infection has also recently been described (58).

A common, but controversial, non-animal model is to use *Galleria mellonella* wax moth larvae. These have been shown to be capable of being used as an infection model for a range of select pathogen agents, including *B. pseudomallei* (59). They have been used to determine the effect of mutations on the virulence of *B. pseudomallei* and *B. mallei* (60) and also to test the efficacy of antibiotic treatments. Thomas et al.

successfully showed using this model that kanamycin, imipenem, ceftazidime, doxycycline and ciprofloxacin prevented the onset of infection by *B. pseudomallei* (61). They also used this model to screen a range of novel antimicrobials and showed that 2 out of 20 provided 75% protection whereas 8 out of 20 provided no protection at all. Results using the *Galleria* model can be highly variable and are often not reproducible. The development of research grade larvae, that are not bred in the presence of antibiotics and are dispatched at the same growth phase are attempts to limit this variability. These advancements however cannot compensate for the lack of an adaptive immune system in *Galleria* and therefore this model is far from matching the response in the human host. However the *Galleria* model of infection can be useful as a tool for the down selection of targets or generation of *in vivo* data for research groups that are not able to perform small animal infections.

1.4. The *B. pseudomallei* genome

The genome of *B. pseudomallei* was first annotated in 2004 by Holden et al (62). The strain was isolated from a 34 year old diabetic female from Vietnam. Designated *B. pseudomallei* K96243, this is widely used as a reference strain to this day. The genome of the pathogen is highly GC rich and comprised of two chromosomes. The larger chromosome, with a size of 4.07 Mbp, encodes genes typically associated with cell growth, metabolism, amino acid biosynthesis, chemotaxis and mobility. The smaller chromosome, with a size of 3.17 Mbp, encodes genes more associated with adaptation as well as many hypothetical genes with no annotations.

Sixteen genomic islands (GIs) were also identified within the genome. The variability of 5 of these islands (chosen as a representative sample) was investigated in 186 isolates both clinical and environmental (63). Certain GIs were found in a high percentage of isolates such as GI16 involved in metabolism, found in 76% of isolates. Others such as GI9, a prophage like island, was found in just 12% of isolates.

In 2008, initial microarray analysis from 94 clinical, environmental and animal isolates from South East Asia was used to identify genes present in all strains - termed the core

genome - and those that are variable amongst isolates - termed the accessory genome. 86% of the genome of the reference strain *B. pseudomallei* K96243 was common to all 94 isolates and was designated the core genome (64). A large percentage (30.8%) of the accessory genome was found to be within GIs. The core genome encodes genes commonly found in many bacteria including essential genes and those associated with virulence. The remaining genome comprises of many hypothetical genes and isolate specific genes, often dependent on if it is a clinical or environmental isolate.

More recently whole genome sequencing (WGS) has been used to compare 106 *B. pseudomallei* isolates to identify genomic differences to a much higher resolution (65). It was shown that the core genome is 5.6 Mbp and the accessory genome (often characterised by a lower GC content) was much larger than that shown using microarrays with each strain having an average of 184kb of novel accessory regions. Moreover the authors showed that the *B. pseudomallei* genome can be classed as an 'open' genome in which the pan-genome (core genome+accessory genome) is 8802 genes, 2897 of with are not associated with *B. pseudomallei* K96243 strain. To extend on this work, WGS of 469 isolates has also been used to show the geographic distribution of *B. pseudomallei* (66). It was shown through SNP analysis of the core genome that *B. pseudomallei* originated from Australia before its spread to Asia, Africa and then to South America and then reintroduction to Asia (Figure 3).

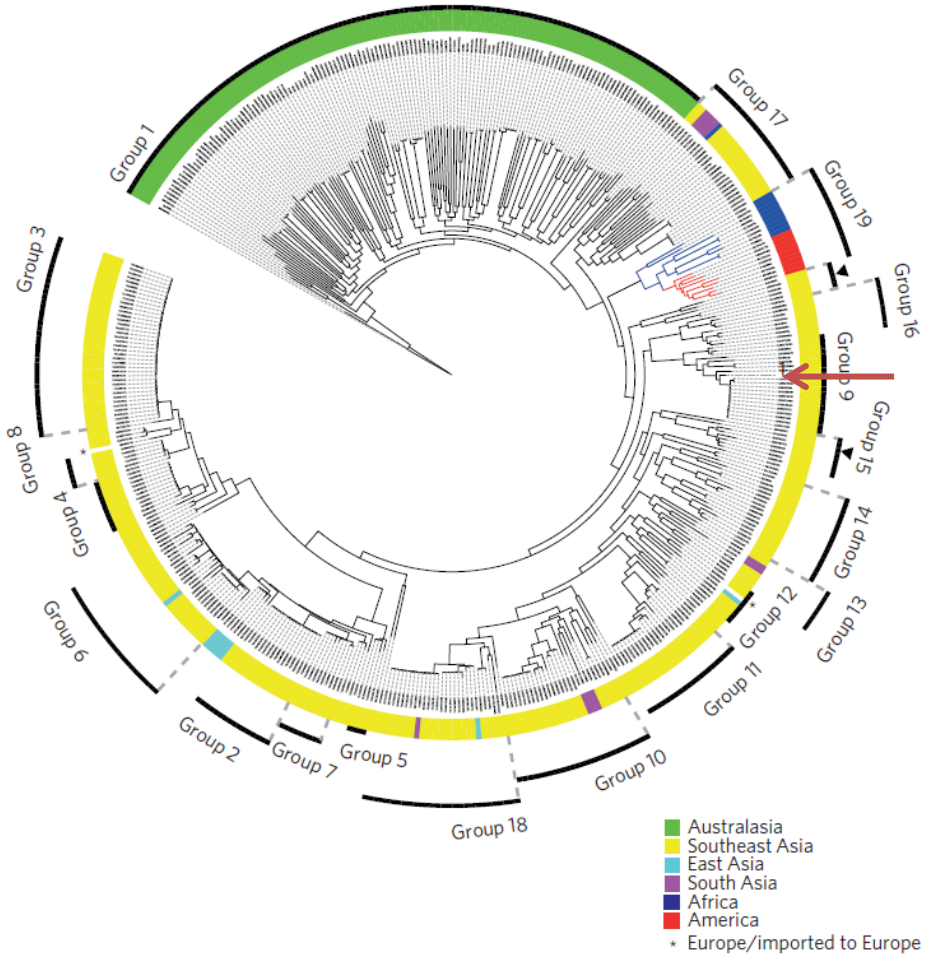

Figure 3 Phylogeny of *Burkholderia pseudomallei*

An SNP-phylogeny tree of the core genome of 469 isolates. Geographical regions are highlighted in different colours. The tree is rooted on *B. pseudomallei* MSHR5619, the most genetically diverse isolate. B. pseudomallei K9642, a reference strain is highlighted by a red arrow. Groups 1 – 19 indicate population clusters. Figure modified from (66).

The most common method to subtype *B. pseudomallei* isolates is to use multilocus sequence typing (MLST). Typically PCR based MLST of *B. pseudomallei* is based on variations within fragments of seven housekeeping genes (67). MLST was performed on 147 isolates of *B. pseudomallei* and *B. mallei* and *B. thailandensis*. Housekeeping loci were identified using *B. pseudomallei* K96243 as the genome sequence. They were able to characterise 71 individual strains from geographically diverse areas. MLST could also correctly differentiate *B. pseudomallei* from *B. thailandensis* species based on their allelic profiles but B. mallei isolates were clustered within B. pseudomallei clusters. The *B. pseudomallei* MLST database (https://pubmlst.org/bpseudomallei/) currently has data on over 5300 isolates with 1647 sequence types. Price et al. used the wealth of genomic information available for *B. pseudomallei* strains to improve previous MLST primers to identify new, more specific primers that also circumvent the problem of known genetic variation between *B. pseudomallei* strains in theses loci (68). A more frequently used method of analysis of differences between isolates of B. *pseudomallei* is to perform WGS and genome analysis (69). This method benefits in that it is not limited to analysis of small number of genes as is the case for MLST and can look at aspects such as recombination, horizontal gene transfer and mutation.

1.5. Virulence and pathogenicity

The success of *B. pseudomallei* as a pathogen is partially due to its ability to survive in phagocytic and non-phagocytic cells as demonstrated by Jones et al (70). Between 10^4 to 10^5 bacteria could be internalised in HeLa, Vero, A549 and CHO cell lines using an inoculum of 10^6 bacteria, indicating the high infectivity of *B. pseudomallei* within cells (70, 71). Given the large genome it is perhaps not surprising that *B. pseudomallei* encodes a vast number of virulence factors that it utilises to become such an effective intracellular pathogen. Such factors contribute to cell adhesion, escape from the phagosome, invasion, actin-based motility, the formation of multi nucleated giant cells and antibiotic resistance. These include virulence factors such as the capsule, flagella, type II, III, IV and type VI secretion systems, lipopolysaccharide (LPS) O- antigen and phospholipases (24, 72).

A powerful tool for genome wide investigation of genes both essential and for virulence of *B. pseudomallei* has been the use of transposon-directed insertion site sequencing (TraDIS) (73). In one study a saturated *B. pseudomallei* transposon library was generated, genomic DNA was isolated and sonicated to break into fragments. Each fragment was sequenced using Illumina HiSeq sequencing. The sequences were mapped to the genome which shows the saturation of transposons throughout the genome. The larger the number of transposons found within a gene the less likely it was to be essential. Those with no or very low numbers of insertions were classed as essential. A number of these genes were confirmed using generation of conditional lethal mutants (73). This approach was taken further to specifically look at genes essential for *in vivo* growth, potentially identifying unknown virulence genes. Previous experiments using signature tagged mutagenesis had identified 33 out of a library of 892 transposon mutants that were attenuated when introduced into the BALB/c model of melioidosis using the intranasal route of infection (74). Genes identified included glycotransferases, capsule polysaccharide biosynthesis, SOS response and DNA repair. To expand and re-examine this data the TraDIS screening approach was used which identified another 105 mutants that were negatively selected in the original mouse infection (75). Outlined below are the main virulence factors and their roles in *B. pseudomallei* pathogenicity.

1.5.1. Capsule and LPS

There are five currently described surface polysaccharides in *B. pseudomallei* (capsular polysaccharides (CPS) type I-IV and an O-polysaccharide (OPS) which forms part of LPS (76-78). Thus far, CPS I is the only antigen shown to play a major role in virulence. CPS 1, specifically *wbcB*, was shown by *lux* fusion to be upregulated when exposed to human serum and can prevent phagocytosis by disrupting complement cascade recognition (79, 80). Mutation of genes found within the CPS 1 gene cluster (*bpsl2786-2810*) were identified using signature tagged mutagenesis screening and resulted in a high level of attenuation in mice (10^5 fold reduction in LD50) and Syrian hamster models of melioidosis (80, 81). Mutation of CPS III and CPS IV did also result in attenuation in a mouse model of melioidosis with an increase in the meantime to death between 7-12 days (82), however all mice succumbed to disease suggesting that these CPS are not as important in virulence as CPS I.

LPS is a major virulence determinant in *B. pseudomallei*. *B. pseudomallei* has multiple LPS variants; three smooth and one rough. A study into the genotypes of these variants revealed that strains exhibiting typical LPS were commonly found in South East Asia but strains displaying atypical LPS were predominantly from Australia (83). This atypical LPS has been shown to be important in resistance to cationic peptides such as polymyxin B (84).The effects of mutations in genes encoding the LPS of *B. pseudomallei* have also been studied; transposon screening revealed three mutants with increased sensitivity to serum, all of which had mutations in the outer polysaccharide moiety of LPS (85). An LPS mutant of *B. pseudomallei* strain SRM117 had an increased internalisation rate in murine macrophages compared to the wildtype strain but could not survive and replicate thereafter (86).

1.5.2. Secretion systems

The ability of a bacterium to secrete factors, both chemical and protein, into its environment, another bacterium or host cell greatly improves its chances of survival and ability to cause infection. In order to accomplish this bacteria encode a range of secretion systems with differing functions dependent on the target and effector protein being secreted (87). *B. pseudomallei* encodes a wide range of secretion systems from multiple families (types). The two main secretion systems important in virulence in many organisms, including *B. pseudomallei*, are the type 3 secretion system (T3SS) and type 6 secretion system (T6SS).

Three T3SS have been identified in *B. pseudomallei* (T3SS1/2/3). Each secretion system is encoded in individual gene clusters comprising of structural and associated proteins. Early studies of these secretion systems in *B. pseudomallei* aimed to identify their importance in virulence. The major inner membrane subunit encoded by *sctU* in the three clusters was mutated in each, effectively inactivating each of the systems. Only Δ$sctU_{B3}$ (inactivated T3SS3) was shown to be attenuated in a Syrian hamster model of melioidosis (88). T3SS-3 (Bsa T3SS-3), is similar to the Inv/Mxi-Spa T3SS of species such as *Salmonella* and *Shigella* (89). Mutants in proteins of this secretion system were unable to escape from vacuoles and form actin tails. These mutants were also attenuated (to varying degrees) in murine mouse models.

BipD is a secreted effector protein of the T3SS. *bipD* mutants provided a small amount of protection against wildtype infection, with those challenged with *bipD* mutants previously, having an increased median time to death and increased survival (up to 60%) (89, 90). The importance of other effector proteins has been studied including BopB and BopE and BapA, BapB and BapC with all mutants being attenuated in murine infection models (89, 91).

Following escape from the phagolysosome *B. pseudomallei* can move throughout the cell and into adjacent cells using a process of actin based motility. This has been shown to be achieved through the utilisation of the autotransporter, BimA. BimA localises to a pole in the cells and can polymerise actin for the formation of actin tails allowing for inter and intracellular movement. Mutation of *bimA* prevents actin tail formation in J774 macrophages (92) while homologues from other *Burkholderia* species can complement this phenotype (93) .

The T6SS is a more recently discovered system that has been the focus of much research over the last decade or so. The secretion system is similar to an inverted bacteriophage-like structure that functions to inject effector proteins into host and other prokaryotic cells (94). Each system is encoded on a gene cluster comprised of approximately 15-20 proteins (94). *B. pseudomallei* has six T6SS. T6SS-1 has been shown to be important for infection of Syrian hamsters. Mutants of this system were unable to form multinucleated giant cells (MNGC) and had defects in actin tail formation. Other T6SS systems were not shown to be important for virulence (95). Regulation of the T6SS-1 was found to be controlled by two pathways dependent on the environment; *B. pseudomallei* in media has regulated expression using BprC whereas intracellular cells were reliant on the two component system, VirAG. Mutants in *virAG* were avirulent in BALB/c mice (96).

Hemolysin Coregulated Protein (Hcp) is a core protein in T6SS and forms the nanotube through which effector proteins are secreted. Recombinant Hcp protein provided up to 80% protection against wildtype K96243 challenge in BALB/c mice (95).

Mass spectrometry comparing culture supernatants of wildtype cells with a mutant with an inactivated T6SS, identified Vgr-5, the tail spike protein of the injection system,

as an effector protein of the T6SS in *B. pseudomallei*. More recently it has been shown that Vgr-5 of *B. thailandensis* is required for cell-cell spread, MNGC formation (expressed immediately prior to MNGC formation) and virulence in mice (97, 98).

1.5.3. Flagella

B. pseudomallei encodes 5 putative clusters encoding genes involved in flagella systems and assembly (62). The literature regarding the importance of flagella in virulence however is currently not conclusive. For example, one study showed that mutations in the flagellin coding gene, *fliC*, had no significant effect in virulence in Syrian hamsters or diabetic rats when infected by the intraperitoneal (IP) route (99). However, mutations made in the same gene by a different group showed that while the mutant had no impairment on its ability to invade human lung cells it was avirulent in BALB/c mice infected by the intranasal or IP route, suggesting that flagella may be involved in virulence but not necessarily adhesion – in these models (100). To further support this *B. pseudomallei fliC* mutants were also shown to have a reduced ability to invade macrophages (RAW264.7) and human lung epithelial cells (A549). It was also noted however that the type III secretion system may also contribute to this phenotype (101).

The role of flagella in *B. pseudomallei* may extend away from virulence within a host, such as its survival in the environment. *B. pseudomallei* is able to outcompete the non-human pathogenic species, *B. thailandensis* through the production of a 30-50kDa secreted compound that can inhibit motility in competition based assays. The compound was shown to inhibit and truncate flagella, although attempts to purify the inhibitory factor failed (102).

1.5.4. Pili

Adherence to cells is an essential step for bacteria to enter host cells before subsequent replication and persistence in an intracellular environment (103). There are a number of mechanisms a bacteria uses to adhere to cells such as adhesins, pili adhesion and non-pili adhesins. Eight type IV pili loci have been identified in *B. pseudomallei* K96243. Important structural genes include *pilA*. A *pilA* mutant was

shown to have reduced adherence to human cell lines (A549, BEAS-2B and RPMI-2650) and attenuation in *Caenorhabditis elegans* and BALB/c mice (104).

1.5.5. Quorum sensing

Induction of virulence genes can be metabolically expensive and immunogenic and as a consequence bacteria promote transcription only upon the cell density reaching a defined threshold. Cell-cell communication allows bacteria to monitor bacterial density levels and is achieved using a process of quorum sensing. Bacteria can then unilaterally express virulence factors in order to increase the probability of overcoming host defences (105). In Gram negative bacteria this communication is achieved by the secretion of small molecules, acyl homoserine lactones (AHL) into the surrounding environment which when a threshold is reached can re-enter the bacterium and regulate gene expression.

In silico and experimental evidence shows that *B. pseudomallei* K96243 encodes at least three *luxI* homologues (AHL biosynthesis), five *luxR* homologues (transcriptional regulators that sense the signals) and a large number of AHLs (at least 7). *B. pseudomallei* strain DD503 contains homologues for two of these *luxI* and four *luxR* genes. Mutants were generated and used to infect BALB/c mice at $1x10^4$ CFU/ml via an aerosol challenge. All mutants were attenuated in mice with an increased time to death in all cases when compared to wildtype (106). In addition this study also showed that there was an increase in the Syrian hamsters infected by the IP route.

Mutations made in of all three AHL synthases encoded by *B. pseudomallei* (*bpsI1, bpsI2* and *bpsI3*) in combination, resulted in increased formation of MNGC in RAW264.7 macrophage cells but not for any of the single mutants. This had no effect on virulence when BALB/c mice were infected with the triple mutant compared to wildtype, with no attenuation observed (107). *In vitro* studies showed that *B. pseudomallei* mutants in N-octanoyl homoserine lactone (C8-HSL) were unable to survive in stationary phase as a result of an inability to withstand increasing alkaline conditions (108).

1.5.6. Autotransporters

Autotransporters (AT) are a family of secreted or outer membrane proteins that have been shown to have an important role in *B. pseudomallei* pathogenesis. AT include invasins, adhesins and actin nucleation factors. *B. pseudomallei* K96243 encodes 11 predicted AT (BatA, BcaA, BpaA-F, BoaA-B and BimA) (109), many of which have been shown to play an important role in adhesion and invasion of human A459 cells (110). A more recent study by Lazar Adler et al. generated marked deletion mutants in all 11 AT of *B. pseudomallei* and assessed their role in replication in J774 macrophages, virulence in BALB/c mice and serum resistance. Eight of which were attenuated in mice (*bcaA*, *boaA*, *boaB*, *bpaA*, *bpaC*, *bpaE*, *bpaF* and *bimA*). The greatest attenuation was in Δ*bpaA* which resulted in a 90 fold decrease in LD_{50}. Δ*bpaC* was shown to have increased sensitivity to serum, suggesting a role in resistance against the complement system (111).

Over the past decade or so, there has been a great deal of research into BimA. Mutation of *bimA* prevents actin tail formation in J774 macrophages (92). It was later shown that a short 13 aa sequence of BimA was shown to be essential for intracellular spread but not for actin polymerisation (112). Homologues from other *Burkholderia* species can complement this phenotype (93) .

1.5.7. Efflux pumps

Burkholderia species are renowned for high intrinsic resistance to many antibiotics (113). There are a number of major proteins or complexes of proteins that play a role in resistance. The first is a membrane bound β-lactamase protein, PenA. Deletion of *penA* resulted in increased sensitivity to many antibiotics in particular ampicillin (256µg/ml to 8µg/ml) and carbenicillin (1024 µg/ml to 32µg/ml). Point mutations (C69Y, S72F and P167S) in PenA resulted in highly increased sensitivity to antibiotics (114). Other mutants had similar resistance profiles by increasing expression of *penA* as a result of a point mutation in the upstream gene region (115).

A second major form of resistance is efflux pumps. There are many families of efflux pump and *B. pseudomallei* encodes multiple systems per family. These include but are not limited to the major facilitator superfamily (MFS), the small multidrug resistance (SMR) family, the ATP-binding cassette (ABC) family and the resistance nodulation cell

division (RND) pumps. *B. pseudomallei* encodes 10 RND pumps (62) including the AmrAB-OprA pump responsible for resistance to aminoglycosides and macrolides (116) and BpeAB-OprB allowing for resistance to fluoroquinolones, macrolides, and tetracycline (117).

1.5.8. Other virulence determinants

1.5.8.1. Morphotype switching

B. pseudomallei can undergo a process called morphotype switching. This is achieved by altering the surface elements allowing it to survive in a range of environments. *In vitro* this can be seen by the presentation of different colony morphologies on Ashdown agar. Peacock et al. identified 7 different colony morphologies and showed that switching can occur in *B. pseudomallei* isolated from human cases of melioidosis, in animal models, during macrophage infection and nutrient starvation (118). The different morphotypes have different altering phenotypes variable biofilm production, swarming and swimming motility and elastase, protease and lipase activity (118).

The ability of *B. pseudomallei* to alter its cellular morphology and virulence determinants has implications during infection. Comparison of colony morphology type II and type III with type I revealed that while there were no differences in growth doubling time, type I was significantly better at intracellular replication in U937 human macrophages. Type I also had increased resistance to H_2O_2 with type III switching to type I or II in oxidative conditions. However, type III was more resistant to the antimicrobial peptide LL-37. The authors also suggest that some morphologies are more adapted to intracellular survival and replication compared to others more suited to persistence (119). Another study has shown how a 'yellow' morphotype in K96243 was more suited to cause infection in gastric environments, including murine stomach colonisation, than its white counterpart (120).

1.5.8.2. Siderophores

B. pseudomallei is able to acquire iron from iron-limiting environments using siderophores. Of 84 clinical isolates tested all 84 were shown to produce siderophores. Supplementation of M9 media with transferrin and siderophore could promote the growth of a low siderophore producing strain, *B. pseudomallei* 316a (121). *B. pseudomallei* also produces the hydroximate siderophore, malleobactin. Malleobactin

of *B. pseudomallei* is able to remove iron from transferrin and lactoferrin (although to a lesser extent) (121, 122). The malleobactin gene cluster had either incomplete or impaired ability to grow in minimal media which had been chelated of iron. This however could by complemented by the addition of recombinant malleobactin (123).

Despite this, it has been demonstrated through the generation of multiple deletion mutants that removal of the malleobactin encoding gene (*mba*), an iron acquisition system gene cluster, pyochelin (*pch*) and haemin uptake loci (*hmu* and *hem*) resulted in full virulence of Bp 1710b in BALB/c melioidosis model. This provides evidence for a so far, unidentified iron utilisation system (124).

1.5.8.3. Haemolysins, proteases and toxins

There is currently limited literature into haemolysins of *B. pseudomallei*, however there is evidence of haemolysins in other *Burkholderia* species. For example *B. cepacia* encodes a haemolysin that results in apoptosis of macrophage-type cells J774.2 shown by DNA degradation associated with programmed cell death. Moreover, the same protein was also able to inhibit growth of *S. aureus* and *P. aeruginosa* (125). More recently, a toxin of the *Burkholderia cepacia* complex (Bcc) was shown to be haemolytic (haemolytic zones on TSA sheep blood agar) with mutation resulting in a decrease in virulence in the *Galleria* model of infection (126). In another study, 91 clinical isolates out of a total of 100 were also shown to produce a weak haemolysin on sheep erythrocyte brain heart infusion agar. Four isolates were also shown to have strong haemolytic activity (also in broth) (127). BPSL1375 of *B. pseudomallei*, a member of the N-acyltransferase family, was shown to have haemolytic activity through visualisation of sheep erythrocytes treated with recombinant BPSL1375 as well as haemolytic zones of *E. coli* strains over expressing BPSL1375 on TSA sheep blood agar (128).

Burkholderia produce proteases, including metallo and serine proteases (129). The importance of proteases in virulence is not clear with conflicting studies, perhaps due to the route of infection. One study showed that the production of a specific metalloprotease was important for virulence in a rat lung infection model (130). However, another group showed that the production of proteases was not essential for virulence (comparing protease positive and negative strains), in a IP SWISS mouse

model of melioidosis (131). A serine protease, MprA, was shown to be sero reactive and could be used to elicit protective immunity in mice, although all mice treated with recombinant MprA succumbed to the disease 25 days after the control group (9 days). It was also demonstrated that the use of protease inhibitors could decrease the lethality of *B. pseudomallei* in *C. elegans* (132).

In 2012 a toxin, *Burkholderia* Lethal Factor 1 (BLF1), was described by Cruze et al. Using structural analaysis on unknown proteins BLF1 was identified as a potential toxin by showing homology *E. coli* cytotoxic necrotizing factor 1 (CNF1-C). Mutation of *blf1* resulted in attenuation in BALB/c mouse model and was toxic to J774 macrophages. Injection of recombinant BLF1 into BALB/c mice via the IP route was lethal by day 14. BLF1 was shown through its interaction with translation initiation factor (eIF4A) to stall translation resulting in the toxic effect on the host cells (133).

1.5.9. Intracellular infection, survival and replication

Following cell adhesion, *B. pseudomallei* can be internalised into phagocytes and neutrophils typically by phagocytosis or can actively infect epithelial cells (70, 71). Once in a host cell it can utilise virulence factors such as the Bsa type III secretion system and its effectors such as BopA and BipD (89) to escape from the phagosome. The speed of escape is extremely short with it being shown that *B. pseudomallei* strain 708a can escape vesicles of RAW macrophages within 15 minutes (134). The longer the bacterium is inside the phagosome the increased likelihood of the phagosome binding to the lysosome and the subsequent destruction of the bacteria. Following escape it then becomes essential to replicate and spread from cell to cell. Transposon library screening identified 9 genes important for the intracellular replication and spread of *B. pseudomallei*. These genes included type III secretion genes, a lipoate-protein ligase and four genes involved in purine, histidine, or p-aminobenzoate biosynthesis (135). Mutants in all nine genes were attenuated in BALB/c model. The ability to replicate and spread is also due in part to its ability to suppress common macrophage killing mechanisms such as the production of nitric oxide (NO). NO release is upregulated by LPS however, *B. pseudomallei* LPS has been shown to result in reduced NO expression compared to other Gram negative bacteria (136). *B. pseudomallei* can suppress expression of two regulators of NO production, SOCS3 and

CIS (137). Following cell-cell spread by actin based motility, using factors such as BimA and IQGAP1 (93, 138), *B. pseudomallei* and induce cell fusion and the formation of MNGC (139).

The intracellular nature of infection by *B. pseudomallei* is most likely to be the primary cause for successful latent reinfection and latent melioidosis. It has been shown to accumulate large granules of polyhydroxybutyrate for use as long-term energy stores; again showing adaptation to long term survival (140).

Despite its successful intracellular lifestyle *B. pseudomallei* it still comes into contact with the host immune response. *B. pseudomallei* produces pathogen associated molecular patterns (PAMPs) such as LPS, lipid A and peptidoglycan. These PAMPS are displayed by host cells had previously degraded invading *B. pseudomallei*. They are recognised by toll-like receptors and pattern recognition receptors and allow the host to coordinate innate and adaptive immune responses. The activation of toll like receptors, specifically TLR4 and TLR2, has been shown as a result of exposure to *B. pseudomallei* LPS and Lipid A (141). Mutation of a toll like receptor adapter protein (myD88) in mice resulted in increased susceptibility to *B. pseudomallei* infection, partially due to in ability to recruit neutrophils to the site of infection (142).

1.6. Peptidoglycan

1.6.1. Structure and function

Peptidoglycan (PG) is comprised of a mesh of linear glycan chains of alternating *N*-Acetylmuramic acid and *N*-Acetylglucosamine residues linked via a 1-4, glycosidic bond. Chains are cross-linked with short peptide chains via *N*-Acetylmuramic acid (143) (Figure 4). The nature of the cross link depicts the type of peptidoglycan and can be species dependent (144). The PG sacculus encompasses the plasma membrane of bacteria to form a cell wall (Gram negative bacteria have a further membrane surrounding this layer). PG maintains the integrity of the bacteria, providing strength, resistance to turgor pressure and acts as a scaffold to which many proteins can anchor (145). As an ever changing molecule, peptidoglycan requires constant turnover and modification to allow it to adapt to the requirements of the bacteria including division, insertion of proteins and macromolecular structures including secretion systems, pores and flagella. As such PG requires a whole host of synthesising, assembly, modifying and recycling enzymes required to maintain its integrity, many of which are targets for antibiotics.

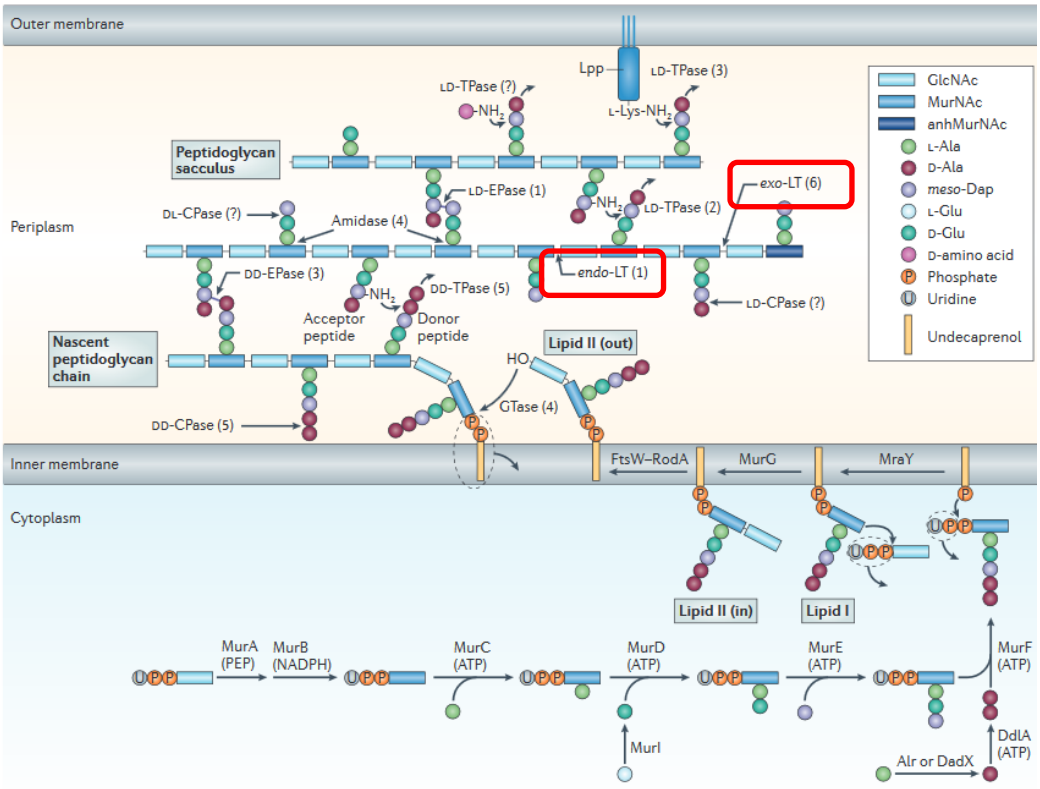

Figure 4: Peptidoglycan biosynthesis and turnover

Peptidoglycan is comprised of a mesh of linear glycan chains of alternating N-Acetylmuramic acid and N-Acetylglucosamine residues linked via 1-4, glycosidic bonds. Chains are cross-linked with short peptide chains via N-Acetylmuramic acid. Peptidoglycan biosynthesis requires a vast number of enzymes in particular the cytoplasmic Mur proteins. Once flipped into the periplasm subunits are assembled into chains. Hydrolysing enzymes such as carboxypeptidases (CPase), amidases, endopeptidases (EPase) and lytic transglycoylases (LT), allow for regulated modification of the peptidoglycan layer particularly during cell growth and division. The exo- and endolytic transglycosylases are highlighted in red boxes. Figure modified from (146)

1.6.2. Peptidoglycan synthesis and turnover

The number of enzymes required for the continued synthesis, turnover and modification of the peptidoglycan layer is vast. Bacteria are continuously synthesising peptidoglycan during cell growth and at the same time hydrolysing in a regulated manner to allow for cell elongation and cell division. The model for the assembly of peptidoglycan was first suggested by Holtje in 1998 and still stands today. Termed the 3-for-1 model (147), it outlines the insertion of 3 new strands and the removal of one old strand. There have been over 20 hydrolysing enzymes identified in *E. coli* split into four main families; endopeptidases, amidases, carboxypeptidases and lytic transglycosylases (Figure 2) (148). The roles of many of these proteins in regards to peptidoglycan synthesis and maintenance is known in *E. coli* but the role they play in other bacterial functions requires continued research, particularly given the vast differences between bacterial species, the niches they occupy and their requirement for such a wide range of enzymes.

1.7. Lytic transglycosylases

A major class of PG modifying enzymes are the lytic transglycosylases (Ltgs). Ltgs are a family of proteins ubiquitous to bacteria. They are muralytic enzymes, which cleave the β-1, 4 glycosidic bond between *N*-Acetylmuramic acid (NAM) and *N*-Acetylglucosamine (NAG) (Figure 4), the same substrate as lysozyme, a well-known muralytic enzyme. However unlike lysozyme, Ltgs are not hydrolases, but cleave to form an intramolecular 1,6-anhydro-muramoyl reaction product and catalyse the release of disaccharide anhydromuropeptides (Figure 5) (149). It is thought that these proteins are essential in cell wall recycling (150). These proteins also have a wide range of functions including cell division and expansion of the sacculus and to an extent the insertion of macromolecular structures such as the Type III and IV secretion systems, flagella, transport systems and type IV pili (149, 151-153). Due to the homology with the resuscitation promoting factors (Rpfs) of *Mycobacteria* species, it is also hypothesised that they are involved in entering the cells into a non-culturable state as and the resuscitation of these cells into a culturable state potentially allowing for latent infection.

There are currently four main families of Ltgs; 1, 2, 3 and 4 (154). Family 1 has been further divided into five subfamilies (155). The family to which an Ltg is categorised is dependent on the motifs located within it. It is known that the number of Ltgs encoded by bacteria ranges from species to species and they are not all necessarily from the same family of Ltg. For example *E. coli* has 8 Ltgs; membrane bound lytic transglycosylase (Mlt) A-G and soluble lytic transglycosylase (Slt)70 (149) from different Ltg families, whereas *P. aeruginosa*, does not encode MltC and MltE but has four MltB proteins. It is unclear as to whether these proteins perform the same functions or act in parallel (i.e. redundancy) with each other. It is also unknown the signals that these proteins respond to and whether they are regulated by the same stimuli will have to be further investigated. However, it is not uncommon for bacteria to encode genes for multiple proteins involved in the same or very similar functions in PG synthesis and assembly (156, 157). Clearly the redundancy of Ltgs indicates the importance of these proteins in bacterial survival and it has been shown that deleting individual genes is not lethal to *E. coli* but multiple deletions are (158).

1.7.1. Overview of current research into lytic transglycoylases

Eight Ltgs have been identified; MltA-G which are all membrane bound and Slt70 which is soluble. Ltgs are classed as either exolytic or endolytic depending on whether the Ltg cleaves the glycosidic bond between the NAG-NAM residues located at the end or within the glycan strand, respectively. Separation of muropeptides released from the *E. coli* sacculus digested with each of the recombinant proteins revealed that all Ltgs have exolytic activity and MltB, MltD, MltE and Slt70 also have some endolytic activity. MltB, MltD and Slt70 were until recently thought to be exolytic only (159). Below outlines an overview of the research into Ltgs so far.

1.7.2. MltA

A membrane bound Ltg was first identified in 1994 which was solubilised and purified from the membrane fraction of an Slt deletion *E. coli* strain, later shown to be an outer membrane lipoprotein (160). This protein was able to digest glycan chains and could form spheroplasts when overexpressed. Mutation of this gene however did not reveal any growth phenotypes (160, 161). There are a number of crystal structures for MltA including *E. coli* and *N. gonorrhoeae* (162, 163). These structures reveal that MltA is vastly different to other Ltg structures, comprised of two large subunits (an additional

subunit for *N. gonorrhoeae*) with a significant groove between, for peptidoglycan binding. This was shown experimentally with inactivated MltA (containing a mutation is the catalytic aspartate residue D308) which was crystallised with chitohexaose, an analogous substrate of Ltgs (164).

MltA has a 3D domain, as it has three conserved catalytic residues. It has been shown that mutation of these residues inactivates MltA (162, 164). This 3D domain has been shown to present in Stationary phase survival proteins (Sps) of Firmicutes. Firmicutes show similarity to *M. tuberculosis* and other *Actinobacteria* as they can enter a dormancy like state in which they can survive in late stationary phase prior to spore formation. This survival has been shown to be as a result of Sps. Sps were first discovered through sequence analysis of Rpf of *M. tuberculosis*. YabE, an Sps of *Bacillus subtilis,* was found to have analogue domains and a similar genomic content to RpfB in which the C' terminal catalytic Rpf domain had been replaced with a so called Sps domain. This Sps domain has low but significant homology with the C terminal, 3D domain of MltA (165). Structural investigation into YuiC, an Sps of *B. subtilis* revealed that YuiC is a stripped down version of MltA and crystallisation with NAG monomers and polymers revealed that the product of YuiC was the 1,6-anydrosugar was the product of the reaction of YuiC (166).

A study into MltA in *Edwardsiella tarda* revealed that overexpression resulted in an increased sensitivity to antibiotics, a small growth defect, decreased motility but perhaps most importantly an increase in virulence in zebra fish. Further, mutation of MltA resulted in a decrease in the LD_{50} (167).

MltA of *Neisseria* species (also referred to as LtgC or GNA33) has been a major focus of research into the Ltgs in *Neisseria*. It was also considered to be a potential vaccine candidate as it elicited a high immune response and the serum of mice injected with recombinant MltA demonstrated bactericidal activity (168). Mutation of *mltA* in *N. gonorrhoeae* resulted in an inhibition in cell division and associated growth defects (169) whilst mutation in *N. meningitidis* was unable to cause bacteraemia and death in infant rats (170).

1.7.3. MltB

MltB was first identified in 1995 in two forms; a larger 'prolipoprotein', MltB, which degraded to the active soluble protein Slt35 (171). MltB was overexpressed in *E. coli* and resulted in rapid cell lysis whereas mutation did not result in any obvious phenotypes (172). MltB produces the second largest amount of reaction products when digesting purified peptidoglycan, after MltA. It is also 10 fold more active in log phase cultures (159). Crystallisation studies of Slt35 show some similarities with Slt70 including a deep catalytic groove for peptidoglycan binding (173). MltB mutants in *P. aeruginosa* were less sensitive to β-lactam antibiotics including cefotaxime and cotrimoxazole due to decreased rate of autolysis. Point mutation in the predicted catalytic glutamate residue (E162A) did not result in an alteration of the minimum inhibitory concentrations (MICs) when compared to wildtype cells, it is suggested that this is due to structural rather than an enzymatic contribution of protein products to β-lactam antibiotics. The mutant had a similar sensitivity to bile salts and no difference in biofilm formation compared to the wildtype strain (174).

1.7.4. MltC

Comparison of the activity of *E. coli* Ltgs by digestion of peptidoglycan and the quantification of the fragments released revealed that MltC was the third most active Ltg after MltA and MltB (159). There was also a 10 fold increase in MltC muropeptides during log phase culture than stationary phase culture suggesting a time dependent regulation of the genes (159). This study also showed that LtgC is primarily exolytic with only 0.5% endolytic activity. The structure of MltC alternates dependent on the endo or exolytic activity of the protein (175). MltC has been shown to be important in motility in *H. pylori*. While flagella expression or assembly was not altered, a decrease in motility was shown to be due to loss of function of peptidoglycan maturation enzymes affecting flagellar functionality (176)**.** MltC has also been shown to play a role in the biofilm formation in *Salmonella enterica* serovar Typhimurium (177).

1.7.5. MltD

MltD, like other Ltgs contains a LysM domain. Structural analysis of the LysM domain of MltD from *E. coli* highlighted the presence of a groove for peptidoglycan binding and important catalytic residues (178). RP-HPLC and glycan chain length analysis of Ltg mutants in *H. pylori* showed it to be redundant to other Ltgs as well as having

endolytic activity. While the growth rate of Δ*mltD* was the same as wildtype it was able to survive in stationary phase for longer (179). Interestingly, mutation of MltD also resulted in an increase in virulence in *Vibrio anguillarum*. The LD_{50} decreased from 3.92×10^3 CFU (wildtype) to 1.01×10^2 CFU (mutant) and the mutant had defects in gelatinase, haemolysin and protease activity and had increased growth rates at sodium chloride concentrations above 2% compared to wildtype (180).

1.7.6. MltE

MltE (previously referred to as EmtA) is unique when compared to other lytic transglycosylases as it is endolytic (cleaves within glycan chains) producing shorter chains, whereas all others are exolytic (cleave from the end of glycan chains) (181). The structure and binding profile of MltE was solved in its free-state but also when bound to chitopentose (chain of five NAG molecules) and also Bulgecin A (an Ltg inhibitor). These structures also revealed the structural basis for endo-specific cleavage as opposed to exo-specific cleavage attributed to MltB and Slt70 (182).

For the first time, it has been recently demonstrated that MltE is required for the assembly of T6SS in *E. coli* (183). There are no genes within T6SS gene clusters that encode lytic transglycosylases (184) therefore Santin et al. proposed a process called domestication of the housekeeping MltE. They showed initially through inhibition of T6SS using the Ltg inhibitor Bulgecin A, that Ltgs were involved in the assembly of T6SS. Through individual mutation of each of the Ltgs encoded by *E. coli* only a mutation in MltE resulted in abolition of Hcp secretion. They also showed through bacterial two hybrid analysis that MltE interacts with TssM (a structural, inner membrane protein) and incubation together resulted in a seven fold increase in activity of MltE (183).

1.7.7. MltF and MltG

MltF is an exolytic Ltg, mutation in *P. aeruginosa* resulted in increased sensitivity to β-lactam antibiotics (including ceftazidime) (185). The structure and activity of MltF from *E. coli* was investigated and found to comprise of two core domains, the N-terminal domain which did not show Ltg or peptidoglycan binding activity and the C-terminal domain, shown to have Ltg activity using turbidometry (degradation of *M. Luteus*) and bioassays (effect on *E. coli* growth following induction) (186).

MltG is the most recently identified Ltg of *E. coli* (187). Using a dye releasing assay alongside an inactivated version (containing E218Q substitution in the predicted catalytic residue) it was shown the MltG was a muralytic enzyme and likely to be endolytic. Mutation did not result in any growth or morphological differences. It was also shown using bacterial two hybrid systems to interact with PBP-1b (187). A continuation of this study in *Streptococcus pneumoniae* showed that MltG is important in peripheral peptidoglycan synthesis (188).

1.7.8. Slt70

Slt70 has been shown to interact with other muralytic enzymes including an endopeptidase and penicillin binding proteins important in cell division (189). Single mutations in *slt70* did not result in increased murein turnover but did when in combination with MltA and MltB mutations. These multiple deletion mutants also had decreased β-lactamase induction leading to increased sensitivity to cefoxitin although not for the single mutation in Δ*slt70* (190).

1.7.9. 'Specialised' Ltgs

While there is a large amount of research suggesting that mutation of the 'typical' Ltgs i.e. MltA-F and slt70, can result in phenotypes such as motility defects, reduced biofilm formation and attenuation *in vivo*, there is a limited amount of evidence that directly links these Ltgs to assembly of virulence factors such as secretion systems, flagella or pili. There are exceptions such as the recent paper on MltE involvement in T6SS assembly (183) (see above). It has been suggested that certain Ltgs involved in macromolecular transport systems as well as the assembly of the T3SS and in Type IV pilus assembly should be called 'specialised Ltgs' (191). For example, the structure of EtgA a T3SS associate protein of enteropathogenic *E. coli* was shown to share features of both Ltgs and hen egg white lysozyme. These include conserved catalytic domains of Slt70 and conserved peptidoglycan binding residues of MltE. Mutation of *etgA* resulted in between 50-90% reduction in T3SS activity dependent on the *E. coli* strain used (192). In addition to this, the virulence of the plant pathogen, *Pseudomonas syringae* is as a result of its T3SS encoded by *hrp* genes. Three Hrp proteins have predicted Slt domains found in Ltgs such as MltD. They also have *hrp* promotor sequences under the control of the *hrp* sigma factor. Overexpression of these genes in

E. coli did result in growth inhibition but not cell lysis. Mutation of one of these Ltg like genes, *hrpH*, resulted in impaired effector protein translocation (193).

There is also research into the involvement of putative Ltgs involved in type IV pilus assembly (191). The type IV pilus is encoded by 14 *pil* genes, 12 of which are essential for conjugation (194). PilT shares homology with slt domains and is found in many type IV pili gene clusters (153).

A protein of *Rhodobacter sphaeroides*, dubbed SltF, also shares an Slt domain. Mutation of *sltF* was shown to result in defects in swimming motility and flagella assembly. It has also been shown that SltF interacts with FlgJ (flagellar rod-scaffolding protein) and suggested that through this interaction, this putative Ltg is localised to the site of flagella assembly (195). Some species of β- and γ-proteobacteria do not encode SltF and this activity is achieved by FlgJ. FlgJ of the α-proteobacteria, including S*almonella enterica* serovar Typhimurium does not have this activity but instead relies on SltF. It has been shown that SltF of *S. enterica* serovar Typhimurium is also essential for flagella assembly (196). More recently it has been shown that SltF has endo-lytic transglycosylase activity, sharing homology with the family 1 Ltgs (155) and that its activity is modulated by FlgB (activation) and FlgF (inhibition) (197).

1.7.10. Mechanism of action

Ltgs act by cleaving the β-1, 4 glycosidic bond between N-acetylmuramic acid (MurNAc) and N-acetylglucosamine (GlcNAc) residues that form the backbone of peptidoglycan to form an intramolecular 1, 6 anydromuramyl reaction product. At the centre of Ltg active site is an acidic residue (typically a glutamate or an aspartate) (164, 198). This acts as an acid/base to allow for cleavage of the bond. Initially acting as an acid, the glycosidic oxygen of the scissile bond is protonated resulting in cleavage of the bond and the formation of an oxocarbenium ion transition state intermediate (199). This is stabilised by the formation of an ozazolinium intermediate using the N-acetyl group. The catalytic residue is then deprotonated using a hydrogen from the C6 hydroxyl group of N-Acetylmuramic acid. This then allows for nucleophilic attack at the C1 group which destabilises the ozazolinium intermediate forming the final 1,6-anhydro reaction product (Figure 5) (155).

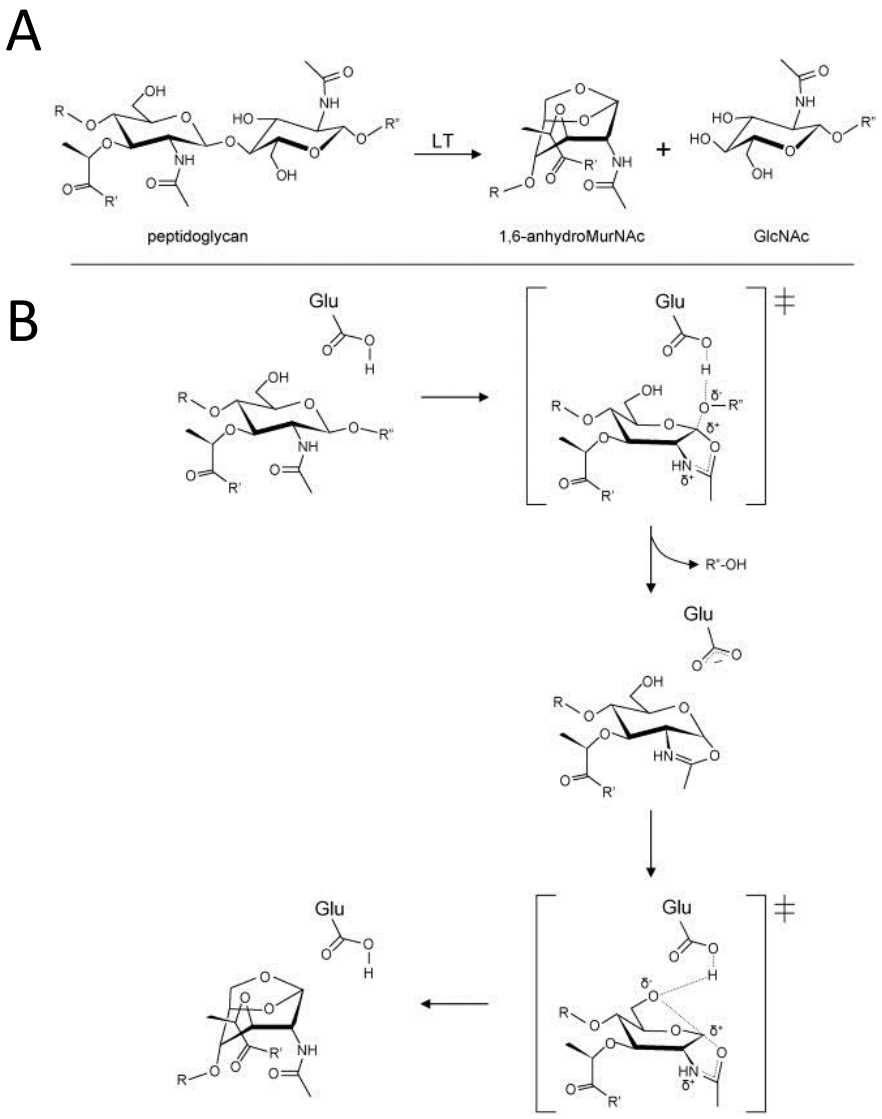

Figure 5 Mechanism of action of lytic transglycosylases

A) Ltgs cleave the β 1,4 glycosidic bond between NAG and NAM residues of peptidoglycan to form 1,6-anhydromuramoyl residues. B) Catalytic glutamate residue protonate the glycosidic bond to form an oxazolinium-ion intermediate. The glutamate can then act as a base to deprotonate the C-6 hydroxyl found on this oxazolinium-ion resulting in its collapse and the formation of 1,6-anhydromuramoyl residues. Figure modified from (155).

1.7.11. Regulation of Ltg activity

Overexpression of muralytic activity can be catastrophic to bacteria, with complete lysis of the peptidoglycan layer and thus cell death. Ltgs have been shown to be autolytic and without regulation will cause the bacterias death (172).

Signal sequences have also been shown to regulate Ltg activity. The signal sequence of MltA of *N. meningitidis* was shown to down regulate expression through post translational modification by the formation of a stem loop structure (200).

Perhaps most likely form of regulation is a physical localisation within the periplasm, as many Ltgs (Mlt class) associate with the inner side of the outer membrane. Furthermore through association with penicillin binding proteins and structural proteins of secretion systems this results in Ltgs being localised within very specific regions of the periplasm (155). Membrane bound Ltgs are secreted into the periplasm and contain a membrane anchor which can further prevent uncontrolled digestion of the sacculus.

Bacteria can also regulate Ltg activity through O-acetylation. O-acetylation occurs in both Gram negative and Gram positive bacteria occurring at the C-6 hydroxyl group *N*-Acetylmuramic acid to prevent degradation from hydrolysing enzymes such as lysozyme. As lysozyme has the same substrate as Ltgs, acetylation can prevent Ltg activity as it is the same hydroxyl group that is targeted by an intermediate of the Ltg mechanism of action (201). Interestingly it has been shown in the Gram positive bacterium *Enterococcus faecalis*, that there was up to a 45% increase in the amount of O-acetylation in viable but non culturable cells (202). Regulation of Ltg activity through O-acetylation could be a factor in the transition from actively growing to non culturable cells.

1.7.12. Inhibitors

Given the escalating problem of antimicrobial resistance it has become imperative for the generation of new antibiotics and an essential part of this process is the identification of new, potential novel, antibiotic targets. Ltgs fit the criteria essential to the success of a new target. Firstly they are unique to bacteria and thus antibiotics will not inadvertently target host cell processes (side effects associated with disruption of commensal bacteria may still occur). Secondly the formation of a unique anhydro-

muramyl reaction product is unique to Ltgs and thus cannot be circumvented by other proteins, a common mechanism in antibiotic resistance. Finally, they have been shown to be important in bacterial processes including growth, division and virulence. There have been recent investigations into developing inhibitors of these proteins. Specific examples include the inhibition of MltB using NAG-thiazoline, a beta-hexosaminidase inhibitor, which was able to reduce Ltg activity (by 61% at 65mM) (203). Perhaps more striking, the addition of Bulgecin A, an O-sulphonated glycopeptide which had previously been shown to inhibit Slt of *E. coli* (204), was able to increase the efficacy of β-lactams in *Neisseria* species (205) . There are also natural inhibitors such as the proteinaceous inhibitor of vertebrate lysozyme, Ivy, which inhibits MltB of *P. aeruginosa* (206). It is hypothesised that these proteins may regulate autolysis in bacteria that are unable to O-acetylate their PG.

1.8. Lytic transglycosylases of *B. pseudomallei* K96243

Using sequence homology to well characterised Ltgs of *E. coli* we have identified 5 putative Ltg-encoding genes on chromosome 1 of *B. pseudomallei* K96243; *bpsl0262 – ltgA*, *bpsl1345 – ltgB*, *bpsl2506 – ltgC*, *bpsl2630 – ltgD*, *bpsl2046 – ltgE*. The proteins are between 35-75kDa and contain features typically associated with cell wall modifying proteins, in particular Ltgs. These include signal sequences, membrane anchors and core Ltg domains sharing features such as goose egg white lysozyme domains and peptidoglycan binding domains such as LysM domains. Potential catalytic sites were also identified. Table 1 outlines the features of each of the identified Ltgs including the potential biological functions each may individually be involved in. Figure 6 provides a schematic of the Ltgs of *B. pseudomallei.*

	Size (bp)	Amino Acids/Mass (Da)	Features	Homology to *E. coli* Ltgs	Potential functions
LtgA (BPSL0262)	1953	651/72,424	29 AA signal sequence, Lysozyme like domain, SLT domain, Ltg superhelical U-shaped and linker domain.	MltE (*E. coli* 42% cover, 32% identity)	T6SS - virulence
LtgB (BPSL1345)	1659	553/60,663	40 AA signal sequence. Secreted or periplasmic protein – no membrane anchor.	MltD (*E. coli* 85% cover, 40% identity) MltE (*E. coli* 41% cover, 34% identity)	Stationary phase survival, virulence, salt tolerance
LtgC (BPSL2506)	1350	450/48,914	53 AA signal sequence. Membrane anchor. Lysozyme like domain.	MltB (*E. coli* 69% cover, 41% identity)	Antibiotic sensitivity
LtgD (BPSL2630)	1056	355/36,677	42 AA signal sequence. Membrane anchor.	Some homology to Slt (*E. coli* 38% cover 33% identity)	
LtgE (BPSL3046)	1116	372/39,978	25 AA signal sequence. Membrane anchor. 3 aspartate (3D) domain containing catalytic site	MltA (*E. coli* 97% cover, 33% identity)	Cell division and septum formation, antibiotic sensitivity, virulence

Table 1 Ltgs of *B. pseudomallei* K96243.

Using sequence homology to well characterised *E. coli* Ltgs, 5 Ltgs were identified on chromosome 1 of *B. pseudomallei* K96243. Protein sequence analysis (BLASTp, InterPro, SignalP) shows domains typical of Ltgs including predicted signal sequences, catalytic sites and membrane anchors. Gene sizes, protein mass and potential contributing functions are shown.

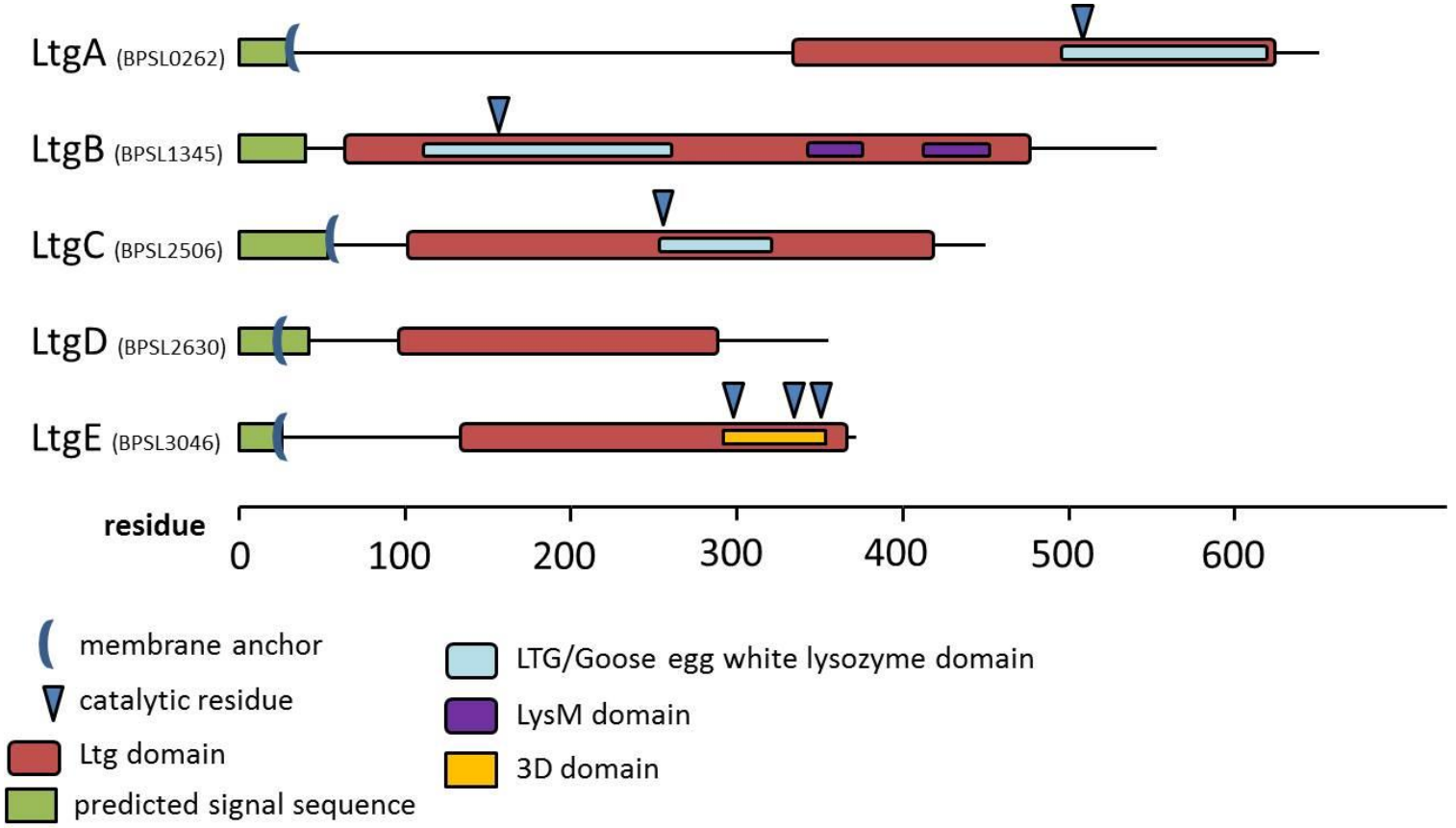

Figure 6 Schematic of *B. pseudomallei* Ltgs

Using sequence homology to well characterised *E. coli* Ltg, 5 Ltgs were identified on chromosome 1 of *B. pseudomallei* K96243. Protein sequence analysis (BLASTp, InterPro, SignalP) shows domains typical of Ltgs including predicted signal sequences, catalytic sites and membrane anchors.

1.9. Project Aims

This project aimed to characterise the Ltgs of *B. pseudomallei* K96243. There were three main aims to this project.

- Clone and express recombinant *B. pseudomallei* Ltgs in *E. coli* and use a range of assays to assess muralytic activity.
- Generate single and multiple *Ltg* unmarked deletion mutants in *B. pseudomallei* K96243 and characterise using phenotypic studies including growth curves, motility, biofilm assays. Virulence will also be assessed *in vivo* using the BALB/c mouse model.
- Develop a method for the generation of non-culturable forms of *Burkholderia* and assess resuscitative capabilities of Ltgs.

Chapter 2

Materials and Methods

2.1. Media

2.1.1. Luria Broth/Agar (LB/LA)

10g tryptone (Difco), 5g yeast extract (Difco) and 10g NaCl were dissolved in 1 litre of distilled water and autoclaved at 121°C for 20 minutes. LA was prepared by the addition of 15g/l of agar.

2.1.2. M9 minimal

5x M9 Minimal Salts; 56.4g 5x M9 Minimal Salts (Difco) was dissolved in 1 litre of distilled water and autoclaved at 121°C for 20 minutes.

M9 minimal media; 200ml 5x M9 minimal salts was added to 800ml sterile distilled water. 2ml sterile 1.0M $MgSO_4$, 0.1ml sterile $CaCl_2$, 20ml of 20% w/v glucose and 0.2% w/v casamino acids (Fisher) was also added.

2.1.3. Yeast Tryptone (YT) broth

10g tryptone and 5g yeast extract were dissolved in 1 litre of distilled water and autoclaved at 121°C for 20 minutes.

2.1.4. Motility plates

Swimming motility plates; 1% w/v Tryptone, 0.5% w/v NaCl, 0.3% w/v Agar.

Swarming motility plates; 1% w/v Tryptone, 0.5% w/v Glucose, 0.5% w/v Agar.

Twitching motility plates; 1% w/v Tryptone, 1% w/v NaCl, 0.5% w/v yeast extract, 1% w/v Agar.

2.1.5. Antibiotics

Unless otherwise stated antibiotics were used at the following concentration;

Antibiotic	**Concentration (µg/ml)**	
Kanamycin	*E. coli* 50	*Burkholderia* 800
Ampicillin		100
Polymyxin B		15

2.2. Bacterial stocks

-80°C stocks were prepared by mixing 800µl of overnight bacterial culture with 400µl of sterile 75% v/w glycerol in 1.5ml cryogenic tubes.

2.3. Culturing of bacteria

Overnight cultures of *E. coli* and *Burkholderia* were prepared by inoculating 5ml of LB (containing appropriate antibiotic) with bacterial cells scraped from -80°C frozen stocks or from a single colony growing on an agar plate. Tubes were incubated at 37°C, with shaking (200rpm), overnight. All work with *B. pseudomallei* was performed in Containment Level 3 laboratories at the University of Leicester or at the Defence Science and Technology Laboratory, Porton Down.

2.4. Cloning

2.4.1. Primers

Custom primers were purchased through Sigma-Aldrich (stock 100µM, working stock 10µM). All primers used in this study can be seen in Appendix 8.5.

2.4.2. Colony Polymerase chain reaction (PCR)

A typical reaction is detailed below;

GoTaq polymerase (Promega)

2µl	5x GoTaq reaction buffer
0.5µl	2mM dNTPs
0.5µl	10µM forward primer
0.5µl	10µM reverse primer
1µl	DMSO
1µl	colony preparation
0.2µl	GoTaq polymerase (5U/µl)
4.3µl	DNase/RNase free water

E. coli colony preparation was prepared by scraping a small amount of a colony from an agar plate and re-suspending in 50µl PBS. The sample was heated at 95°C for 10 minutes to release DNA before centrifugation at 13200rpm for 2 minutes to pellet cellular debris. *B. pseudomallei* colony preparation was prepared in a similar manner

but the conditions increased to 100°C for 30 minutes (validated for removal from the containment level 3 laboratory).

A typical protocol PCR is outlined below;

(30 cycles of steps 2-4)

1)	Initial denaturation	95°C	2 min
2)	Denaturation	95°C	30 sec
3)	Annealing	50-60°C	30 sec
4)	Extension	72°C	1 min/kb
5)	Final extension	72°C	5 min
6)	Incubation	4°C	indefinitely

2.4.3. High fidelity polymerase chain reaction

Q5 High fidelity DNA polymerase (New England Biolabs, NEB)

A typical reaction is detailed below;

10µl	5X Q5 Reaction Buffer
5µl	2mM dNTPs
2.5µl	10µM reverse primer
2.5µl	10µM forward primer
10µl	5X Q5 High GC Enhancer
<1000ng	DNA template
0.5µl	Q5 High-Fidelity DNA Polymerase (0.02U/µl)
Up to 50µl	DNase/RNase free water

PCR protocol (30 cycles of steps 2-4)

A typical reaction is detailed below;

1)	Initial denaturation	98°C	30 sec
2)	Denaturation	98°C	10 sec
3)	Annealing	50-60°C	20 sec
4)	Extension	72°C	20 sec/kb

5)	Final extension	72°C	2 min
6)	Incubation	4°C	indefinitely

2.4.4. DNA gel electrophoresis

A 1% w/v agarose gel was made by adding 1g of agarose in 100ml of Tris-acetate-EDTA buffer and microwaved until completely dissolved. 0.5 µg/ml ethidium bromide solution (Fisher) was added and the gel cast. DNA samples were combined with 6x loading dye (Thermo Fisher Scientific) and loaded onto the gel (5µl DNA:1µl loading dye). Electrophoresis was performed at 100V for one hour. DNA bands were visualised by exposure to UV light.

2.4.5. Restriction Digests

DNA digests were performed using restriction enzymes and buffers supplied by NEB according to their protocols. A typical diagnostic digest contained; 300ng of DNA, 1µl of 10x NEB restriction enzyme buffer, 10 units of restriction enzyme(s). The final volume was adjusted to 10µl with DNA/RNAase free water. A typical cloning digest contained; 1-2µg of DNA, 5µl of 10x NEB restriction enzyme buffer, 25 units of restriction enzyme(s). The final volume was adjusted to 50µl with DNase/RNase free water. Samples were incubated at 37°C for 2 hours.

2.4.6. DNA isolation

2.4.6.1. Plasmid purification

Plasmid DNA was purified from 5ml of an *E. coli* overnight culture using the GenElute Plasmid Miniprep Kit (Sigma-Aldrich) according to the manufacturer's protocol. Plasmid was eluted in 30-100µl DNase/RNase free water. Midipreps for large scale purification were performed using CompactPrep Plasmid Midi Kit (Qiagen) from a 50ml *E. coli* overnight culture. Plasmid was eluted in 200µl of DNase/RNase free water. Plasmid purity was assessed using DNA gel electrophoresis (presence of clear bands) and Nanodrop (ThermoFisher Scientific). A nanodrop 260/280nm absorbance ratio of between 1.8-2.2 was classed as pure DNA.

2.4.6.2. gDNA extraction

1ml of an overnight culture was pelleted and the bacteria resuspended in 750µl of lysis buffer (10mM NaCl, 20mM Tris-HCl, 1mM EDTA, 0.5% (w/v) SDS, 100 µg/ml Proteinase

K and RNase A). Tubes were incubated at 55°C overnight to lyse cells before decontamination and removal from the containment level 3 facility. An equal volume of phenol: chloroform: isoamyl alcohol 25:24:1 was added and inverted ~500 times before centrifugation at 12000xg for 20mins. The aqueous layer was removed and the phenol/chloroform treatment repeated a further two times. The resulting aqueous layer was mixed with an equal volume of chloroform: isoamyl alcohol 24:1 and inverted ~200 times before centrifugation. This was repeated. 0.1 volume of 3M sodium acetate (70µl) and 1 volume of isopropanol (700µl) were added and the mixture incubated at 4°C for 1 hour before pelleting of DNA by centrifugation at 12 000xg for 30 minutes. The supernatant was removed and the DNA pellets washed with ice-cold 70% (v/v) ethanol. The DNA was further washed with 96-100% ethanol before allowing the pellet to air-dry. The gDNA was resuspended in 200µl of TE buffer. A 0.8% (w/v) agarose gel was used to assess quality and a nanodrop was used to determine the concentration of purified gDNA.

2.4.7. Sequencing

Sequencing was performed using the Sanger sequencing SUPREMERUN service at GATC biotech. Purified plasmid DNA was provided at 50ng/µl. PCR products were provided at 5-10ng/µl. Sequencing data was analysed using FinchTV (Geospiza) and Nucleotide BLAST (https://blast.ncbi.nlm.nih.gov/Blast.cgi).

2.4.8. Ligation reactions

Ligation reactions were performed using T4 DNA ligase (Promega) with the following composition.

Ligase Buffer (10X)	10 µl
Vector DNA	~100 ng
Insert DNA	~20 ng
Nuclease-free Water	to 10 µl
T4 DNA Ligase	1 µl

Reactions were incubated at room temperature for 2 hours (room temperature) or 16 hours (16°C).

2.4.9. Transformation by heat shock

50µl Alpha-Select competent *E. coli* Cells (Bioline) were defrosted on ice from -80°C stocks. Approximately 50ng of purified plasmid DNA or 5µl of ligation reaction was added to the cells and left to incubate, on ice, for 15 minutes. The tubes were transferred to a water bath set to 42°C for precisely 40 seconds before being placed back on ice for a further 3 minutes. 1ml of SOC media (Sigma-Aldrich) was added to the bacteria and tubes were incubated at 37°C with shaking for one hour. Following incubation 100µl of neat and 10^{-1} diluted transformation mixture was plated onto selective agar plates. The antibiotic used was dependent on the antibiotic resistance cassette on the plasmid being selected for. Plates were incubated at 37°C for 24-48 hours. Competent *E. coli* BL21(DE3) (Bioline) or *E. coli* C41(DE3) (Lucigen) were used in transformations generating strains for protein expression.

2.4.10. Site directed mutagenesis

Site directed mutants were generated as per the manufactures protocol (GeneArt® Site-Directed Mutagenesis System, ThermoFisher Scientific). Briefly, plasmid DNA containing the Ltg gene of interest was methylated at 37°C for 20 minutes before PCR amplification using primers containing the target mutation. The linearised, amplified plasmid containing the mutation was recombined before transformation into *E. coli* DH5α. Plasmid DNA was purified and sequenced before a protein overexpression *E. coli* strain (BL21(DE3) or C41(DE3)) was transformed.

2.5. SDS-PAGE

A 12% v/v SDS-PAGE gel comprised of the following;

Resolving gel; 3.6ml Acrylamide/Bis 19:1, 40% (w/v) solution (Fisher), 5.4 ml water, 3ml (1.5M Tris HCl pH8.8, 0.4% SDS), 60µl 10% (w/v) ammonium persulphate, 60µl Tetramethylethylenediamine

Stacking gel; 0.75ml Acrylamide/Bis 19:1, 40% (w/v) solution (Fisher), 3.66 ml water, 0.5ml (0.5M Tris HCl pH6.8, 0.4% SDS), 20µl 10% w/v ammonium persulphate, 20µl Tetramethylethylenediamine

Gels were assembled into SDS-PAGE tanks (Geneflow) and filled with SDS PAGE buffer (14.4 g glycine, 15g Tris base, 1g SDS - dissolved in 1 litre of water).

Protein samples were combined with 4x sample buffer (8ml glycerol, 4.8ml 1M Tris HCl pH6.8, 1.6g SDS, 8mg Bromophenol blue, 6.2ml water, 10mM Dithiothreitol).
Samples were loaded alongside 5µl BLUeye Prestained Protein Ladder (Geneflow) and gels run at 200V for approximately 60 minutes.
Proteins were visualised by Coomassie staining (2.5 g/L Coomassie Brilliant Blue was dissolved in 40% v/v methanol and 10% v/v acetic acid) overnight followed by destaining in water.

2.6. Western blot

Following separation of proteins by SDS-PAGE the gel was placed on a nitrocellulose membrane between two Whatman filter papers. The membrane and filter papers were soaked briefly in Western transfer buffer (25 mM Tris base pH8.3, 192mM glycine and 20% v/v methanol). Gel, membrane and papers were assembled into a blotting system (Geneflow). Proteins were transferred for 2 hours at 150mA. The membrane was blocked by soaking in 2% w/v skimmed milk powder in PBS for 30 minutes. All incubations were carried out on a roller to ensure constant agitation. The membrane was rinsed in PBS and incubated in primary antibody (mouse anti-poly histidine, Sigma Aldrich) in 1% PBS at 4°C overnight (1:2000). The membrane was washed three times in PBS with 0.1% Tween 20 before incubation in secondary antibody (anti-mouse IgG-AP, Sigma Aldrich) in 1% w/v skimmed milk powder in PBS (1:10000) for 1 hour. The membrane was washed in PBS with Tween 20 as above. Approximately 5ml of BCIP/NPT liquid substrate system (Sigma) was added to the membrane and incubated in the dark until bands became visible. To stop the reaction the membrane was rinsed thoroughly in water.

Chapter 3

Expression of recombinant Ltgs and assessment of muralytic activity

3.1. General Introduction

The production of recombinant proteins has become an essential part in biochemical studies into their physiological roles. Overexpression in *E.coli* can produce large amounts of protein, relatively inexpensively and often with little optimisation. Ideally used in combination with mutant phenotype studies, recombinant protein assays can help to uncover the function, understand regulation and modification, interacting partners as well as the factors influencing stability of the protein.

Recombinant protein production is relatively straight-forward. Briefly, a gene of interest is cloned into an expression vector, of which there is vast choice that vary in promoter, copy number, tags and fusion proteins, cloning sites, antibiotic markers, protease cleavage sites e.g. for tag removal. The vector is then used to transform an *E. coli* strain; again there is a wide range, the strain used may depend on factors such as the proteins stability or its solubility. *E. coli* has a fast growth rate, can be easily transformed with foreign genetic material and requires inexpensive media and growth conditions and a high culture density can be achieved. Transformants can then be cultured in large quantities, protein production induced and the cells harvested for purification. Once lysed the protein is purified on a columns dependant on the properties of the protein such as terminal tags, hydrophobicity or charge and affinity to ligands or antibodies for example. In an ideal situation it is possible to have recombinant protein in as little as one to two weeks.

The process outlined above however, is idealistic and often there is much optimisation needed to achieve satisfactory yields. There are problems that need to be overcome including the metabolic burden of production of recombinant protein (207) and potential toxicity of the proteins – although this can occasionally be overcome using alternative expression strains (208). Rapid production of protein can lead to inclusion bodies as protein aggregates due to high concentration and uneven distribution within the cell. Inclusion bodies are often prevented by decreasing temperature or inducer concentration, changing media or co-expression with chaperon proteins or solubility enhancing tags.

3.1.1. Methods to assess muralytic activity

Recombinant protein assays in this study were aimed to investigate the muralytic activity of lytic transglycoylases of *B. pseudomallei*. One such example is zymography. This consists of an SDS-PAGE gel impregnated with lyophilised *Micrococcus luteus*. *M. luteus* has a thick cell wall and is particularly susceptible to cell wall hydrolases. Lyophilised *M. luteus* produces an opaque background when added to an SDS-PAGE gel whereas other bacteria, particularly Gram-negative bacteria produce a more translucent or even transparent gel which would require much more intensive downstream processing and staining. The protein is separated on this specialised SDS-PAGE gel in its denatured form. The SDS is removed through multiple washes in distilled water and replaced by a non-denaturing detergent such as Triton-X100. The gel is placed into various refolding buffers of differing composition and pH. If the protein is refolded and is muralytic it can digest the cell wall present in the gel forming a clearance band. The band can be further enhanced by staining and alkaline treatment.

While this assay is a good indicator of muralytic activity it is not completely definitive. It has been noted that a clearance band may be possible if the protein simply binds to the peptidoglycan, not necessarily hydrolysing it (191). It can also be quite subjective with only highly active enzymes producing a very definitive clearance band. Given this, an additional method is often required which does not rely on interpretation of a qualitative result but rather produces quantitative data.

Artificial lysozyme substrates are available such as 4-Methylumbelliferyl β-D-N,N',N''-triacetylchitotrioside (MUF Tri-NAG), or alternatively, fluorescently labelled peptidoglycan can be used in assays that release a fluorophore when digested by muralytic enzymes. This would require the protein to be in active in solution using conditions that may be different to that used in zymography. It is also possible to digest purified peptidoglycan and separate the released muropeptides using liquid chromatography. Muropeptide analysis coupled with mass spectrometry can reveal the nature of fragments released, the relative quantity and any modifications present in these fragments. This is a highly sensitive and specialised method but perhaps the most informative (159) . This approach has previously involved a process of

peptidoglycan purification that can take 1-2 weeks but recently this has been achieved in as little as 24 hours (purification, digestion, separation and MS) (209).

There are also indirect methods to test for activity. Included in which is the overexpression of secreted cell wall enzymes in a host bacterium, such as *E. coli*. This method was used when showing muralytic activity of the original Rpf in *M. luteus* (210). The premise is that as bacteria express large amounts of a muralytic enzyme it is translocated to the periplasm and can hydrolyse or otherwise modify the peptidoglycan and thus compromising the cell wall potentially resulting in lysis. This can be measured by a reduction in optical density following induction of the protein. This method has been used to show the activity of Rpf of *M. luteus* and the soluble Ltg, Slt70 of *E. coli* (211, 212).

One aspect to be considered when producing large amounts or recombinant Ltg was the localisation and purification method needed. In particular; the risk of toxicity or cell lysis as a result of over expression of the muralytic enzyme. As such, two versions of each gene were cloned. One encoding the whole protein, along with its native signal sequence; this protein would be exported into the periplasm where it was more likely to be active (due to post translational modifications and folding as it is secreted) but have a higher risk of cell lysis due to its proximity to the peptidoglycan substrate. This version was used predominantly in overexpression growth analysis. The second version was cloned without this signal sequence (predicted using online software, SignalP and ExPASy), allowing recombinant protein to localise in the cytoplasm. This would allow for the production of larger quantities of protein needed for recombinant protein assays and crystallography while also reducing the laborious and technical process of purification of recombinant Ltg from membrane fractions.

3.2. Chapter aims

- Cloning, expression and purification of *B. pseudomallei* K96243 Ltgs.
- Assess the muralytic activity of recombinant *B. pseudomallei* Ltgs using a variety of assays. Investigate important catalytic residues using site directed mutagenesis.

3.3. Materials and Methods

Primers used in the generation of *E. coli* strains overexpressing recombinant Ltg can be found in (Appendix 8.5, Table 8) along with restriction sites and expected PCR product sizes. All strains generated can be found in (Appendix 8.2, Table 5). Ltg protein sequences including predicted signal sequences, membrane anchors and catalytic residues can be found in (Appendix 8.1). All strains containing pET expression vectors were cultured on LA and LB containing ampicillin (100µg/ml).

3.3.1. Generation of expression plasmids

Ltg encoding regions were PCR amplified from *B. pseudomallei* K96243 genomic DNA using Q5 DNA polymerase and corresponding primers Ltg(B/C/D/E)_pET23_For/Rev for amplification of the gene with the native secretion signal sequence, and Ltg(B/C/D/E)_pET15_For/Rev for amplification without the predicted signal sequence. Fragments were ligated into the cloning vector; pGEM-T Easy (Promega). *E. coli* DH5α (Bioline) was transformed with each of the pGEM- constructs. Blue/white phenotype screening allowed for the selection of positive clones and diagnostic digests were performed for further confirmation using appropriate restriction enzymes. Plasmids were sequenced using M13_For/Rev primers (GATC-biotech). The gene products were digested from pGEM using the appropriate restriction enzymes (Appendix 8.5) before ligation into the expression vectors pET23a and pET15bTEV. pET15bTEV contains a Tobacco Etch Virus (TEV) protease cleavage site for removal of the N-terminal polyhistidine tag. pET23a encodes a C-terminal polyhistidine tag suitable for genes encoding an N-terminal signal sequence. *E.coli* DH5α (Bioline) was transformed with each of the constructs and positive clones were identified using diagnostic digests. *E. coli* BL21(DE3) or C41(DE3) strains were transformed with purified plasmid DNA.

3.3.2. Expression and purification of non-secreted LtgE, LtgB and LtgC

E. coli C41(DE3) was transformed with pET15bTEV-*ltgE* or pET15bTEV-*ltgB*. Strains were grown in LB-Amp (100µg/ml) at 37°C, 200rpm, until an OD_{600} of 0.6. The bacterial

cultures were chilled on ice for 1-2 hours before induction with Isopropyl β-D-1-thiogalactopyranoside (IPTG) at a final concentration of 0.05mM (LtgE) and 0.5mM (LtgB). Cultures were incubated at 18°C overnight, with shaking, then harvested by centrifugation at 6000xg for 20 minutes. The pellet was washed in buffer containing 25mM Tris pH8.5, 150mM NaCl before final resuspension in 40ml of binding wash buffer. Bacteria were lysed by sonication (4x40 second bursts). The soluble fraction was separated by centrifugation at 25000xg for 30 minutes, before loading onto a gravity flow Ni^{2+}chelating column (Ni Sepharose 6 Fast Flow, GE Healthcare Life Sciences) (GE Healthcare). The column was washed with 30 column volumes of binding buffer (25mM Tris pH8.5, 500mM NaCl) followed by 10 column volumes of wash buffer (binding buffer containing 60mM imidazole). Recombinant protein was eluted in 7x1ml of 250mM imidazole in binding buffer. The first and last fractions were discarded and the remaining 5ml were pooled for gel filtration. Gel filtration was used to remove imidazole and low molecular weight impurities using a GE Healthcare Superdex column on an AKTA FPLC system. A constant flow of buffer (20mM Tris pH8.5, 150mM NaCl, 20mM KCl) was maintained at 1ml/min. Fractions of 1ml were collected. SDS-PAGE and Western blots using anti-polyhistidine IgG antibodies (Sigma) were used to test the purity of the protein.

E. coli BL21(DE3) was transformed with pET15bTEV::*ltgC*. Cultures were grown at 37°C to an OD_{600} of 1.0 (without induction). The culture was harvested, lysed and the recombinant protein purified as for LtgB and LtgE above.

3.3.3. Expression and purification of secreted LtgE

E. coli BL21(DE3) pET23-*ltgE* was grown to an OD_{600} 0.6 at 37°C, with shaking at 200rpm. Cultures were induced with IPTG at a final concentration of 0.5mM for 4 hours. Culture was harvested by centrifugation at 6000xg for 20 minutes, French pressure cell pressed (20,000 psi) and soluble protein isolated from the membrane using one of two methods. The first used ultracentrifugation and dissolving in buffer containing Triton X-100 as outlined previously (213). The second, a simplified version, involved centrifugation at 30,000xg for 30 minutes. The supernatant was harvested and dialysed against buffer containing 50mM Tris HCl, 150mM NaCl, 20mM MgCl2, 2% (v/v) Triton X-100. Recombinant protein was then purified on a gravity flow

Ni^{2+}chelating column (Ni Sepharose 6 Fast Flow, GE Healthcare Life Sciences). The pelleted fraction was resuspended in the above buffer and stirred on ice for 15 minutes to disrupt the cell membrane to release membrane bound proteins. The larger, insoluble fraction was separated by centrifugation at 30,000xg and LtgE purified using the protocol described above for purification of non-secreted LtgE. The presence of soluble protein was confirmed using Western blots as outlined in Chapter 2.2.6.

3.3.4. Growth of *E. coli* strains overexpressing secreted Ltgs

Overnight cultures of BL21 (DE3) or C41(DE3) pET23-*ltg* strains were used to inoculate 20ml of LB-Amp (100µg/ml). Cultures were grown at 37°C, with shaking at 200rpm. Every hour 1ml of culture was removed and the OD_{600} measured. At an OD_{600} of 0.6 cultures were induced with IPTG 0.5mM (final concentration). OD_{600} were measured hourly for 9 hours.

3.3.5. Zymography

A single colony of *M. luteus* was inoculated into 10ml of LB and incubated overnight at 37°C, shaking at 200rpm. This was used to inoculate 2 litres of LB before incubation at 37°C for 48 hours, to exponential growth phase. The bacteria were harvested by centrifugation at 6000xg for 20 minutes. The pellet was washed with PBS and frozen at -20°C overnight before being lyophilised for 48-72 hours. The lyophilised *M. luteus* was ground into a fine powder and stored at room temperature before use in zymograms.

An SDS-PAGE gel containing 1.5% (w/v) lyophilised *M. luteus* was prepared. Protein samples were run an SDS-PAGE gel (Chapter 2.2.5). Gels were washed twice in distilled water (10 minutes per wash), cut into strips and soaked in refolding buffers of differing pH and composition. The conditions investigated included 25mM citric acid, 25mM phosphate and 25mM Tris buffer and with and without manganese (1mM) or magnesium (5mM). Gels were incubated overnight at 37°C. When required the clearance bands were enhanced by staining in 0.1% (w/v) methylene blue containing 0.01% (w/v) potassium hydroxide.

3.3.6. Hydrolysis of MUF Tri-NAG using LtgB

For storage and activity assays recombinant LtgB was filter sterilised using 0.22µm filter units (Merck Millipore). 180µl of 25mM sodium phosphate buffer at pH6 and

1.8µl of 600nM MUF Tri-NAG substrate was added to a black 96 well plate. 10µl of either recombinant LtgB, 10µl of denatured recombinant LtgB, 10µl of 1mg/ml lysozyme (positive control) or 10µl of denatured 1mg/ml lysozyme was added to the wells. Denaturation was achieved by heating samples in a thermocycler at 95°C for 20 minutes. The plate was incubated in the dark at 37°C overnight. 10µl of NaOH was added to each of the wells to stop the reaction followed by incubation for 5 minutes at room temperature. The amount of umbelliferon released was measured using 364nm excitation and 448nm emission filters in a Varioskan plate reader (ThermoFisher Scientific). Mean and standard deviation were determined for replicates and subtracted from background buffer control.

3.3.7. Solving the crystal structure of LtgE

Preparation of protein for crystallisation

Non-secreted recombinant LtgE was purified as above, fractions corresponding to the molecular weight of LtgE (38kDa) were collected and analysed by SDS-PAGE. Fractions with the highest LtgE concentration and minimal degradation were pooled and further concentrated to ~5mg/ml by centrifugation at 4000xg in a 10,000Da cut off filter (Merck Millipore) Following concentration of recombinant LtgE to 5mg/ml crystallisation conditions were screened 0.1µl drops (protein:buffer) using PACT *premier*™ HT-96 (Molecular Dimensions) screening buffers.

Solving the crystal structure of LtgE

LtgE crystals were grown in 0.1M Bis-tris propane (pH7.5), 0.2M potassium sodium tartrate, 14% 8K Polyethylene glycol (PEG) using 1.5µl drops. Drops were incubated for two weeks at 4°C. The crystal was preserved in cryo-preservative consisting of the crystallisation buffer with the addition of 30% v/v glycerol and stored in liquid nitrogen. Following X-ray diffraction, molecular replacement and refinement using the structure of LtgE homologues (*E. coli* and *N. gonorrhoea*) was performed. Analysis of X-ray diffraction pattern and solving of the crystal structure was performed by Professor Russell Wallis (University of Leicester).

3.3.8. Generation and purification of anti-LtgE polyclonal antibody

3.5mg of recombinant LtgE in PBS was sent to Gemini biosciences for the production of polyclonal Anti-LtgE antibodies in rabbits. Two rabbits were injected with 4 inoculums of LtgE (0.5mg per inoculum). Serum was purified from the final bleeds of both rabbits. In the interest of time only IgG antibodies from 'rabbit 4' was purified. 50ml of serum was mixed 50:50 with PBS before loading in four aliquots onto a Protein A column on an AKTA FPLC system. IgG antibodies were eluted in 100mM glycine pH2.4 (1ml fractions) into 100µl of 1M Tris pH 8.5. Eluted antibodies were concentrated using a 100,000kDa cut off filter. A working stock was made by mixing in equal parts with 100% glycerol and stored at -20°C. Remaining antibodies were stored at -80°C. The validity of the antibody was assessed using Western blots using recombinant protein. Anti-LtgE antibodies were diluted 1:10000, 1:20000, 1:40000, 1:80000 and 1:100000. Secondary monoclonal anti-rabbit antibody was used as a secondary antibody at a dilution of 1:10000.

3.3.9. Digestion of peptidoglycan with LtgE, separation and visualisation of muropeptides profile.

E. coli peptidoglycan was isolated and analysed as described previously (158, 214). Peptidoglycan was digested for with 5µl LtgE (100µg/ml) in 25mM Tris at pH 8. The addition of protein was repeated daily for 3 days. Muropeptides were reduced sodium borohydride.

3.4. Results and discussion

3.4.1. Cloning of plasmids for expression of recombinant Ltg

3.4.1.1. Secreted Ltg

Three constructs were generated containing coding regions for the full length LtgB, LtgD and LtgE, including secretion signals. This would allow for expression of secreted versions of the Ltgs to observe the effect of overexpression on the growth of *E. coli*.

ltgB, ltgD and *ltgE* coding regions (including the N-terminal signal sequence) were amplified by PCR. Following purification and digestion the fragments were cloned into the expression vector pET23a (containing a C-terminal polyhistidine-tag) to generate pET23a-*ltgB,* pET23a-*ltgD* and pET23a-*ltgE* (Figure 7). pET23a-*ltgB* was transformed into *E. coli* C41(DE3) and pET23a-*ltgD* was transformed into *E. coli* BL21(DE3). Due to time constraints pET23a-*ltgE* was not used for protein expression trials but could be used in future experiments. The constructs for the expression of SDM LtgB (E154A and E154K) and LtgD (E182A and E182K) were also generated.

Purification of recombinant LtgE from membrane fractions was possible but proved laborious with minimal yields (see section 3.4.3.1). As a result constructs for the expression of non-secreted Ltgs were also generated.

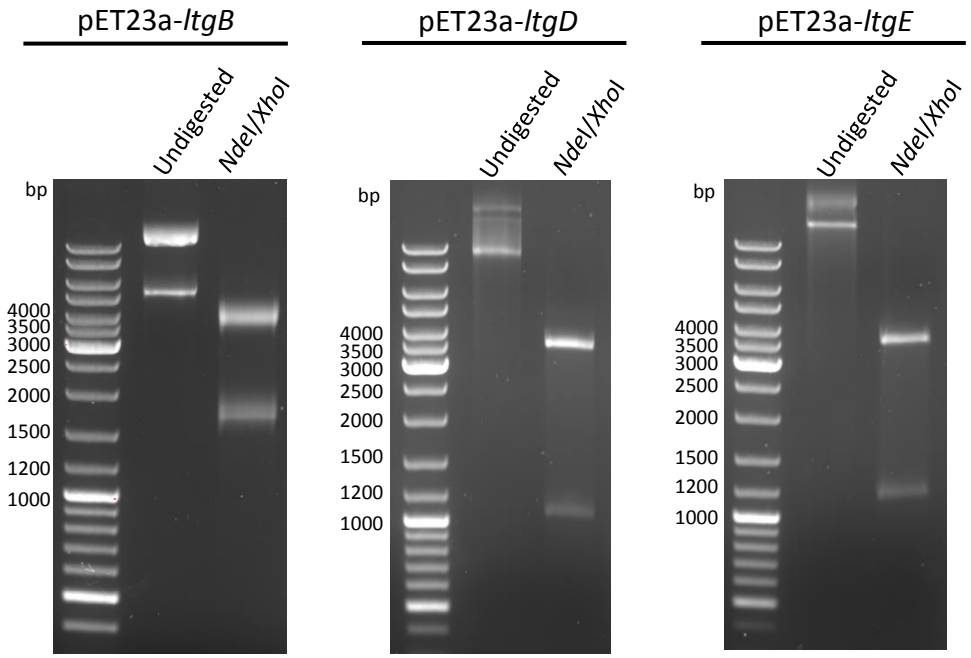

Figure 7: Diagnostic digests of pET23a-ltg constructs for overexpression of secreted Ltgs in *E. coli*.

ltg genes cloned in between *Nde*I and *Xho*I sites of pET23a. Diagnostic digests were performed on purified plasmid DNA to show the presence of the insert. Undigested plasmids were run as control in the lane immediately next to the ladder. Expected sizes – pET23a vector; 3660bp plus either - *ltgB*; 1671bp *ltgD*; 1076bp *ltgE*; 1132bp

3.4.1.2. Non-secreted Ltg

Three constructs were generated for the overexpression of non-secreted LtgB, LtgC and LtgE. PCRs of *ltgB, ltgC*, and *ltgE* were performed for the amplification of the *ltg* encoding region minus the N-terminal signal sequence. Following purification and digestion the fragments were cloned into the expression vector pET15b-TEV (containing an N-terminal polyhistidine-tag) to generate the following constructs; pET15bTev-*ltgB*, pET15bTEV-*ltgC* and pET15bTev-*ltgE* (Figure 8). pET15bTEV-*ltgB* and pET15bTev-*ltgE* constructs were successfully transformed into *E. coli* C41(DE3), pET15bTEV-*ltgC* was transformed into *E. coli* BL21(DE3). A construct for the expression of SDM LtgE containing a D343A point mutation was also generated and transformed into C41(DE3).

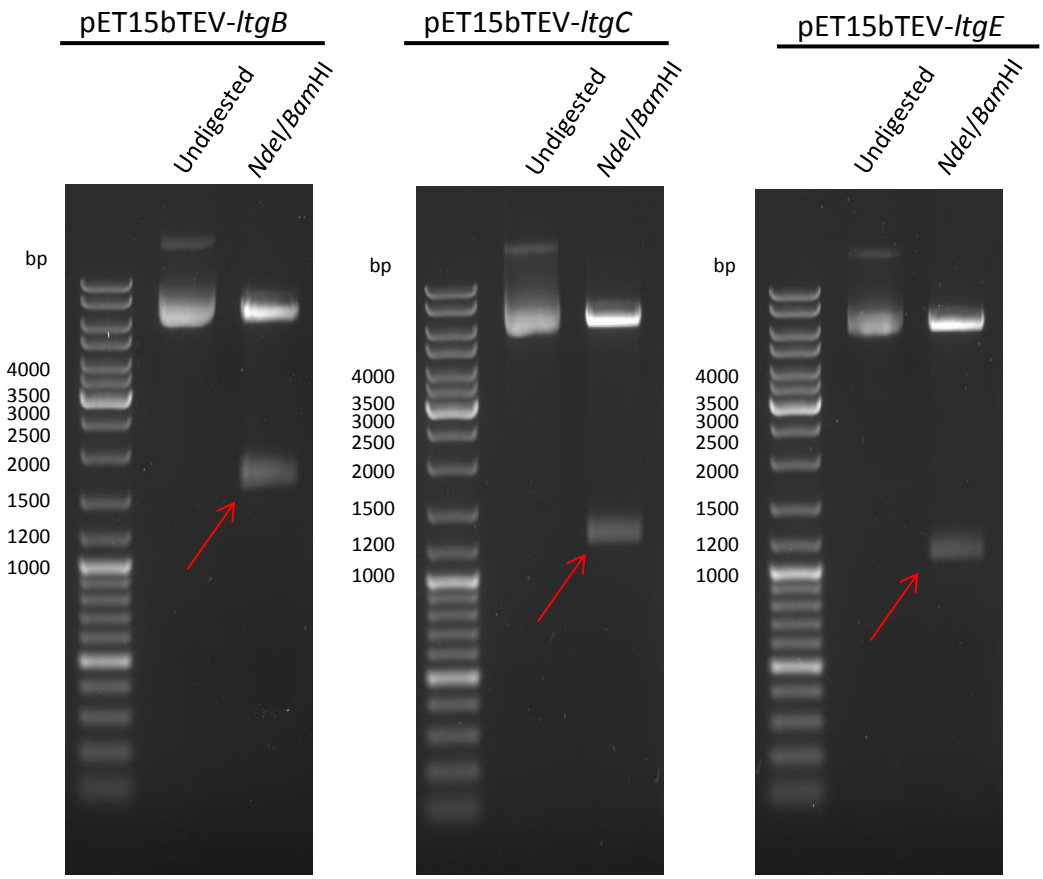

Figure 8: Diagnostic digests of pET15bTEV-ltg constructs for overexpression of non-secreted Ltgs in *E. coli*.

ltg genes were cloned between the *Nde*I and *Bam*HI sites of pET23a. Diagnostic digests were performed on purified plasmid DNA to show the presence of the insert. Undigested plasmids were run as controls in the lane immediately next to the ladder. Expected sizes – pET15bTEV vector; 5800bp plus - *ltgB*; 1554bp *ltgC*; 1221bp *ltgE*; 1071bp

3.4.2. LtgA

Multiple attempts were made to clone *ltgA* as a secreted and non-secreted form into an expression vector. Unfortunately, all were unsuccessful. pET vectors have leaky promotors (215) and therefore if this protein is expressed even at basal levels it may be at a level too toxic *E. coli*. This was seen with LtgB in which the secreted form could only be cloned into an *E. coli* strain more suitable for toxic protein expression (C41(DE3)) (Chapter 3.3.3.2).

LtgA shares the greatest homology with MltE of *E. coli*. However, given that there were issues in regards to cloning of LtgB which also shares homology with MltE; it would seem unlikely that the class of protein would be the cause of the problem in regards to this cloning. This explanation however, does not account for why the non-secreted version was also unable to be cloned. LtgA is the largest of the 5 Ltgs and contains a goose egg white lysozyme domain and shares homology with Slt domain. Other possibilities including a protein sequence not optimised for *E. coli* expression or alternatively, though less likely, the DNA sequence could be toxic. At the time of cloning focus was heavily placed on other parts of the project and maybe given more time and an increased trouble shooting process then this problem would be resolved.

3.4.3. LtgE

3.4.3.1. Expression of recombinant LtgE

Preliminary experiments showed that secreted and non-secreted LtgE could be expressed and purified. As the protein could be purified from the membrane fraction this confirms the *in silico* analysis and is coherent with the literature on MltA (162, 216), that suggests that this protein contains a membrane anchor, is secreted into the periplasmic space and bound to the membrane. However, the signal sequence and membrane anchor made purification problematic and laborious yielding a maximum of 200µg of protein from 3 litres of bacterial culture. Conversely, a similar volume of culture expressing non secreted LtgE yielded approximately 3mg of recombinant protein (approx. 60pg/ml of culture). Given this and the volume of recombinant LtgE needed for assays and crystallisation, it was necessary to optimise purification of the non-secreted version of LtgE. Optimal conditions for expression of LtgE were found induction with 0.05mM IPTG, at 18°C overnight, using *E. coli* C41(DE3). Soluble

recombinant LtgE was expressed and purified by affinity chromatography using a nickel chelating column followed by size using gel filtration. LtgE was purified as a single peak by gel filtration indicating little aggregation or degradation (Figure 9A) with a molecular weight of approximately 40kDa (compared against purification of known standards), which corresponds to the predicated molecular weight of LtgE which is 38.8kDa. Fractions from this peak were concentrated and visualised using SDS-PAGE and Western blot using anti-poly histidine IgG antibodies (Figure 9B).

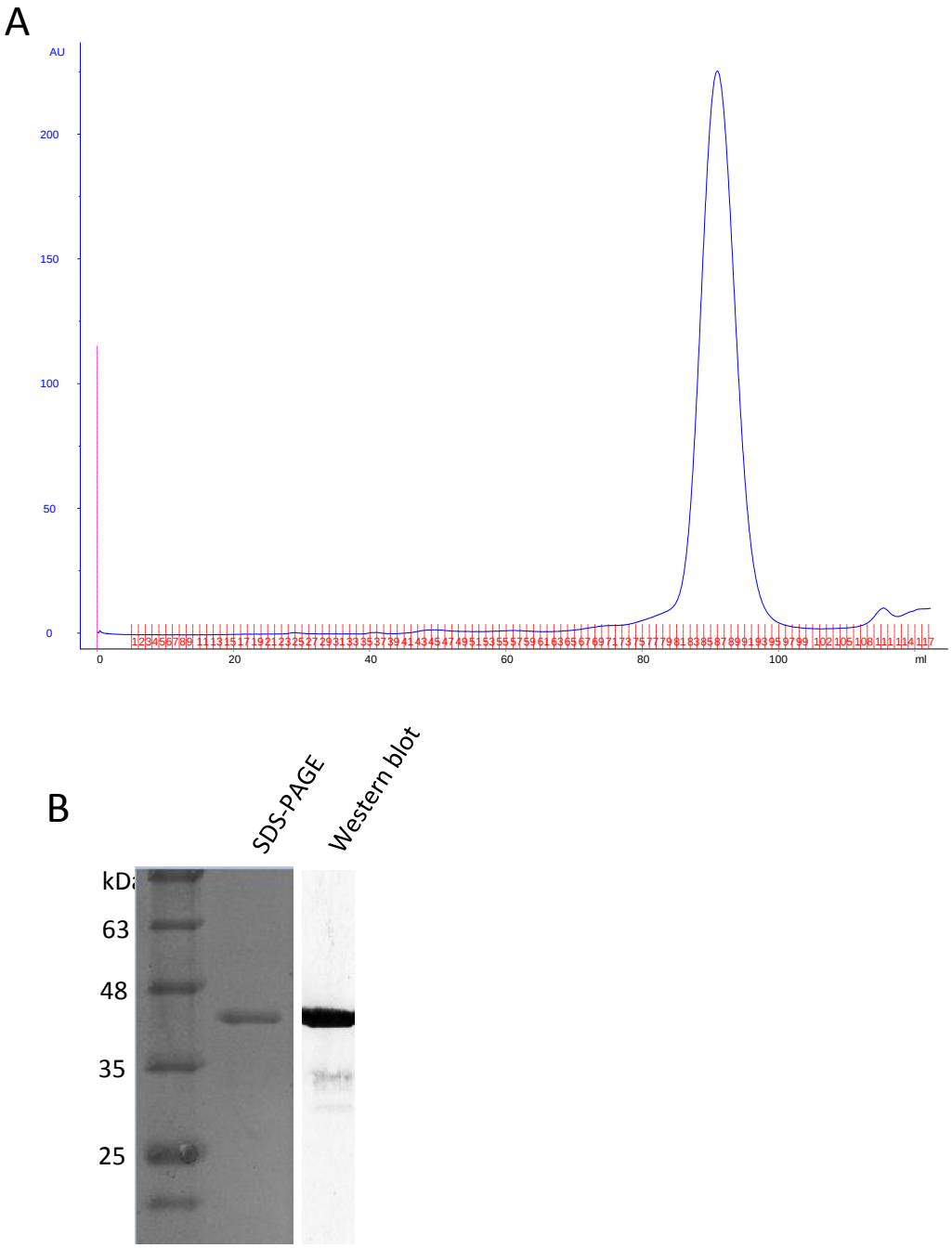

Figure 9: Gel filtration, SDS-PAGE and Western blot of recombinant LtgE.

E. coli C41(DE3) pET15bTEV-ltgE$_{NS}$ produced soluble protein that was extracted and purified on a nickel chelating column. (A) Gel filtration resulted in a single peak indicating a stable protein with little degradation or aggregation. (B) This was confirmed by SDS-PAGE and Western blot using anti-poly histidine antibodies (LtgE encodes an N' terminal poly-His tag). LtgE has a predicted molecular mass of 38.6 kDa.

3.4.3.2. Solving of LtgE X-ray crystal structure

A HT-96 screen revealed two sphere like crystals with 0.1M Bis-Tris propane, 0.2M potassium sodium tartrate, 20% v/v polyethylene glycol (PEG) at pH 6.5 and 7.5 at room temperature (Figure 10A). A second screen comparing crystallisation in pH 6.5 and 7.5 conditions was set up with the addition of additives from a HR2-428 additive screen (Hampton Research). The addition of 3-(1-Pyridinio)-1-propanesulfonate (final concentration 0.2M) resulted in increasingly ordered crystals at pH7.5 at 4°C (Figure 10B). However, due to poor diffraction, optimisation was further required to increase the size and purity of the crystal. A screen was set up with increased drop size (1.5µl) as well as a range of precipitant, PEG, concentrations (18-28%). Final conditions for optimal crystal growth were found to be 0.1M Bis-Tris propane, 0.2M potassium sodium tartrate, 14% 8K v/v PEG at pH 7.5 at 4°C. This resulted in the growth of a ~0.2mm crystal following 12 days of growth (Figure 10C).

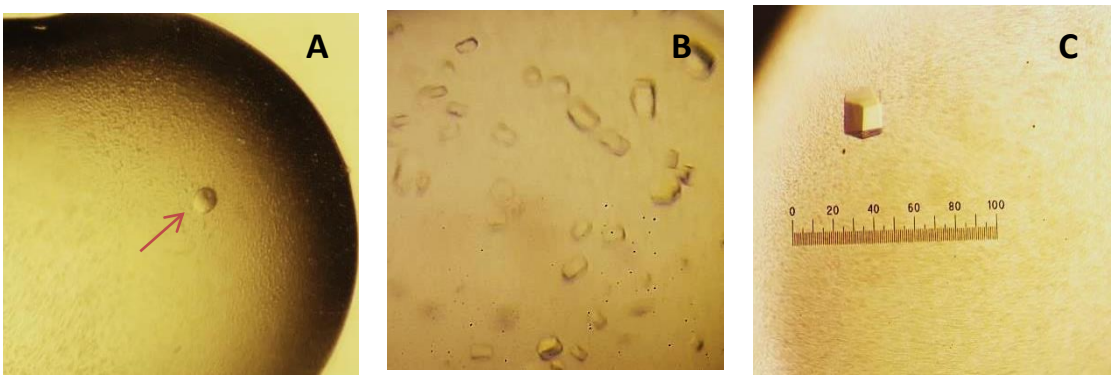

Figure 10: Crystallisation of LtgE for X-ray crystallography

Recombinant LtgE (lacking N' terminal signal sequence) was purified and concentrated to ~5mg/ml. A) 0.1µl drops using a PACT *premier*™ HT-96 screen revealed sphere like crystals with 0.1M Bis-Tris propane, 0.2M potassium sodium tartrate, 20% v/v polyethylene glycol (PEG) at pH 6.5 and 7.5. B) Additional additive screening further optimised the of crystal structure by the addition of 2.0M 3-(1-Pyridinio)-1-propanesulfonate (final concentration 0.2M), resulting in more ordered crystals at pH7.5 only. C) Increased drop size (1.5µl) and a range of PEG concentrations (18-28%) were evaluated and resulted in larger, more ordered crystals at 14% v/v 8K PEG (without additive). This crystal was able to diffract when exposed to X-rays and was used to solve the structure of LtgE.

This crystal could be successfully diffracted and the structure was solved by Professor Russell Wallis (University of Leicester). The final resolution of the structure was 1.75Å. The X-ray structure shares structural homology with LtgE from other bacteria including MltA of *E. coli* and MltA homologue of *N. gonorrhoeae* (Figure 11). All proteins have two main domains with *N. gonorrhoeae* having an additional smaller third domain (hypothesised to be involved in protein-protein interactions) (162). There is also a significant groove between the two domains in which it has been shown in *E. coli* to bind peptidoglycan (164).

Given this structure and comparing the active sites of other homologues in which the structure has also been solved, it is possible to infer potential catalytic sites. MltA contains a 3D domain so named for its 3 active site aspartates. BLASTp analysis suggested three possible catalytic sites in the 3D domain of LtgE; D300, D331 and D343. Given structural homology and the site directed mutant data from *E.coli* and *N. gonorrhoeae* MltA (162, 164) it was hypothesised that D343 was the most suitable candidate for a catalytic residue in LtgE.

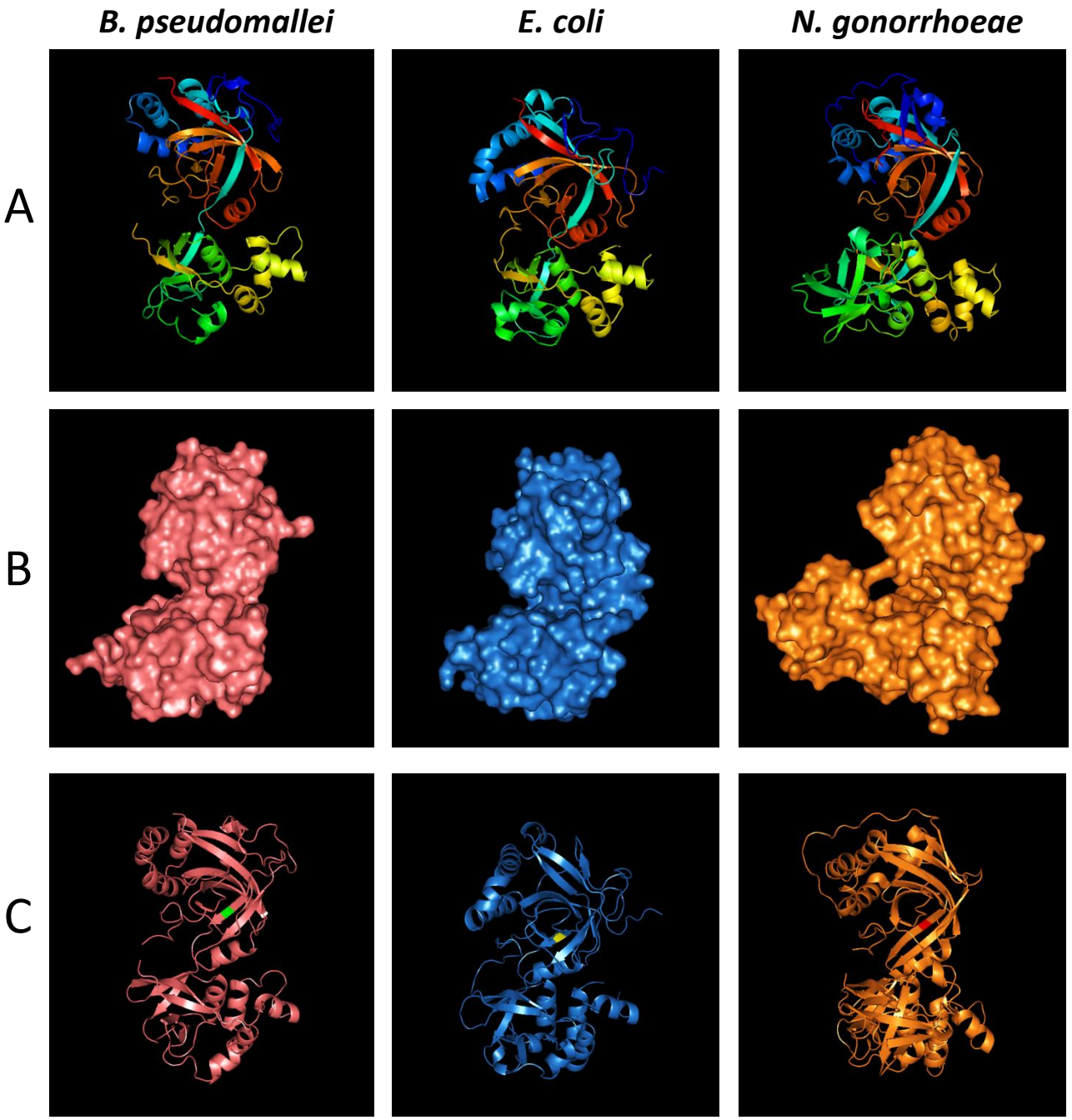

Figure 11: Crystal structure of *B. pseudomallei* LtgE and its MltA homologues in *E. coli* and *N. gonorrhoeae*.

A) Cartoon structure coloured in a red to blue spectrum from N' to C' terminus respectively. In all three proteins the polypeptide chain goes from the first domain into the second and back into the first domain. B) Protein surface demonstrates that the two domains are separate and form a groove between them, presumably for the insertion of a peptidoglycan substrate. C) The catalytic aspartate (D343) residue of LtgE (highlighted green) can be predicted using conserved aspartates from the *E. coli* (yellow) and *N. gonorrhoeae* (red) homologues. Each of these aspartate residues are located in similar areas of the protein, exposed to the outer surface and located within the groove between the two domains.

3.4.3.3. Assessment of LtgE muralytic activity

All assays for the assessment of LtgE activity were performed using gel-filtrated recombinant LtgE. However, zymograms were also successful using protein eluted straight from the Immobilized Metal Affinity Chromatography column as imidazole used to elute the protein was removed from the protein sample during SDS-PAGE.

Zymography

A zymogram for LtgE revealed a clearance band that developed within 1-2 hours, indicating that this protein was refolded successfully and could digest the lyophilised cell wall within the gel (Figure 12). The optimum buffer for activity was 25mM Tris pH 7 containing 1mM $MnCl_2$. As buffer pH was dropped below 6 or above 8 the clearance band faded or disappeared completely indicating this was due to the activity of the protein. Furthermore to confirm that the catalytic residue of LtgE was D343, a site directed mutant was constructed and purified in which this residue was substituted for alanine (D343A). Alanine is a small non polar, inert, residue that would be unlikely to cause unwanted alternative chemical reactions. Recombinant mutated protein was purified alongside wildtype protein and observed by SDS-PAGE. 200ng of protein was loaded onto the gel. Zymograms using the same quantity of protein were performed (Figure 12). Wildtype protein was shown to be active, producing a clearance band, whereas mutated protein showed a complete loss of activity (absence of a clearance band) confirming that D343 is an important catalytic residue. Due to time constraints it was not possible to investigate the roles that the other aspartates (D300 and D331) or other residues have in the catalytic site.

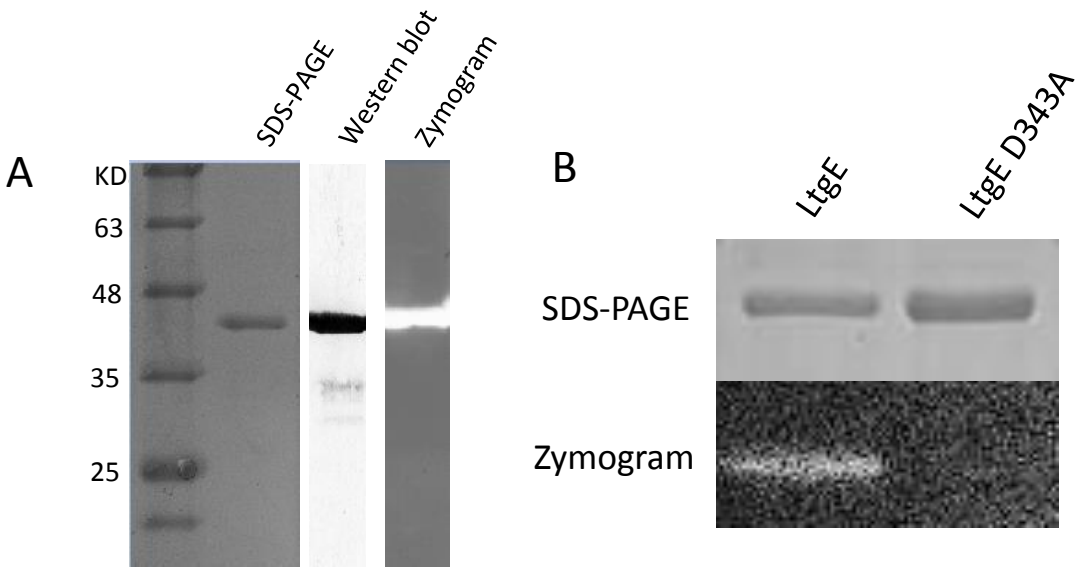

Figure 12: Assessing the muralytic activity of LtgE using zymography

(A) Zymogram shows LtgE can degrade the lyophilised *M. luteus* cell wall at an optimum condition of 25mM Tris pH 7 + 1mM $MnCl_2$. The clearance band corresponds with the LtgE band on SDS-PAGE and Western blot. B) Mutation of aspartate residue 343 to alanine (D343A) results in loss of activity in zymography.

Evaluation of LtgE activity through degradation of M. luteus in solution

To further evaluate the muralytic activity of LtgE, lyophilised *M. luteus* was resuspended in 25mM citric acid buffer pH 6 and LtgE was added (2µg). Activity could be seen by a decrease in optical density over the course of 5 hours (Figure 13). The rapid digestion of the substrate indicates that LtgE is highly active. The protein could be inactivated by heating at 95°C for 10 minutes, although a slight decrease in optical density suggests perhaps low level residual activity. The lysozyme control (from commercial preparation) showed a very rapid decrease in optical density indicating that this assay could be used to show muralytic activity.

While these results were reproducible, given time constraints and the amount of recombinant protein available different concentrations of protein were unable to be tested. It would have been interesting to see if addition of potential inhibitors such as Bulgecin A or Rpf inhibitors available in our laboratory could prevent this lysis. In addition, future experiments could increase denaturing conditions beyond heating at high temperatures (such as DTT and iodoacetamide treatment) to remove any of the residual activity. This could be an important control if this experiment were to be used as a screen for inhibitors.

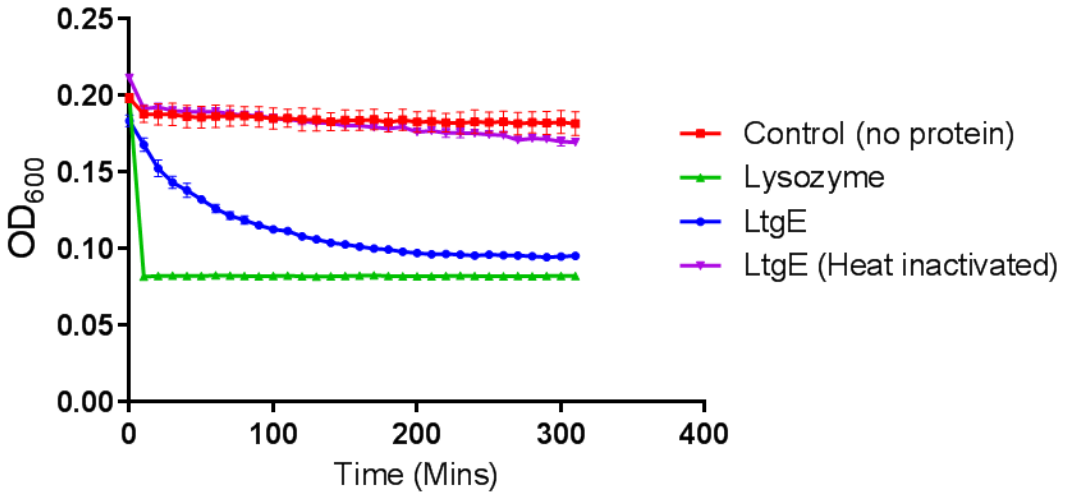

Figure 13: LtgE can degrade lyophilised *M. luteus* in solution.

Lyophilised *M. luteus* cell wall was mixed with 25mM citric acid pH6 (20µg/ml). Triplicate wells were inoculated with LtgE, heat inactivated LtgE, lysozyme positive control or buffer controls. Optical density was measured using a Varioskan every 10 minutes. LtgE can digest the *M. luteus* as seen by a reduction in OD. Heat inactivated protein was unable to degrade the cell wall. Data shown in combined data from three independent experiments.

Digestion of purified peptidoglycan

A preliminary experiment was performed comparing the digestion of purified peptidoglycan with recombinant LtgE with mutanolysin, a highly active muralytic enzyme which also cleaves the β-N-acetylmuramyl-(1-4)-N-acetylglucosamine linkage of bacterial cell walls. This did reveal some addition peaks when muropeptides were analysed by reverse-phase HPLC and compared to samples only digested with mutanolysin (Figure 14). It is possible that the fragments generated by LtgE cleavage were too large to be detected by RP-HPLC, therefore could only be seen when co-digested with mutanolysin. The nature of these unique peaks is unclear, however given the elution time of these additional peaks it is a good indicator that these are anhydro-products and that LtgE is indeed a lytic transglycosylase.

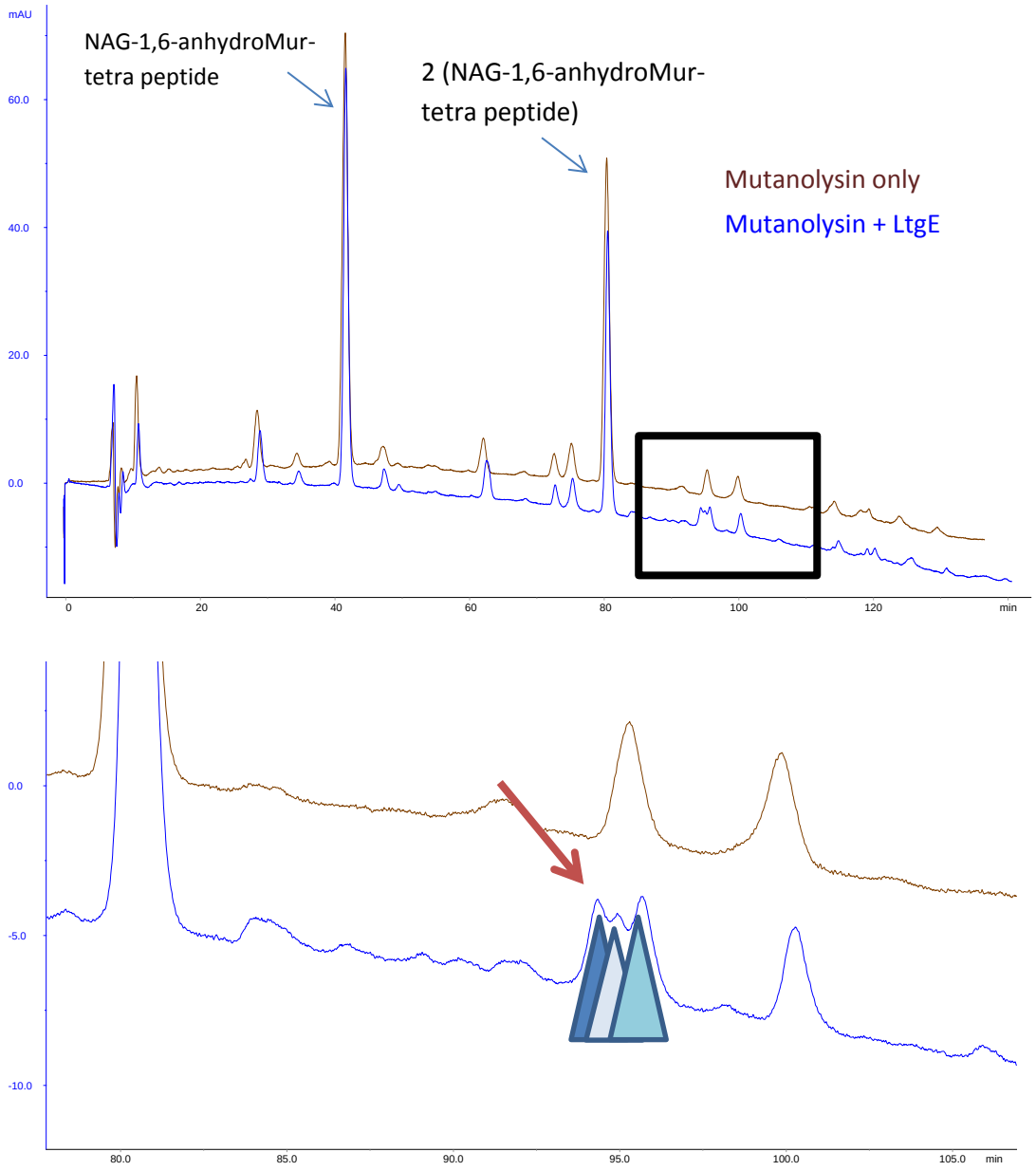

Figure 14: Digestion of purified peptidoglycan by LtgE

Purified peptidoglycan was digested with recombinant LtgE alongside mutanolysin Muropeptides were separated by RP-HPLC. Additional peaks can be seen when compared to samples only digested with mutanolysin. The nature of these unique peaks is unclear, however anhydro-products, such as those formed by lytic transglycosylase activity, are eluted at a later time given their increased hydrophobicity. Therefore given the elution time of these additional peaks it is a good indicator that these are anhydro-products and that LtgE is indeed a lytic transglycosylase.

Before further repeats were performed, and to find optimal conditions for digestion of peptidoglycan by LtgE (for RP-HPLC) a screen was set up investigating various conditions. LtgE was added to citric acid buffer at pH4 or Tris pH 6 or 8 containing FITC-labelled peptidoglycan and incubated at either 30°C or 37°C. Mutanolysin and lysozyme were used as controls. The results suggest that LtgE is most active at pH8 at 37°C. The activity is reduced slightly at pH6 or by reducing the incubation temperature to 30°C. Using a buffer of pH4 abolishes this activity. The optimal condition for double digestion appears to be pH8 at 37°C (Figure 15). The fact that LtgE appears to be more active at 37°C than at 30°C is in contrast to literature for MltA of *E. coli* (160).

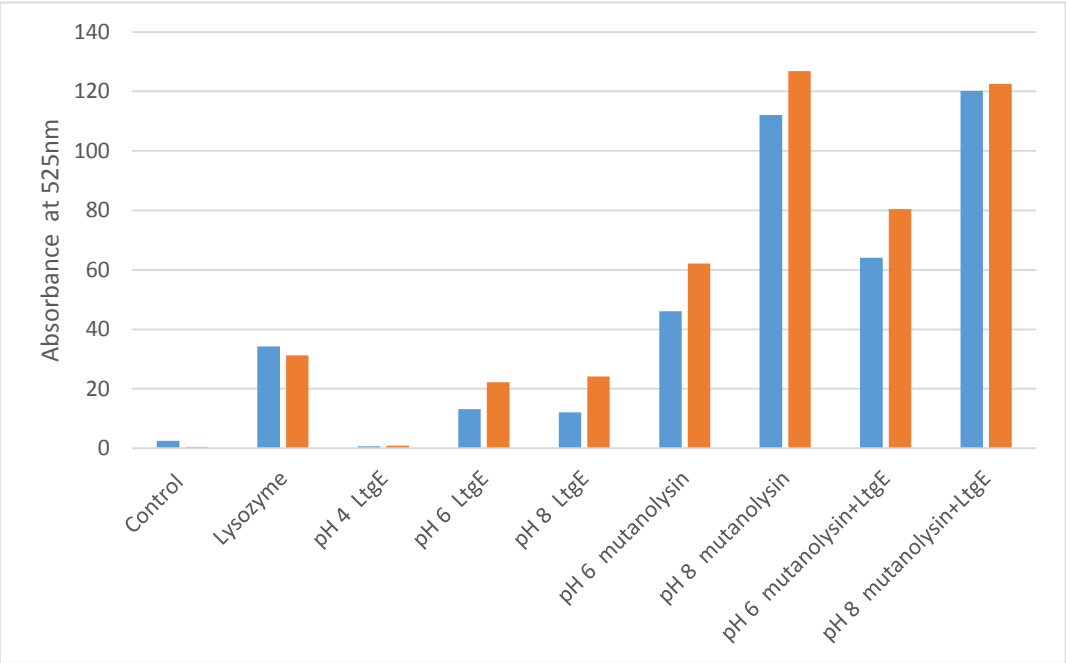

Figure 15: Finding optimal conditions for future peptidoglycan digestion.

FITC labelled peptidoglycan was digested with LtgE and/or mutanolysin at a range of pH buffers at 30 or 37°C. Optimal conditions are pH8 and 37°C as measured by the maximum release of FITC florescence at 525nm. There was no activity at pH4. Lysozyme and buffer controls are included (pH6). Blue bars - 30°C, Orange bars - 37°C. This experiment was only performed once.

3.4.4. LtgB

3.4.4.1. Expression of recombinant LtgB

C41(DE3)-pET15bTEV-*ltgB* was cultured in LB-Amp (100µg/ml) and induced with 0.5mM IPTG at 18°C. Soluble protein was purified on a nickel chelating sepharose column. SDS-PAGE and Western blot analysis using anti-poly histidine IgG antibodies revealed that, unlike LtgE, there was a heavy amount of degradation suggesting instability in the protein (Figure 16). This is similar to Slt35 which is the soluble fragment of MltB (217), although there is not a high level of homology between MltB and LtgB.

Future experiments would aim to optimise conditions to prevent this degradation to allow for study of the full length protein, perhaps by minimising toxic effects by decreasing expression rates. Alternatively, and perhaps a more suitable option would be to clone a shorter version that would correspond to the degraded version of LtgB, similar to the approach used previously for Slt35 (217). This is likely a natural processing and cleavage of LtgB as a mechanism of regulation as LtgB does not have a predicted membrane anchor found in other Ltgs. It is important to note that Western blot analysis showed only recombinant protein still containing to a C-terminal poly-histidine tag and any protein cleaved from the C-terminal end would not be detected.

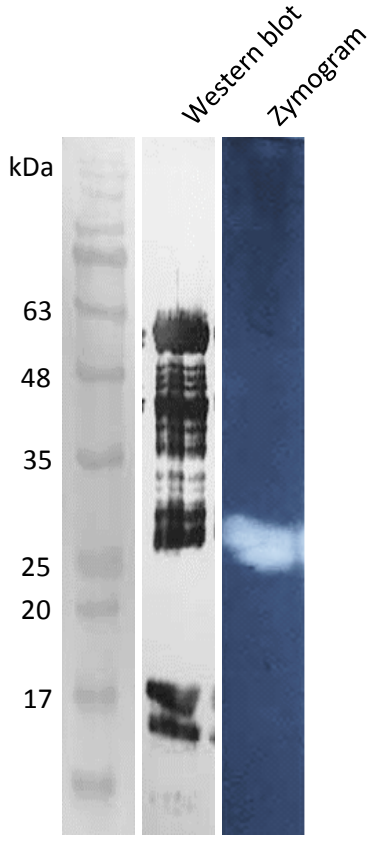

Figure 16: Western blot and zymogram of LtgB.

LtgB was expressed and purified on a nickel chelating column. Western blot analysis using anti-polyhistidine IgG antibodies reveal heavy degradation but successful expression of LtgB. Zymography shows a clearance band indicating that LtgB does have muralytic activity; however the size corresponds to approximately 25kDa, smaller than the predicted full length of protein 57kDa. This suggests that the protein degrades to a smaller, active form.

3.4.4.2. Assessment of LtgB muralytic activity

Zymography

LtgB muralytic activity could be shown using zymography with the optimal conditions for observation of a clearance band being 25mM Tris pH 7.5 with 5mM $MgCl_2$. Unlike LtgE, in which the clearance band corresponded to the predicted size of LtgE, the clearance band seen for LtgB corresponds to one of the degraded forms of the protein (approximately 25kDa) rather than the full length protein (57 kDa) (Figure 17). This degradation appears to have a significant effect on the activity of the protein supporting the hypothesis that degradation is natural processing of the enzyme to an active form rather than nonspecific degradation.

Cleavage of artificial lysozyme substrates

An alternative method to assay muralytic activity in a quantitative manner is the cleavage of the artificial lysozyme substrate MUF Tri-NAG. Cleavage of glycan bonds between the sugar residues resulted in detectable umbelliferon released. LtgB, lysozyme, heat inactivated LtgB and heat inactivated lysozyme was added to buffer containing MUF Tri-NAG and incubated at 37°C overnight before inactivation with 10M NaOH. Umbelliferon release was measured by absorbance at 448nm. A relative light units (RLU) score (taking into account protein concentration) of greater than 1.0 corresponds to an enzyme that has muralytic activity. LtgB was shown to have muralytic activity (3.9 RLU). The activity of the protein was high, only 2 fold less than the commercial lysozyme control (6.6 RLU). Heat inactivation of LtgB resulted in substantial loss in activity (0.08 RLU). Dilution of the protein also reduced the RLUs released, as expected.

This experiment was not reproducible when the protein was dialysed to remove imidazole as opposed to gel filtration indicating that the protein may be unstable and long dialysis may result in complete degradation of the protein. This is not surprising given the degradation that can be seen on SDS-PAGE and Western blots. Prolonged storage at 4°C also resulted in degradation. The instability of the protein is most likely a natural mechanism of regulation especially as this protein does not encode a membrane anchor. Protein-protein interaction studies may reveal if LtgB forms part of complexes as a form of regulation by localisation.

	Active protein	1:10 diluted active protein	Heat inactivated protein
LtgB	3.9 ± 0.30	0.23 ± 0.02	0.08 ± 0.02
Lysozyme	6.6 ± 0.16	0.725 ± 0.08	4.72 ± 0.73

Table 2: Measurement of muralytic activity of LtgB using an artificial lysozyme substrate

LtgB was added to buffer containing an artificial lysozyme substrate, MUF- TriNAG. Mean and standard deviation were calculated. Results are displayed as relative light units. Results show that LtgB is a muralytic enzyme with activity greater than 1 RLU. Heat inactivation could successfully denature the protein.

Effect of LtgB overexpression on E. coli growth

Evidence that overexpression of LtgB was toxic to *E. coli* was first demonstrated during generation of strains for the overexpression of secreted LtgB. The effect of overexpressing secreted LtgB on *E. coli* growth was investigated using C41(DE3) strains as it was not possible to transform BL21(DE3) strain. This is most likely because pET vectors have leaky promoters indicating that even without induction there was a basal level of expression which was toxic to the cell. This however, was not detectable by Western blot for LtgB but could be seen for LtgC (Chapter 3.3.5.2). BL21 (DE3) is routinely used for protein expression, however given the toxic effect of Ltg overexpression, a more suitable strain was used. C41(DE3) has been engineered to be less susceptible to toxic proteins and increase soluble expression of proteins (208). C41(DE3) could be transformed with pET23-*ltgB* although colonies were much smaller than those transformed with of the empty vector control indicating that there was basal expression of protein which has some toxicity to C41(DE3).

LtgB has a single predicted catalytic glutamate (E154). This conserved residue is found in many lytic transglycosylases and lysozymes including the well characterised MltE, Slt70 and Slt35 (MltB) protein from *E. coli* (173, 198). Mutation of E154 to either the small non-polar amino acid alanine, or to the oppositely charged amino acid lysine, resulted in a decreased toxicity of the protein. This was seen initially by the successful transformation of BL21(DE3) with pET15bTEV-*ltgB*(E154A) and pET15bTEV-*ltgB*(E154K). To investigate this further, growth experiments using C41(DE3)::pET23a-*ltgB* and C41(DE3)::pET23a-*ltgB* (E154A/K) strains were performed. Growth curves revealed that upon induction of LtgB there is rapid decrease in optical density, with growth restored three hours post induction. Mutation of the predicted catalytic glutamic acid residue from glutamate to alanine or lysine prevented cell lysis. This adds further evidence that this is indeed the catalytic residue. The alanine substitution appears to be more suitable for restoring growth towards empty vector control levels; however, the substitution does not restore growth completely, indicating residual toxicity of the protein (Figure 17A).

Western blot analysis shows that wildtype and mutated proteins are soluble following one hour of induction (Figure 17B). This suggests that mutation of the catalytic residue

does not result in the protein becoming insoluble and thus any absence of activity is due to inactivation of the protein. Western blots on wildtype protein show expression of soluble protein which correlates with the decrease in OD (cell lysis). The recovery of growth observed three hour post induction is as a result of loss of soluble LtgB protein.

Reasons for these results are unclear but it is possible that either the bacteria stop expressing this protein or can target it for degradation explaining the absence of bands on Western blot (loss of histidine tag). Mutation in the promoter region may prevent expression and it is these bacteria that are able to grow. Alternatively, the bacteria may have mutations allowing it to become resistant to ampicillin and thus the requirement for maintenance of the toxic LtgB expressing - ampicillin resistance encoding plasmid - is lost. More investigation would be needed to understand the exact nature of the bacteria which are able to grow after three hours induction, for example, bacteria could be screened for both ampicillin resistance and *ltgB*.

Further work would aim to investigate the extent cross reactivity between LtgB and RpfB of *Mycobacteria* species such as resuscitation of non-culturable forms of *Mycobacteria*. In a pilot experiment recombinant LtgB was added to an experiment monitoring *M. smegmatis* growth which did indicate promotion of growth and a decrease in lag phase, but the nature of the experiment and the results were questionable and would require much more optimisation. It would also be preferable to identify muropeptide fragments released by LtgB activity using RP-HPLC coupled with mass spectrometry.

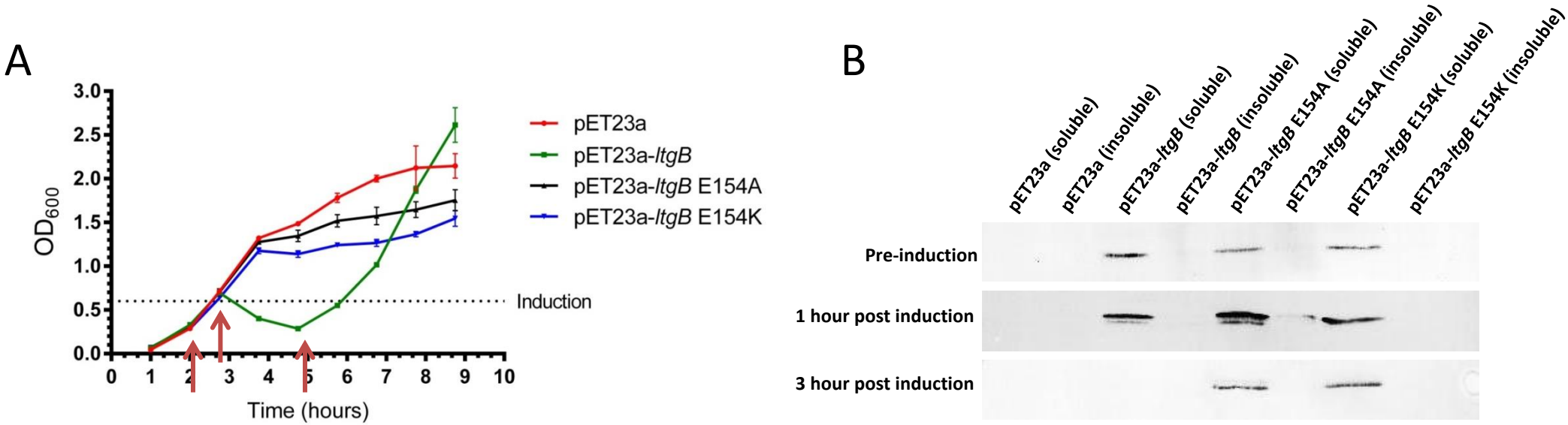

Figure 17: Lysis by overexpression of LtgB can be prevented by site directed mutagenesis of the catalytic glutamate 154 residue.

E. coli C41 (DE3) strains were grown in LB-Amp at 37°C. Fresh media was inoculated with the overnights (1:100) and grown to an OD_{600} of 0.6. Cultures were induced with 0.5mM IPTG. OD_{600} readings were recorded every hour. Arrows indicate time points in which protein extraction was carried out. A) Induction of LtgB results in rapid lysis of *E. coli* cells. This can be seen by a drop in optical density immediately after induction. E154A or E154K mutation could prevent this lysis. B) Western blots using anti-polyhistidine IgG antibodies were performed using cell extracts at time points indicated by arrows. Blots indicate that the during cell lysis LtgB is expressed as soluble protein. However, when growth recovers there is a loss of soluble protein suggesting the bacteria are no longer expressing the toxic protein. LtgB E145A/K are soluble at all time points tested indicating that this residue is essential for the toxic effect of this protein.

3.4.5. LtgD

3.4.5.1. Effect of LtgD overexpression on *E. coli* growth

To assess the effect of LtgD muralytic activity, growth curves of *E. coli* LtgD overexpressing strains (containing the pET23a-*ltgD* plasmid) were carried out as for LtgB. The catalytic residue of LtgD was predicted to be a glutamic acid residue (E182). Site directed mutation of the catalytic site with either alanine or lysine was carried out on pET23a-*ltgD* to generate plasmids pET23a::*ltgD* E182A and pET23a::*ltgD* E182K.

Growth curves of *E. coli* BL21(DE3) pET23a-*ltgD* and pET23a-*ltgD* E128A/E128K expressing strains were performed (Figure 18). LtgD expression caused immediate inhibition of cell growth and cell lysis that was unable to be recovered, this indicates that this protein is highly toxic for *E. coli* and most likely causes substantial damage to the cell wall. If LtgD was more stable than LtgB, it may remain in the cells for a much longer period of time and therefore the toxic effect would be much longer lasting. E182A mutation does not appear to elevate this toxic effect, with the growth pattern being similar to that of expressing wildtype LtgD. LtgD E182K mutation resulted in a substantial increase in lag phase but induction did not appear to cause cell lysis over an 8 hour period. However, all three strains still have impaired growth when compared to *E. coli* containing the empty plasmid. All strains grew in a similar way to the empty vector control when they were not induced (data not shown).

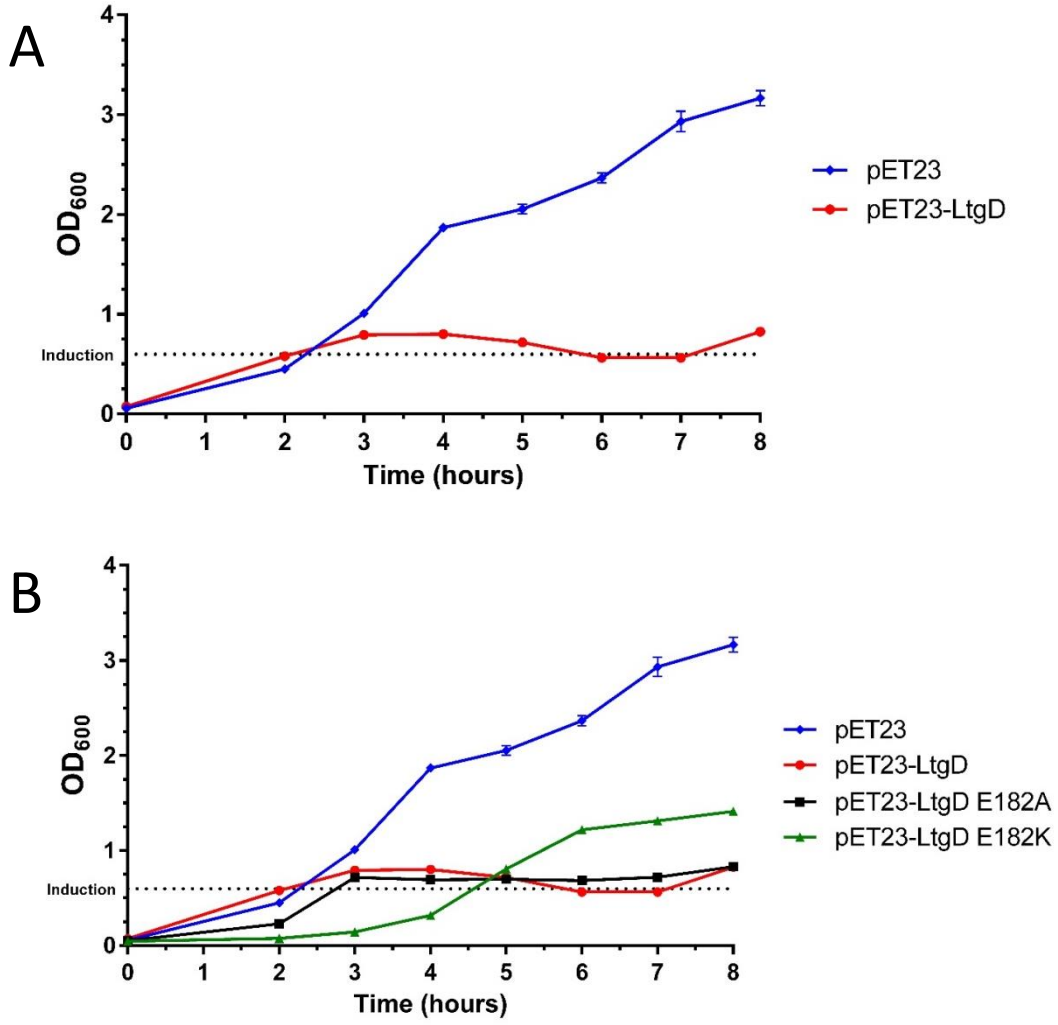

Figure 18: Growth curves of LtgD overexpressing *E. coli* strains

Overnight cultures of *E. coli* BL21(DE3) pET23a-LtgD/E182A/LE182K strains were grown in LB-Amp at 37°C. Fresh media was inoculated with the overnight culture and grown to an OD_{600} of 0.6. Cultures were induced with 0.5mM IPTG. OD_{600} readings were recorded every hour. (A) Overexpression of LtgD causes immediate arrest of *E. coli* growth with potential cell lysis occurring (B) E182K mutation appears to increase lag phase of *E. coli* growth but does not appear to cause the toxic effect of wildtype protein. E182A does not appear to have any effect.

The fact that mutation of the catalytic site does not abolish this toxic activity could mean a number of things. The most obvious being that the catalytic residue mutated is not the correct residue and it is not essential for the activity of the protein. Given that Ltgs are known to have glutamates as their catalytic residues (198), it may be that the catalytic site is an alternative glutamate residue. There are 10 glutamate residues in total in LtgD, one of which is just 8 residues away (E190) from the predicted catalytic glutamate (E182). As mutation to lysine did result in minor reversal in in this phenotype it would suggest that E182 does play a role in catalysis but that there are multiple residues important for catalysis and mutation of multiple residues is required for abolition of activity. If this protein is highly active and therefore highly toxic to the cell when over expressed, then even residual activity may be enough to prevent growth of *E. coli* . Recombinant protein assays similar to those performed for LtgE and LtgB would be useful to understand the extent of protein inactivation as a result of these mutations as well as the stability of the protein. It is also possible that mutation does not result in inhibition of binding of the substrate, simply the formation of anhydro-muramyl reaction product. This mutated protein may bind the peptidoglycan irreversibly preventing access to other proteins required at the site of cleavage causing a toxic effect on the cell.

3.4.6. LtgC

3.4.6.1. Expression of recombinant LtgC

Protein expression trials (including SDS PAGE and Western Blot analysis) indicated that there was a large amount of soluble protein produced, with little degradation, even without induction. Following induction there was significant degradation of the protein, in an attempt to limit this, purification was performed on non-induced cultures.

3.4.6.2. Assessment of LtgC muralytic activity

Zymography using LtgC resulted in a clearance band indicating the protein has muralytic activity (Figure 19). LtgC also degrades to a smaller more active form. The predicted size of LtgC is 44.5kD however, the protein migrates on an SDS-PAGE at approximately 55kDa. It is not clear why this occurs but it may have unusual confirmation, be resistant to the denaturing processes in sample preparation or form complexes with itself or other proteins. A second band can be seen on the Western blot at approximately 22kD, it is this band that appears to be active on zymogram. LtgC is predicated to have an Ltg/goose egg white domain, similar to LtgB and RpfB. Therefore, it may be that this domain is only active if the remaining protein is removed. This would correlate with the evidence for LtgB degradation and activity.

.

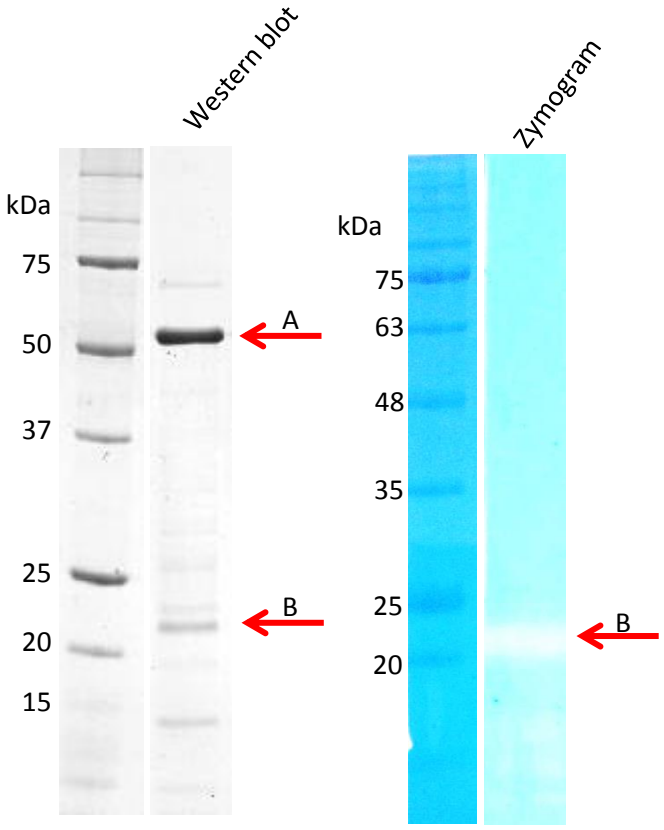

Figure 19: Purification and activity of LtgC by zymogram

E. coli BL21(DE3) pET15bTEV-*ltgC* was cultured in LB-Amp (100µg/ml) at 37°C to an OD_{600} of 1.0. Soluble protein was extracted and purified on a nickel chelating column. Expected protein size; 44.5 kDa, the predominant band 'A' migrates higher than is expected ~55kDa, a smaller band, 'B', can also be seen on the Western blot and produces a clear band on zymogram

3.5. Final Discussion

Muralytic activity of LtgB, LtgC and LtgD was shown successfully using the quantitative assay zymography. Zymograms were also used to provide data on the importance of the catalytic aspartate residue (D343) of LtgE with a D343A mutation resulting in a complete loss of a clearance band. Zymograms and Western blot analysis reveal that both LtgB and LtgC degrade to a smaller more active form. This is not surprising in regards to LtgC which shares homology with MltB. MltB degrades to a soluble form (slt35) (171). This instability is reasonably well studied and has been shown to be influenced by the presence of Na^{+} and Ca^{2+} ions (218). Therefore the data generated with LtgC agrees with literature on MltB of *E. coli*. LtgB contains a goose egg white lysozyme domain similar to Rpfs of *mycobacteria* and shares significant homology with MltE, the predominant exolytic enzyme of *E. coli*. Other domains present such as the LysM domain are most likely for substrate binding (219, 220). While there is no evidence of proteolytic cleavage of MltE in the literature, results here suggest that LtgB does undergo proteolytic cleavage. It would be preferential to identify this shorter protein region by mass spectrometry and overexpress this shortened version in *E. coli* to further study this protein in greater detail.

Despite this uncertainty into the true nature of this degraded form of LtgB, a quantitative assay was carried out using the artificial substrate MUF Tri-NAG. This assay is useful not only to assess the level of muralytic activity but also, to some extent, the nature of the substrate cleaved. The release of umbelliferon shows that LtgB can cleave the glycosidic bond in these short glycan fragments. Interestingly, this assay was unsuccessful with LtgE. It is likely that LtgE can only cleave the glycosidic bond in larger peptidoglycan fragments. Given the homology between LtgB and MltE which is largely an endolytic enzyme (159), it is not surprising that LtgB can cleave short peptides given that this would reflect the end of a glycan chain. It would have been interesting to see if LtgC (active by zymography and also containing a goose egg white lysozyme domain) was also able to cleave these short sugar repeats or whether larger fragments are needed as is likely the case for LtgE.

A MUF assay or an optimised version of the FITC-labelled PG digestion assay used for LtgE could make very good high throughput screening assays for the investigation of

potential inhibitors. Initially it would be preferable to assess known inhibitors of Ltgs such as Bulgecin A as a proof of concept, but in theory it would be possible to very rapidly screen a library of inhibitors to assess their ability to prevent Ltg activity. Given the X-ray crystal structure we have solved for LtgE, it may also be possible to rationally design inhibitors to target the active site or prevent peptidoglycan binding through occupation of the groove seen between domains.

E. coli growth curves that measure the effect of Ltg overexpression on *E. coli* growth were utilised for LtgB and LtgD. These assays were successful, particularly in regards to LtgB which was couple with Western blot analysis to investigate protein expression and solubility. Upon induction of protein expression both LtgB and LtgD resulted in very rapid reduction in growth, presumably because of cell lysis as a result of compromised peptidoglycan although more thorough investigations would be needed before this could be concluded. While this growth could be rescued in LtgB (by the absence of soluble protein) this was not the case for LtgD and growth did not recover. SDM could restore growth for LtgB but had less of an effect with LtgD, which is likely to be due to a highly damaging effect of LtgD and residual activity of mutated protein.

3.6. Summary

In this chapter secreted and non-secreting Ltg protein expression strains were generated. The muralytic activity of all Ltgs, apart from LtgA, was assessed using a range of approaches and assays, some of which can be optimised to allow for high throughput inhibitor screening. The X-ray crystal structure of LtgE was solved and is an excellent candidate for search of inhibitors. The catalytic site of LtgE was investigated and shown that D343 is essential for its activity. The catalytic sites of other Ltgs were investigated primarily with *E. coli* over expression growth curves. The following chapters (4 and 5) outline the generation and characterisation of *B. pseudomallei ltg* deletion mutants.

Chapter 4

Generation of *ltg* deletion, overexpression and complemented strains

4.1. Introduction

There are a number of well-established methods for inactivation or deletion of genes from a target genome. One method, typically used when performing large scale mutagenesis, is to use a transposon. Libraries of transposon mutants can be screened to identify essential and non-essential genes, both *in vitro* and *in vivo*. Perhaps most relevant for this study, this technique has been used to identify essential and virulence genes in *Burkholderia* species (73, 75, 221). Alternatively, these libraries could be used to identify genes involved in specific processes including, but not limited to, nutrient metabolism, motility, biofilm formation or antibiotic resistance. Drawbacks include polar effects and integration into the gene in non-functional regions which could result in genes been falsely annotated as non-essential .

A more targeted method is for the insertion within or replacement of the gene with selectable marker, typically an antibiotic resistance cassette, allowing for easy selection of mutants. This can be important for selection of unfavourable mutations, for example mutation of gene important in growth and metabolism. Selectable markers also allow for assessment of the proportion of mutants to wildtype strains in competition assays both *in vitro* and *in vivo*. This approach has been successfully used to investigate genes in *B. pseudomallei* examples include genes important in biofilm formation (222), auto transporters (111) and virulence (223).

The gold standard method for generating mutants is to make an unmarked deletion of a target gene. Homologues recombination occurs between flanking regions upstream and downstream of the gene of interest and those within an introduced suicide vector during which the gene is excised from the genome. The absence of selectable markers means that the strain can be grown without selective pressure and allows for multiple mutations without the need for multiple selectable markers.

A rapidly advancing technology is the suppression, editing or targeting of genes using the clustered regularly interspace short palindromic repeat (CRISPR) system. This effectively utilises a bacterial immune mechanism to generate RNA-guided nucleases to a target gene. The most commonly used protein is the CRIPSR associated protein 9 nuclease (cas9). A guide RNA could be incorporated into cas9 protein and introduced

into a host bacterium. The cas9 protein then recognises the target DNA and perform a number of desired functions including, cleavage, excision, insertion, gene activation and DNA modification (224). At the time of this writing there are no publications on the use of CRISPR to generate mutants in *Burkholderia* spp.

When mutation of a gene results in marginal or non-obvious phenotypes an alternative method is to overexpress the protein of interest potentially resulting in an exaggeration of phenotype. This could have obvious negative effects particularly if overexpression is toxic to the bacteria however it also allows you to artificially induce expression of a gene to beyond wildtype levels. Overexpression of genes in pathogenic bacteria, particularly genes encoding potential virulence factors, must be carefully considered due to potential increased pathogenicity.

There are significant challenges when generating mutants in *B. pseudomallei*. Firstly the bacterium has a large genome comprised of two chromosomes encoding almost 6000 genes (62). A large genome suggests an increased redundancy making phenotypic assays problematic as paralogues can compensate for the loss of a particular gene. In addition, the *B. pseudomallei* GC rich genome can be problematic with cloning of suicide vectors, for example primer design for PCR (62). The classification of *B. pseudomallei* as a select-agent and potential biothreat has resulted in strict regulation on genetic manipulation of the organism (225), in particular, the choice of selectable markers that can be introduced. These are limited to kanamycin, gentamycin, polymyxin B, chloramphenicol and zeocin. The intrinsic resistance of *Burkholderia* to gentamycin and polymyxin B or the high levels of antibiotic needed to be effective (kanamycin and zeocin) poses further problems (226). While genetic manipulation of *Burkholderia* is not as advanced as it is for species such as *E. coli* or *Mycobacteria*, there are a range of tools that have been used for the generation of mutants. These include the suicide plasmids pDM4 (227), pMo130 (228) and pKNOCK (229). There have also been a number of studies that have utilised transposons to generate *Burkholderia* mutant libraries (74, 81, 135, 230). There are also a number of plasmids suitable for expression of proteins in *Burkholderia* for use in complementation. These include pMo168 (228) and broad host range vectors such as pBHR1 and PBBR1 series (231).

4.2. Chapter aims

- Generate single and multiple unmarked *ltg* mutants in *B. pseudomallei* K96243 and confirm mutations using PCR and southern blots
- Generate complementing *ltg* mutant strains
- Generate *B. thailandensis* and *B. pseudomallei* strains containing an LtgE overexpression plasmid

4.3. Materials and Methods

Appendix 8.5 table 8 outlines all primers (including expected PCR product sizes and encoded restriction sites) used in generation of constructs for deletion mutants.

4.3.1. Generation of constructs for allelic exchange

Primers were designed to amplify upstream (FR1) and downstream (FR2) flanking regions of *ltg* genes (LtgB/C/D/E_FR1/2_For/Rev). For cloning purposes additional restriction sites were introduced to the primer sequences. Primers were designed to produce PCR fragments of between 750 and 1500bp. Where possible, flanking regions were designed so homologous recombination occurred within intergenic regions. The primers also included 6 or 9bp of the gene itself. Flanking regions were amplified by PCR using Q5 High fidelity DNA polymerase and *B. pseudomallei* K96243 genomic DNA as a template. Fragments were purified using QIAquick gel extraction kit (QIAGEN) before ligation into the pGEM-T Easy vector. *E. coli* DH5α (Bioline) was transformed with pGEM-T easy constructs and plated onto LA-Amp (100µg/ml) and X-gal (80µg/ml). Transformants with correct plasmids were identified by blue/white screening and diagnostic digests. Purified plasmids containing the correct sized inserts were sent for sequencing (GATC Biotech). Flanking regions were digested from pGEM-T easy, purified and ligated into the suicide plasmid pMo130 (232). *E. coli* S17-1 (λ*pir*) was transformed by electroporation with 5µl of ligation reaction (BioRad Gene Pulser Xcell™, 2.5Kv, 25µF, 200Ω, 2mm cuvette). Transformants were selected on LA-Kan (50µg/ml). Diagnostic digests of the final constructs were performed before conjugation into *B. pseudomallei* K96243.

4.3.2. Transformation of *B. pseudomallei* K96243 by conjugation.

All manipulations with *B. pseudomallei* were done in category 3 containment laboratory in accordance with the approved Code of Practice. pMo130-*ltg* suicide vectors were transformed into *B. pseudomallei* K96243 by conjugation as described previously (232). Briefly, 500µl of an overnight culture of the donor *E. coli* strains and recipient *B. pseudomallei* K96243 were centrifuged at 12000xg for 2 minutes. Cell pellets were washed in 10mM $MgSO_4$ before final resuspension in 100µl of 10mM $MgSO_4$. A donor and recipient suspensions were combined and four 25µl aliquots were spotted onto LA plates. Control donor and recipient strains were also spotted onto separate plates. Plates were incubated overnight at 37°C. The following day the spots were scraped and resuspended in 1ml of PBS. 200µl was plated onto multiple LA-Kan (800µg/ml) and polymyxin B (15µg/ml) plates and incubated for 48-72 hours to select for single crossover mutants.

Potential single crossover mutants were cultured in LA- Kan (800µg/ml) to ensure resistance before sub-culturing in YT media overnight. Subculturing removed the selective pressure to allow for secondary homologous recombination between the second flanking region on the plasmid and the homologous region on the chromosome. Cultures were serially diluted and plated onto YT agar containing 20% (w/v) sucrose and incubated for 48 hours at 37°C.

Potential double crossover mutants were screened by patching colonies from 20% sucrose supplemented plates onto LA and LA-Kan (800 µg/ml) and incubated at 37°C for 24-48 hours. Those colonies that grow on LA and not on LA-Kan were screened using PCR and Southern blots.

4.3.3. Confirmation of gene deletion by PCR

Kanamycin sensitive putative double crossover mutants were screened by colony PCR using both gene specific (LtgB/C/D/E_GS_For/Rev) and flank screening primers (LtgB/C/D/E_out_For/Rev). Boiled lysates were prepared as outlined in Chapter 2.4.2.

4.3.4. Southern Blot

Preparation of digoxigenin (DIG)-labeled probe; 1µg of plasmid DNA containing the flanking region for the probe (Δ*ltgB* – FR1, Δ*ltgD* – FR2, Δ*ltgE* – FR1) and was

restriction digested as detailed in (Chapter 2.4.5) using appropriate restriction sites. The flanking region was purified using gel extraction. 1µg of template DNA was added with dH_2O to a final volume of 16µl and the sample was denatured by heating at 95°C for 10 minutes. Once cooled 4µl of DIG-High prime (DIG High Prime DNA Labelling and Detection Starter Kit I, Roche) was added and incubated at 37°C for 1 hour. The reaction was stopped by adding 2µl of 0.2M EDTA and heating at 65°C for 10 minutes. Southern blot; 1µg of gDNA from both wildtype and mutant strains was digested with appropriate restriction enzymes overnight at 37°C. Digested DNA was resolved on a 0.8% (w/v) agarose gel at 25V for 6-8 hours. The gel was rinsed in distilled water, depurinated by incubation in 0.25M HCl for 15 minutes (twice); denatured by soaking gels in 0.5M NaOH, 1.5M NaCl for 15 minutes (twice) and neutralised in 0.5M Tris-Cl pH 7.5, 3M NaCl for 30 minutes. The gel was rinsed in dH_2O between each washing step. The DNA was transferred to a positively charged nylon membrane using capillary action using 20X SSC buffer overnight. The DNA was fixed to the membrane by UV-crosslinking (UV straterLinker^{TM} 2400, Invitrogen) twice. Hybridisation of the DIG-labeled probe to the target DNA was performed at 65°C for 24 hours, with constant agitation. The membrane was washed repeatedly and immunoenzymatic detection reactions were performed following manufactures protocol (DIG High PRIME DNA labelling and Detection Starter Kit I, Roche).

4.3.5. Electroporation of *B. pseudomallei* for uptake of plasmid DNA

B. pseudomallei wildtype, Δ*ltgE* strains and *B. thailandensis* E555 were made electrocompetent as previously described (233). Briefly 1ml of overnight culture was centrifuged for 1 minute at 12000xg. Cells were washed three times in 300mM sucrose before a final resuspension in 100µl 300mM sucrose. 50ng of purified plasmid DNA (pMo168 and pMo168-*ltgE*) was added to the electrocompetent cells in a 2mm electroporation cuvette. Cells were transformed by electroporation using a Gene Pulsar Xcell Electroporation System (2.5kV, 25µF capacitance, 200Ω resistance). 1ml of LB was added and the bacteria were incubated at 37°C, 150rpm, for one hour prior to plating onto LA-Kan (800µg/ml).

4.3.6. *In cis* complementation of *ltgE* deletion mutants

A plasmid used for *in cis* complementation was constructed containing the *ltgE* encoding region with 200bp of the upstream region containing the putative promoter and ribosome binding site. This region was PCR amplified from *B. pseudomallei* K96243 gDNA using Q5 DNA polymerase and primers LtgE_Comp130_For/Rev . The PCR product was digested using appropriate restriction sites (Appendix 8.5) and ligated into pMo130. In addition, a downstream flanking region for the insertion of the plasmid in the intergenic region immediately down stream of *bpsl3330* was PCR amplified using primers LtgE_compFR2_For/Rev and ligated into the complementing plasmid. The construct was electroporated into *E. coli* S17-1(λ*pir*) and used in conjugation experiments with the *B. pseudomallei* Δ*ltgE*, Δ*ltgEB*, Δ*ltgEBD*, Δ*ltgEBDC* strains. Single crossover strains were selected for on LA-Kan (800µg/ml), polymyxin (15µg/ml). Single crossover complementing mutants were generated using this plasmid. Site directed mutagenesis was also carried out on the plasmid to generate a D343A mutation in *ltgE* as outlined in Chapter 2.4.10 using primers LtgE_D343A_Rev/Rev. A control strains containing an integrated plasmid with just the flanking region were also generated.

4.3.7. Generation of *Burkholderia* strains overexpressing LtgE

The *ltgE* open reading frame with 250bp of the upstream region (encoding promoter and ribosome binding sites) was PCR amplified using Q5 DNA polymerase from *B. pseudomallei* K96243 gDNA using primers LtgE_168comp_For/Rev. PCR fragments were PCR purified and ligated into pGEM-T easy, screened by diagnostic digest using appropriate restriction enzymes (appendix 8.5) and sequenced using M13_For/Rev primers. The fragments were ligated into the replicative vector pMo168 and *E. coli* JM109 (Promega) was transformed with the ligation reaction and plated onto LA-Kan (50µg/ml). Purified plasmid, pMo168-*ltgE,* was electroporated into *B. thailandensis* E555 and *B. pseudomallei*. Transformants were selected for on LA-Kan (800µg/ml).

4.3.8. Purification of RNA

20ml of *B. pseudomallei* strains were grown in LB to an OD_{600} of 0.4 and harvested by centrifugation. The pellet was resuspended in 1ml TRIzol (ThermoFisher Scientific).

200µl of chloroform was added to each tube, vortexed for 30 seconds and incubated at room temperature for 10 mins. The samples were centrifuged at 16000xg for 15 minutes at 4°C. The aqueous phase was transferred to a fresh tube and 200µl of chloroform was added. The tubes were centrifuged again and the top aqueous phase was transferred to a fresh tube. 0.8x volumes of isopropanol was added and mixed by inversion before storing at -20°C overnight. Tubes were centrifuged and the pellet washed in 500µl 70% v/v cold ethanol before further centrifugation. The pellet was washed in 100% cold ethanol and centrifuged again. The supernatant was removed and the pellet air dried for 5-10 minutes. The pellet was resuspended in 50µl RNase free dH_2O.

RNA samples were RNase treated twice using TURBO DNA-free™ Kit (ThermoFisher Scientific). RNA concentrations and purity was measured using a nanodrop.

4.3.9. Reverse transcriptase PCR (RT-PCR)

Reverse transcription reactions were set up using SuperScript® II Reverse Transcriptase kit (ThermoFisher Scientific) according to manufacturer's protocol. Briefly the following RT-PCRs were set up; 1µg/100ng/10ng/1ng of RNA, 1µl of 10mM dNTP mix, 1µl of 2mM reverse gene specific primers (16S_Rev and LtgE_GS_Rev), Sterile RNase/DNase free water up to 12µl. The mixture was heated to 65°C for 5 minutes before cooling to 4°C. 4µl of 4X First-strand buffer and 2µl 0.1M Dithiothreitol was added and gently mixed by pipetting. The tubes were incubated at 42°C before 1µl of SuperScript II RT was added. Samples were incubated at 42°C for 50 minutes before inactivation by heating at 70°C for 15 minutes. PCRs using 16S and LtgE gene specific primers; 16S_(For/Rev) and LtgE_GS_(For/Rev) using cDNA as the template were set up using GoTaq polymerase protocols. PCRs were visualised by DNA gel electrophoresis using 2% w/v TAE agarose.

4.4. Results and discussion

4.4.1. Overview

We have identified 5 Ltgs in *B. pseudomallei* K96243 (*bpsl0262*, *bpsl1345*, *bpsl2506*, *bpsl2630* and *bpsl3046*) designated LtgA-E, respectively. These genes are located on chromosome 1 and are not in genomic islands or in any operons. The *ltg* encoding regions and their adjacent genes can be seen in (Figure 20).

The strategy for generating mutants in these genes was first to construct a suicide vector, pMo130, containing upstream and downstream flanking regions of the gene of interest for homologous recombination. These plasmids would then be conjugated into *B. pseudomallei* to allow for allelic exchange. Finally, double cross over mutants would be screened for the presence of the gene. A schematic outlining this approach can be seen in (Figure 21).

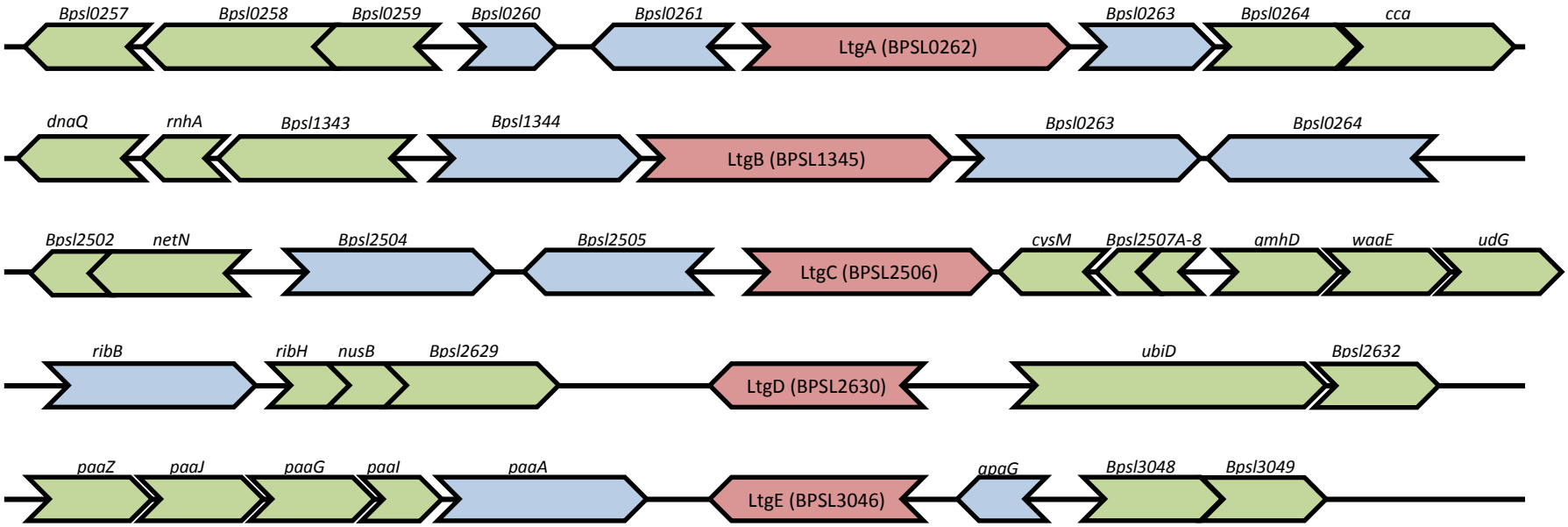

Figure 20: Simplified schematic of chromosomal regions containing Ltgs of *B. pseudomallei* K96243.

Genes depicted with right pointing arrows are on the positive strand, genes depicted with left pointing arrows are on the negative strand. Red genes are Ltg A-E. Blue genes are independent genes, not in operons. Green genes are operons.

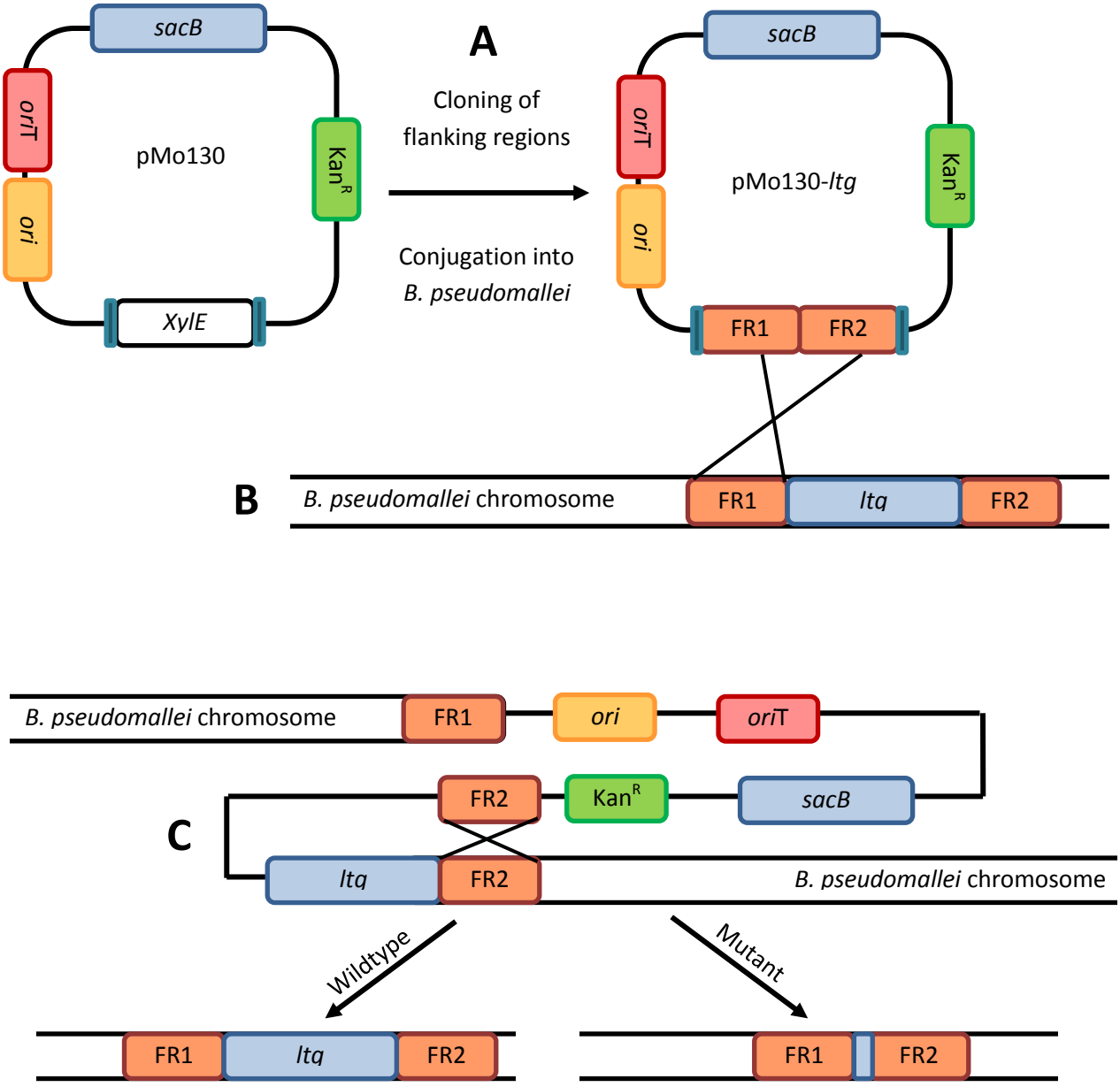

Figure 21: Schematic representation of homologue recombination to generate *ltg* deletion mutants.

(A) Upstream (FR1) and downstream (FR2) flanking regions were cloned into the suicide plasmid pMo130 and conjugated into *B. pseudomallei*. (B) The suicide vector undergoes homologous recombination into the chromosome. (C) The second recombination results in two possible outcomes; wildtype genotype or excision of the gene. Note – this schematic shows recombination initially with FR1 followed by FR2, in reality recombination with FR2 could precede that of FR1.

Following PCR amplification fragments were purified and digested with appropriate restriction enzymes before ligation into pMo130. Four suicide plasmids were successfully constructed (pMo130Δ*ltgB*, pMo130Δ*ltgC* and pMo130Δ*ltgD,* pMo130Δ*ltgE)* (Figure 22). Successful cloned pMo130Δ*ltg* constructs were used to transform a donor *E. coli* strain S17-1(λpir) by electroporation for use in conjugations.

Repeated attempts were made to generate pMo130Δ*ltgA* but all were unsuccessful. Only one flanking region was successfully inserted into the suicide vector. Given that positive transformants were confirmed by diagnostic digest it may be possible that there was insertion of the second flanking region but the *Xba*I site used in this cloning may have been methylated and thus would not have been digested resulting in a negative diagnostic digest. To negate this, future cloning could incorporate an alternative restriction site into the flanking region, a neighbouring restriction site could be used in diagnostic digests, an alternative screening method could be used such as colony PCR in combination with sequencing or a methylase negative cloning strain could be used.

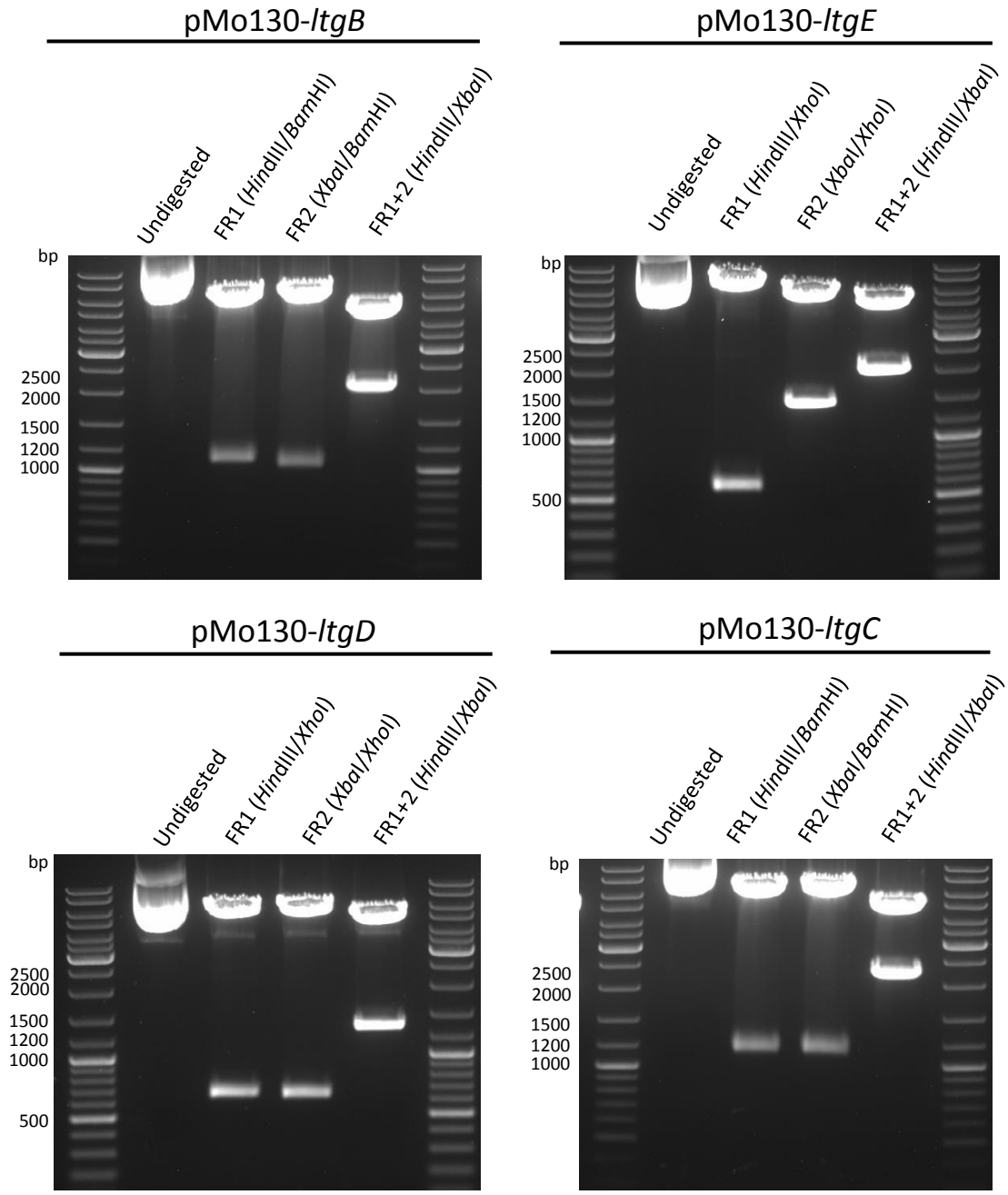

Figure 22: **Diagnostic digests of plasmids for use in allelic exchange to generate Ltg deletion mutants in *B. pseudomallei* K96243.**

Upstream (FR1) and downstream (FR2) flanking regions were cloned into the suicide plasmid pMo130. Diagnostic were performed to show the presence of FR1, FR2 and ligation of FRI and FR2. Expected sizes – **LtgB;** FR1-1056bp, FR2-1021bp, FR1+2-2071bp **LtgC;** FR1-1135bp, FR2-1126bp, FR1+2-2261bp **LtgD;** FR1-663bp, FR2-658bp, FR1+2- 1315bp **LtgE;** FR1-580bp, FR2-1385bp, FR1+2-1959bp

4.4.2. Generation and confirmation of *ltg* deletion mutants

ltg mutants were confirmed by PCR and/or Southern blot. A schematic for this screening process can be seen in Figure 23. Initially conjugations were performed for allelic exchange to generate four single Ltg mutants (Δ*ltgB*, Δ*ltgC*, Δ*ltgD* and Δ*ltgE*). The total number of single crossover (SCO) colonies was; Δ*ltgB* SCO - 6, Δ*ltgC* SCO - 12 , Δ*ltgD* SCO - 13, Δ*ltgE* SCO – 6. *Sac*B selection was used to select for double cross over mutants. The number of mutant genotype for the screened double cross overs was; Δ*ltgB* – 20/20, Δ*ltgC* – 5/8 , Δ*ltgD* – 4/20, Δ*ltgE*–1/30. All remaining colonies were either wildtype or resulted in incorrect/unusual PCR products. Multiple mutants were made following the same process using single mutants as the recipient strain. A list of all mutants generated can be found in (Appendix 8.3) . PCR screening, sequencing and Southern blots were all utilised to confirm the presence of the mutation. PCR screening utilised primers between 200 and 400 bp upstream and downstream of the gene of interest which produced PCR products of approximately 400-600bp and 1-2kb for wildtype and *ltg* mutant strains respectively. PCRs using gene specific primers were also performed to demonstrate excision of the gene.

For Southern blots probes were generated using the flanking region 1 (upstream flank) for Δ*ltgB* and Δ*ltgE* and flanking region 2 (downstream flank) for Δ*ltgD*. Wildtype and Δ*ltgB* gDNA was digested with the restriction enzymes *Bam*HI and *Age*I and all bands were of the expected size. Wildtype and Δ*ltgE* gDNA was digested with the restriction enzymes *Bgl*II, *Bam*HI and *Acl*I and all bands were of the expected size. Wildtype and Δ*ltgD* gDNA was digested with the restriction enzymes *Cla*I and *Pst*I. *Cla*I band sizes were as expected however *Pst*I band sizes were higher than expected. There was a decrease in size for the mutant, which does support evidence that the mutant was successfully created. Possible reasons for the unexpected sizes are the presence of a single nucleotide polymorphism in the K96243 strain being used compared to the annotated strain and thus the absence of the expected restriction site, methylation of the *Pst*I site, incomplete digestion of gDNA, a mistake and an alternative restriction enzyme was added instead of *Pst*I although this is unlikely. A Southern blot for Δ*ltgC* was not completed but PCR and sequencing show this mutant was successfully generated. Confirmation of the generation of Δ*ltgB,* Δ*ltgC*, Δ*ltgD* and Δ*ltgE* by PCR and

Southern blot can be seen in Figure 24, Figure 25, Figure 26 and Figure 27 respectively Confirmation of the generation of multiple *ltg* deletion mutants can be seen in Figure 28.

B. pseudomallei has the ability to produce multiple colony morphologies (118) which have varying phenotypes including motility, LPS, secretome, pathogenicity for example. Double cross over mutants were selected that had the same colony morphology therefore any differences observed in the characterisation studies were due to excision of the gene rather than natural colony morphology variation.

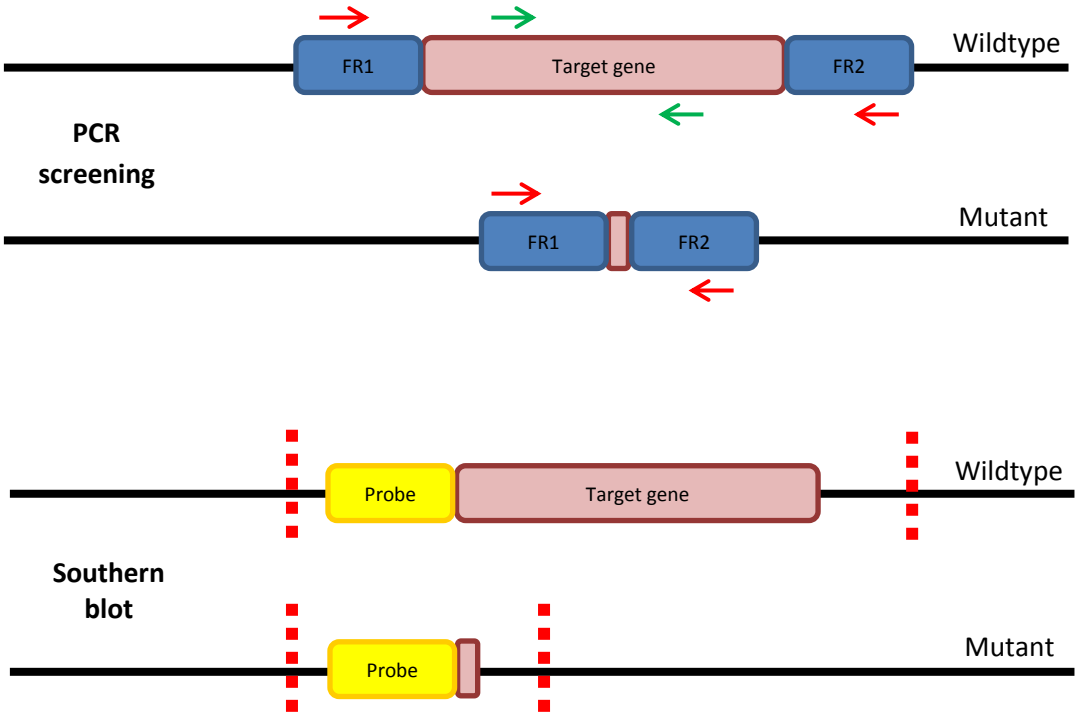

Figure 23: Schematic of PCR and Southern blot screening of deletion mutants.
PCR screening

Flanking region primers (red arrows) are used to PCR amplify a region outside of the target gene. Gene specific primers (green arrows) are used to PCR amplify a region of DNA only found within the target gene. Deletion of this gene results in a negative reaction as the primer binding sites are lost. **Southern blot screening**; gDNA is digested using specific restriction sites (demonstrated as red dotted lines) and probed using a DIG-labelled probe. Deletion of the gene results in smaller digested products which can be visualised by Southern blot using Anti-DIG antibodies.

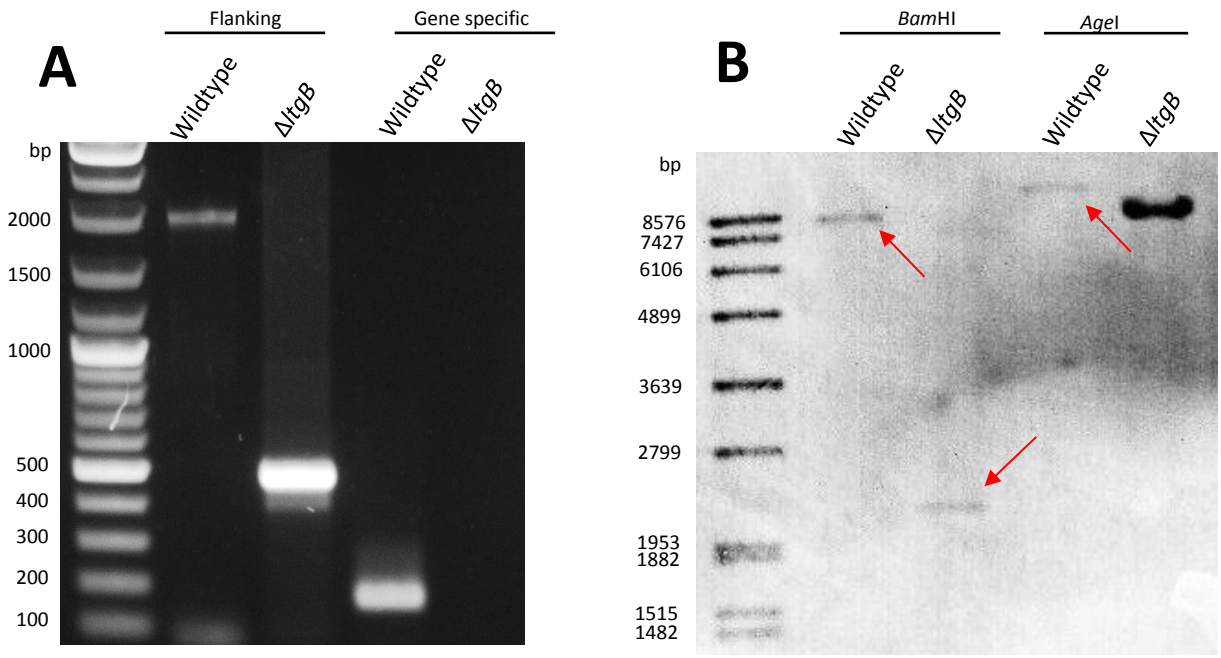

PCR Screening	Wildtype	Δ*ltgB*
Flanking (screening primers)	1943bp	475bp
Gene specific primers	170bp	No product

Southern Blot	Wildtype	Δ*ltgB*
***Bam*HI**	8kb	2.1kb
***Age*I**	9.9kb	8.4kb

Figure 24: Confirmation of *ltgB* mutation by Southern blot and PCR

A) PCR screens using flanking region primers and gene specific primers were performed. Wildtype and Δ*ltgB* gDNA was used as templates. Expected band sizes can be seen in the table above. **B) Southern blot** digested gDNA probed with DIG labelled Flanking region 1 (upstream flank) that was used to generate this mutant. Expected band sizes can be seen in the table above. Arrows have been added where bands may appear faint.

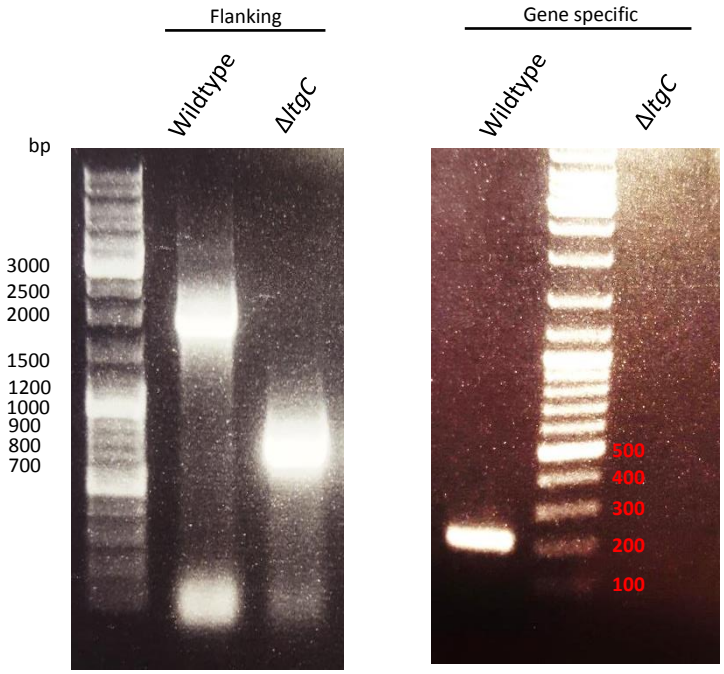

PCR Screening	Wildtype	Δ*ltgC*
Flanking (screening primers)	1846bp	710bp
Gene specific primers	208bp	No product

Figure 25: Confirmation of *ltgC* mutation by PCR

PCR screens using flanking region primers and gene specific primers were performed. Wildtype and Δ*ltgC* gDNA was used as templates. Expected band sizes can be seen in the table above.

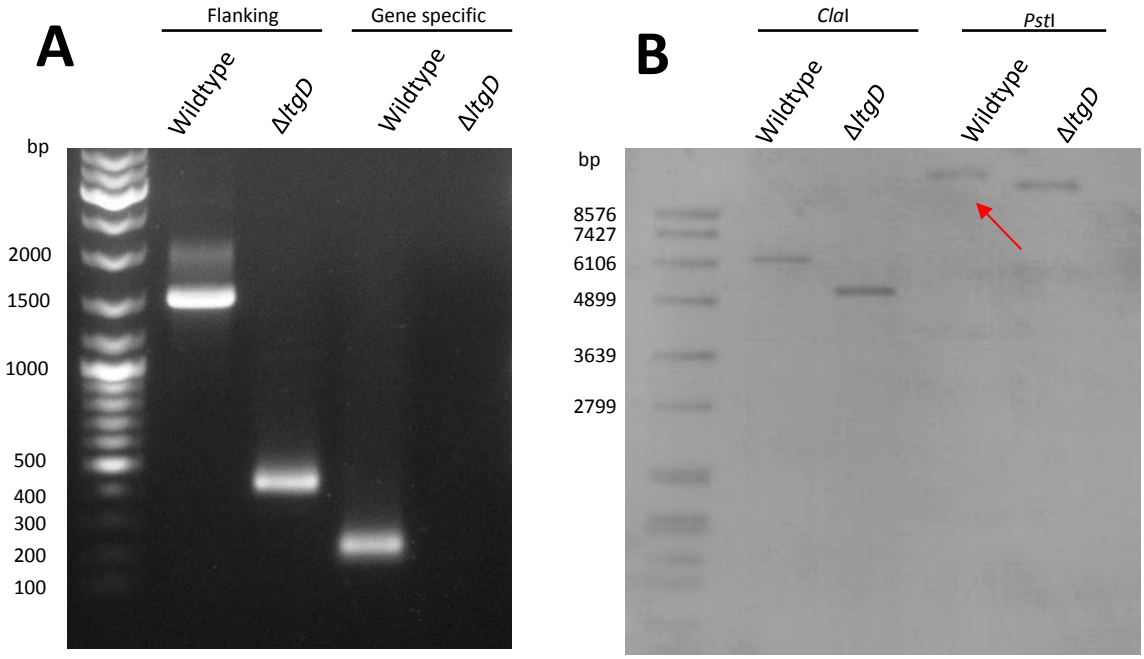

PCR Screening	Wildtype	Δ*ltgD*
Flanking (screening primers)	1461bp	405bp
Gene specific primers	230bp	No product

Southern Blot	Wildtype	Δ*ltgD*
ClaI	6.1kb	5.0kb
PstI	5.3kb	4.3kb

Figure 26: Confirmation of *ltgD* mutation by Southern blot and PCR

A) PCR screens using flanking region primers and gene specific primers were performed. Wildtype and Δ*ltgD* gDNA was used as templates. Expected band sizes can be seen in the table above. **B) Southern** blot digested gDNA probed with DIG labelled Flanking region 2 (downstream flank) that was used to generate this mutant. Expected band sizes can be seen in the table above. Arrows have been added where bands may appear faint.

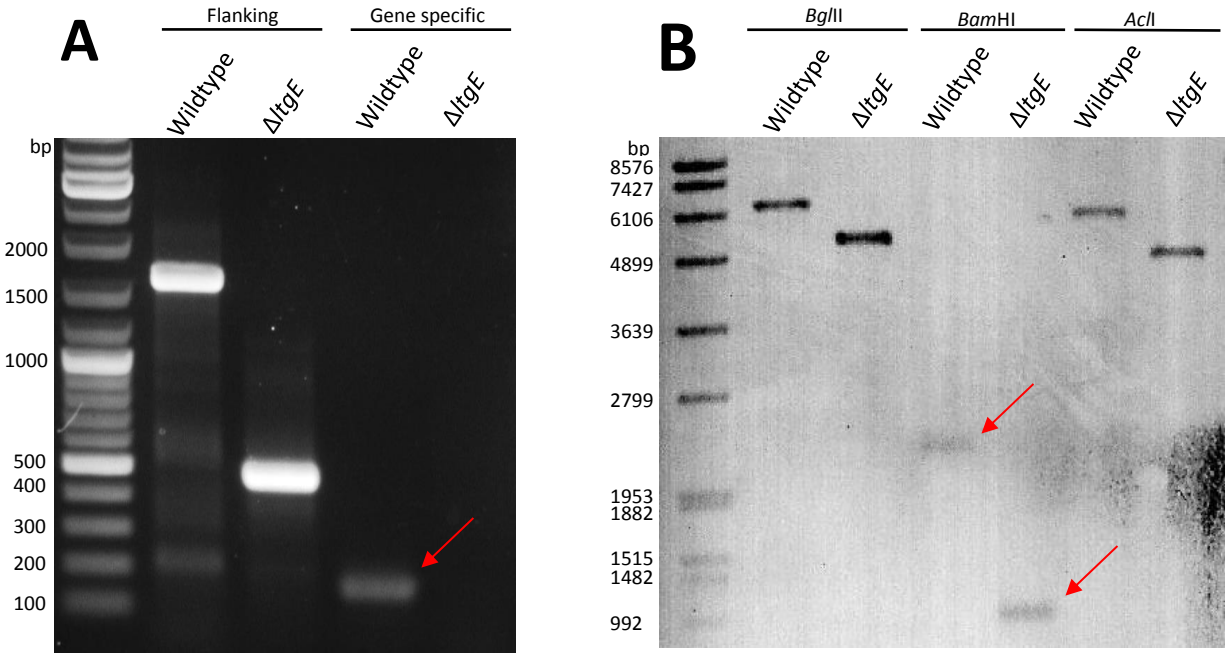

PCR Screening	Wildtype	Δ*ltgE*
Flanking (screening primers)	1571bp	478bp
Gene specific primers	150bp	No product

Southern Blot	Wildtype	Δ*ltgE*
BglII	6.3kb	5.1kb
BamHI	2.2kb	1.1kb
AclI	5.9kb	4.8kb

Figure 27: Confirmation of *ltgE* mutation by Southern blot and PCR

A) PCR screens using flanking region primers and gene specific primers were performed. Wildtype and Δ*ltgE* gDNA was used as templates. Expected band sizes can be seen in the table above. **B) Southern blot** digested gDNA probed with DIG labelled Flanking region 1 (upstream flank) that was used to generate this mutant. Expected band sizes can be seen in the table above. Arrows have been added where bands may appear faint.

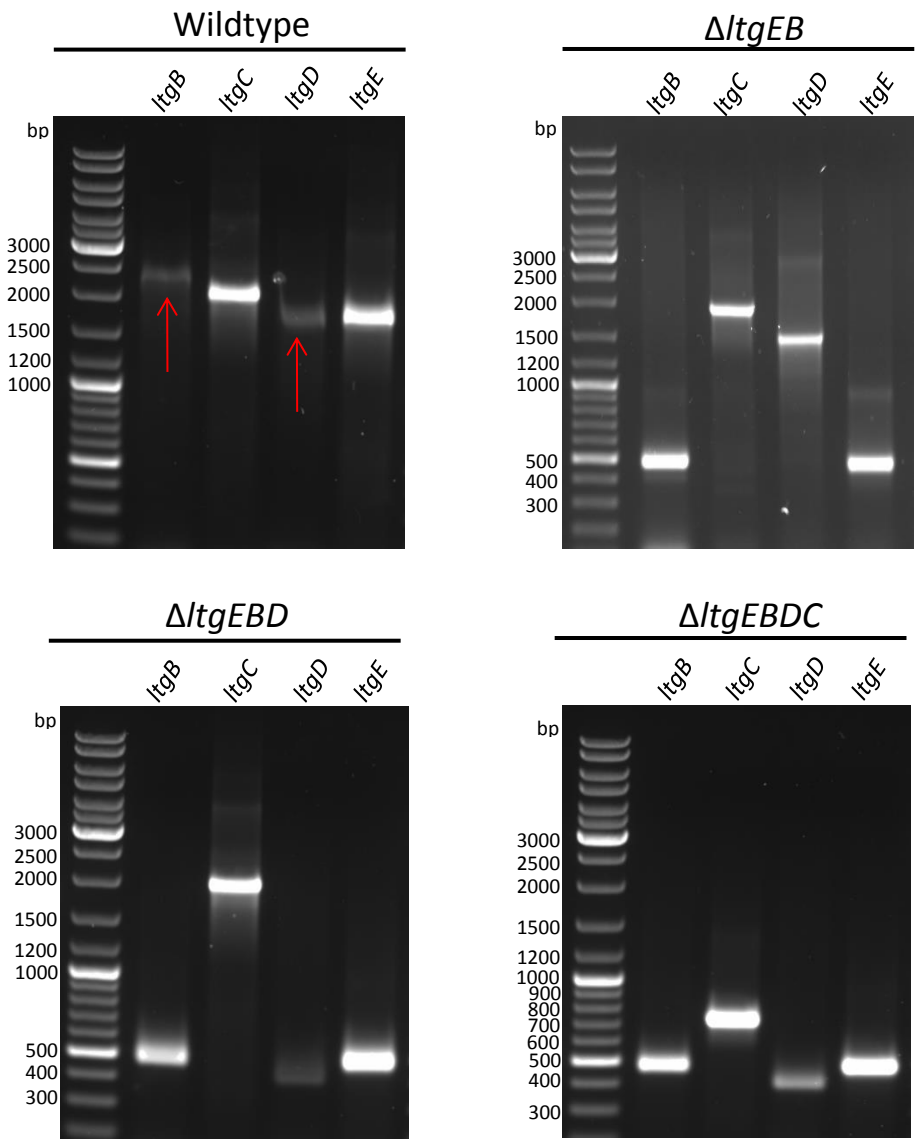

Figure 28: Confirmation of multiple *ltg* mutations by PCR

Gene regions were amplified using primers independent of the flanking regions used to generate mutants. PCR fragments were sequenced to further confirm the presence of the mutation. Wildtype, Δ*ltgEBD* and Δ*ltgEBDC* gDNA was used as templates. PCR product sizes expected; ***ΔltgB;*** wildtype 1943bp, Δ*ltgB* 475bp ***ΔltgC;*** wildtype 1846bp, Δ*ltgC* 716bp ***ΔltgD;*** wildtype 1461bp, Δ*ltgD* 405bp ***ΔltgE;*** wildtype 1571bp, Δ*ltgE* 478bp

4.4.3. Generation of *Burkholderia* strains overexpressing LtgE

In addition to generating *ltgE* mutants, *Burkholderia* strains overexpressing LtgE were generated. pMo168 is a low copy number plasmid with a kanamycin selection cassette. *ltgE* was cloned along with its native promoter to allow for overexpression of LtgE under wildtype conditions. The LtgE encoding region along with 250bp upstream containing putative promoter and ribosome binding site were PCR amplified from *B. pseudomallei* gDNA. This was cloned into the replicative vector pMo168. The ligation reaction was electroporated into S17-1(λpir). pMo168-*ltgE* plasmid DNA was purified and electroporated into *B. thailandensis* and *B. pseudomallei* K96243.

The *ltgE* encoding region was cloned into the IPTG inducible plasmid pME6032 studies. While cloning was successful, induction of this plasmid did not appear to result in expression of the gene even under very high IPTG concentrations, therefore this plasmid was disregarded in favour of the non-inducible plasmid pMo168-*ltgE* (data not shown).

4.4.4. Generation of Δ*ltgE* complementing strains

pMo168-*ltgE* was electroporated into Δ*ltgE* Δ*ltgEB*, Δl*tgEBD* and Δ*ltgEBDC* mutants for *in trans* complementation. Transformants were selected using LA-Kanamycin (800µg/ml). Δ*ltgE*::pMo168-*ltgE* was successfully created however overexpression of LtgE had a toxic effect on the multiple deletion mutants with either only very small colonies which could not be cultured or unsuccessful transformations occurring. As such *in cis* complementation was used to reintroduce a single copy of *ltgE* back onto the chromosome of Δ*ltgE* and multiple deletion mutants. *ltgE* with 200bp upstream region, containing the promoter and ribosome binding site, were cloned into the suicide vector pMo130. In addition to this, an upstream flanking region was cloned that allowed for integration of the plasmid onto the chromosome downstream of *bpsl3330*. This plasmid was designated pMo130::ltgEcomp. Unfortunately, despite multiple attempts, cloning of the downstream flanking region that would have allowed for the allelic exchange for insertion of the LtgE encoding region and removal of plasmid DNA was unsuccessful. As a control to ensure that complementation was not due to other plasmid components an *in cis* complemented control was also generated

in which the same suicide vector was integrated except without the *ltgE* encoding region (pMo130-comp control).

Chapter 3.3.2.3 showed that D343A point mutation could prevent recombinant LtgE activity. To investigate the effect of this mutation in complementation studies, pMo130-*ltgE*comp was used in a SDM reaction to replace the catalytic aspartate residue (D343) with alanine. Strains were produced expressing mutated version of LtgE (ΔltgE::pMo130-*ltgE* D343A and ΔltgEBDC::pMo130-*ltgE* D343A). All complemented strains generated can be seen in Appendix 8.3.

4.4.4.1. Semi-quantitative analysis of RNA expression.

To semi-quantify expression levels of *ltgE* in *ltgE* complemented strains, RT-PCR was set up using serial dilutions of RNA (1µg, 100ng, 10ng, 1ng). 16S gene specific primers were used as a positive control and a reverse transcriptase control confirming the samples were free from gDNA were also included. Results indicate that Δ*ltgE* mutant does not express *ltgE* supporting the PCR and Southern blot evidence. Secondly, both the complemented and SDM complemented strains express *ltgE*. Finally, expression levels appear to be similar across the wildtype and complemented strains. Controls show that there is expression of the housekeeping 16S gene, indicating RNA was added to the reactions and that there was no gDNA contamination as there were no bands present in controls (Figure 29).

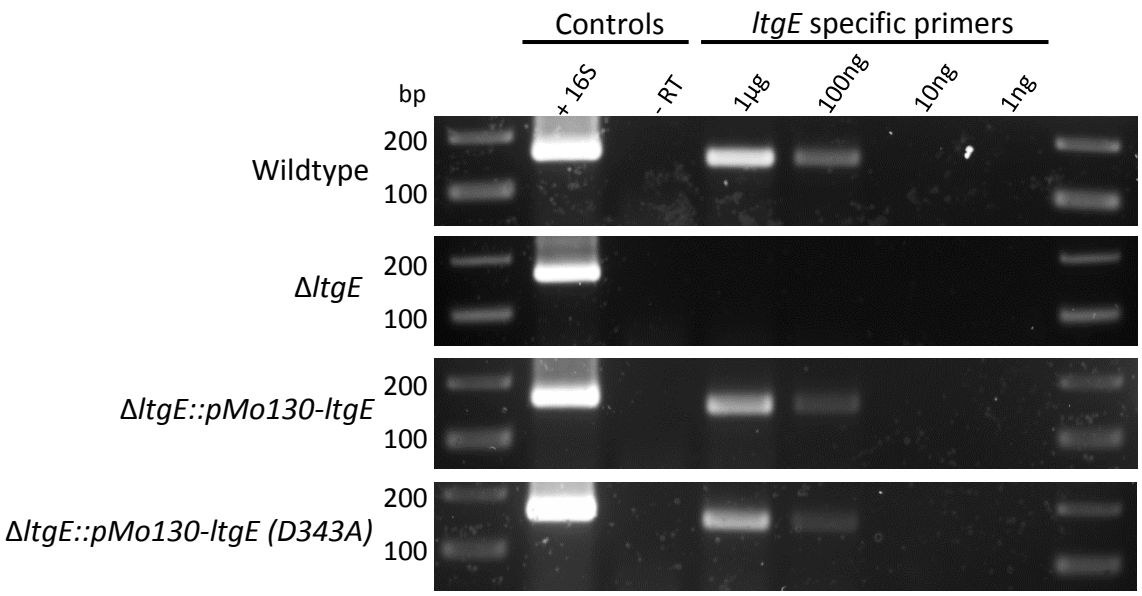

Figure 29 Reverse transcription PCR (RT-PCR) to show *ltgE* expression.

RNA was extracted from 20ml of *B. pseudomallei* culture (OD_{600} 0.4) using phenol: chloroform treatment. Samples were digested twice with DNAase and purified using RNAeasy columns to remove gDNA. RT-PCR was performed to generate cDNA using 16Srev primers and LtgE gene specific primers. 10 fold serial dilution of RNA were made with an initial concentration of 1µg of RNA. PCR was carried out using *ltgE* gene specific primers and 16S gene specific primers for the positive control (1µg RNA only for controls). Expression can be seen for wildtype, complemented mutant (Δ*ltgE*::pMo130-*ltgE*) and inactivated complemented mutant (Δ*ltgE*::pMo130-*ltgE* (D343A)). Dilutions reveal that expression levels appear to be equal for all strains. A reverse transcriptase control (-RT) shows that there is no contamination with gDNA.

4.5. Summary

Given the redundant nature of Ltgs, which has been demonstrated in other Gram negative bacteria including *E. coli* and *S. enterica* serovar Typhimurium (159, 177), it was unclear whether there would be significant phenotypes observed for individual *ltg* mutants. As such, multiple deletion strains were constructed. Four single *ltg* mutants were successfully generated the fifth, Δ*ltgA*, was unable to be generated due to multiple failed attempts to generate the suicide vector. Double, triple and quadruple mutants were also created along with *in cis* complementing strains. *B. thailandensis* and *B. pseudomallei* overexpressing LtgE were also generated.

There are potentially a huge number of bacterial functions that could be compromised by alteration of peptidoglycan. These include cell growth and division, capsule and LPS assembly, membrane permeability and virulence. In order to try and understand the role of these functions a number of phenotypes were tested. These were growth, cellular morphology and length (analysed by phase and scanning electron microscopy), motility, biofilm formation, minimum inhibitory concentrations and virulence in mice. Results of these phenotypic assays can be seen in Chapter 5.

Chapter 5

Phenotypic characterisation of *ltg* deletion mutants and overexpression strains

5.1. Introduction

Bacteria often possess multiple Ltg encoding genes indicating their importance. While it is likely that some of these Ltgs have highly specialist functions there is also potentially a high level of redundancy as has been seen for Ltgs of other bacterial species (155, 159, 177, 234). Such redundancy poses a substantial problem in identifying specific functions of an individual Ltg, as multiple gene knock out mutants may be required for a phenotypic difference to be seen. While, as far as we are aware, this is the first study into the function and importance of the Ltgs encoded by *B. pseudomallei* there are a number of studies of Ltg mutants in other bacteria. These include, but are not limited to *E. coli*, *P. aeruginosa*, *S. enterica* Serovar Typhimurium, *N. gonorrhoeae* and *H. pylori*. Ltg mutations in these bacteria result in variable phenotypes. For example, mutation of three *Ltg* genes in *E. coli* did not lead to any growth phenotypes (160), however mutation of six *ltg* genes led to the formation of small chains, indicating defects in cell division (158). Single and double Ltg mutants in 4 out of 8 Ltgs encoded by *P. aeruginosa* revealed either an increase or decrease in sensitivity to certain β-lactams depending on the Ltg involved, while the loss of four other Ltgs had no effect on antibiotic tolerance at all. This suggests that certain Ltgs may form part of protein complexes as well indicating that expression of Ltgs may occur at different stages of the cell cycle and at different locations and expression levels (185). This is not the only reported shift in antibiotic susceptibility of *ltg* mutants in Gram-negative bacteria. *E. coli* mutants lacking six Ltg genes were shown to have increased susceptibility to antibiotics that are typically poorly active against Gram-negative bacteria including erythromycin and vancomycin. It was also shown that Ltgs were needed for the induction of β-lactamase (235).

Ltg redundancy has also been reported in *S. enterica* Serovar Typhimurium in which two Ltgs (MltE and MltC) are involved, in combination, in the regulation of biofilm formation by altering expression of a master regulator, CsgS (177). Single deletions in the six remaining *ltgs* with all other double mutants, had no effect on biofilm formation. This *mltEC* double mutant also demonstrated a difference in morphology when grown in media lacking salt (low osmotic pressure). This was as result of incomplete cleavage of the peptidoglycan septum as well as increased cell membrane

permeability (177). This phenotype was also seen in a single *ltg* mutant, Δ*ltgC* (a homologue of *mltA*) of *N. gonorrhoea* which displayed incomplete separation of cells and exhibited abnormal growth patterns compared to wildtype cells (169). A double knock out mutant (Δ*ltgAD*) is required to prevent the release of peptidoglycan monomers, a feature of *N. gonorrhoea* infection. These mutations however, had no effect on growth or cell separation (236).

There are bacterial species that do not possess a large number of Ltgs. For example, *H. pylori* encodes genes for two Ltgs, *slt* and *mltD*. Single mutations made in both of these were shown to have non-redundant features with Δ*mltD* resulting in increased viability during stationary phase than both wildtype and Δ*slt* (179).

The effect of Ltg overexpression has been shown in *S. enterica* Serovar Typhimurium in which six of its Ltgs were individually overexpressed. Overexpression of one Ltg, MltE, resulted in enhanced red dry and rough (rdar) colony morphology. The rdar morphology is associated with the biofilm mode of growth as well as desiccation resistance (177). Prolonged overexpression of MltE in *E. coli* resulted in chaining bacteria which were unable to complete division (181).

There are potentially a huge number of bacterial functions that could be compromised by alteration or modification of peptidoglycan structure. These include cell growth and division, capsule and LPS assembly, membrane permeability and virulence. In order to try and understand the functions of the *ltgs* of *B. pseudomallei* a number of phenotypes were tested. These were growth, cellular morphology and length (analysed by phase contrast and scanning electron microscopy), motility, biofilm formation, minimum inhibitory concentrations and virulence in BALB/c mice.

5.2. Chapter aims

- Characterise the effect of *ltg* mutations on *B. pseudomallei* growth, morphology, motility, biofilm formation, antibiotic susceptibility and virulence in BALB/c mice.
- Investigate the effect of LtgE overexpression on *B. thailandensis* and *B. pseudomallei* using growth curves and phase contrast microscopy.

5.3. Materials and methods

5.3.1. Analysis of *B. pseudomallei* growth

Overnight cultures of wildtype and *ltg* mutant strains were grown and subcultured (in triplicate) into 5ml of LB (1:100 inoculum). Cultures were incubated at 37°C, with shaking (150rpm). OD_{600} readings (CO8000 Cell Density Meter, VWR) and CFU counts were measured at regular intervals. Growth experiments were repeated twice and data combined.

5.3.2. Overexpression of LtgE in *B. thailandensis* E555 and *B. pseudomallei* K96243

B. thailandensis E555 pMo168 and pMo168-*ltgE* were grown in LB-Kan (800µg/ml) for 48 hours OD_{600} readings were measured every 30 minutes. Following this bacteria were lysed in sample buffer for analysis of protein expression by SDS-PAGE and Western blot using Anti-LtgE IgG antibodies. Cells were fixed in 4% w/v paraformaldehyde (PFA) overnight and visualised by phase contrast microscopy. *B. pseudomallei*::pMo168 and pMo168-*ltgE* were also grown in LB-Kan (800µg/ml) for 48 hours before fixation in 4% PFA and phase contrast microscopy.

5.3.3. Analysis of bacterial cell length using phase contrast microscopy

Overnight cultures of *B. pseudomallei* wildtype and *ltg* mutant strains were grown in LB to an OD_{600} 0.8 and fixed overnight in 4% (w/v) PFA. Phase contrast microscopy was performed using a Nikon Eclipse Ni-E microscope and bacterial cell length was measured at x1000 magnification using NIS-Elements software. Bacteria were measured in 20 fields of view; any bacteria in which the poles were not visible/dubious were disregarded. The mean length, standard error and standard deviation were measured for each strain.

5.3.4. Preparation and visualisation of *ltg* mutants by Scanning Electron Microscopy (SEM)

Overnight cultures of *B. pseudomallei* wildtype and *ltg* mutants were grown in LB to an OD_{600} of 0.8. Cells were washed in PBS before fixation in 2.5% v/v glutaraldehyde in PBS for 24 hours. Fixative was removed by two washes in PBS. 50µl of the sample was added to a small glass coverslip treated with Poly-L-Lysine for 10 minutes. A secondary fixation was carried out in 1% w/v osmium tetroxide for 90 minutes. Samples were washed in deionised water several times followed by subsequent 30 minute washes in 30%, 50%, 70% and 90% v/v ethanol. Two final 30 minute washes in 100% analytical grade ethanol were performed. The slides were washed in 3:1 ethanol/hexamethyldisilazane (HMDS) for 30 minutes followed by 1:3 ethanol/HMDS for 30 minutes and finally 100% HMDS for 30 minutes (twice). Excess HDMS was removed and allowed to air dry (in fume cupboard) overnight. Slides were mounted and sputter coated in gold (Emitech SC7640 sputter coater, 90 seconds, 20mA Au). Bacteria were viewed on a Hitachi S3000H Scanning electron microscope with an accelerating voltage of 10kV.

5.3.5. Minimum inhibitory concentration (MIC) assays

Overnight cultures of *B. pseudomallei* wildtype and *ltg* mutants were grown in Muller Hinton broth overnight before subculturing (1:100) and growing for 2 hours at 37°C. Cultures were diluted (1:10) and used to inoculate 96 well microtiter plates containing 2 fold serial diluted wells of a 96 well plate containing the appropriate antibiotics; ceftazidime, co-trimaxazole, doxycycline, meropenem, imipenem or carbenicillin (Sigma Aldrich) with a final inoculum of 10^5 bacteria per well (confirmed by CFU counts). Plates were sealed and statically incubated for 24 hours at 37°C before MIC results were recorded. The MIC was the lowest concentration for which there was no growth. Experiments were repeated 3 times.

5.3.6. Analysis of *B. pseudomallei* motility

Overnight cultures of *B. pseudomallei* wildtype and *ltg* mutants were grown in LB and subcultured 1:10 for 2 hours. 1ml of each culture was centrifuged and washed in PBS. Optical densities were adjusted so they were ±0.01. Swimming and twitching motility plates were inoculated by touching a sterile tip into prepared culture and stabbed into an appropriate agar plate. Swimming plates were incubated at 30°C for 24 hours.

Twitching plates were incubated at 37°C for 24 hours. Swarming plates were inoculated from a swimming plate that had been incubated for 24 hours and incubated at 37°C for 16 hours. Halo radii were measured.

5.3.7. Biofilm formation

Overnight cultures of *B. pseudomallei* wildtype and *ltg* mutants were grown in LB and subcultured 1:10 for 2 hours. 8 wells of a 96 well plate were inoculated with 100µl of each strain. Plates were sealed and incubated at 30°C for 72 hours. Non-adhered planktonic cells were carefully removed and wells washed once in distilled water. 125µl of 1% w/v crystal violet was added carefully to each well and incubated at room temperature for 20 minutes. Excess dye was removed and the wells washed twice in distilled water. 300µl of ethanol was added to each well and repeatedly pipetted to resuspend the dye. Plates were incubated on a gently rocking platform for 30 minutes. Crystal violet absorbance was measured at 590nm. Experiments were repeated 4 times the data combined and standard error calculated.

5.3.8. Assessment of mutant virulence using BALB/C mouse model

5.3.8.1. Preparation of *B. pseudomallei* for bacterial challenges

B. pseudomallei median lethal dose (MLD) study

10µL of wildtype *B. pseudomallei* K96243 was inoculated from frozen stock into 50ml LB. Cultures were incubated with shaking at 180rpm at 37°C overnight. After overnight growth the OD_{600} was measured and adjusted to 0.4 to provide a starting inoculum of approximately 10^8 CFU/ml. The culture was serially diluted in PBS to provide challenge doses of $1x10^1$, $1x10^2$, $1x10^3$, $1x10^4$, $1x10^5$ and $1x10^6$ CFU. 5 mice were challenged per group.

Ltg mutant virulence study

10 µL of *B. pseudomallei* K96243 strains (**First study**; wildtype, Δ*ltgB*, Δ*ltgC*, Δ*ltgD*, Δ*ltgE*, Δ*ltgE*::pMo130-*ltgE*, Δ*ltgEBDC* and Δ*ltgEBDC*::pMo130-*ltgE*. **Second study**; wildtype, Δ*ltgE* and Δ*ltgE*::pMo130-*ltgE*) was inoculated from frozen stock into 50ml LB or LB-Kan (800µg/ml). Cultures were incubated with shaking at 180rpm at 37°C overnight. After overnight growth the OD_{600} was measured and adjusted to 0.38 and

serially diluted in PBS to provide a challenge dose of approximately 5 x 10^3 CFU (first study) or 1 x 10^4 CFU (second study). The neat culture was diluted 2 fold in PBS for the first animal experiment (to give approximately 5x10^7 CFU/ml) and used undiluted in the second experiment. A 10 fold dilution series into PBS was prepared for both experiments and the 10^{-3} was used as the prepared inoculum. CFU counts were confirmed through multiple trials before preparing the challenge for mice.

5.3.8.2. Challenges

All murine infections were carried out at Defence Science and Technology Laboratory (Dstl, Porton Down, Salisbury Wiltshire, UK) under the Animal (Scientific Procedures) Act 1986. Predetermined humane end points were employed where possible and animals were culled via cervical dislocation in accordance with schedule 1 of the Animal (Scientific Procedures) Act 1986. 6-8 week old female BALB/c mice (Charles River) were caged in groups of 5 in an isolator and allowed to acclimatise for at least 7 days.

Mice were challenged with 100µl from the prepared inoculum via the IP route. For the MLD study 5 mice were challenged per group and for the *ltg* mutant studies 10 mice were used per group. CFU counts were confirmed by plating onto LA plates. The mice were observed twice daily (or more where necessary) for signs of infection and mortality for 35 days. At day 35 all remaining survivors were culled and the spleen, liver and lungs were removed. The organs were weighed and homogenised through a 40µm cell strainer (FisherScientific) into 1ml PBS. The homogenate was 10 fold serially diluted into PBS and 2 times 100µl strips were streaked onto LA plates. Plates were incubated for 72 hours at 37°C. An average count was recorded and CFU/ml calculated. CFU/g was calculated by dividing CFU/ml by weight of the organ. The remaining homogenate was added to 10ml LB and incubated statically at 37°C for 7 days before checking for *B. pseudomallei* growth by performing a streak onto LA.

5.3.9. Statistical analysis

Mean, standard deviation and standard error were calculated using Microsoft Excel software. Statistical analysis was performed using Graphpad Prism. Motility, biofilm and cell length analysis were analysed using one way ANOVA to compare each mutant against wildtype or unpaired T-test when comparing two strains only. Logrank test was

used to compare survival data for mouse studies. Mann-Whitney tests were used to compare bacterial counts found in organs between each strain.

5.4. Results

5.4.1. Single *ltg* deletions do not affect growth of *B. pseudomallei*

Before more complex phenotypic characterisation, it was essential to test potential growth defects in the *ltg* mutants. This was assessed by performing growth curves on *B. pseudomallei* wildtype, Δ*ltgB*, Δ*ltgC,* Δ*ltgD,* Δ*ltgE* and Δ*ltgEBDC*. Strains were inoculated from an overnight stock into fresh media and the OD and CFU counts were measured at regular time points over the course of 48 hours.

Results showed that growth, measured by optical density, did not reveal any differences between wildtype and any of the *ltg* mutants (Figure 30A). In order to assess doubling time of the strains the data set was narrowed to exponential phase with time points 2 and 4 hours chosen. Doubling times were calculated using Graphpad prism using nonlinear exponential growth equation and were; wildtype - 0.8614 hours (51 mins), Δ*ltgB* - 0.7614 hours (45 mins), Δ*ltgC* - 0.8038 hours (48 mins), Δ*ltgD* - 0.7829 hours (49 mins), Δ*ltgE* - 0.7686 (46.2mins), Δ*ltgEBDC* 0.8243 (49 mins). While this is not unexpected for single mutants it is surprising that the removal of four important cell wall modifying enzymes, as in Δ*ltgEBDC.*

CFU counts revealed a 2 fold decrease in growth between wildtype and Δ*ltgEBDC* throughout the duration of the experiment. While initial inoculum volume was the same for both wildtype and Δ*ltgEBDC*, the starting CFU count was 2 fold lower for Δ*ltgEBDC*. This was seen in repeat experiments. Colony morphology did not appear to be affected in any of the single *ltg* mutants. However, Δ*ltgEBDC* produced smaller colonies (Figure 30B) than wildtype and required approximately 24 hours of additional incubation before colonies were countable. The reduced CFU count and the smaller colonies suggest a growth defect that could not be assessed using OD readings. Such results could be explained by morphological differences between wildtype and Δ*ltgEBDC* which may alter light scattering in OD readings of Δ*ltgEBDC* cultures.

In order to calculate the doubling time for the growth curve measured by CFU two approaches were used. The first used linear regression to generate an equation of a straight line (y=mx+c) which was used to generate the doubling time using set CFU counts. The second was to use non-linear regression using an exponential growth equation. Both analyses were performed using Graphpad prism.

For the first method only time points from the exponential phase were used. The time points chosen were 3, 6 and 7.5 hour as following this the cultures were in stationary phase. To generate a linear regression (y=mx+c) for both curves the data was log transformed using the equation Y=Log(Y). Analysis using linear regression was performed to generate the equations; Wildtype (Y = 0.2621*X + 6.991) and Δ*ltgEBDC* (Y = 0.2601*X + 6.449) where Y is the CFU count, and X is time (hours). By rearranging the equations it was possible to work out, given set CFU counts of $1x10^7$ and $2x10^7$, the doubling time of the strains. The doubling time of wildtype was 1.149 hours (1hr 9min 25sec) and the doubling time for Δ*ltgEBDC* was 1.157 hours (1hr 8 min 56sec). Using this method there is no difference between the growth rates of the two strains. It is therefore unclear why there is consistently a two fold differences across the growth curve.

The second method used the raw, non-transformed data, the growth rate constant (K values) were calculated to be 0.5345 and 0.7974 for wildtype and Δ*ltgEBDC* respectively. The doubling times (ln(2)/K) to be wildtype; 1.297 hours (1hr 17mins) and Δ*ltgEBDC*; 0.8693 hours (52 mins). This would suggest that the doubling time of the mutant was actually quicker than the wildtype in the exponential growth phase.

Overall, the results indicated that deletion in individual *ltg* genes does not result in growth defects as measured by doubling time (by OD) with values of between 45-51 minutes. CFU counts reveal that Δ*ltgEBDC* does not have a growth defect when calculating doubling time using linear regression equation and perhaps even quicker growth when calculating doubling time using an exponential growth equation. This then presents problems explaining why Δ*ltgEBDC* is consistently lower in counts throughout the duration of the experiment. It may be that the transition from liquid

media to solid media cause stress on a portion of the population resulting in the lower CFU counts. More time points are needed before a more accurate picture can be seen.

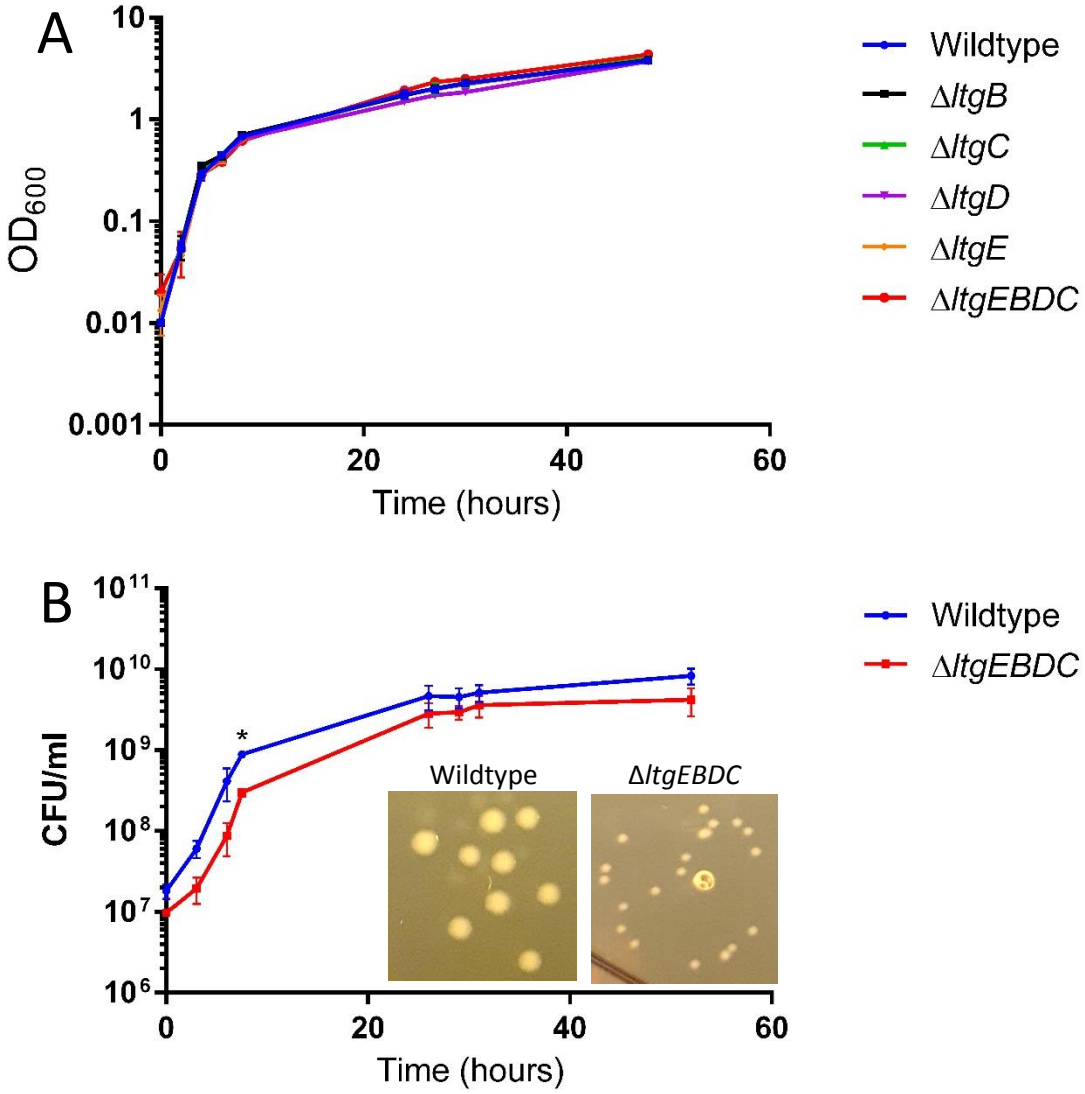

Figure 30: Growth curves of *ltg* deletion mutants.

A) There is no difference between wildtype and *ltg* mutants when measuring growth by optical density. B) CFU counts were performed on wildtype and Δ*ltgEBDC*. Removal of four Ltgs results in slightly attenuated growth. Δ*ltgEBDC* colonies were smaller than wildtype for the first 24 hours (images were adjusted to accurately show colony sizes).

Graphs are the results of two independent experiments combined.* indicates an additional time point in one experiment.

5.4.2. Overexpression of LtgE results in a growth defect and elongated cell morphology in *B. thailandensis*

LtgE was overexpressed in *B. thailandensis E555* (*B. thailandensis*::pMo168-*ltgE*) to investigate the effect on cell growth and morphology. Overexpression of LtgE resulted in major growth defects in *B. thailandensis E555*. When compared to an empty plasmid control there was an apparent increase in log phase and a decreased exponential phase (Figure 31A). This resulted in approximately 50% reduction in OD during the stationary phase compared to the empty vector control. Overexpression of LtgE using pMo168-*ltgE* was confirmed by Western blot analysis using anti-LtgE polyclonal antibodies (Figure 31B).

Phase contrast microscopy of these strains revealed a significant alteration in cellular morphology. LtgE overexpressed *B. thailandensis* produced extremely elongated, filament like bacteria. This was likely due to increased cell length and a defect in cellular division. This difference in morphology can also be seen when LtgE is overexpressed in *B. pseudomallei* (Figure 31C).

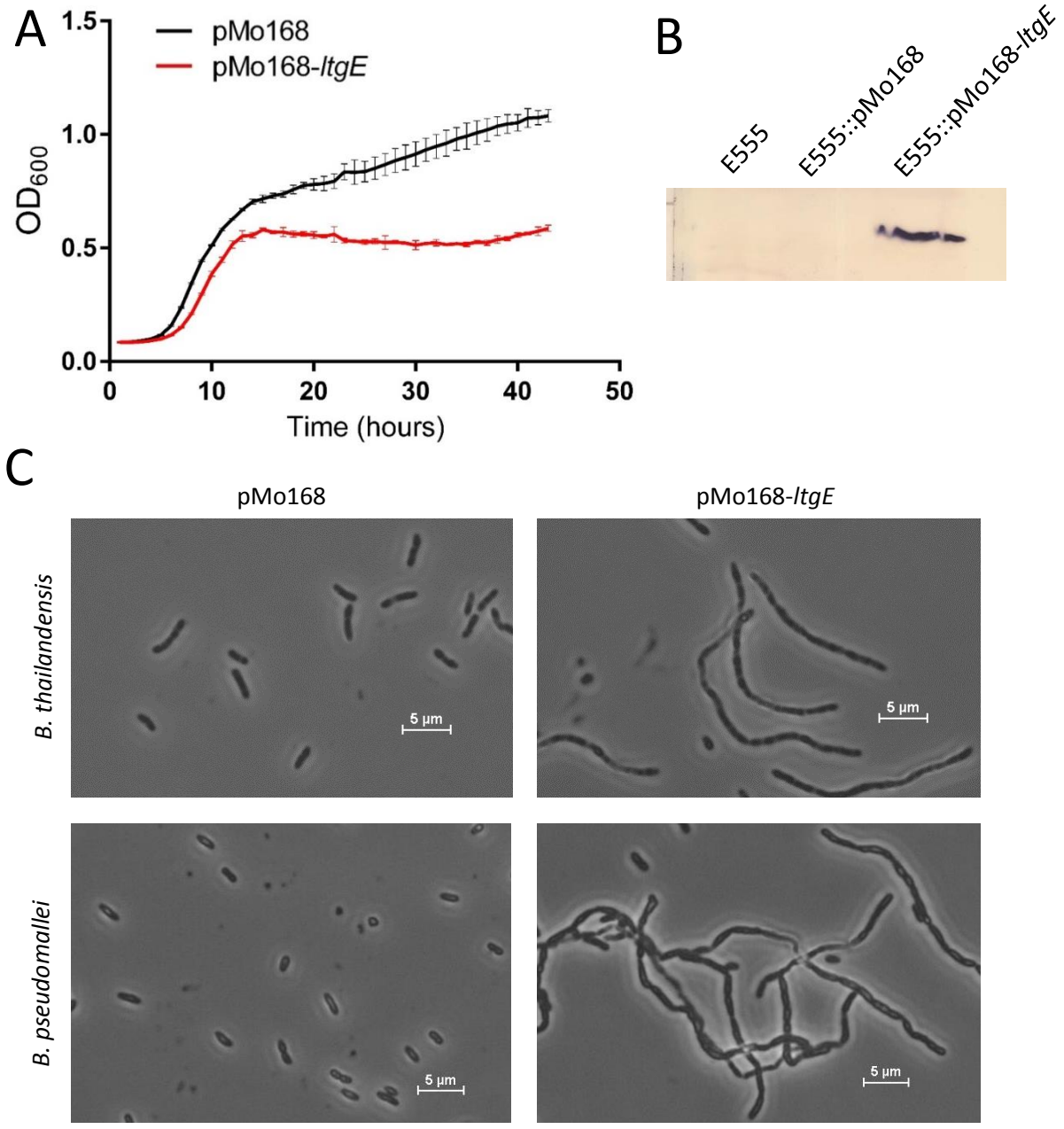

Figure 31: Overexpression of LtgE in *Burkholderia* inhibits growth and causes extreme cell elongation and chaining.

A) *B. thailandensis* E555 pMo168 and pMo168-*ltgE* were grown in LB-Kan (800µg/ml) for 48 hours with the OD measured every 30 minutes. Overexpression of LtgE causes a growth defect with an increase in the lag phase and a reduced exponential phase. B) Western blot using anti-LtgE antibodies confirms the expression of LtgE in *B. thailandensis* E555::pMo168-*ltgE* C) Cells were fixed in 4% PFA and visualised by phase microscopy. Morphological differences can be seen where bacteria form long, filament like chains. This phenotype could also be seen for *B. pseudomallei*.

5.4.3. Scanning Electron Microscopy revealed dramatic differences in the morphology of *ltg* mutants

SEM was used to visualise *ltg* mutants in much greater detail than phase contrast microscopy used for assessing LtgE overexpressing strains. Results show that cellular morphologies of Δ*ltgB*, Δ*ltgC* or Δ*ltgD* were the same as wildtype; with equal cell length and width and no obvious cell division defects. Cells also appear to be bipolar and rod shaped (Figure 32).

Δ*ltgE* does have morphological differences with elongation of cell length compared to wildtype cells. Furthermore, given that all strains were fixed during the exponential phase and thus are rapidly dividing, it appears that the Δ*ltgE* mutant has a defect in cell division which can be shown by the presence of thin sections between daughter cells (not observed in wildtype cells). Removal of multiple *ltg* genes extenuates these phenotypes with Δ*ltgEB* having further elongated cell length along with the presence of curved and twisted bacteria (Figure 32). It would appear that with the removal of these *ltgs* the peptidoglycan is substantially altered and the rod shaped morphology of typical *B. pseudomallei* is lost. These twisted bacteria are also present in the triple mutant, Δ*ltgEBD,* although at a lower frequency. There is however, a substantial increase in the number of chaining bacteria suggesting an amplification of the cell division defect. Interestingly, the individual bacterial cells are not always uniform in length in these chains (Figure 32). Δ*ltgEBDC* were again longer in length with it often not possible to locate the poles cells. In addition, it became increasingly difficult to identify individual cells within chains suggesting almost total inhibition of septum formation (Figure 32). Δ*ltgBDC* does not have this extenuated cell length and defects in cell division with cells being almost wildtype in their morphology.

In cis complementation using *ltgE* could successfully prevent the chaining and division defects of Δ*ltgE* and this could be seen more prominently when used to complement Δ*ltgEBDC*. Δ*ltgEBDC::*pMo130-*ltgE* was restored to almost wildtype morphology with restored cell length and no obvious defects in cell division (absence of thin sections between daughter cells and reduced chaining). The morphology of Δ*ltgEBDC::*pMo130-*ltgE* appeared to be equivalent to Δ*ltgBDC*, as expected. This shows the importance of LtgE in terms of cellular morphology and cell division. It also highlights redundancy

with in the *ltg* genes with the most extenuated phenotypes seen only with multiple deletion mutants. Mutation of the catalytic aspartate residue (D343A) prevented complementation supporting data generated in recombinant protein assays (chapter 3.3.2.3). Δ*ltgEBDC::*pMo130 control cells had the same morphology as Δ*ltgEBDC* cells indicating that complementation was due to expression of *ltgE* and not to influencing factors on the plasmid backbone.

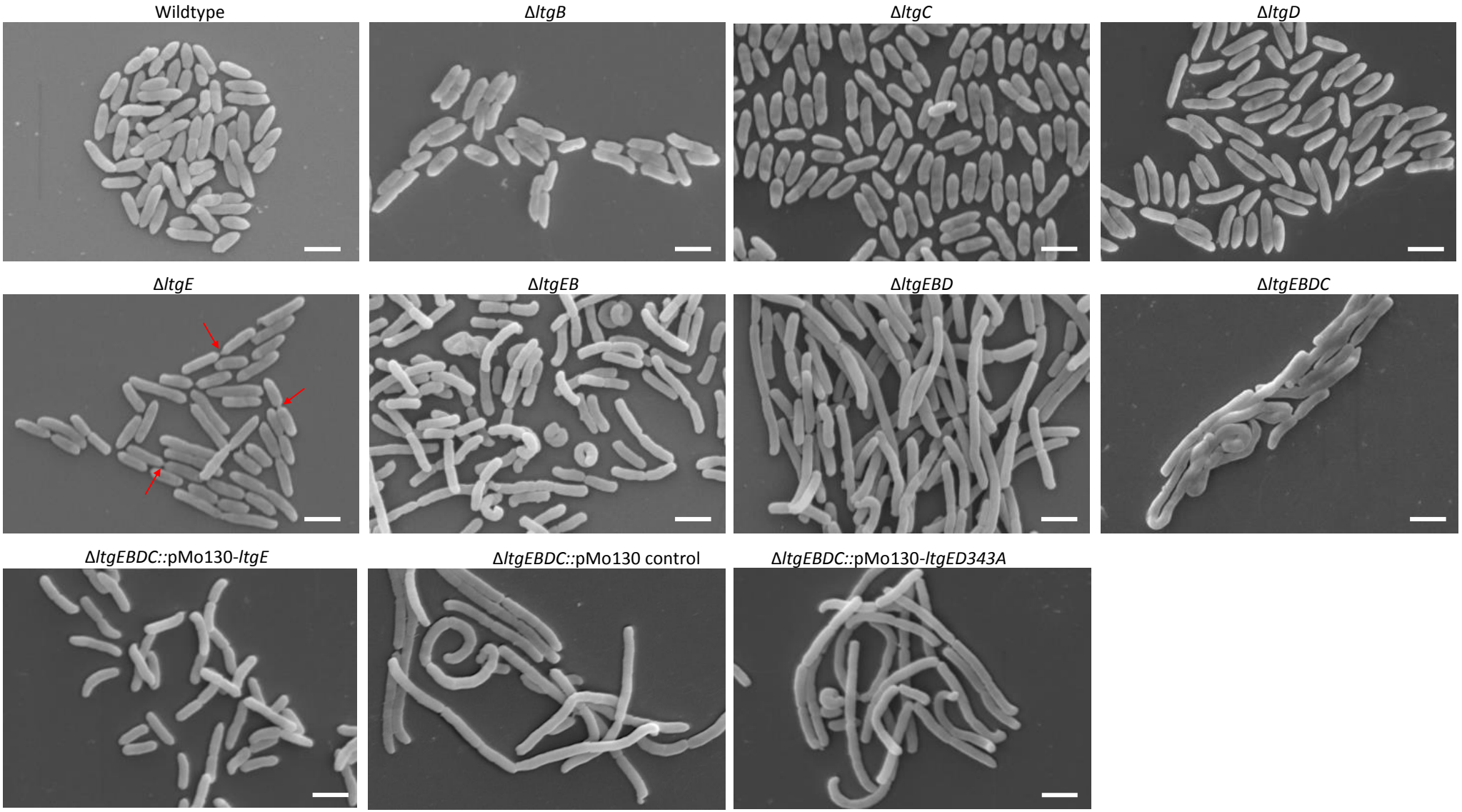

Figure 32: Scanning electron microscopy images of *ltg* mutants.

No major morphological differences can be seen between wildtype and Δ*ltgB,* Δ*ltgC* or Δ*ltgD*. Δ*ltgE* have an increase in cell length and thin sections between daughter cells suggesting incomplete cell division (see red arrows). Multiple deletion mutants results in chaining bacteria and increased individual cell length. Complementation could be achieved *in cis*. A Δ*ltgEBDC comp control* has no significant differences when compared to Δ*ltgEBDC* showing that integration of empty pMo130 does not result in any complementation. Mutation of catalytic aspartate 343 to alanine (D343A) prevents complementation. Scale bar - 2µm

5.4.4. Analysis of cell length using Phase contrast microscopy

To quantify the observations associated with mutating *ltgE* seen using SEM, phase contrast microscopy of wildtype, Δ*ltgE*, Δ*ltgEB* and Δ*ltgEBD,* Δ*ltgEBDC,* Δ*ltgDBC,* Δ*ltgE*::pMo130-*ltgE*comp, Δ*ltgEBDC*::pMo130-*ltgE*comp, Δ*ltgE*::pMo130-*ltg*Ecomp D343A, Δ*ltgEBDC*::pMo130-*ltgE*comp D343A and Δ*ltgEBDC*::pMo130-*ltgE*comp control mutants was performed to analyse overall cell length. The mean length and standard error of bacterial size can be seen in Figure 33.

Results show that for *ltgE* deletion mutants the mean length of bacteria increases with the each *ltg* deleted. Δ*ltgE* had a 50% increase in length compared to wildtype as expected given the increased cell length and defects in cell division seen by SEM. Removal of two *ltg* genes (Δ*ltgEB*) resulted in a mean cell length increasing by 85% compared to wildtype. Deletion of a third gene (Δ*ltgEBD*) resulted in a mean cell length of approximately 3 times that of the wildtype. Finally deletion of a fourth *ltg* (Δ*ltgEBDC)* increased the cell length further with a mean cell length 3.5 times that of wildtype cells. Comparison of Δ*ltgEBDC* to the complemented strain, Δ*ltgEBDC::*pMo130-*ltgE,* and with the triple mutant (Δ*ltgDBC*) shows that Δ*ltgEBDC::*pMo130-*ltgE* and Δ*ltgDBC* are of similar length and therefore, *ltgE* is responsible for this extended length and chaining phenotypes seen. Furthermore, the fact that the wildtype and the Δ*ltgDBC* mutant are only marginally different (2.3µm and 2.68 µm respectively) indicates that there is redundancy as the differences in elongation or division were only observed when in combination with the *ltgE* mutation. This is further evidence to suggest that *ltgE* plays an essential role in cell length and separation. The D343A point mutation prevented complementation, demonstrating that this residue is essential for the activity of the protein *in vitro*. The length of cells containing the *in cis* empty plasmid shows that integration of the plasmid backbone is not responsible for the complementation seen.

There is a large amount of deviation, particularly in the multiple deletion mutants due to the presence of vary variable lengths of bacteria, some being wildtype in size with others extraordinarily long. Shorter bacteria are likely to be as a result of division or shearing from a longer chain. However, given the large sample size it is clear that

removal of *ltgs* results in increased cell length, both through increased individual cell length and failure to complete division.

Strain	Mean cell length (St. dev.)	Minimum	Maximum	Number of bacteria measured
Wildtype	2.3 (0.6)	1.0	5.1	771
Δ*ltgE*	3.5 (1.1)	1.5	12.7	905
Δ*ltgEB*	4.3 (1.9)	1.5	21.9	1069
Δ*ltgEBD*	7.1 (3.6)	1.4	36.6	795
Δ*ltgEBDC*	7.98 (4.9)	2.02	45.44	1123
Δ*ltgE*-comp	2.21 (0.78)	0.87	7.72	1145
Δ*ltgEBDC*-comp	2.89 (1.38)	0.92	15.27	886
Δ*ltgBDC*	2.68(0.8)	1.25	8.52	805
Δ*ltgEBDC*-comp *ltgE* D343A	7.87 (4.91)	1.99	41.2	623
Δ*ltgEBDC*-comp control	7.8 (5.28)	1.75	37.69	787

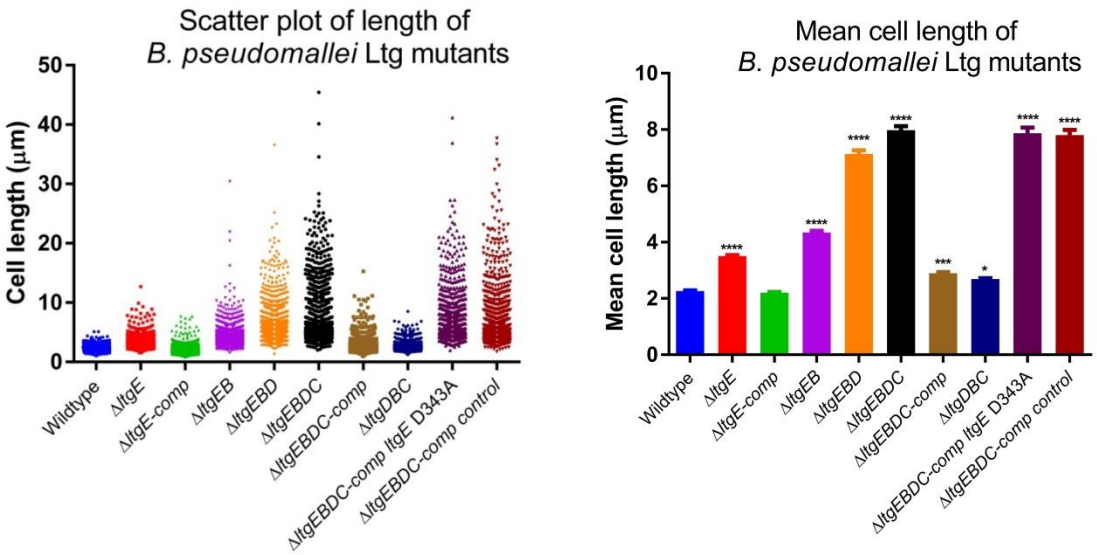

Figure 33 Bacterial length of *ltg* deletion mutants.

Strains were grown to an OD_{600} of 0.8 and fixed in 4% PFA. Cells were visualised by phase contrast microscopy and cell length measured for all bacteria in 20 fields of view. A scatter plot shows the wide spread of bacterial cell length, particularly in multiple *ltgE* deletion mutants. Standard error was used in the error bars in the mean cell length graph. Cell length increases with each *ltg* deletion but only in strains containing a mutation in *ltgE*. Complementation could restore wildtype cell length in Δ*ltgE* and could partially restore wildtype cell length in Δ*ltgEBDC::*pMo130-*ltg*E. Mutation of the catalytic site D343A prevents this complementation. * p<0.05 ***p<0.001 ****p<0.0001

5.4.5. Single *ltg* mutations impair swimming, swarming and twitching motility

The ability of bacteria to relocate itself, typically towards nutrients or away from toxic and harmful substances, is essential to its survival and often plays an important role in its virulence. There are three main mechanisms of motility - swimming, swarming and twitching. Swimming and swarming motility are flagella based methods; they differ in that swimming is motility in liquid media whereas swarming is motility across the surface, typically associated with movement across the surface of biofilms (237). Twitching motility is a result of extension, anchoring and retraction of type IV pili, important in adhesion to cells and colonisation, features important in virulence (238). By using plates containing varying concentrations of agar and of different nutrient composition it is possible to assess different types of motility.

Results from the swimming motility assay indicate that all four single *ltg* mutants have significantly reduced swimming motility when compared to wildtype. While the reduction in Δ*ltgB, ΔltgC* and *ΔltgD* (means of 13.3mm, 16.4mm, 16.3mm respectively compared to wildtype 18.5mm) is not dramatic there are reductions in motility. Whether this is direct (implications in flagella assembly) or indirect (result of alternative abnormalities such as cellular morphology) is unclear using this approach. Δ*ltgE* had a much greater reduction in swimming motility (mean radius of 7.3mm), a 40% reduction from wildtype (Figure 34A). Given the morphological defects of Δ*ltgE* it may be that these cells are unable to assemble the polar localised flagella, particularly where there are implications in cell division. *In-cis* complementation of *ltgE* restored wildtype phenotype. Δ*ltgEBDC* is effectively non-motile (mean radius of 3mm), with the halo being only marginally bigger than the inoculation site. Approximately 70% of wildtype swimming motility can be restored by *in cis* complementation with *ltgE* (13.4mm).

Swarming motility assays revealed that only Δ*ltgE* had significantly reduced swarming motility (mean radius 14.4 compared to wildtype 21.2mm), with individual mutations in the other *ltgs* not having a significant effect on motility (Figure 34B) and Δ*ltgEBDC* is again, non-motile (2.1mm). Given the difference between the mean radius of Δ*ltgE* and Δ*ltgEBDC* it is clear that there is redundancy within the Ltgs. There are only motility defects in mutants containing *ltgC*, *ltgD* and *ltgB* when in combination with

Δ*ltgE* therefore, loss of any of these genes can be compensated by the action of another, at least for swarming motility.

Given time constraints twitching motility was evaluated in a smaller number of mutants. Δ*ltgB* and Δ*ltgE* mutants appeared to have the greatest reduction in motility compared to wildtype (Figure 34C) with mean radii of 19.4mm and 16.6mm respectively compared to wildtype (21.4mm). Twitching motility is associated with type IV pili extension and retraction suggesting that implications for type IV pili assembly in these mutants. Δ*ltgD* did not have significantly different motility.

The swimming motility of various *ltgE* complemented and SDM mutants were also assessed (Figure 34D). The results show that complementation was not possible in the single Δ*ltgE* or multiple Δ*ltgEBDC* mutants when the catalytic aspartate residue (D343) was substituted for alanine. Integration of the pMo130-control plasmid had no effect on motility showing that complementation was solely due to the re-introduction of *ltgE.*

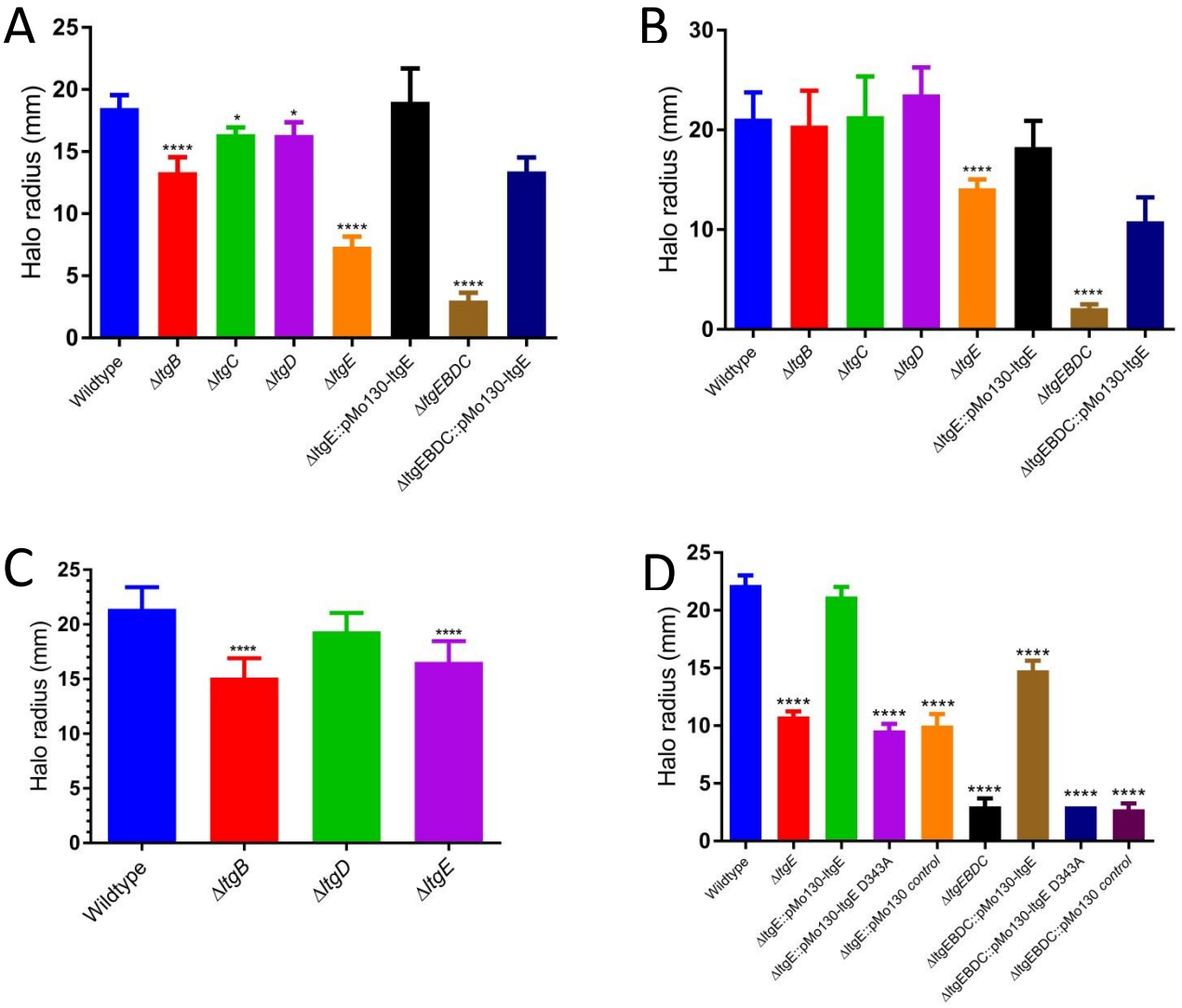

Figure 34; Motility of *ltg* deletion mutants.

A) All single *ltg* mutants have significantly reduced swimming motility. Δ*ltgE* has approximately 40% reduction in motility, which can be complemented *in cis* B) Δ*ltgE* is the only single deletion mutant with significantly reduced swarming motility. Δ*ltgEBDC* is immotile but 50% of wildtype motility can be complemented *in cis* using *ltgE*. C) Δ*ltgB* and Δ*ltgE* both demonstrate a small, but significantly reduced, twitching motility suggesting they could be involved with type IV pili assembly. D) Insertion of empty *in cis* complementing plasmid had no complementing effect in swimming motility; SDM mutation of catalytic residue (D343A) can prevent complementation.

A One-way ANOVA analysis was performed comparing Ltg mutant strains to wildtype (n=7), *p<0.05, ****p<0.0001.

5.4.6. *ltgB, ltgC* and *ltgD* play a significant role in biofilm formation.

A crystal violet based biofilm assay was optimised to find conditions in which maximum amount of biofilm was produced. Conditions included incubation temperature (30 and 37°C), tissue culture treated or non-tissue culture treated plates and incubation time (24, 48 or 72 hours). The greatest biofilm levels were found to be produced 30°C in tissue culture treated plates with incubation for 72 hours (data not shown). This condition was used in all subsequent experiments. Due to variation between individual experiments results of replicate experiments were combined and the standard error calculated.

These assays indicate that Δ*ltgB*, Δ*ltgC* and Δ*ltgD* all have a significant reduction in biofilm formation (Figure 35). It is unclear whether this is directly a decrease in the adherence and development of bacterial community on the surface of the well or if this community existed but was more loosely attached and thus was more easily removed than the wildtype strain during wash steps. Δ*ltgE* does not have significantly reduced biofilm compared to wildtype. Δ*ltgEBDC,* surprisingly, had approximately 95% increase in biofilm production; this increase can be restored to wildtype levels by *in cis* complementation with *ltgE*.

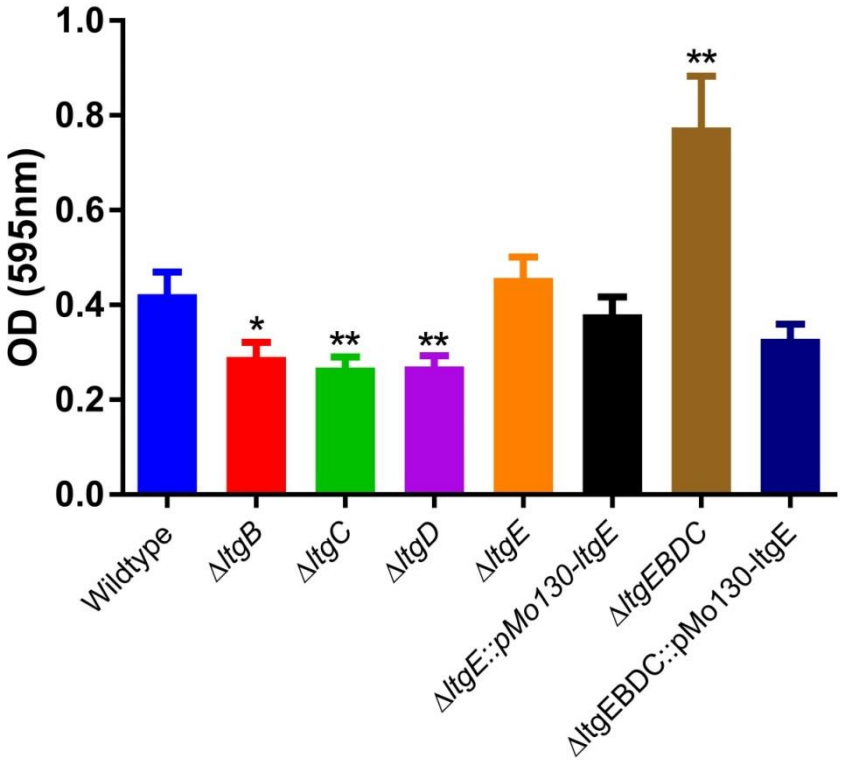

Figure 35: Formation of biofilms by *ltg* mutants

Crystal violet assays show that Δ*ltgB*, Δ*ltgC* and Δ*ltgD* all have significantly reduced biofilm formation. Δ*ltgEBDC* has significantly increased biofilm production, potentially due to aggregation of chained bacteria or settling of non-motile bacteria. Data shown in combined data from four independent experiments with 8 wells per strain per experiment, standard error bars are shown. A one way ANOVA statistical analysis was performed (comparison to wildtype). *p<0.05, **p<0.01.

5.4.7. Δ*ltgEBDC* has a small increase in sensitivity to carbenicillin, doxycycline and ceftazidime

It has been shown that mutation of *ltgs* can result in increased sensitivity to certain antibiotics (174, 235). *B. pseudomallei* is intrinsically resistant to many antibiotics causing a substantial problem in the treatment of melioidosis (239).To investigate whether disruption of the peptidoglycan layer and potential membrane integrity would to allow for increased uptake of antibiotic, MIC assays were performed. Six antibiotics (ceftazidime, meropenem, imipenem, carbenicillin, co-trimoxazole and doxycycline) were chosen, four of which are routinely used to treat melioidosis and two other cell wall targeting β-lactam antibiotics. Results of these MICs are shown in Table 3. Data shown is from replicate experiments recorded after 24 hours of incubation, from two replicate experiments with 4 replicate wells per experiment. All strains have equal sensitivity to meropenem, imipenem and co-trimoxazole (2µg/ml). There is a 2 fold difference between wildtype and Δ*ltgEBDC* for carbenicillin, doxycycline and ceftazidime. This difference is not as drastic as one might expect given the dramatic differences in cell morphology. Screens to test a wider range of compounds could be used to assess susceptibility to antibiotics and antimicrobial peptides not tested here.

	Wildtype	Δ*ltgB*	Δ*ltgC*	Δ*ltgD*	Δ*ltgE*	Δ*ltgEBDC*	ΔltgEBDC::pMo130-*ltgE*
Meropenem	2	2	2	2	2	2	2
Imipenem	1	1	1	1	1	1	1
Co-trimoxazole	64	64	64	64	64	64	64
Carbenicillin	1024	1024	1024	1024	1024	512	512
Doxycycline	2	2	2	2	2	1	1
Ceftazidime	16	16	16	16	16	8	8

Results are displayed as µg/ml

Table 3: MICs reveal a small increase in antibiotic sensitivity Δ*ltgEBDC*.

MICs show that single *ltg* mutants have no increased sensitivity to the antibiotics evaluated. There were two fold increases in sensitivity for the Δ*ltgEBDC* mutant for carbenicillin, doxycycline and ceftazidime. Results were reproducible and are displayed as average values from duplicate experiments (four replicate wells per experiment). Concentrations are in µg/ml.

5.4.8. Δ*ltgB*, Δ*ltgD and* Δ*ltgE* are attenuated in IP BALB/c model of melioidosis

An MLD study was performed to determine the MLD of the wildtype *B. pseudomallei* strain used to generate the *ltg* mutants. Multiple passages and repeated freeze thawing of glycerol stocks could result in decreased virulence compared to strains used in the literature. Wildtype challenges were prepared containing $1x10^6$, $1x10^5$ $1x10^4$, $1x10^3$, $1x10^2$ and $1x10^1$ CFU. 5 mice were challenged per group by the IP route and monitored over 35 days. Mice challenged with $1x10^4$ CFU, $1x10^5$ CFU and $1x10^6$ CFU all reached the humane end point by day 3 (with the exception of one mouse for $1x10^5$ CFU, which survived to day 26). Mice infected with the lower inoculums started to succumb to infection from day 20. By the end of the experiment there was the following survival rates; $1x10^3$ CFU – 40%, $1x10^2$ CFU 60%, $1x10^1$ CFU 60% (Figure 36). The MLD was calculated to be 150 CFU using the Reed and Muench method (240).

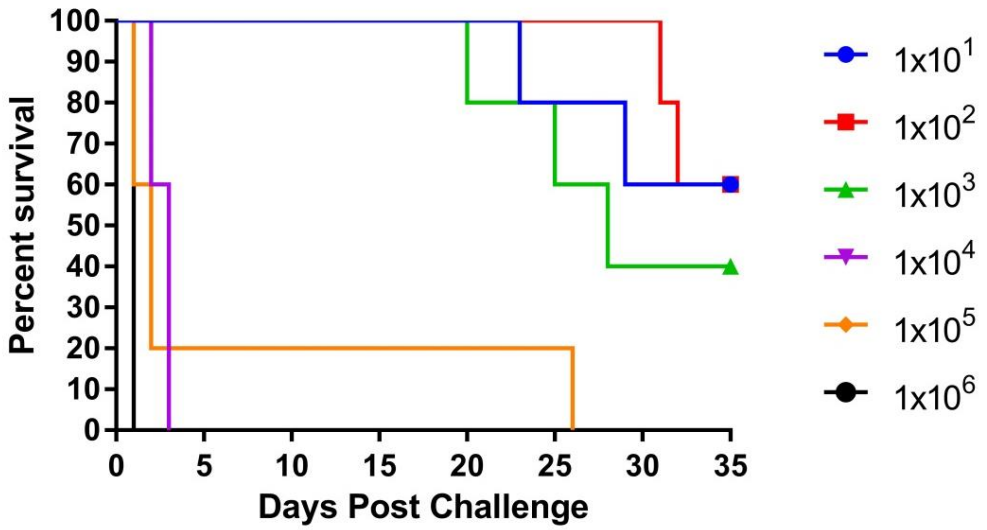

Figure 36: Survival data of BALB/c mice challenged with wildtype *B. pseudomallei*.

5 mice per group were challenged by the IP route with $1x10^{1-6}$ CFU. Mice challenged with $\geq 1x10^{4}$ succumbed to infection within 3 days (with the exception of one mouse). Mice challenged with a lower CFU count began to reach humane end points at day 21 onwards. The MLD was calculated to be 150 CFU.

In order to assess the virulence of the *ltg* mutants (Δ*ltgB*, Δ*ltgC*, Δ*ltgD*, Δ*ltgE,* Δ*ltgE::*pMo130-*ltgE,* Δ*ltgEBDC* , Δ*ltgEBDC*::pMo130-*ltgE*) 10 mice per group were challenged with approximately $5x10^3$ CFU via the IP route. The final challenge counts were; Wildtype - $1.38x10^4$, Δ*ltgB* – $3.17x10^3$, Δ*ltgC* - $6.97x10^3$, Δ*ltgD* -$4.23x10^3$, Δ*ltgE* - no counts, Δ*ltgE*::pMo130-*ltgE* – $3.57x10^3$, Δ*ltgEBDC* – $3.57x10^3$, Δ*ltgEBDC*::pMo130-*ltgE* - $1.67x10^3$ CFU. As there were no CFU counts for the Δ*ltgE* challenge the resultant data was treated with caution.

The results indicated that Δ*ltgB*, Δ*ltgD* Δ*ltgE* and Δ*ltgEBDC* were significantly different to wildtype with Mantel-Cox Log Rank test values of 0.020, 0.009, 0.000 and 0.000 respectively (Figure 37). Therefore, each of these strains was attenuated in the BALB/c melioidosis mouse model. Δ*ltgC* was not significantly different but the statistical value was close to the threshold of 0.05 with a test value of 0.058. Complementation of Δ*ltgE* could only partially restore wildtype virulence and did not restore any level of virulence in Δ*ltgEBDC*, both were significantly different to wildtype using Mantel-Cox Log Rank test with test values of 0.003 and 0.000 respectively. This is not unexpected for Δ*ltgEBDC* given that each of these genes is likely to play a role in the cellular processes and 3 out of 4 were attenuated. This was an important result as it was unknown whether single mutations would be sufficient to attenuate or if multiple mutations would be required.

At day 35 bacterial loads in the spleen, lung and liver for the surviving mice were enumerated. While there were mice that had cleared all bacteria for all of the strains tested, there were also mice that had *B. pseudomallei* colonising in all organs (Figure 38A). Whether these mice would have relapsed or could control the level of attenuated bacteria is unclear. It was difficult to assess the level of successful complementation as reintroduction of *ltgE* to Δ*ltgE* strains did result in the loss of two mice, however as the challenge dose for Δ*ltgE* mice received was unknown this cannot be accepted as partial complementation. The bacterial loads for the surviving mice were higher for the Δ*ltgEBDC* infected mice whereas the Δ*ltgEBDC*::pMo130-*ltgE* infected mice appeared to have cleared the infection (Figure 38B).

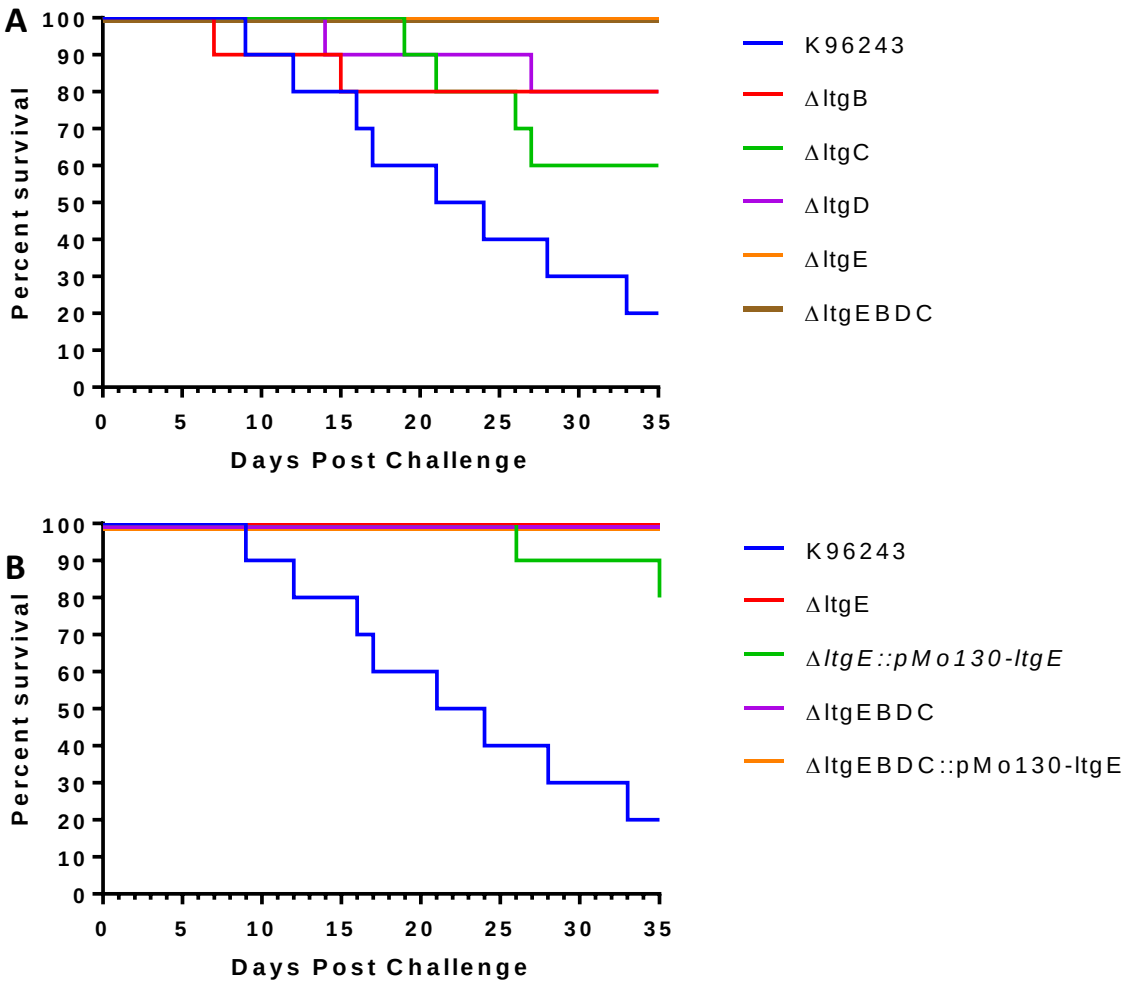

Figure 37: Survival of BALB/c mice challenged with *ltg* mutants

10 BALB/c mice were challenged by the IP route with wildtype, *ltg* mutants or *ltg* complemented strains and monitored over 35 days. Mice reaching a predetermined humane end point were culled. A) Δ*ltgB*, Δ*ltgD,* Δ*ltgE* and Δ*ltgEBDC* were all significantly attenuated compared to wildtype with Δ*ltgC* close to being attenuated. All mice survived challenge with Δ*ltgE* and Δ*ltgEBDC* (although exact challenge count for Δ*ltgE* was unknown). B) Complementation with *ltgE* could partially complement wildtype phenotype in *ltgE* single mutant but not for Δ*ltgEBDC*.

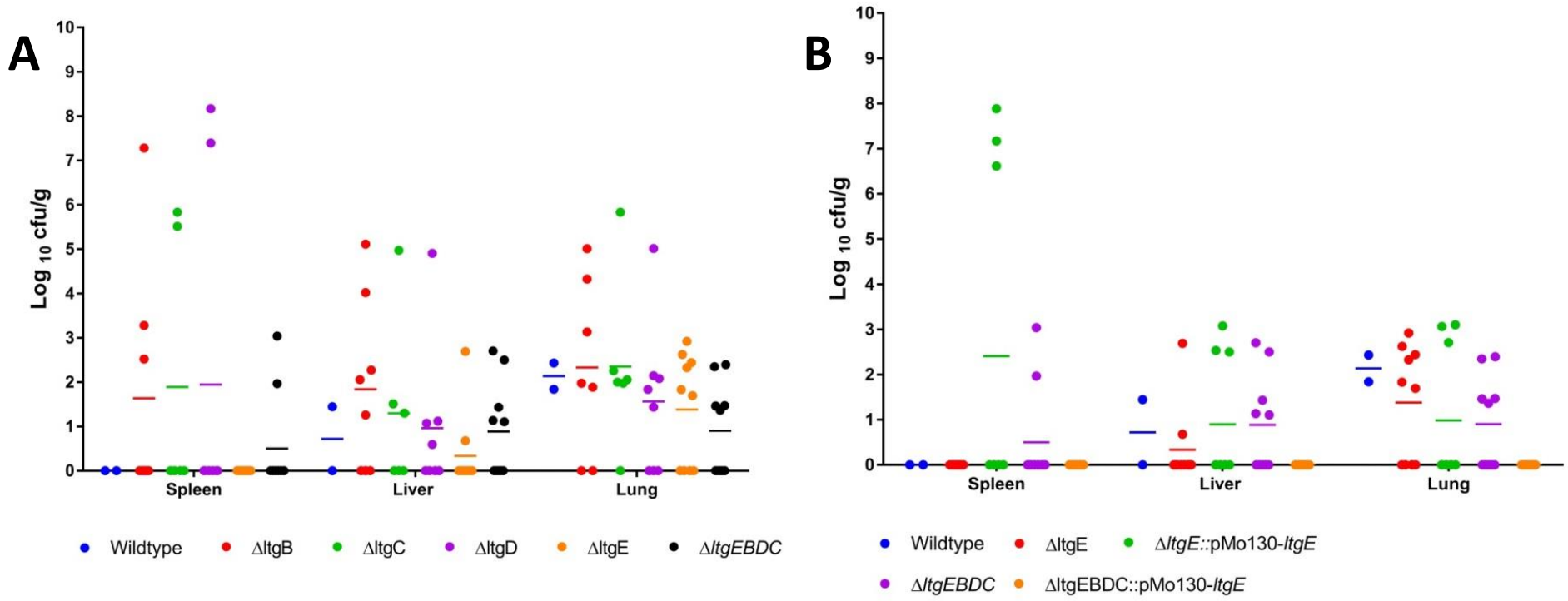

Figure 38: Assessment of bacterial load in the organs of surviving mice challenged with *ltg* mutants.

A) A comparison of all mutants showed that all bacteria were present in at least one organ for all strains, although overall at relatively low levels. There were elevated counts in a small number of spleens of mice challenged with *ltgB*, *ltgC* and *ltgD.* There were more mice containing *B. pseudomallei* in their lungs that spleen B) Complementation with *ltgE* resulted in a small increase in counts for spleen and liver but not for lung. Complementation of Δ*ltgEBDC* resulted in bacterial clearance from all organs, rather than returned to wildtype levels. Δ*EBDC* was detected in all organs.

Given that the Δ*ltgE* challenge dose was not determined and that this was the only mutant that has a complementing strain, it was decided to repeat the experiment including wildtype, Δ*ltgE* and Δ*ltgE*::pMo130-*ltgE* strains. Mice were challenged with an increased CFU dose of approximately 1-2x10^4 CFU by the IP route, final counts of challenges were; wildtype – 2x10^4, Δ*ltgE* – 1.9x10^4, Δ*ltgE*::pMo130-*ltgE*comp – 1.4x10^4 CFU. At the end of the 35 day experiment all mice challenged with wildtype and 1 challenged with Δ*ltgE* succumbed to infection (Figure 39A). Unexpectedly, all Δ*ltgE*::pMo130-*ltgE* strains survived. Given the complementation demonstrate *in vitro*, that the wildtype challenged mice died and 90% of Δ*ltgE* challenged mice survived then it was expected that mice challenged with complemented strain would also succumb to infection. Organ counts from the surviving mice showed that many of the mice had cleared the infecting bacteria or had low levels of infection (Figure 39B). There were two mice in the group challenged with the complementing strain that had enlarged livers and spleens and high bacterial loads. It is likely that if the experiment was extended these mice would have succumbed to infection. Interestingly it appeared that both strains in most mice were unable to colonise the spleen with counts of zero bacteria for both groups. There did appear to be increased levels of bacteria within the lung. It may be that LtgE plays an important role in colonisation of the spleen. There was however, no significant difference between the Δ*ltgE* and Δ*ltgE*::pMo130-*ltgE* bacterial loads in any of the organs.

Results of the second experiment followed a similar trend to the first experiment with *ltgE* being attenuated (90% survival rate). For this study however, the challenge dose was known to be 1x10^4 CFU. This challenge only resulted in the death of one mouse indicating that *ltgE* is an important virulence determinant in *B. pseudomallei*. 6 of the remaining 9 mice had completely cleared the bacteria from the liver and 7 had cleared from the spleen. However, *B. pseudomallei* could be recovered for all strains from the lung. It is surprising given the route of infection was IP and therefore one might expect the spleen and liver to contain more bacteria. It is unclear why Δ*ltgE* may be able to establish infection in the lungs over the liver and spleen.

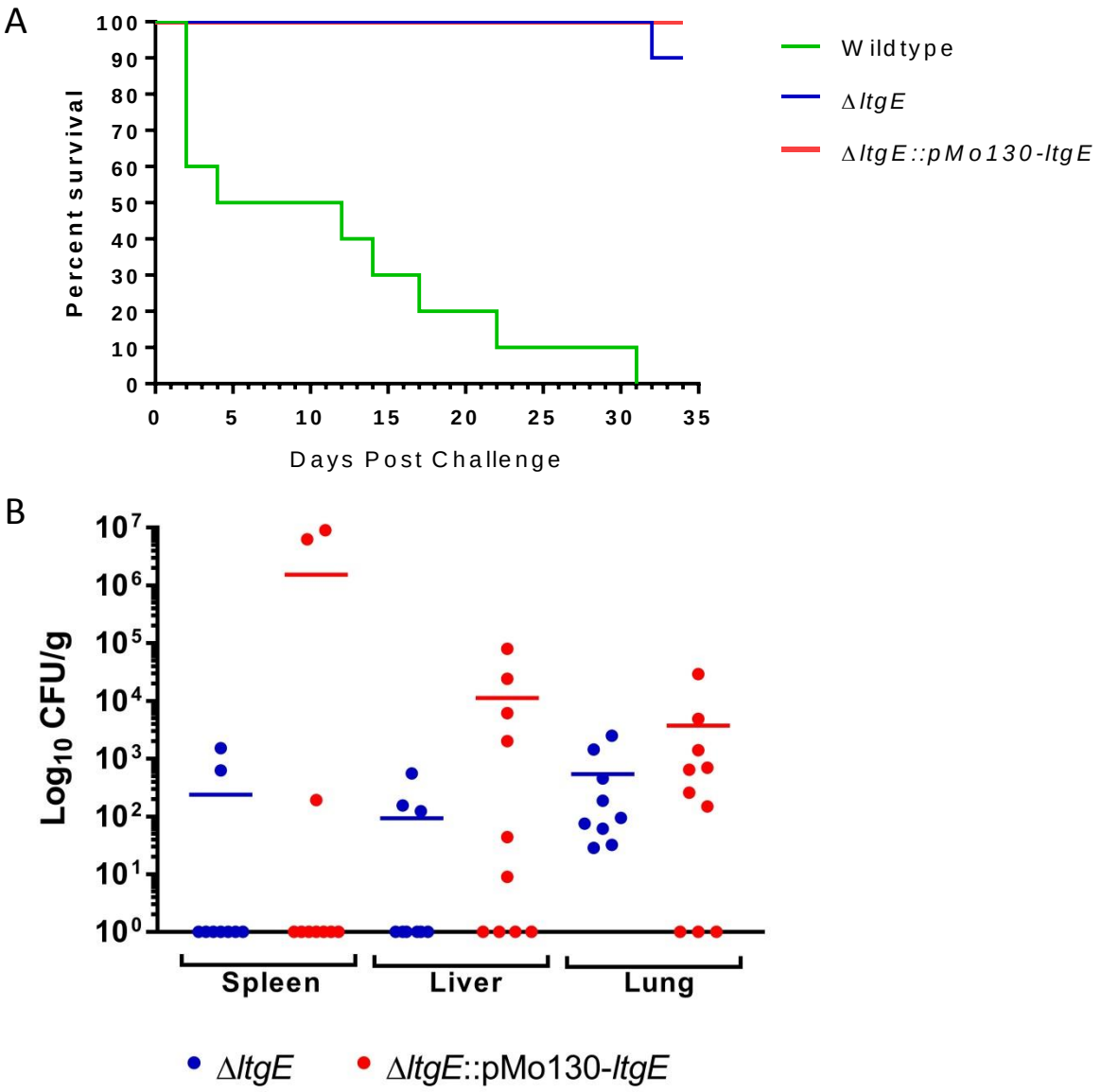

Figure 39: **Survival and bacterial load of mice challenged with Δ*ltgE***

A) 10 BALB/C mice per group were challenged with 1x10^4 CFU of *B. pseudomallei* wildtype, Δ*ltgE* or Δ*ltgE*::pMo130-*ltgE* (complemented) strains. All wildtype mice succumbed to disease and 90% of mice challenged with Δ*ltgE* and 100% mice challenged with the complemented strain survived the study. All surviving mice were culled and their organs processed to calculate bacterial load. B) Bacterial loads were measured from spleen, liver and lungs. Data was adjusted to CFU/g of organ. Δ*ltgE* and the complemented strain were largely unable to colonise the spleen although two mice in the complemented group had very high levels of bacteria (>10^6). There was no statistical significance between strains in any organ.

Unfortunately, complementation did not restore wildtype virulence and no mice succumbed to infection. The higher counts in all three organs seen for two of the mice challenged with the complemented strain may have developed into a chronic form of melioidosis if the experiment was extended. This lack of complementation was unexpected as *in vitro* complementation in motility and morphological experiments was successful. The lack of complementation seen could be due to a number of factors. Firstly, it may be that reintroduction of the gene resulted in a toxic effect on the bacteria. This however, would be more likely if the gene was under a constitutively expressing promoter or on a multicopy plasmid. *ltgE* was placed under its own native promoter and therefore would express under wildtype conditions. RT-PCR performed *in vitro* indicated that *ltgE* was expressed at a similar level to wildtype. The second explanation is that integration of the plasmid resulted in unwanted polar effects. The protocol followed is that outlined in (228) with the integration site designed to be downstream of *bpsl3330*. As it was not possible to insert the upstream flanking region into the complementing plasmid only single cross over integrates were generated. Flanking region 2 was located within *bpsl3329*, the last gene in an operon of 9 genes. If integration disrupted expression of *bpsl3329* (unknown function but part of an operon involved in fatty acid biosynthesis) or *bpsl3330* (hypothetical protein) then this could influence virulence in mice especially since fatty acid biosynthesis is known contribute to virulence. Another possibility is that the plasmid was inherently unstable within the chromosome as it was only a single cross over. If over the course of infection the plasmid was lost then there would not be successful complementation. This however is unclear as bacteria from organs for mice challenged with ΔltgE::pMo130-ltgE were plated onto both LA and LA-Kan (800µg/ml). When comparing the counts on LA verses LA-Kan (Figure 40), it would appear that there is no difference between the two medias when comparing median and interquartile range. There the number of mice that were deemed to have negative counts was much greater when plated onto LA-Kan compared to LA, suggesting some instability of the plasmid.

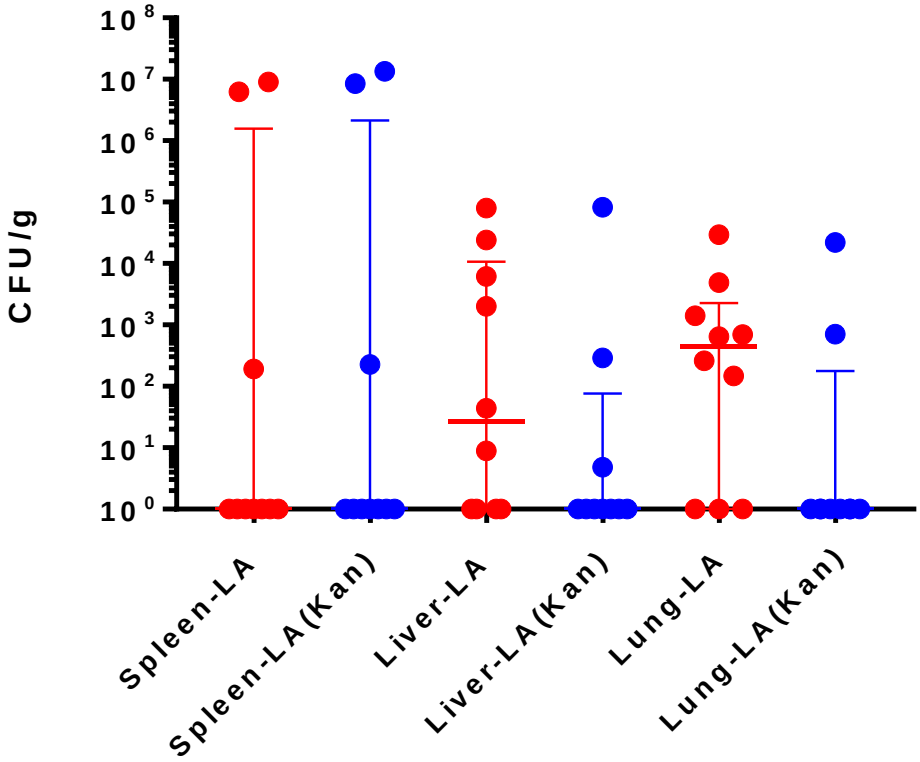

Figure 40: Comparison of Δ*ltgE*::pMo130-ltgE organ counts plated onto LA and LA-Kan

Bacterial loads from organs of mice challenged with Δ*ltgE*::pMo130-*ltgE* were plated onto both LA and LA-Kan (800µg/ml) to assess loss of integrating plasmid. The scatter graph shows the median with the interquartile range. These results suggest there is not a significant loss of integrating plasmid. However across many of the mice there are more bacterial counts when plated on LA rather than LA-Kan, suggesting some instability in the integration site of the plasmid.

There are a number of approaches to try and address some of these questions. Firstly whole genome sequencing or sequencing of the region of insertion could be performed to identify the exact site of integration. Secondly RT-PCR could be performed on neighbouring genes to the integration site to ensure that there are no polar effects from integration of the plasmid. A replicative vector could be used for complementation instead. This was not be possible with multiple deletion mutants as generation of Δ*ltgEB*, Δ*ltgEBD*, Δ*ltgEBCD* containing *ltgE* expressing pMo168-*ltgE* was unsuccessful, possibly due to the toxic effect of overexpression of muralytic enzymes on stressed cells. However, this plasmid could be introduced to a single Δ*ltgE* mutant and could complement *in vitro*. This approach would negate any risk of polar effects but could cause problems when overexpressing cells in an *in vivo* environment. Fourthly, if reintegration into the chromosome under the native promoter is preferable, then alternative integration sites could be explored or an alternative cloning approach could be utilised to insert the second recombination flanking region into the plasmid used. Finally virulence studies using the control complemented strain (containing only the integrated, empty pMo130 plasmid) or MLD studies comparing wildtype strain and the control complementing strain could also be performed to see the effect of plasmid integration on virulence.

5.5. Discussion

Given the redundancy bacteria employ with regards to Ltgs, as has been demonstrated in other Gram negative bacteria including *E. coli, S. enterica* serovar Typhimurium and *P. aeruginosa*, it was unclear whether there would be significant phenotypes for individual *ltg* mutations in *B. pseudomallei*. As such, multiple deletion mutants were constructed and characterised alongside the single *ltg* mutants.

Given that deletion of seven murine hydrolases of *E. coli* (including Ltgs) had no effect on the rate of growth (158) it was not expected that single *ltg* mutants would reveal a significant growth difference to wildtype in *B. pseudomallei*. Removal of 4 out of 5 important cell wall modifying enzymes did not result in a dramatic effect on the viability of the bacterium; Δ*ltgEBDC* grew almost to a wildtype level. The quadruple mutant, unlike the single mutants, was the only strain to show any attenuation of growth *in vitro* with an approximate 2 fold reduction in growth over 72 hours, however there was no difference between doubling times. This could only be seen when measuring growth by CFU indicating potential morphological differences and potential difficulties in the transition from liquid to solid media. This was however, only under the single condition tested. It may well be that there would be substantial growth defects under stressful conditions such as; hypoxic, acidic, osmotic pressures and conditions more associated with *in vivo* growth and high peptidoglycan turn over. It would be useful to assess combinations of *ltg* mutations to see which mutations are required in order to replicate this growth defect.

SEM and measurement of cell length using phase contrast microscopy revealed LtgE as a key protein in cell division and cell elongation. This could be extended through the generation of multiple deletion mutants also containing a mutation in *ltgE*. This correlates with previously published data on MltA of *N. meningitidis* (170). Double, triple and quadruple mutants had increased cell length and chaining forming filament like bacteria. Given these phenotypes it is remarkable that Δ*ltgEBDC* remains viable and can grow to densities greater than 10^9 CFU/ml. This morphology however, may explain the 2 fold difference between wildtype and Δ*ltgEBDC* CFU counts in growth curves while there was no difference by optical density readings. It is likely that the chaining bacteria increase optical density readings and cause problems when the

colonies are formed. These morphological differences are only seen in mutants containing the *ltgE* mutation. These elongated cells have similar morphologies to those seen in *S. enterica* serovar Typhimurium multiple *ltg* mutants [8]. Although unlike the *B. pseudomallei* mutants generated this study, this was seen only seen when grown in media lacking salt. Furthermore sub MIC antibiotic induced filaments of *B. pseudomallei* had a similar phenotype and had decreased lysis of monocytic cells, although this phenotype was reversible upon removal of the antibiotics (241).

Δ*ltgB*, Δ*ltgC* and Δ*ltgD* single deletion mutants did not display obvious morphological differences even in combination, with Δ*ltgDBC* only having a marginal increase in cell length compared to wildtype. This indicates that these genes may not be involved in functions such as in septum formation, cell shape and cell elongation. This however, does not mean that they are not involved, just that potential differences may be too small to be seen by SEM or under the conditions tested here. Complementation studies revealed that LtgE D343A was unable to complement as the wildtype protein could. This along with recombinant protein assays adds to the evidence of the importance of this residue in the catalytic residue of the protein. If LtgE is deemed a suitable target for the development of a future antibiotic, understanding its activity and catalytic residues is essential.

It may well be that there is an underestimation of the cell length in the *ltgE* multiple deletion mutants as only cells that had clearly defined poles were measured, and longer cells may have been disregarded. An alternative method to measure these cells may be to use flow cytometry or the use of a cell sorter could be used to separate bacteria according to their size to allow for a more focused investigation of some of these phenotypes. For example, TEM could be performed using a sample solely consisting of cells greater than 10µm to investigate defects in cell division.

The poor growth and the altered cellular morphology as a result of overexpression of LtgE suggest a severe loss of integrity of the peptidoglycan layer. In wildtype cells muralytic proteins are tightly controlled. The morphological differences observed are would likely be dependent on the level of peptidoglycan degradation in addition to protein expression levels and plasmid copy number. It has been shown that

interference with murine hydrolases and Ltgs results in increased release of muropeptides (when overexpressed) which, in turn, results in the increased expression of β-lactamase (235, 242). An interesting observation with the *B. thailandensis* strain overexpressing LtgE came from a pilot experiment utilising a simple assay based on the cleavage of a chromogenic, highly sensitive β-lactamase substrate, nitrocefin. This experiment suggested LtgE overproduction led to increased β-lactamase activity most likely due to increased release of peptidoglycan fragments indicative of exposure to β-lactam antibiotics. Crude cell lysate from pMo168 and pMo168-*ltgE* expressing strains (same OD) resulted in an observable change of colour for the strain overexpressing LtgE (observation, data not recorded). A more quantifiable experiment would be needed to determine the levels of increased β-lactamase expression. This would correlate with data in *E. tarda* in which overexpression of MltA resulted in increased antibiotic sensitivity to β-lactam antibiotics including ampicillin, carbenicillin and ceftriaxone (167).

Given that similar antibiotic induced filaments in *B. pseudomallei* had decreased cytotoxicity in THP-1 cells (243), it is likely that the *ltg* mutant filament-like morphologies would have also have implications *in vivo*. Given that *B. pseudomallei* is an intracellular pathogen, this chaining and increased cell length could have implications for cellular processes such as escape from the phagosome, cell-cell spread and the formation of MNGC, features important in intracellular invasion and *B. pseudomallei* infection (244). Specifically, the formation of filaments may prevent polar localisation, assembly and functioning of virulence factors. Such virulence factors in *B. pseudomallei* include flagella and T6SS-5 (essential for cell-cell spread) which are both located at the poles of the cells (100, 245). Recently, it has been shown in *P. aeruginosa* that type IV pili machinery is localised to sites of cell division prior to cell division. If this is true for *B. pseudomallei* and that cell division is hampered, as is the case with Δ*ltgE,* then it is unlikely that there will be assembly of type IV pili and thus twitching motility would be impaired (246).

To investigate the effect these filament like morphologies on polar localised virulence factors, the motility of these mutants was assessed. Swimming motility of all single *ltg* mutants was significantly lower than that of the wildtype. If each Ltg is involved, either

directly or indirectly, in certain aspects important for bacterial motility such as quorum sensing, two component regulatory systems and flagella assembly then it could explain why all mutants have reduced swimming motility. Conversely, the fact that Δ*ltgB*, Δ*ltgC* and Δ*ltgD* do not have reduced swarming motility is also interesting. Swarming motility is associated more typically with biofilms and there may be an alteration in expression of Ltgs between swimming and swarming motility. *ltgE* again appears to be the most influential Ltg in these phenotypes, most likely due to the morphological differences seen, with chaining likely impacting the assembly of flagella. It may well be LtgE is also directly involved in flagella assembly, although evidence of LtgE (MltA) in other bacteria does not support this hypothesis. MltE of *E. coli* has been shown to involved in the assembly of the T6SS (183). LtgA and LtgB of *B. pseudomallei* share some homology with MltE, therefore it may be that LtgA or LtgB directly are directly involved in flagella assembly. In addition the flagella operon (*bpsl2072-0278*) and other flagella associated genes are in close proximity on the genome to *ltgA* (*bpsl0262*). This would be worth investigating.

Biofilms are a community of bacteria adhered to a surface surrounded by a secreted extracellular matrix. Biofilms can have serious implications in disease including antibiotic tolerance, failure to clear infection and are an important feature of many nosocomial infections (247). The effect mutating *ltg* genes on biofilm production was investigated. The significantly reduced biofilm formation in Δ*ltgB*, Δ*ltgC* and Δ*ltgD may* correlate with the swimming and twitching motility data. As flagella and pili are used in bacterial adhesion and if their functioning is compromised then bacterial adhesion and biofilm formation may also be comprised. *ltgB* does have a some homology with MltE (E. coli 41% cover, 34% identity) which when overexpressed in *S. enterica* serovar Typhimurium resulted in increased biofilm mode of growth – although the mutant did not (177). Interestingly Δ*ltgE* did not result in altered biofilm production but Δ*ltgEBDC* increased biofilm production. There are a number of possible explanations for this increase in biofilm formation. Firstly, the unusual cell morphology of the cells could make the cells leaky or cause an increase in production of extracellular matrix to compensate for its potentially more vulnerable state. Secondly, the unusual cell morphology causes the bacteria to aggregate over the 72 hours and adheres to the

surface non-specifically as opposed to formation of true biofilm. This could be extended to the third explanation in that these cells are effectively non motile and thus would settle to the bottom of the well to bind non-specifically. It is interesting that Δ*ltgE* had no difference in biofilm production which indicates that the cellular defects caused by the mutation do not influence biofilm formation. While it was shown Δ*ltgB*, Δ*ltgC* and Δ*ltgD* mutations in combination do not result in drastic differences in cellular morphology the individual phenotypes seen here indicate individual roles in biofilm formation. There are a number of factors that each Ltg could influence in regards to biofilm formation. These include secretion of surfactants, secretion and sensing of acetyl homoserine lactones in quorum sensing and the secretion of polysaccharide matrix.

MICs were performed to investigate whether mutations in *ltgs* would compromise the cell membrane in such a way that it would lead to increased susceptibility to antibiotics. This has been shown previously to be the case in *P. aeruginosa* (174), *Campylobacter jejuni* (248) and *E. coli* (235). *B. pseudomallei* has intrinsic resistance to many antibiotics which is a substantial problem in the treatment of melioidosis (239). Mutation of *ltg* genes did not reveal any vast differences for 6 antibiotics tested (four of which are routinely used to treat melioidosis). There was a two fold increase in sensitivity for the quadruple mutant for doxycycline, carbenicillin and ceftazidime. These differences are not as dramatic as one might expect given that the peptidoglycan should be severely compromised given the absence of 4 Ltgs. It is also interesting that there is a small difference in doxycycline as this is a protein synthesis inhibiting antibiotic that binds to the 30S ribosomal subunit blocking aminoacyl tRNA suggesting that Δ*ltgEBDC* is more permeable than wildtype. It may be that other non-cell wall targeting antibiotics are also able to cross the bacterial periplasmic and outer membranes. Furthermore, it may be that bacterial cell wall dysregulation results in the overexpression of antibiotic resistance mechanisms including β-lactamases, efflux pumps and antibiotic targets.

The direct role of Ltg in virulence is not well understood even in bacterial species for which most current Ltg research is based. Muropeptide analysis showed that mutation of *ltgA* and *ltgD* of *N. gonorrhoeae* abolished peptidoglycan monomer release(234),

these anhydro-muramyl reaction products have been shown to cause damage to ciliated cells in fallopian tubes (249) and cause system arthritis when injected into rats (250). An MltA mutant in *N. meningitidis* was unable to cause bacteraemia in infant rats (170) and a study into an MltB homolog in *Brucella abortus* (encoded by *BAB_RS22915*) directly showed the importance of this Ltg in virulence in BALB/c mice (251). The *BAB_RS22915* mutant had no defects in adhesion or invasion of RAW264.7 cells but did have decreased intracellular survival and significantly decreased colonisation of spleens in mice and while the bacteria was able to persist it caused no pathological damage. While there were some issues with animal experiments in this study it was possible to show that Ltgs play an important role in virulence in the IP BALB/c melioidosis model. All but Δ*ltgC* were significantly attenuated. In order to assess the level of attenuation MLD studies with the separate mutants would have to be performed. Δ*ltgE* appeared to be the greatest contributor to virulence with 100% and 90% survival rates in the first and second experiment respectively. Many of the surviving mice were able to clear the infecting bacteria although low levels were still found, predominantly in the lung. This result is very promising and helps in the understanding of the importance of these proteins in virulence, an area that is lacking in the literature. Furthermore given that there is homology and shared catalytic domains between some of these Ltgs it may be possible to target multiple proteins with a single inhibitor increasing the attenuation or perhaps even rendering the bacterium avirulent.

Overall these experiments have shown the importance of LtgE and its role in cell elongation and cell division and with its mutation causing a number of downstream phenotypes such as motility defects and attenuation in mice. While there have been phenotypes seen for the other ltg mutants it is more difficult to identify the exact contribution or cause of the *ltgs* in these phenotypes. Future experiments would aim to continue to investigate this using macrophage invasion and replication assays, investigation of secretion systems and flagella assembly. Protein:protein interaction studies would also be paramount in understanding the exact roles of LtgB, LtgC and LtgD. There is also limited information known about the regulation of Ltgs or under which conditions they are expressed. It would be possible to perform RNA analysis in a

variety of growth conditions, particularly those associated with *in vivo* growth, to investigate differences in expression levels. Once established it would also be possible to do RNAseq to look for other pathways also regulated under similar conditions identify other potential functions of Ltgs, particularly focused on peptidoglycan remodelling. Another approach would be to look more holistically using an –omics approach, for example, membrane proteomics or secretomics to see if the protein profile of mutants is different to that from wildtype. Finally it would be preferential to purify peptidoglycan from these mutants and perform muropeptide analysis. All of the above, along with the data generated during this study, would allow for a comprehensive understanding of the roles Ltg play in *B. pseudomallei*.

5.6. Summary

In this chapter single and multiple *ltg* deletion mutants were assessed for phenotypic differences. These mutants were characterised on their ability to grow, their morphology and cell length, motility, biofilm production, antibiotic sensitivity and virulence. Δ*ltgE* was shown to have the largest differences out of all other single mutants in many of the phenotypes tested, most likely due to defects in cell division and cell elongation. Many of the phenotypes seen here are similar to phenotypes in *ltg* mutants of other bacteria suggesting that inhibitors of Ltgs could potentially be used as a broad spectrum antibiotic.

Chapter 6

Investigation of non-culturable *Burkholderia*

6.1. Introduction

6.1.1. Non culturable bacteria

Non-culturable (NC) bacteria, sometimes referred to as viable but non culturable (VBNC) bacteria, cannot be cultured on conventional growth media. This is to say, they are unable to form colonies and sometimes do not grow in liquid broth, but remain intact and metabolically active. For this reason they are still considered to be live (252, 253). VBNC bacteria pose a great problem to human health for a number of reasons predominantly that routine diagnostic tools often rely on the culturing of bacteria leading to false negatives in the presence of VBNC bacteria. This could lead to potentially severe prognosis implications. Sterile samples, such as blood have been suggested to contain many dormant bacteria originating from gut microbiome that given favourable conditions can shift to a pathogenic state (254). VBNC bacteria in the body could resuscitate into actively growing bacteria leading to latent infection. In addition, water treatment facilities routinely test water for human consumption and despite advances in detection predominantly use culture based detection methods. The same problems arise in the research environment where a particular stress, whether environmental or therapeutic, that results in a decrease in viability could in reality be as a result of the bacterium entering a NC state.

NC bacteria were first reported in 1982 with *E. coli* and *Vibrio cholerae* upon exposure to high salinity conditions (255). This observation lead to a huge amount of research into this physiological state including gene expression profiles, proteomics, physiological changes, antibiotic resistance and infection capabilities, in particular dormancy and latent infection (256-258) . The concept of dormancy and resuscitation to cause latent infection is not new, and is a well-studied field particularly in *M. tuberculosis* (259) a hallmark bacteria for latent infection. Given this and the number of bacteria that have been observed to enter a NC state it may well be that many current infections are actually a result of reactivation of a bacteria that entered the body many months or even years prior to the current infection. Many pathogenic bacteria have been shown to have the capacity to become NC. These include, but are not limited to; *E. coli* spp, *Campylobacter* spp, *H. pylori*, *Salmonella* spp, *Enterococcus*

spp, *Vibrio* spp, *Listeria monocytogenes*, *Rhizobium leguminosarum* in addition to the well characterised *M. tuberculosis* (253, 257, 258, 260).

Sputum samples are known to have a heterogeneous population of bacteria. *M. tuberculosis* found within sputum samples has been shown to have both culturable and so called 'differential culturable' bacteria that are tolerant to first line drugs (261, 262) . It is the differential culturable bacteria that are more resistant to antibiotics (263) and require external factors, found in cell filtrate to resuscitate into culturable bacteria. Such factors include resuscitation promoting factors but a recent study has shown that sputum from tuberculosis patients both with and without HIV-1 contained a range of Rpf dependent, Rpf independent, cell filtrate dependent, cell filtrate independent and actively growing *Mycobacteria* within each sputum sample. This highlights the complexity of the populations *in vivo* and the difficulties that can arise from targeting essentially the same organism but one that can exist in multiple states, with different phenotypes in a single host (262).

The number of bacteria that can be cultured from environmental samples is small when compared to the total number of bacteria in the sample. While detectable by various methods they are for the most part non-culturable. In recent years inventions such as the 'ichip' that allow for the diffusion of growth factors past bacteria, have allowed for the cultivation of previously unculturable bacteria from soil samples (264), even leading the discovery of a new novel antibiotic (265).

6.1.2. Conditions leading to non culturability

The stresses that result in this phenomenon are wide and varied and include nutrient starvation, temperature, peroxide stress, UV exposure, osmotic pressure, oxygen concentrations and pH stress. Many of these conditions are typical of stressful environmental and host niches. Whether resuscitation is simply dependent upon removal of the stress or is more complex process it may be bacteria and condition dependent. There may also be factors that allow for this resuscitation such as specific proteins and chemical signals such as quorum sensing, for example (266). It is also known that reactivation can result from contact with amoeba (267). Some bacteria, including mycobacteria can be resuscitated to growing forms when supplemented with specialist media such as culture supernatant. Culture supernatant contains a large number of secreted proteins and other chemicals such as siderophores (268) which may act upon these dormant, NC bacteria to reinitiate growth and potentially the reactivation of infection. One such family of proteins which can be found in the culture supernatant and has been shown to resuscitate dormant Actinobacteria are the resuscitation promoting factors (Rpfs) (269-271). These proteins have been shown to have muralytic activity and share homology with Ltgs (272, 273). This indicates that resuscitation may be dependent upon rearrangement of peptidoglycan. Peptidoglycan analysis of *Enterococcus faecalis* comparing growing verses VBNC state has been performed. It was shown that the VBNC state (induced by cold exposure) resulted in 9% increase in crosslinked muropeptides in addition to an increase in the activities of penicillin binding proteins and muramidases (274). In a further study by the same group *E. coli* VBNC were shown to be more coccoid in shape as well as having increased peptidoglycan crosslinking and a shortening of average glycan chain length (275). It is therefore likely that the remodelling of peptidoglycan is an important feature of the VBNC state. Homology between Rpfs and Ltgs in other organisms, including *B. pseudomallei*, could suggest that the remodelling of peptidoglycan by Ltgs allows bacteria to enter or leave a dormant/NC state.

6.1.3. Detection of non culturable bacteria

While typical culturing methods are not suitable, these bacteria can be detected or visualised using a number of techniques. In the late 1970's the detection of non culturable bacteria was achieved by supplementing sea water (containing NC bacteria) with very low levels of specific nutrients (yeast extract and nalidixic acid). The yeast extract promoted growth while the nalidixic acid prevented replication/division of these bacteria resulting in elongated cells. While this did not result in actively dividing bacteria that would allow for the formation of colonies on plates, it did however result in increased cell size detectable using various microscopic techniques (276).

A more commonly used technique is the use of the BacLight™ Live/Dead kit which involves staining a bacterial sample with two stains, a green-fluorescent SYTO® 9, which stains all bacteria and red-fluorescent propidium iodide, which stains membrane damaged cells i.e. non-viable. These bacteria can then be visualised using fluorescence microscopy or can be quantified using flow cytometry.

An alternative method is the detection of gene expression using RT- PCR or qRT-PCR. As the bacteria are technically still live there is still basal levels of gene expression. This has successfully been used for the detection of water contaminating *Vibrio* species (277, 278). However, this does not differentiate between live and dead bacteria, just the presence or absence of a DNA template. This has been circumvented through the use of propidium monoazide coupled with RT-PCR allowing for only the detection of viable cells in a sample and not lysed bacteria. This is because propidium monoazide is unable to permeate membranes and thus cannot enter live cells (monoazide inhibits qPCR amplification). Therefore any extracellular DNA cannot be used as a template. This method has been used to detect *Legionella pneumophila* in contaminated water samples (279). Other methods to detect VBNC include solid phase cytometry (280), MALDI-TOF (281) and even the use of phage to assess the level of VBNC in a population (282).

6.1.4. Non culturable *Burkholderia*

While it is known that *B. pseudomallei* is capable of surviving for a long time in nutrient poor environments (283, 284), there is a limited amount of research into non culturability in *Burkholderia*. Certain conditions have however been shown or been

suggested to allow *B. pseudomallei* to enter a NC state. These include pH stress, high osmotic pressure, cold, oxidative stress, chlorination and UV exposure. Table 4 outlines details of conditions suggested to form NC *Burkholderia*.

pH levels below 4.5 were shown to result in a drop in a loss in culturability (by CFU count) however, flow cytometry results suggested that the level of viable cells remained constant even at the lowest pH tested of 3.5 (140). Cold shock is a common mechanism to force bacteria into a nonculturable state (253, 285) and while it is known that *B. pseudomallei* appear to die when stored at 4°C it is possible that this is not due to cell death but in reality cells becoming NC. One study, investigating the ability of bacteria to survive in distilled water, showed that at 5°C none of the pathogens tested (including *B. pseudomallei*) were culturable after 30 days but using Solid-phase cytometry they demonstrated metabolic activity and showed esterase activity indicating viability (286). They also showed that the effect of this experiment was as a result of cold exposure not nutrient starvation as *B. pseudomallei* was still culturable after 30 days at 25°C in distilled water whereas *B. mallei*, a closely related species and the cause of Glanders, was not (286). When stored at 25°C in distilled water *B. pseudomallei* remained viable for 16 years with Live/Dead counts of 3.8×10^7 cells/ml and 1.4×10^5 cells/ml respectively, however, colony counts on agar of 1.0×10^6 CFU/ml suggested that a proportion of cells were in a NC state.

Another common technique used for generating NC bacteria is osmotic pressure. One study showed that the number of culturable *B. pseudomallei* reduced when NaCl concentrations increased to concentrations above 2.5% (w/v). However, flow cytometry counts used to detect the number of viable cells, remained constant. This was not the case for lower osmotic pressures (140).

There are a number of studies that have shown that H_2O_2 may play a role in the nonculturable state in many Gram negative bacteria including *Vibrio vulnificus, E. coli* and *S. enterica* serovar Typhimurium (253) and while there are studies into the effect of H_2O_2 on *Burkholderia* there is little in terms of inducing dormancy or a NC state. UV exposure and chlorine exposure have been shown to produce a decrease in culturability and suggested could be causing a NC state in *Burkholderia* (287-289).

Despite the lack of detailed research into the state of *Burkholderia* when subjected to such stresses, these papers do indicate that the bacteria is certainly capable and in the case of low pH and high osmotic pressure may actually produce a very high level of NC cells. An aim of this project was to investigate some of these conditions and to generate and optimise a protocol of the production of NC *Burkholderia* for use in resuscitation studies.

Condition tested	Detail	Strain	Reference
pH	CFU counts decreased sharply when pH dropped below 4.5. However, flow cytometry results suggest that the level of viable cells remains constant (lowest pH tested was 3.5). Potentially up to 10^7 bacterial count/ml VBNC compared to no culturable cells.	No strain stated.	(290) (140)
Temperature	Temperatures evaluated ranged from 0-48°C. At temperatures less than 4°C there is a significant loss in the ability to culture *B. pseudomallei*. Optimum temperature is between 24-32°C. There is no mention in this reference of the nature of the bacteria at either end of the temperatures tested. It may be that the cells were in a VBNC state but did not show as CFU. There is suggestion that culturing *B. pseudomallei* in liquid media for 48 hours at 42°C results in rapid growth and depletion of nutrients and the resulting sediment can consist of approximately 80% VBNC cells. Gilbert and Rose showed that *B. pseudomallei* were still culturable after 30 days at 25°C whereas *B. mallei* were not. However at 5°C none of the pathogens tested were culturable but using Solid-phase cytometry they demonstrated metabolic activity.		(289) (286)
Water	Stored at 25°C in distilled water *B. pseudomallei* remained viable for 16 years with live/dead counts of 3.8×10^7 cells/ml and 1.4×10^5 cells/ml respectively. However CFU counts of 1.0×10^6 CFU/ml suggested that a proportion of cells were in a VBNC state. There was a difference in phenotype between those in the original culture verses those that had been stored in distilled water for a prolonged period of time. Prolonged freezing resulted in a large number of the bacteria dying.	207a	(284) (283)
NaCl (osmotic stress)	The number of culturable cells (CFU count) decreases sharply when NaCl concentrations rise above 2.5% (w/v) however the flow cytometry count used to detect the number of viable cells remains constant. There were no VBNC cells at lower osmotic pressures.	NCTC 13177	(140)
H_2O_2	There are a number of studies that have shown that H_2O_2 has been a suitable chemical to induce a VBNC state in many gram negative bacteria including *Vibrio vulnificus, Escherichia coli,*		

	S. enterica serovar Typhimurium. There are studies investigating the effect of H_2O_2 on *Burkholderia* but little in terms of inducing a VBNC state.		
UV	This is a questionable study that states that *B. pseudomallei* has increased sensitivity to UV than other bacterial species. However another study showed that they were no more susceptible to UV. Neither study mentions the entry of *B. pseudomallei* into a VBNC state. A third study investigated the effect of sunlight on *B. pseudomallei*. Cells kept in the dark remained at a constant level throughout the experiments. Exposed cells were "killed with a kinetic studied through 5xLog_{10} inactivation". They make no mention of the state of the *B. pseudomallei*, simply that there was a decrease in CFU when exposed to sunlight.	NCTC 13177 DM98	(288) (289)
Chlorine	The levels of chlorine or monochloramine needed to disinfect water were tested at 5 or 25°C and at pH 7 or 8. The membrane integrity and metabolic activity were investigated in order to test for VBNC cells. Highest results recorded; 7.8mg - min/litre for free available chlorine (FAC) at pH 8 and 5°C and 550 mg - min/litre for monochloramine at pH 8 and 5°C. Metabolic alternative viability assay (Esterase cleavage of a fluorescent substrate by metabolically) showed a 3-log reduction; pH7 – 5°C; chlorine range from 0.2 to 3.7mg/litre. Alternative viability assay. Solid-phase cytometry counts of untreated controls were identical to plate culture results (1.1 x 10^6 CFU/ml. The cytometry detected 1.5 to 4 log_{10} greater cell numbers than plating after disinfection exposure for all tested strains. The 4-log10 Ct values calculated from the cytometry data for each strain and disinfection condition were up to five times higher than those obtained by plate recovery methods.		(287)

Table 4: Overview of conditions suggested to produce non culturable *Burkholderia*.

6.2. Chapter aims

- Review literature on non-culturable forms of *Burkholderia* to identify conditions that may be suitable for development of a non culturability model
- Test multiple conditions that reduce the culturability of *B. thailandensis* while retaining a viable population Live/Dead staining
- Attempt to resuscitate these non-culturable bacteria using a range of conditions including the use of recombinant Ltg or Ltg overexpression.

6.3. Materials and Methods

6.3.1. Incubation of *B. thailandensis* in high osmotic pressure conditions.

Triplicate cultures of *B. thailandensis* strains E264 and E555 were grown to OD_{600} 1.0 in LB (37°C, 200 rpm). The bacteria were washed once in sterile dH_2O before being transferred to dH_2O (two groups), dH_2O at pH4 (pH lowered using HCl to pH4 before being autoclaved), dH_2O containing 5% (w/v) NaCl while ensuring the OD remained at 1.0. 1 in 10 dilutions were made of each sample using the appropriate media to produce an OD_{600} of 0.1. One set of dH_2O incubated samples was transferred to 4°C. Cultures were left for 30 days and CFU counts taken at regular intervals.

6.3.2. Live/dead staining

Live/Dead staining was performed using the Live/Dead® *Bac*Light™ Bacterial Viability Kit (ThermoFisher) using an abridged manufacturers protocol. Briefly the test culture (1-5ml) was centrifuged at 3000g for 10 minutes to pellet cells. Cell were washed in 1ml of saline twice before resuspension in 200µl of fresh saline containing 0.5µl of Syto 9 and propidium iodide stains at a ratio of 1:1 respectively. The cell suspension was incubated in the dark for 20 minutes at room temperature before 5µl was loaded on to a glass slide and visualised by fluorescence microscopy using the following excitation/emissions - SYTO 9; 485⁄498nm, Propidium iodide; 535⁄617nm. The same fields of view were also visualised using phase contrast microscopy.

6.3.3. Determination of bacterial culturability using most probable number method

The concentration of bacteria in liquid media was calculated using a modified most probable number (MPN) method (291). MPN assays are based upon Poisson distribution of growth in a dilution series. 7 columns (6 replicates plus a control column) of a 96 well plate were loaded with 90µl appropriate media into each well (LB/5 fold diluted LB/LB containing 5mM magnesium/ M9 minimal media (0.5%

Casamino acids, 2% glucose)/ M9 containing ~3µg of LtgB/M9 containing ~3µg of LtgE/ 50% v/v *B. thailandensis* culture supernatant (mixed in fresh LB)/50% v/v *M. tuberculosis* culture supernatant (mixed in fresh LB)). *B. thailandensis* culture supernatant was prepared by growing 50ml of *B. thailandensis* in LB overnight. The bacteria were harvested by centrifugation at 6000g for 10 minutes. The supernatant was filter sterilised twice through 0.2 µm filters (Merck Millipore) to ensure all bacteria were removed. Culture supernatant was used immediately. *M. tuberculosis* culture supernatant was prepared as described previously (292).

Cultures were homogenised by vortexing to ensure minimal clumping. 10µl of cell suspension was loaded into each well of the first row of the multi-well plate. 1:10 serial dilutions were made into each of the subsequent rows. Plates were sealed and incubated at 37°C for up to 2 weeks. Results were examined and the number of positive wells was recorded for each replicate. Experiments were set up for each of the triplicate cultures. MPN counts were calculated using Microsoft Excel MPN calculator software, developed by Professor Peter Wilrich, University of Berlin.

6.4. Results

Pilot experiments to test the effect of cold shock, high osmotic pressure and low pH on *B. thailandensis* E264 were carried out. B. thailandensis was chosen for pilot experiments due to its similarity to *B. pseudomallei* but with the ease of being classed as a containment level two organism. Bacteria were subjected to different stresses including incubation in dH_2O (control), dH_2O at pH4, exposure to 5% (w/v) NaCl (these three were tested at room temperature) and dH_2O at 4°C. CFU counts were recorded every day for 21 days and Live/Dead staining was performed at the end of the experiment. Only cultures incubated in 5% (w/v) NaCl resulted in complete loss of culturability over 21 days (Figure 41). Exposure to low temperature resulted in a small decrease in culturability.

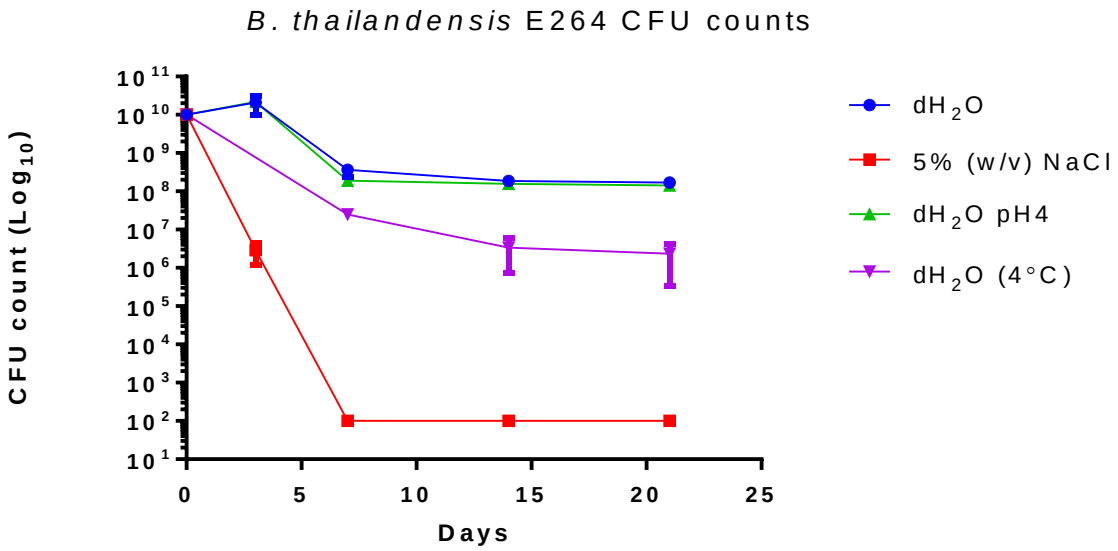

Figure 41: Effect of various stresses on culturability of *B. thailandensis* E264

Graph showing the CFU counts (CFU/ml) of *B. thailandensis* E264 subjected to stresses over 21 days. Preliminary results indicate that 5% NaCl (w/v) was effective at decreasing culturability to the limit of detection (100 CFU/ml), while pH4 and dH_2O did not result in a vast decrease in culturability. Note all cultures started at $>10^{10}$ CFU/ml at T_0, however the exact colony count was unknown due to insufficient dilutions.

It was unclear whether the counts for bacteria exposed to pH4 were reliable as the pH measurement taken of the water at the end of the experiments showed that the bacteria were able to neutralise the water. A weak buffer such as 20mM citric acid may be used to prevent this. Live cells were observed by Live/Dead staining (data not recorded) and as such LB and M9 minimal media was inoculated with each of the three samples for *B. thailandensis* E264 5% (w/v) NaCl. This was to determine if these bacteria were culturable in liquid media or if they were truly NC. Initial results indicated that after 24 hours there was no growth, but between 48 and 72 hours later 50% of samples began to show signs of growth. To try and ascertain the number of NC bacteria (on solid media), Most-Probable Number assays (MPNs) were set up. MPNs allow you to estimate, through serial dilutions, the number of bacteria that are able to grow in liquid medium. The results however, indicated that there was no growth in LB (no positive wells scored). Presumably the initial growth in LB and M9 minimal media was due to a very low number of culturable bacteria and the additional days of exposure to the high salt conditions could have potentially either killed these cells or made them NC.

It was decided to switch to a *B. thailandensis* strain most similar to the target organism, *B. pseudomallei*. *B. thailandensis* E555 is a capsulated strain that displays features similar to *B. pseudomallei* including colony morphology and intracellular macrophage survival (293). The next stage in the model progression was to select the stress condition that appeared to most promising. While results for low pH exposure could not be properly determined from the pilot study, osmotic pressure did cause the highest drop in culturability out of the conditions tested while also having the presence of live bacteria by Live/Dead staining.

To try and identify the optimal concentration of NaCl to use, LB containing various concentrations of NaCl was inoculated with the same volume of *B. thailandensis* E555 overnight and incubated at 37°C overnight. Optical densities were measured the following day. Between concentrations of 2.5% and 3% (w/v) NaCl there is a dramatic reduction in growth (measured by optical density) and at 5% (w/v) there was no increase in growth (Figure 42).

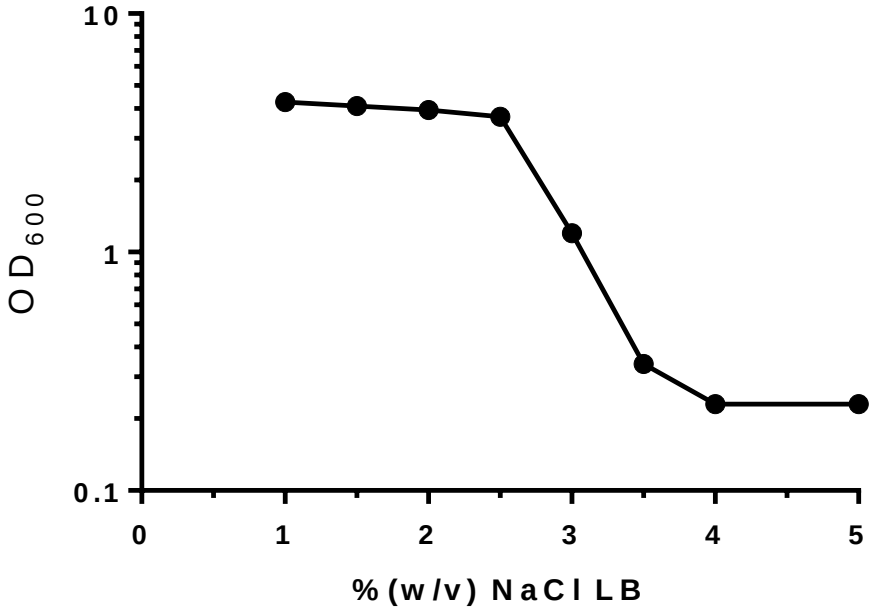

Figure 42: Growth of *Burkholderia thailandensis* E555 when exposed to LB containing increasing concentrations of NaCl

LB containing various concentrations of NaCl were inoculated with the same volume of bacterial culture and incubated overnight. Optical densities were measured the following day. A reduction in growth can be seen at concentrations above 2.5% (w/v) NaCl and no growth at 5% (w/v). This experiment was only performed once.

An experiment was devised to assess the ability of *B. thailandensis* to survive in dH_2O containing 2.5, 4 and 5% (w/v) NaCl. These concentrations were chosen because 2.5% (w/v) appeared to be the maximum salt concentration that E555 had unaffected growth, 4% because E555 could still grow even if it at very low levels and 5% as there is no growth. dH_2O without the addition of NaCl was used to demonstrate that any effect was due to NaCl concentration and not solely due to nutrient starvation.

In a similar set up to the previous non culturability experiment, triplicate cultures were grown to OD_{600} 1.0 washed in dH_2O and resuspended in the appropriate NaCl concentration to an OD of ~0.1. CFU counts and MPN counts using LA/LB were taken every 24 hours for 7 days. Results indicated that NaCl did reduce the culturability of *B. thailandensis* E555 on solid media but also in LB liquid media (Figure 43A/B). CFU and MPN counts dropped from $x10^{6-7}$ to just 100-1000 CFU/ ml. The most severe drop occurred between 0 and 72 hours, with the rate of decrease in culturable cells appearing to slow thereafter. The resuscitation index, RI, (LogMPN-LogCFU) allows you to easily assess whether there are more bacteria growing in liquid media or on solid media. Scores greater than 0 indicate that more bacteria are growing on solid media whereas a score of less than 0 indicate more bacteria are growing in liquid media. The RI for this experiment revealed broadly that more bacteria grew in liquid than in solid media (Figure 43C). The RI score is at a maximum of -1 for bacteria exposed to 4% NaCl, indicating a maximum of a log difference. While this is not a huge difference it may be that this is beyond the variation of the two methods to assess viability counts but actually some of the bacteria in the population are in a non culturable form. The ideal situation would result in a much lower RI, but this may be a promising start. Interestingly, a decreasing RI was seen in the 4% NaCl exposed group post 120 hours.

Live/Dead staining of bacteria exposed to 7 days of 5% NaCl revealed that there are a high percentage of cells (between 40 to 60%) that appear to be alive despite not producing high CFU or MPN counts (Figure 44).

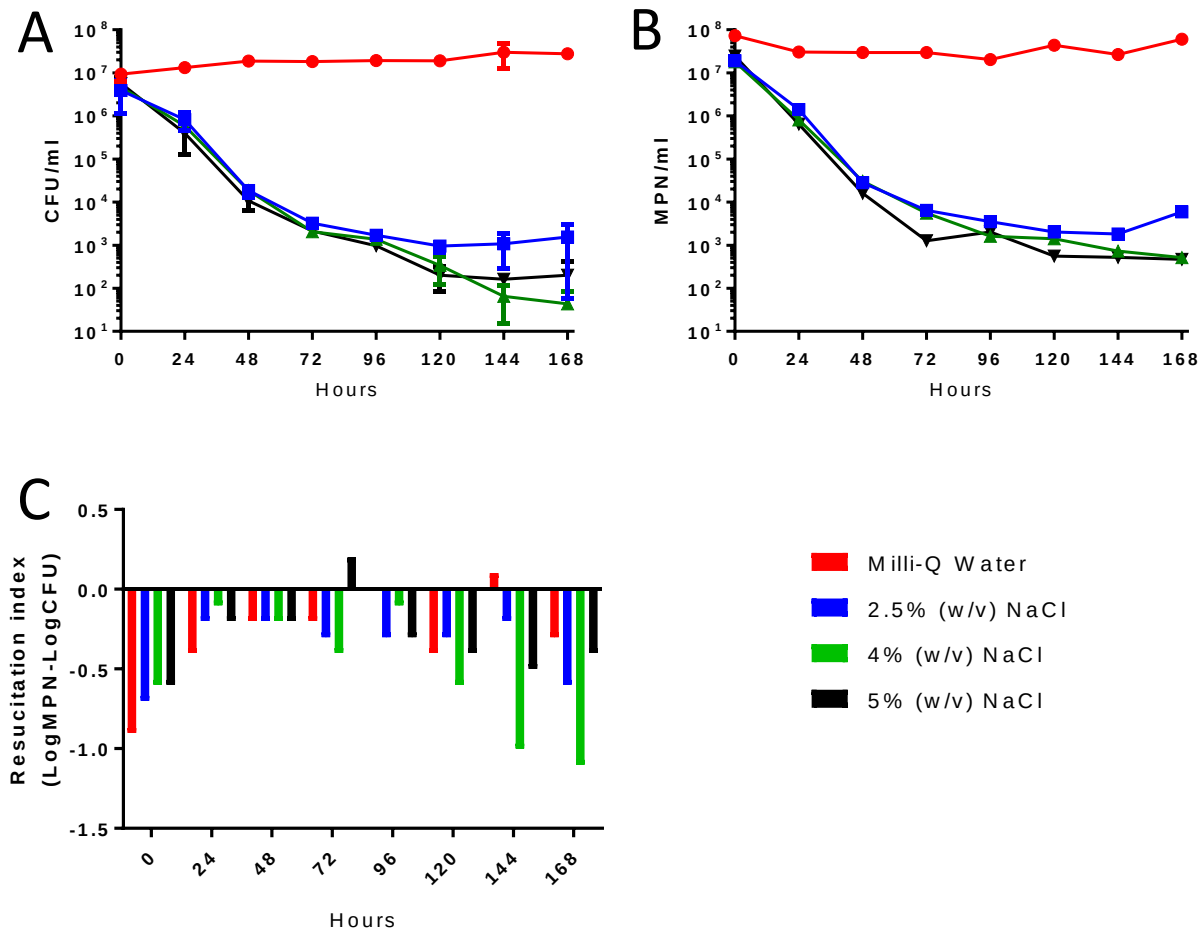

Figure 43: CFU and MPN counts of *B. thailandensis* E555 when exposed to various NaCl concentrations

Culturability decreases dramatically in all NaCl concentrations tested in both (A) CFU and (B) MPN counts over the course of the experiment. The most dramatic reduction occurs in the first 48-72 hours. Note; the limit of detection for CFU counts is 10 CFU. The counts at the end of the experiment (168 hours) for both MPN and CFU are approximately a log higher for the 2.5% w/v exposed cells compared to the 4 and 5% w/v exposed cells. C) Resuscitation index (RI) (LogMPN-LogCFU) was <0 indicating that more bacteria grew on agar than in liquid culture. There is a decreasing RI for bacteria exposed to 4% NaCl as time passes 120 hours.

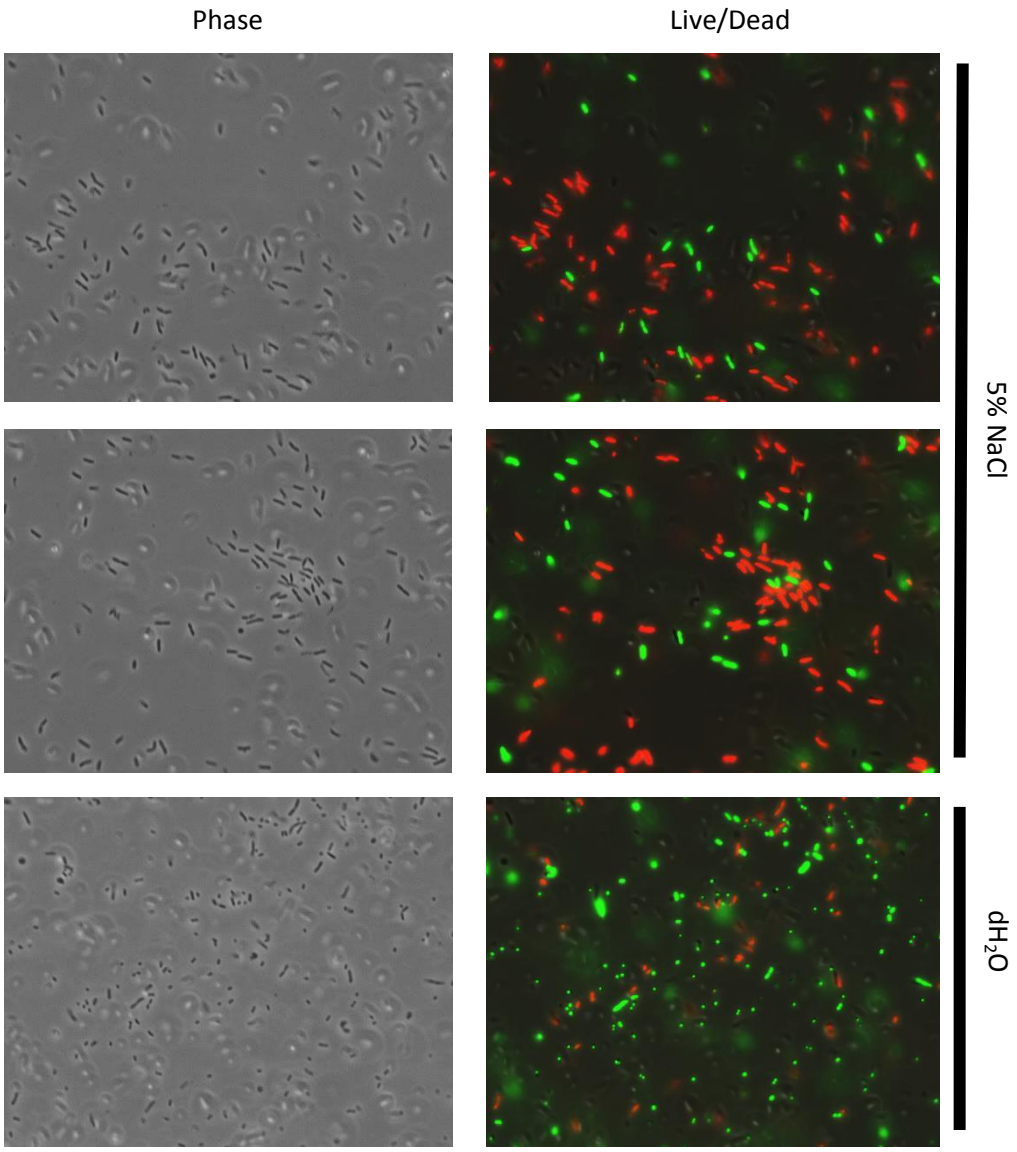

Figure 44: Live/Dead staining of *B. thailandensis* E555 exposed to 5% NaCl

B. thailandensis E555 strains were cultured in dH_2O and dH_2O water containing 5% NaCl for 7 days. Live/dead staining shows roughly 40-60% viable (green), cells despite not being able to be cultured on LA. Bacteria subjected to dH_2O only are almost all viable, but have substantially more coccoid morphology than those treated with NaCl.

As there were approximately x10^7 bacteria at the beginning of the experiment (by CFU count) and by the end counts had dropped to x10^2-x10^3 CFUs/ml (0.0001-0.001% survival), Live/Dead staining indicates that there are much more live bacteria than are reflected by CFU/MPN counts as there are 40-60% of the sample that are live. This suggests that there are a large number of potentially non-culturable bacteria in the population. Images taken of cells exposed only to dH_2O revealed a high percentage of live bacteria (>90%), however many of these bacteria appear to be much smaller, and more coccoid shaped. These results were reproducible across three independent experiments.

The focus of the investigation then turned to resuscitation of these dormant/NC cells. It may be that LB (used in the MPN assays) was too nutrient rich and substrate accelerated death was occurring when attempting to resuscitate them (294). Alternative media were tested in an attempt to resolve this. MPN counts using M9 minimal media, LB (diluted 5 fold) and LB supplemented with 10mM magnesium were set up using bacteria exposed to 2.5% and 5% (w/v) NaCl. None of these conditions however resulted in resuscitation. The addition of 5µg of recombinant LtgB and LtgE was also tested but this also failed, this is likely due to the fact that *Burkholderia* is a Gram-negative bacterium and poses the issue of translocation of the protein across the outer membrane, an issue not relevant to Rpfs of *Mycobacteria* spp.

B. thailandensis strains overexpressing LtgE were used to investigate resuscitation. The lack of compatible *E. coli* plasmids and inducible *Burkholderia* plasmids posed a substantial drawback. The *ltgE* encoding region was cloned into the IPTG inducible pME6032 plasmid that has been successful *in cis* complementation in *Burkholderia* before (111, 295). However as stated in Chapter 4.3.2 there was no evidence of LtgE expression that had been seen for pMo168-*ltgE* (under the control of the LtgE native promoter). It was hypothesised that expression at the levels seen using pMo168-*ltgE* would be toxic and above those likely to be expressed if used in resuscitation. Therefore, it was decided to proceed with the inducible plasmid in the chance that there was low level expression. *B. thailandensis E555* pME6032-*ltgE* was put through the osmotic stress NC model but failed to resuscitate when exposed to IPTG even at very high concentrations (1M), this is likely due to a failure to express the protein or

because LtgE could not resuscitate the bacteria. Given more time this would have been tested using reverse transcriptase PCR.

The NC model was set up using *B. thailandensis* pMo168 and pMo168-*ltgE*. CFU counts dropped to the limit of detection (100 CFU/ml) for both strains as seen previously (Figure 45). MPN assays were set up to see if any of the NC bacteria could resuscitate to actively growing cultures. A wide range of conditions were tested; LB, LB (diluted 1:5), M9 minimal media (0.5% Casamino acids, 2% glucose), M9 + 2µg LtgB, M9+ 2µg LtgE, 50% v/v *B. thailandensis* culture supernatant (mixed in fresh LB) and 50% v/v *M. tuberculosis* culture supernatant (mixed in fresh LB). However, there was no growth in any media following 7 days of incubation. Given more time this experiment would have been repeated and optimised as the starting culture was $6x10^4$ CFU/ml when ideally it should be much higher ($1x10^{6-7}$CFU/ml). There was difficulty in matching CFU count to OD for both strains; this is likely due to the toxic effect of LtgE overexpression as seen in Chapter 5.3.2. This experiment would have to be redesigned to account for any cellular morphological differences that can result in fluctuations in OD.

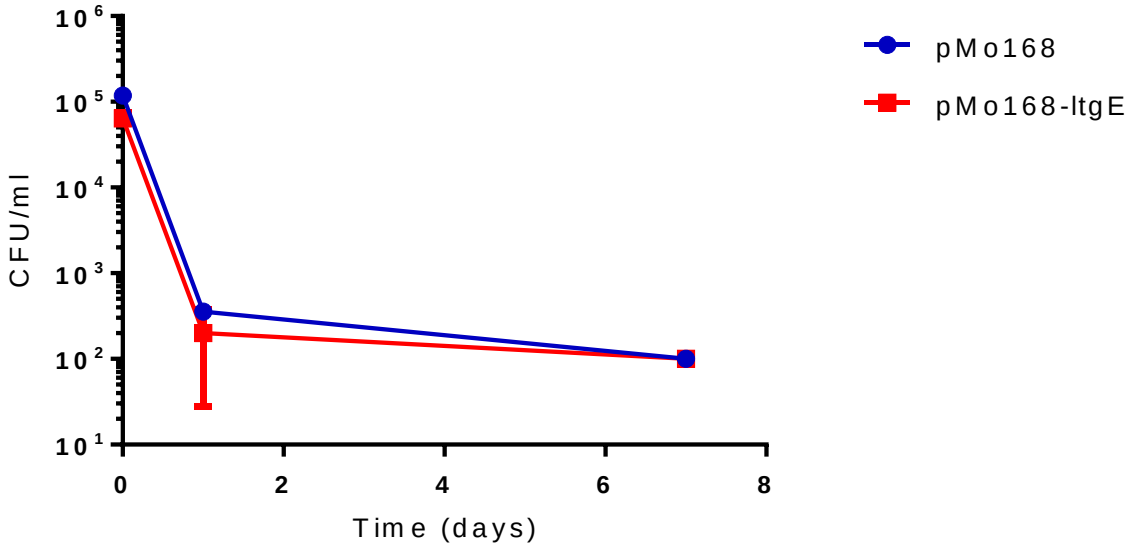

Figure 45: CFU count of *B. thailandensis* E555::pMo168 and pMo168-*ltgE* strains - when exposed to 5% NaCl

Culturability measured by CFU count dropped to the limit of detection (100 CFU/ml) as previously demonstrated however, there was no resuscitation in various media. pMo168-*ltgE* had approximately two fold difference in starting CFU count, likely due to the toxic effect of overexpressing LtgE in *B. thailandensis*.

6.5. Discussion

Using exposure to high salt levels it was possible to prevent culturability on solid media while leaving a large proportion of cells viable, at least by observations using Live/Dead staining. Given the rapid reduction in culturability and the reasonable retention of 'viable' bacteria it would appear that osmotic stress would be a suitable model to develop. There are a number of possible experiments that could be performed in order to develop this model. These include continuing to develop methods to express Ltg only when the cells are in a nonculturable state using a more suitable inducible plasmid. The native *ltgE* promoter used in pMo168-*ltgE* could be removed and replaced an inducible promoter. Ideally a very sensitive promoter would be used where the level of expression could be very tightly regulated to assess the levels of mRNA expression needed for resuscitation. Given the protocols outlined in Chapter 3 for the purification of recombinant Ltgs and the generation of the *ltg* mutants, it would have been interesting to see the whether this model could be progressed to see if Ltgs are directly involved in the generation of non-culturable forms of *Burkholderia*.

Aside from the resuscitation aspect it would also be interesting to assess the metabolism or even gene expression of these potentially nonculturable cells. Given the half-life of mRNA is only a matter of minutes, positive results using RT-PCR would suggest that these nonculturable cells are still viable. Housekeeping genes could be assessed and it would be interesting to see the level of mRNA levels for Ltg.

To assess the ability of Ltg protein to resuscitate NC cells the out membrane of the cells could be disrupted using a weak detergent such as Triton X-100 or the antibiotic polymyxin B. There is also a possibility that the cells visualised are not non –culturable in the traditional sense but bacteria in a different physiological state. They may be technically still live but they may not be able to resuscitate and a more suitable model may be needed to enable *Burkholderia* to enter a true nonculturable state. This however, is unlikely to be the case as it has been shown in other bacteria that osmotic pressure is able to force a non culturable state (296).

It has also been speculated that the stresses involved in generating a VBNC population result in damaged or injured cells that when exposed to atmospheric oxygen during plating results in formation of reactive oxygen species (ROS). These levels of ROS result in cell death and as a consequence colonies do not grow on plates. The addition of ROS scavengers such as catalase, pyruvate or glutamate has been shown to resuscitate VBNC cells (297-299). It would therefore be appropriate to assess whether the addition of ROS scavengers to media would allow for the resuscitation of the non culturable *Burkholderia* generated using this high osmotic pressure model.

It would be interesting to assess the virulence capabilities of nonculturable forms of *Burkholderia*. For example *Vibrio harveyi* in a VBNC state are no longer virulent in zebra fish or indeed mice (dependent on the length of time cells were in a VBNC) however resuscitation restored this lethality (300, 301). This could be assessed using *B. thailandensis* in a macrophage or *Galleria mellonella* model or potentially with *B. pseudomallei* in established murine models.

6.6. Summary

This chapter has outlined the development of a NC model for *Burkholderia thailandensis* using high salt concentrations. By using concentrations of NaCl greater than 2.5% it was possible to reduce the culturability of bacteria to the limit of detection while retaining 40-60% 'viable' bacteria according to live/dead staining. Unfortunately, it was not possible to resuscitate these bacteria using the conditions employed in these experiments but developing an inducible system for the expression of Ltgs may result in resuscitation.

Chapter 7

Final discussion

Peptidoglycan remodelling during cell growth and division is essential not just for the insertion of new precursors but also to maintain the integrity of the dividing cells during this crucial period. Many of the antibiotics used today target peptidoglycan biosynthesis, remodelling and modification enzymes given the unique nature of peptidoglycan to bacteria. However, decades of misuse and overuse in both the clinical and agricultural setting has led to an ever increasing number of drug resistant bacteria resulting in infections that are becoming more difficult, lengthier and costly to treat. The desire to identify new, novel antibiotic targets has become of paramount importance. Enzymes acting upon the peptidoglycan layer remain excellent targets for antibiotics and there are a number of proteins that are yet to be fully investigated as potential new targets. One such class of enzymes are the lytic transglycosylases. These proteins cleave the peptidoglycan layer using a unique mechanism of action resulting in a product that cannot be circumvented by other classes of proteins. Ltg cleavage allows for the localised degradation of peptidoglycan, particularly during cell growth and division to allow for the insertion of new peptidoglycan precursors or in certain cases the insertion of large macromolecular structures such as type VI secretions systems and flagella. While Ltgs have been the focus of much attention in model bacteria such as *E. coli*, *Salmonella* and *Neisseria* species, their importance in many other bacteria remains unknown, particularly in regards to biological functions and virulence. One such organism is *B. pseudomallei*. *B. pseudomallei* has a high mortality rate, is inherently resistant to many antibiotics and can remain undeterred in the host for many years before reactivation to cause latent infection. The desire for new antibiotics targeting *B. pseudomallei* is not just from the clinical community, with 89,000 deaths per annum (11), but also from a defence perspective given that *B. pseudomallei* is a schedule 5 pathogen and a potential biothreat.

Using sequence analysis to homologues in *E. coli* along with information in the literature, 5 putative Ltgs on chromosome 1 of *B. pseudomallei* K96243 were identified (Chapter 1). All 5 Ltgs have features typical of cell wall modifying enzymes including; predicted signal sequences for localisation into the periplasm and four out of five (LtgB excluded) have predicted membrane anchors which enable to protein to localise within the membrane. Other features include domains such as goose egg white

lysozyme domains, peptidoglycan binding domains such as LysM domains and conserved Ltg catalytic residues, typically glutamates. This project aimed to investigate these proteins initially in terms of their muralytic activity and then their role in the biological functions of *B. pseudomallei*.

It was unclear given the number of proteins and the redundancy of Ltgs and other cell wall hydrolases in other bacteria whether there would be any phenotypic differences between wildtype and single *ltg* mutants. While mutations were not lethal (indicating that these proteins are not essential for growth *in vitro*); *ltgB*, *ltgC*, *ltgD* and *ltgE* mutants all displayed individual phenotypes in various assays including motility, biofilm formation, cell morphology and virulence.

It became apparent using SEM and analysis of cell length that *ltgE* plays an important role in cell elongation and division. This is in agreement with research into LtgE homologues (MltA) in other bacteria such as *N. gonorrhoeae* in which mutation of MltA, was shown to cause defects in cell septation and cell separation (169). This phenotype could be greatly enhanced through the generation of multiple deletion mutants. Interestingly, only mutants containing a mutation Δ*ltgE* showed high levels of chaining and elongated cell length further suggesting that *ltgE* is essential for maintaining cell morphology and separation during growth and division. Despite the fact that there are no obviously morphological differences between the wildtype cells and the individual *ltgB, ltgC* and *ltgD* mutants or the *ltgDBC* mutant there must be a small level of redundancy given that the removal of each of these genes could increase the phenotype of *ltgE* deletion mutants.

The effect of these cell division defects on biological functions was also investigated. I hypothesised that the function of polar virulence factors could be influenced by chaining and the biological functions that rely on them may also therefore be affected. Through motility assays it was possible to show that these morphological defects resulted in decreased swimming and twitching motility although other functions such as biofilm formation were unaffected. Other Ltgs were also shown to be important in motility although it is unknown why this is the case. Like SltF in *R. sphaeroides* one or more of these Ltgs may be involved directly in assembly of flagella (195, 197). More

investigation would be needed to definitively say this, these could include protein: protein interactions between these Ltgs and flagella assembly proteins, the use anti-flagella component antibodies to assess the assembly of flagella in these *ltg* deletion mutants or perhaps electron microscopy directly looking for the presence or absence of flagella. It is also interesting that *ltgB, ltgC* and *ltgD* mutants all had significantly reduced biofilm formation. Biofilm formation is reliant on a number of factors including flagella, pili, quorum sensing and the production of extracellular matrix (247). As swimming and swarming motility is affected in these *ltg* mutations it is perhaps not surprising that there are also defects in biofilm formation. However, further work could aim to investigate the biofilm defects in more detail again through protein:protein interaction studies between Ltgs and components know to contribute to biofilm formation and measurement of AHL concentration by *ltg* mutants. This could be useful particularly as the treatment of melioidosis is lengthy and prolonged treatment in hospitals increases the chance of biofilm formation potentially providing additional complications in the clearance of *B. pseudomallei* from the host. Furthermore biofilms are known to contain a substantial population of persister cells and prevent successful treatment by antibiotics (302). Understanding the functions of Ltgs in biofilm formation could help to reduce the risks associated from this mode of growth.

Perhaps the most important finding was that 3 out of the 4 *ltgs* evaluated, were shown to be important in virulence of *B. pseudomallei* in the BALB/c mouse model of melioidosis. There is a very limited amount of literature that directly shows the importance of Ltgs in the virulence of pathogens, as such it was difficult to predict the outcome of the studies was likely to be. While it is useful to understand the mechanisms and functions of Ltgs, this research has shown that mutations results in significant defects in the ability of *B. pseudomallei* to cause infection. Moreover, the quadruple *ltg* deletion mutant, Δ*ltgEBDC*, was highly attenuated with no mice succumbing to infection. As many of these Ltgs share domains it may be possible to target many of these proteins with a single inhibitor. *ltgE* again, appeared to be the most important Ltg in infection with survival rates of 90% and 100%. A number of experiments could be performed to try to further understand the exact nature of

these attenuations. Such experiments could include macrophage infections, assessment of actin tail and MNGC formation. Membrane proteomics and secretomics could also be performed to assess the presence of important structural and effector proteins of secretion systems important in virulence such as T3SS and T6SS.

While the 2 fold decreases in MIC observed for Δ*ltgEBDC* are not as dramatic as expected, a relatively small range of antibiotics were investigated. Using high throughput screening it may be able to identify drugs that have a much greater effect on the *ltg* mutants, in particular those targeting the cell wall. There are implications of disrupting the cell wall one of the most important being the increased production of β-lactamase. Through combination treatment with a β-lactamase inhibitor there may be greater sensitivity to antibiotics in the *ltg* mutants.

During this study I have optimised the production of recombinant Ltgs of *B. pseudomallei* in *E. coli*, in particular LtgE. I was also able to show using a range of approaches the muralytic activity of these proteins including assays suitable for high through put screening of inhibitors such as FITC-labelled peptidoglycan degradation and the MUF Tri-NAG assay. We were also able to solve the crystal structure of LtgE and use it along with data from other well characterised homologues to predict the catalytic site. Through site directed mutation of aspartate D343 it was possible to abolish activity in zymogram. This could also be shown in vitro as this mutation was also able to prevent complementation in *ltgE* complemented strains. These results, the methods developed and the crystal structure of LtgE, would be an excellent tools for the development of new inhibitors to target LtgE directly.

Rpf inhibitors were briefly investigated to see if Ltg activity was affected. These inhibitors rapidly dropped out of solution in zymograms and the MUF tri-NAG assay. This was not optimised and a more systematic approach could be taken in the future. Unfortunately LtgE activity in solution was only proven in the final weeks of my research and therefore I was unable to test the activity in the presence of inhibitors using FITC-labelled peptidoglycan.

Given the results seen in regards to motility, biofilm formation and virulence, particularly in relation to LtgE, it suggests that Ltgs are a suitable new target for novel antivirulence drug development. Classical antibiotics cause growth arrest or death of the bacteria, antivirulence drugs aim to disarm the pathogen in order to prevent colonisation and progression of the disease. They also have the added benefit that they would not kill commensal bacteria and as they do not target vital cellular process the likelihood of resistance is much lower than classical antibiotics. Given this, there has been increasing research into this antivirulence approach over the last decade (303). Specific examples of this being a successful approach include the use of inhibitors of the adhesins FimH in *E. coli* to prevent urinary tract infections (304) and reduce symptoms of Crohn's disease (305). There are drawbacks however, in using virulence proteins as drug targets. While recombinant protein assays can allow you identify inhibitory concentrations, the efficacy and potency of a drug is typically assess using MICs, however this approach may not be possible for antivirulence drugs if they often do not cause an obvious inhibition of growth. This is the case for LtgE and also other virulence determinants such as T3SS and T6SS proteins whose deletion does result in substantial decrease in virulence and could potentially be excellent drug targets, do not result in substantial growth defects. As such, initial high through put screening is reliant on cell based assays or whole cell protein specific assays followed by small animal models. High-throughput cell based assays have been used to identify inhibitors of quorum sensing in *P. aeruginosa* (306). An alternative approach, used to identify inhibitors of the T3SS in *Yersinia pestis* has been to use the *luxAB* reporter gene construct under the promoter of a chaperon for a T3SS effector protein. In the presence of an inhibitor the genes are not expressed and an absence of luciferase expression (307).

At this time, without an observable effect on growth, LtgE inhibitor screening would largely be based on recombinant protein assays such as the FITC labelled peptidoglycan assay. However future experiments could aim to identify measurable whole-cell phenotypes that may allow for high throughput screening of inhibitors. These could include detection of secreted proteins (assuming mutation results in alteration in the secretome) or if mutation results in defects in cell invasion or

replication then high through put screening could be performed using a cell based approach. This could also allow you to identify concentrations in an MIC-like manner.

Finally, a basic model for the generation of nonculturable forms of *Burkholderia* was also established. Using exposure to high salt levels it was possible to prevent culturability of B*. thailandensis* while leaving a large proportion of these cells viable, at least using Live/Dead staining. Development of this model could determine whether Ltgs are directly involved in the generation of nonculturable forms of *Burkholderia*. From a research perspective it would also be interesting to assess the muropeptide profile of these ltg deletion mutants, particularly in regards to *O*-acetylation which has been shown to important in VBNC *E. faecalis* (202).

Overall I believe this project has been successful in investigating for the first time, the nature and functions of these proteins in *B. pseudomallei.* Moreover, I have shown correlation with data of homologous proteins contributing to our understanding of these proteins in a wider range of bacteria. I have developed a number of strains that can be used to further understand the roles of these proteins particular in regards to non culturability and virulence factor assembly. Through the optimisation LtgE expression and purification, the muralytic activity assays developed and the solving of the crystal structure of LtgE, the tools are in place for the next stages of rational design or high throughput inhibitor screening to investigate the druggability of LtgE.

These results regarding LtgE are being written to be submitted as a manuscript for publication.

Chapter 8

Appendix

8.1. Protein sequences

LtgA (BPSL0262)

Green; predicted signal sequence, Yellow; predicted membrane anchor, Red; predicted catalytic glutamate

Protein sequence

MSTSLFRVYRAVAAPLVAIALAAVAAACAAQTADEASSNDDRVFVQLREAARRNDPVRAAQLAALIPNYPAPSYLEYF
QIKPQLFDSAGHARLDAPDAPVLSFLSRYDGQAIADRMRNDYLLVLGARHDWRAFDEQYKRFVLDDDTQVKCYALES
RASRGENVADMARELLVEPKYYGDACVDLITALATNKQFSSDDVWAQVRLAYEQNYTTLGGKIADALGPRPVGFDQV
TSAPPLFLARGVGSDATSRQLALVAITRMARNDPEAAAGQLASLASTLSAAEQAIGWGEIGYQATVKRLPQAASWYRK
SMDAPLSNPAYEWRVRAALLAGDWPMVRRSIEQMPERLRDDTAWIYWRGRALKESGDTLKANQEFERIAGQFNFY
GQLAGEELGQKTTIPPRTKVTDAEIDAMSKVPGFALAQRFYALNLRLEGNREWNWPLRGMTDRQLLAAAEYGKRVDL
LDRTVNTADRTTAEHDFSLRYPSPYRDIVERYARTNGLDVEWAYGLIRQESRFITNARSTVGAGGLMQLMPATAQLVA
KKLGLGTVSRAQMHDIDTNVQLGTWYLSDIYQKFDDSAVLATAGYNAGPGRPAQWRQVLTRPVEGAIFAETIPFNET
REYVKNVLSNETYYAALFEKKPQSLKARLGFIAP

LtgB (BPSL1345)

Green; predicted signal sequence, Red; predicted catalytic glutamate

Protein sequence

MLTRSTHFRTIACNFQPLEAEIFMRFLLSALLVLTLAACAGTGPTAQNPAASDPQAASDYLRKSASAKETVDVDKQSVG
DLTTADSDLWARIRRGFQMPDLQSDLVDMQASWYAQRPDYVQRMTERSQKYLYHIVEELESRHMPTELALLPFIESA
YNPQALSVAKAAGMWQFMPATGRTFNLKRNMWQDERRDVLASTSAALDYLSRLHDMFGDWYLALAAYNWGEGN
LQRAIARNQAAGLPTDYQSLRMPNETRNYVPKLQAVKNIVTNPQQYGLTLPEIPNHPYFVTVTTSRDIDVTVAAKLANL
PLDEFKSLNPSFSKPVILGATQPQILLPFDNAAAFEKGLKSYDGQLSSWTAYTVTERARPAAIAEKIGVDADTLMQVNKI
PAGMRLKPGSTIVVPRTDDDDEDISADVAENGVLAMEPDVPDTRKMLIRVRRKQSMEALASRYGVSVAQLRGWNRT
RRAVVMPGQTMVLHVPVGRAVPAEPGPERIATSVGGGRIERASLHTGGKASSRGRKAGPAAKASAKAATKSGAKAAP
AKTAGRKTTKKK

LtgC (BPSL2506)

Green; predicted signal sequence, Yellow; predicted membrane anchor, Red; predicted catalytic aspartate

Protein sequence

MSVILPRNRPSRPLRFDMIFHQPAAPASLAFRLRFPLAALSLAATLFASAAVAQTQPAAAVVAQEPAQPQSQSQSQSQ
LQPQPQPQPQPQPSVQQGQTFEEEIIPQRYANNAKIDAFIADMVARHDFDANALHALFARVSYSATAAKLVMPAPSP
AVKNWRVYQSRFLDAVRVNAGVKFWRANQGTLQRASTEFGVPPEVIVGIIGVETIYGRYMGNFRTLDALTTLAFDYPN
TPNRDARQATFRKNLEDFLVWTRDSQLDPTGVLGSYTGAVGIPQFLPSSIRDYAVDYDGNGHIDLRASQADAIGSVAN
YLKQHGWETGRPVVWNIAPDTGSQGVAQAAADGRPEPHWVLSQLLRAGLVLDEPSVNIASEASTPVTVVDLPTPGR
ATEYKLGLQNFYVLTRYNRSFFYALAVYQLGERVKAQMEASGALTPSPADAATGSPAAQPPSE

LtgD (BPSL2630)

Green; predicted signal sequence, Yellow; predicted membrane anchor, Red; predicted catalytic glutamate

Protein sequence

MLRAVLRRGTRVSHHLFSVVGCCAVAVALALWLLPNVRGTLAAKVMPFVSAAVQAGPARLLSGHPLPTFGPANADES
ESVNADAAPSTTAAPADAGAMLDAARNSPSPVSLAKLIPTQRVAADARDDRVLASNREQALVATYLARRYRVAQEPV
GQLVKAAFQTGRDVGLDPLLILAVMAIESGFNPYAESGVGAQGLMQVMSKVHSDKFEYFGGTDAALQPVVNIQVGA
LVLKDCIARGGSLAGGLRLYVGATTPDDGGYGAKVIGERDRLRDVARGRKVSIYASQQPAQGAVTVATVSTSSGATQK
RVRTTLDGAHPLTIKAAAAPKAPQQDDVSADTAASSKHETASPELGT

LtgE (BPSL3046)

Green; predicted signal sequence, Yellow; predicted membrane anchor, Red; predicted catalytic aspartates

Protein sequence

MGFSRRLAGWAAAVAAAALLAACVGSPVRQGARPAGAAIVPGQIAAARLTPVAWQQVPGWQDDSLIGATIALRQN
CARLARQANWQRACAAAMRLDDLDVGSARTFFETYFTPFQFANNDGTLDGLVTGYYEPLLHGSRVRRGPYQYALYR
WPAGYRAGASMPARAQLMRSGALSGNELVWVDDPIEAFFLQVQGSGRVVLDDGTVMRVGYGGTNNQPYRSIGKW
LLDHGELGAGQATMQGIKAWARANPSRVDALLDTNPRFVFFREMPSQEDVPHGGADGPVGALGVPLTPERSIAVDP
SSIPLGTPVFLQTTRPMTNAPLNRLVFAQDVGTAIKGGVRADYFWGLGDDAGDQAGRMKQNGRMWLLFPNS-

8.2. *E. coli* strains

***E. coli* strain**	**Properties**
C41(DE3)::pET23a-*ltgB*	Expression of recombinant LtgB (secreted)
C41(DE3)::pET23a-*ltgB* E154A	Expression of recombinant LtgB (secreted) containing a site directed mutation in glutamate 154 to alanine
C41(DE3):: pET23a-*ltgB* E154K	Expression of recombinant LtgB (secreted) containing a site directed mutation in glutamate 154 to lysine
C41(DE3)::pET23a-*ltgD*	Expression of recombinant LtgD (secreted)
C41(DE3)::pET23a-*ltgD* E128A	Expression of recombinant LtgD (secreted) containing a site directed mutation in glutamate 128 to alanine
C41(DE3)::pET23a-*ltgD* E128K	Expression of recombinant LtgD (secreted) containing a site directed mutation in glutamate 128 to lysine
C41(DE3)::pET23a-*ltgE*	Expression of recombinant LtgE (secreted)
C41(DE3)::pET23a-*ltgE* D300A	Expression of recombinant LtgE (secreted) containing a site directed mutation in aspartate 300 to alanine
C41(DE3)::pET23a-*ltgE* D331A	Expression of recombinant LtgE (secreted) containing a site directed mutation in aspartate 331 to alanine
C41(DE3)::pET23a-*ltgE* D343A	Expression of recombinant LtgE (secreted) containing a site directed mutation in aspartate 343 to alanine
C41(DE3)::pET15bTev-*ltgB*	Expression of recombinant LtgB (non-secreted)
Bl21(DE3)::pET15bTev-*ltgC*	Expression of recombinant LtgC (non-secreted)
C41(DE3)::pET15bTev-*ltgE*	Expression of recombinant LtgE (non-secreted)
C41(DE3)::pET15bTev-*ltgE* D343A	Expression of recombinant LtgE (non-secreted) containing a site directed mutation in aspartate 343 to alanine
S17-1 (λ*pir*)::pMo130-*ltgB*	Conjugation of suicide vector the generation of a deletion mutant in *ltgB*
S17-1 (λ*pir*)::pMo130-*ltgC*	Conjugation of suicide vector for the generation of a deletion mutant in *ltgC*
S17-1 (λ*pir*)::pMo130-*ltgD*	Conjugation of suicide vector for the generation of a deletion mutant in *ltgD*
S17-1 (λ*pir*)::pMo130-*ltgE*	Conjugation of suicide vector for the generation of a deletion mutant in *ltgE*

S17-1 (λ*pir*)::pMo130-*ltgE*comp	Conjugation of suicide vector for *in cis* complementation of *ltgE*
S17-1 (λ*pir*)::pMo130-*ltgE*comp D343A	Conjugation of suicide vector for *in cis* complementation of *ltgE* (containing a D343A mutation)
S17-1 (λ*pir*)::pMo130-*ltgE*comp control	Conjugation of suicide vector used for *ltgE* complementation – containing only integrative elements and not complementing gene

Table 5: *E. coli* strains generated in this study

8.3. *Burkholderia pseudomallei* strains

***Burkholderia pseudomallei* strain**	**Properties**
K96243	Wildtype strain (62)
K96243 Δ*ltgB*	Unmarked deletion mutant in *ltgB*
K96243 Δ*ltgC*	Unmarked deletion mutant in *ltgC*
K96243 Δ*ltgD*	Unmarked deletion mutant in *ltgD*
K96243 Δ*ltgE*	Unmarked deletion mutant in *ltgE*
K96243 Δ*ltgEB*	Unmarked deletion mutant in *ltgE* and *ltgB*
K96243 Δ*ltgEBD*	Unmarked deletion mutant in *ltgE*, *ltgB* and *ltgC*
K96243 Δ*ltgEBDC*	Unmarked deletion mutant in *ltgE*, *ltgB,* ltgD and *ltgC*
K96243 Δ*ltgDB*	Unmarked deletion mutant in *ltgD* and *ltgB*
K96243 Δ*ltgDBC*	Unmarked deletion mutant in *ltgD, ltgB* and *ltgC*
K96243 Δ*ltgE*::pMo130-*ltgE*	Unmarked deletion mutant in *ltgE* complemented *in cis* with *ltgE*
K96243 Δ*ltgEBDC*::pMo130-*ltgE*	Unmarked deletion mutant in *ltgE*, *ltgB,* ltgD and *ltgC* complemented *in cis* with *ltgE*
K96243 Δ*ltgE*::pMo130-*ltgE D343A*	Unmarked deletion mutant in *ltgE* complemented *in cis* with *ltgE* (containing a D343A mutation)
K96243 Δ*ltgEBDC*::pMo130-*ltgE D343A*	Unmarked deletion mutant in *ltgE*, *ltgB,* ltgD and *ltgC* complemented *in cis* with *ltgE* (containing a D343A mutation)
K96243 Δ*ltgE*::pMo130 control	Unmarked deletion mutant in *ltgE* 'complemented' *in cis* with empty suicide vector pMo130
K96243 Δ*ltgEBDC*::pMo130 control	Unmarked deletion mutant in *ltgE*, *ltgB,* ltgD and *ltgC* 'complemented' *in cis* with empty suicide vector pMo130
K96243::pMo168	Wildtype strain containing empty pMo168
K96243::pMo168-*ltgE*	Wildtype strain containing pMo168-*ltgE* for overexpression of LtgE

Table 6: *B. pseudomallei* strains generated in this study

8.4. *B. thailandensis* strains

***Burkholderia thailandensis* strains**	**Properties**
E555	**Wildtype strain (293)**
E555::pMo168	**Wildtype strain containing empty pMo168**
E555::pMo168-*ltgE*	**Wildtype strain containing pMo168-*ltgE* for the overexpression of LtgE**
E264	**Wildtype strain**

Table 7: *B. thailandensis* strains generated in this study

8.5. List of primers

Name	SEQUENCE 5' – 3'	Restriction site	Purpose	PCR product sizes (bp)
16S_For	GACACGGCCCAGACTCCTAC		16S for RT-PCR control	176
16S_Rev	CCGGTACCGTCATCCACTCC		16S for RT-PCR control	
LtgA_pET15_For	ACACATATGGCGCAGACCGCCGACGAAGCGTCGT	*Nde*I	Non-secreted LtgA	1881
LtgA_pET15_Rev	ACAGGATCCTTACGGCGCGATGAAGCCGAGGCGA	*Bam*HI	Non-secreted LtgA	
LtgA_pET23_For	ACACATATGTCAACCAGCCTTTTTCGAGTATAT	*Nde*I	Secreted LtgA	1965
LtgA_pET23_Rev	ACAGAATTCCGGCGCGATGAAGCCGAGGCGAGC	*Eco*RI	Secreted LtgA	
LtgB_E154A_For	CGCTGCTGCCGTTCATCGCATCGGCGTACAACCCGCAGG		Insertion of point mutation (E154A) in LtgB	
LtgB_E154A_Rev	CCTGCGGGTTGTACGCCGATGCGATGAACGGCAGCAGCG		Insertion of point mutation (E154A) in LtgB	
LtgB_E154K_For	CGCTGCTGCCGTTCATCAAATCGGCGTACAACCCGCAGG		Insertion of point mutation (E154K) in LtgB	
LtgB_E154K_Rev	CCTGCGGGTTGTACGCCGATTTGATGAACGGCAGCAGCG		Insertion of point mutation (E154K) in LtgB	
LtgB_GS_For	CGTTGGAAGCCGAGATTT		*ltgB* gene specific	170
LtgB_GS_Rev	GACGTCGACGGTTTCTTT		*ltgB* gene specific	
LtgB_out_For	CGTTCACGTTGATGCGCGAGT		Confirmation screening of Δ*ltgB*	Wildtype - 1943
LtgB_out_Rev	ATCACGATCACCGGTAAGACG		Confirmation screening of Δ*ltgB*	Mutant - 475
LtgB_FR1_For	ATAAAGCTTACAACTACATCTGGCTCGTGT	*Hind*III	FR1 for *ltgB* deletion mutant	1056
LtgB_FR1_Rev	ATAGGATCCTTGCGCAAGTAGTCCGAA	*Bam*HI	FR1 for *ltgB* deletion mutant	
LtgB_FR2_For	ATAGGATCCAAGTAAGACGAAAGGGCGCGC	*Bam*HI	FR2 for *ltgB* deletion mutant	1021
LtgB_FR2_Rev	ATATCTAGAAACCCGCAGAACGCATACAGC	*Xba*I	FR2 for *ltgB* deletion mutant	
LtgB_pET15_For	ACACATATGGGCACCGGGCCGACCGCCCAAAAT	*Nde*I	Non-secreted LtgB	1554
LtgB_pET15_Rev	TACTGGATCCTTACTTCTTCTTCGTCGTCTTGC	*Bam*HI	Non-secreted LtgB	
LtgB_pET23_For	ACACATATGTTGACGCGAAGCACGCACTTTCGT	*Nde*I	Secreted LtgB	1671
LtgB_pET23_Rev	ACTCTCGAGCTTCTTCTTCGTCGTCTTGCGGCC	*Xho*I	Secreted LtgB	
LtgC_GS_For	CTCGAAGATTTCCTCGTCTG		*ltgC* gene specific	208
LtgC_GS_Rev	CGTGCTGCTTCAGATAGTT		*ltgC* gene specific	
LtgC_out_For	TGTAATCGATGTGCGCCTGCG		Confirmation screening of Δ*ltgC*	Wildtype - 1846
LtgC_out_Rev	AGGTTCGACTGCTCGCTTGCG		Confirmation screening of Δ*ltgC*	Mutant – 710

LtgC_FR1_For	ATAAAGCTTTCGTAGTCGGCTTCGACGAGC	*Hind*III	FR1 for *ltgC* deletion mutant	1135
LtgC_FR1_Rev	ATAGGATCCATTGCGGCTGCGCCGGCTCTT	*Bam*HI	FR1 for *ltgC* deletion mutant	
LtgC_FR2_For	ATAGGATCCGAATGACGCCGACGCGGCGCG	*Bam*HI	FR2 for *ltgC* deletion mutant	1126
LtgC_FR2_Rev	ATATCTAGAAAGACACGATCGGCAATA	*Xba*I	FR2 for *ltgC* deletion mutant	
LtgC_pET15_For	TGCCATATGGCCGTCGCGCAAACGCAGCCC	*Nde*I	Non-secreted LtgC	1221
LtgC_pET15_Rev	ACAGGATCCTCATTCGGACGGCGGCTGTGC	*Bam*HI	Non-secreted LtgC	
LtgC_pET23_For	ACACATATGTCGGTTATACTGCCCCGAAAT	*Nde*I	Secreted LtgC	1366
LtgC_pET23_Rev	ACTCTCGAGTTCGGACGGCGGCTGTGCGGC	*Xho*I	Secreted LtgC	
LtgD_E182A_for	CTCGCCGTGATGGCGATCGCATCCGGCTTCAATCCGTAT		Insertion of point mutation (E182A) in LtgD	N/A
LtgD_E182A_for	CTCGCCGTGATGGCGATCGCATCCGGCTTCAATCCGTAT		Insertion of point mutation (E182A) in LtgD	
LtgD_E182A_rev	ATACGGATTGAAGCCGGATGCGATCGCCATCACGGCGAG		Insertion of point mutation (E182K) in LtgD	N/A
LtgD_E182A_rev	ATACGGATTGAAGCCGGATGCGATCGCCATCACGGCGAG		Insertion of point mutation (E182K) in LtgD	
LtgD_GS_For	AGGTCCATTCGGACAAGTTC		*ltgD* gene specific	230
LtgD_GS_Rev	ATCACCTTCGCGCCATAA		*ltgD* gene specific	
LtgD_out_For	ACGGTACATATACCGTTTCTC		Confirmation screening of Δ*ltgD*	Wildtype - 1461 mutant - 475405
LtgD_out_Rev	TCAATATCCGCGTCGGAAACA		Confirmation screening of Δ*ltgD*	
LtgD_FR1_For	ATAAAGCTTATCTTTGTATTTCATGAAGAA	*Hind*III	FR1 for *ltgD* deletion mutant	663
LtgD_FR1_Rev	ATACTCGAGCAACATCTGCGCATGCCGCTCACT	XhoI	FR1 for *ltgD* deletion mutant	
LtgD_FR2_For	ATACTCGAGACCTGACGAAATCGGCGGCAA	XhoI	FR2 for *ltgD* deletion mutant	650
LtgD_FR2_Rev	ATATCTAGAGCAAGCTGTTCGGGCGCTAAC	XbaI	FR2 for *ltgD* deletion mutant	
LtgD_pET23_For	TGCCATATGTTGCGCGCAGTGCTGCGTCGCGGGA	*Nde*I	Secreted LtgD	1076
LtgD_pET23_Rev	ACACTCGAGGGTACCGAGCTCCGGGCTGGCCGTC	*Xho*I	Secreted LtgD	
LtgE_Comp130_For	ATCGAGCCAGATCTACGCTGCACTGAGCGCGGCGTCGC	*Bgl*II	*ltgE* including upstream region for insertion into pMo130 for *in cis* complementation	1347
LtgE_Comp130_Rev	GGATATCCCCGGGTCACGAATTCGGAAACAGCAGCCA	*EcoRV* *Sma*I	*ltgE* including upstream region for insertion into pMo130 for *in cis* complementation	
LtgE_compFR1_For	TGCGATCGCTAGCCATCAAACGGCCGACCGTGGTGGACATTC	*Nhe*I	FR1 for integration of in cis complementing plasmid downstream of *bpsl3330*	1190
LtgE_compFR1_Rev	CAGCTTTCAGATCTGGCTCGATCAAAATCCCTTCCAGTAATCG	*Bgl*II	FR1 for integration of in cis complementing plasmid downstream of *bpsl3330*	

LtgE_compFR2_For	AGATATCCCCGGGGCAGCCGGCGCGGCGGACGCCGGCGCAACC	*EcoRV* *Sma*I	FR2 for integration of in cis complementing plasmid downstream of *bpsl3330*	1000
LtgE_compFR2_Rev	CCACTCGCAAGCTTCGTCGCGTTCGACAACCGCTGCCCGCAC	*Hin*dIII	FR2 for integration of in cis complementing plasmid downstream of *bpsl3330*	
LtgE_D343A_Rev	GCCGAGCCCCCAGAAATAGGCGGCCCGCACGCCGCCCTTG		Insertion of point mutation (D343A) in LtgE	N/A
LtgE_D343A_For	CAAGGGCGGCGTGCGGGCCGCCTATTTCTGGGGGCTCGGC		Insertion of point mutation (D343A) in LtgE	N/A
LtgE_GS_For	TATCAGTACGCGCTCTACC		*ltgE* gene specific	150
LtgE_GS_Rev	CTGCACCTGCAGAAAGAA		*ltgE* gene specific	
LtgE_out_For	GCCGCGCACGCTGCACTGAGCGCG		Confirmation screening of Δ*ltgE*	Wildtype - 1571 Mutant - 478
LtgE_out_Rev	CGATACGTCCGGTCGCGCGTCGAA		Confirmation screening of Δ*ltgE*	
LtgE_168_Comp_For	TATGGATCCCACGATGCGCGGCGCGTATTTTT	*Bam*HI	*ltgE* including upstream region for insertion into pMo168 for *in trans* complementation/overexpression studies	1447
LtgE_168_Comp_Rev	ACTTCTAGATCACGAATTCGGAAACAGCAGCCA	*Xho*I	*ltgE* including upstream region for insertion into pMo168 for *in trans* complementation/overexpression studies	
LtgE_FR1_For	ATAAAGCTTAGCTATTTGCCGGAacaatcc	*Hin*dIII	FR1 for *ltgE* deletion mutant	580
LtgE_FR1_Rev	ATACTCGAGGCTAAAACCCATACAATGTCC	*Xho*I	FR1 for *ltgE* deletion mutant	
LtgE_FR2_For	ATACTCGAGAATTCGTGATCCTGTGATCTC	*Xho*I	FR2 for *ltgE* deletion mutant	1385
LtgE_FR2_Rev	ATATCTAGACGCGCATCCACGCTTCGTCAG	*Xba*I	FR2 for *ltgE* deletion mutant	
LtgE_pET15_For	ACACATATGTCTGTCGGCTCGCCGGTGCGGCAG	*Nde*I	Non-secreted LtgE	1071
LtgE_pET15_Rev	ACTGGATCCTCACGAATTCGGAAACAGCAGCCA	*Bam*HI	Non-secreted LtgE	
LtgE_pET23_For	ACACATATGGGTTTTAGCCGGCGGCTTGCC	*Nde*I	Secreted LtgE	1132
LtgE_pET23_Rev	ACTCTCGAGCGAATTCGGAAACAGCAGCCA	*Xho*I	Secreted LtgE	
M13_For	TGTAAAACGACGGCCAGT		Sequencing and colony screening of pGEM T-easy inserts	
M13_Rev	CAGGAAACAGCTATGACC		Sequencing and colony screening of pGEM T-easy inserts	

Table 8: Primers used in this study

Chapter 9

References

1. Yabuuchi E, Kosako Y, Oyaizu H, Yano I, Hotta H, Hashimoto Y, et al. Proposal of Burkholderia gen. nov. and transfer of seven species of the genus Pseudomonas homology group II to the new genus, with the type species Burkholderia cepacia (Palleroni and Holmes 1981) comb. nov. Microbiol Immunol. 1992;36(12):1251-75.

2. Sawana A, Adeolu M, Gupta RS. Molecular signatures and phylogenomic analysis of the genus Burkholderia: proposal for division of this genus into the emended genus Burkholderia containing pathogenic organisms and a new genus Paraburkholderia gen. nov. harboring environmental species. Frontiers in Genetics. 2014;5(429).

3. Lowe W, March JK, Bunnell AJ, O'Neill KL, Robison RA. PCR-based Methodologies Used to Detect and Differentiate the Burkholderia pseudomallei complex: B. pseudomallei, B. mallei, and B. thailandensis. Current issues in molecular biology. 2014;16:23-54.

4. Smith MD, Angus BJ, Wuthiekanun V, White NJ. Arabinose assimilation defines a nonvirulent biotype of Burkholderia pseudomallei. Infect Immun. 1997;65(10):4319-21.

5. Smith MD, Wuthiekanun V, Walsh AL, Pitt TL. Latex agglutination test for identification of Pseudomonas pseudomallei. Journal of clinical pathology. 1993;46(4):374-5.

6. Merritt A, Inglis TJ, Chidlow G, Harnett G. PCR-based identification of Burkholderia pseudomallei. Revista do Instituto de Medicina Tropical de Sao Paulo. 2006;48(5):239-44.

7. Rainbow L, Hart CA, Winstanley C. Distribution of type III secretion gene clusters in Burkholderia pseudomallei, B. thailandensis and B. mallei. J Med Microbiol. 2002;51(5):374-84.

8. Thibault FM, Valade E, Vidal DR. Identification and discrimination of Burkholderia pseudomallei, B. mallei, and B. thailandensis by real-time PCR targeting type III secretion system genes. J Clin Microbiol. 2004;42(12):5871-4.

9. Whitmore AKCS. An account of the discovery of a hitherto undescribed infective disease occurring among the population of Rangoon. Indian Medical Gazette. 1912;47:262-7.

10. Whitmore A. An account of a glanders-like disease occurring in Rangoon. Journ of Hyg. 1913:1 - 37.

11. Limmathurotsakul D, Golding N, Dance DAB, Messina JP, Pigott DM, Moyes CL, et al. Predicted global distribution of Burkholderia pseudomallei and burden of melioidosis. Nature Microbiology. 2016;1:15008.

12. Limmathurotsakul D, Wongratanacheewin S, Teerawattanasook N, Wongsuvan G, Chaisuksant S, Chetchotisakd P, et al. Increasing incidence of human melioidosis in Northeast Thailand. Am J Trop Med Hyg. 2010;82(6):1113-7.

13. Cheng AC, Currie BJ. Melioidosis: epidemiology, pathophysiology, and management. Clinical microbiology reviews. 2005;18(2):383-416.

14. Dance DA. Melioidosis as an emerging global problem. Acta Trop. 2000;74(2-3):115-9.

15. Currie BJ, Dance DA, Cheng AC. The global distribution of Burkholderia pseudomallei and melioidosis: an update. Trans R Soc Trop Med Hyg. 2008;102 Suppl 1:S1-4.

16. Limmathurotsakul D, Kanoksil M, Wuthiekanun V, Kitphati R, deStavola B, Day NP, et al. Activities of daily living associated with acquisition of melioidosis in northeast Thailand: a matched case-control study. PLoS Negl Trop Dis. 2013;7(2):e2072.

17. Cheng AC, Jacups SP, Gal D, Mayo M, Currie BJ. Extreme weather events and environmental contamination are associated with case-clusters of melioidosis in the Northern Territory of Australia. Int J Epidemiol. 2006;35(2):323-9.

18. Liu X, Pang L, Sim SH, Goh KT, Ravikumar S, Win MS, et al. Association of melioidosis incidence with rainfall and humidity, Singapore, 2003-2012. Emerg Infect Dis. 2015;21(1):159-62.

19. Hoppe I BB, Rohde M, Kreft A, Häussler S, Reganzerowski A, Steinmetz I. Characterization of a Murine Model of Melioidosis: Comparison of Different Strains of Mice. American Society for Microbiology. 1999:2891-900.

20. Ngauy V, Lemeshev Y, Sadkowski L, Crawford G. Cutaneous melioidosis in a man who was taken as a prisoner of war by the Japanese during World War II. Journal of clinical microbiology. 2005;43(2):970-2.

21. Howe C SA, Spotnitz M. The pseudomallei group: a review. The Journal of Infectious Disease. 1971;124(6):598-606.

22. Maharjan B, Chantratita N, Vesaratchavest M, Cheng A, Wuthiekanun V, Chierakul W, et al. Recurrent melioidosis in patients in northeast Thailand is frequently due to reinfection rather than relapse. Journal of clinical microbiology. 2005;43(12):6032-4.

23. Panida Kanaphun NT, Yupin Suputtamongkol, Pimjai Naigowit, David A. B. Dance, Michael D. Smith and Nicholas J. White. Serology and Carriage of Pseudomonas pseudomallei: A Prospective Study in1000 Hospitalized Children in Northeast Thailand. J Infect Dis. 1993;167(1):230-3.

24. Galyov EE, Brett PJ, DeShazer D. Molecular insights into Burkholderia pseudomallei and Burkholderia mallei pathogenesis. Annual review of microbiology. 2010;64:495-517.

25. Lewis K. Persister cells, dormancy and infectious disease. Nat Rev Micro. 2007;5(1):48-56.

26. Wiuff C, Zappala RM, Regoes RR, Garner KN, Baquero F, Levin BR. Phenotypic tolerance: antibiotic enrichment of noninherited resistance in bacterial populations. Antimicrob Agents Chemother. 2005;49(4):1483-94.

27. Nierman WC, Yu Y, Losada L. The In vitro Antibiotic Tolerant Persister Population in Burkholderia pseudomallei is Altered by Environmental Factors. Front Microbiol. 2015;6.

28. Barnes KB, Hamblin KA, Richards MI, Laws TR, Vente A, Atkins HS, et al. Demonstrating the Protective Efficacy of the Novel Fluoroquinolone Finafloxacin against an Inhalational Exposure to Burkholderia pseudomallei. Antimicrob Agents Chemother. 2017;61(7).

29. Hamad MA, Austin CR, Stewart AL, Higgins M, Vazquez-Torres A, Voskuil MI. Adaptation and antibiotic tolerance of anaerobic Burkholderia pseudomallei. Antimicrob Agents Chemother. 2011;55(7):3313-23.

30. Butt A, Higman V A, Williams C, Crump M P, Hemsley C M, Harmer N, et al. The HicA toxin from Burkholderia pseudomallei has a role in persister cell formation. Biochemical Journal. 2014;459(Pt 2):333-44.

31. Lau SK, Sridhar S, Ho CC, Chow WN, Lee KC, Lam CW, et al. Laboratory diagnosis of melioidosis: past, present and future. Exp Biol Med (Maywood). 2015;240(6):742-51.

32. Suntornsut P, Wongsuwan N, Malasit M, Kitphati R, Michie S, Peacock SJ, et al. Barriers and Recommended Interventions to Prevent Melioidosis in Northeast Thailand: A Focus Group Study Using the Behaviour Change Wheel. PLoS Negl Trop Dis. 2016;10(7):e0004823.

33. Peacock SJ, Chieng G, Cheng AC, Dance DA, Amornchai P, Wongsuvan G, et al. Comparison of Ashdown's medium, Burkholderia cepacia medium, and Burkholderia pseudomallei selective agar for clinical isolation of Burkholderia pseudomallei. Journal of clinical microbiology. 2005;43(10):5359-61.

34. Harris PN, Ketheesan N, Owens L, Norton RE. Clinical features that affect indirect-hemagglutination-assay responses to Burkholderia pseudomallei. Clinical and vaccine immunology : CVI. 2009;16(6):924-30.

35. Koehler C. The small Tim proteins and the twin Cx3C motif. Trends in Biochemical Sciences. 2004;29(1):1-4.

36. Houghton RL, Reed DE, Hubbard MA, Dillon MJ, Chen H, Currie BJ, et al. Development of a prototype lateral flow immunoassay (LFI) for the rapid diagnosis of melioidosis. PLoS Negl Trop Dis. 2014;8(3):e2727.

37. Robertson G, Sorenson A, Govan B, Ketheesan N, Houghton R, Chen H, et al. Rapid diagnostics for melioidosis: a comparative study of a novel lateral flow antigen detection assay. J Med Microbiol. 2015;64(8):845-8.

38. Lau SKP, Tang BSF, Curreem SOT, Chan T-M, Martelli P, Tse CWS, et al. Matrix-Assisted Laser Desorption Ionization–Time of Flight Mass Spectrometry for Rapid Identification of Burkholderia pseudomallei: Importance of Expanding Databases with Pathogens Endemic to Different Localities. Journal of Clinical Microbiology. 2012;50(9):3142-3.

39. Mahenthiralingam E, Bischof J, Byrne SK, Radomski C, Davies JE, Av-Gay Y, et al. DNA-Based diagnostic approaches for identification of Burkholderia cepacia complex, Burkholderia vietnamiensis, Burkholderia multivorans, Burkholderia stabilis, and Burkholderia cepacia genomovars I and III. J Clin Microbiol. 2000;38(9):3165-73.

40. Raja NS, White NJ, Simpson AJ. Burkholderia pseudomallei (Melioidosis) and B. mallei (Glanders).

41. McEniry DW, Gillespie SH, Felmingham D. Susceptibility of Pseudomonas pseudomallei to new beta-lactam and aminoglycoside antibiotics. The Journal of antimicrobial chemotherapy. 1988;21(2):171-5.

42. Dance D. Treatment and prophylaxis of melioidosis. Int J Antimicrob Agents. 2014;43(4):310-8.

43. Inglis TJJ. The Treatment of Melioidosis. Pharmaceuticals. 2010;3(5):1296-303.

44. Peacock SJ, Limmathurotsakul D, Lubell Y, Koh GC, White LJ, Day NP, et al. Melioidosis vaccines: a systematic review and appraisal of the potential to exploit biodefense vaccines for public health purposes. PLoS Negl Trop Dis. 2012;6(1):e1488.

45. Nelson M, Prior JL, Lever MS, Jones HE, Atkins TP, Titball RW. Evaluation of lipopolysaccharide and capsular polysaccharide as subunit vaccines against experimental melioidosis. Journal of Medical Microbiology. 2004;53(12):1177-82.

46. Scott AE, Christ WJ, George AJ, Stokes MG, Lohman GJ, Guo Y, et al. Protection against Experimental Melioidosis with a Synthetic manno-Heptopyranose Hexasaccharide Glycoconjugate. Bioconjug Chem. 2016;27(6):1435-46.

47. Casey WT, Spink N, Cia F, Collins C, Romano M, Berisio R, et al. Identification of an OmpW homologue in Burkholderia pseudomallei, a protective vaccine antigen against melioidosis. Vaccine. 2016;34(23):2616-21.

48. Propst KL, Mima T, Choi KH, Dow SW, Schweizer HP. A Burkholderia pseudomallei Delta purM Mutant Is Avirulent in Immunocompetent and Immunodeficient Animals: Candidate Strain for Exclusion from Select-Agent Lists. Infection and Immunity. 2010;78(7):3136-43.

49. Norris MH, Propst KL, Kang Y, Dow SW, Schweizer HP, Hoang TT. The Burkholderia pseudomallei Delta asd Mutant Exhibits Attenuated Intracellular Infectivity and Imparts Protection against Acute Inhalation Melioidosis in Mice. Infection and Immunity. 2011;79(10):4010-8.

50. Sarkar-Tyson M, Smither SJ, Harding SV, Atkins TP, Titball RW. Protective efficacy of heat-inactivated B. thailandensis, B. mallei or B. pseudomallei against experimental melioidosis and glanders. Vaccine. 2009;27(33):4447-51.

51. Puangpetch A, Anderson R, Huang YY, Saengsot R, Sermswan RW, Wongratanacheewin S. Comparison of the protective effects of killed Burkholderia pseudomallei and CpG oligodeoxynucleotide against live challenge. Vaccine. 2014;32(45):5983-8.

52. Jernigan DB, Raghunathan PL, Bell BP, Brechner R, Bresnitz EA, Butler JC, et al. Investigation of bioterrorism-related anthrax, United States, 2001: epidemiologic findings. Emerg Infect Dis. 2002;8(10):1019-28.

53. Rotz LD, Khan AS, Lillibridge SR, Ostroff SM, Hughes JM. Public health assessment of potential biological terrorism agents. Emerg Infect Dis. 2002;8(2):225-30.

54. Titball RW, Russell P, Cuccui J, Easton A, Haque A, Atkins T, et al. Burkholderia pseudomallei: animal models of infection. Trans R Soc Trop Med Hyg. 2008;102 Suppl 1:S111-6.

55. Sellers RS, Clifford CB, Treuting PM, Brayton C. Immunological Variation Between Inbred Laboratory Mouse Strains. Veterinary Pathology. 2011;49(1):32-43.

56. Nelson M, Dean RE, Salguero FJ, Taylor C, Pearce PC, Simpson AJH, et al. Development of an acute model of inhalational melioidosis in the common marmoset (Callithrix jacchus). International Journal of Experimental Pathology. 2011;92(6):428-35.

57. Nelson M, Nunez A, Ngugi SA, Sinclair A, Atkins TP. Characterization of lesion formation in marmosets following inhalational challenge with different strains of Burkholderia pseudomallei. Int J Exp Pathol. 2015;96(6):414-26.

58. Yingst SL, Facemire P, Chuvala L, Norwood D, Wolcott M, Alves DA. Pathological findings and diagnostic implications of a rhesus macaque (Macaca mulatta) model of aerosol-exposure melioidosis (Burkholderia pseudomallei). J Med Microbiol. 2014;63(Pt 1):118-28.

59. Sprynski N, Valade E, Neulat-Ripoll F. Galleria mellonella as an infection model for select agents. Methods in molecular biology (Clifton, NJ). 2014;1197:3-9.

60. Schell MA, Lipscomb L, DeShazer D. Comparative genomics and an insect model rapidly identify novel virulence genes of Burkholderia mallei. J Bacteriol. 2008;190(7):2306-13.

61. Thomas RJ, Hamblin KA, Armstrong SJ, Müller CM, Bokori-Brown M, Goldman S, et al. Galleria mellonella as a model system to test the pharmacokinetics and efficacy of antibiotics against Burkholderia pseudomallei. International Journal of Antimicrobial Agents. 2013;41(4):330-6.

62. Holden MT, Titball RW, Peacock SJ, Cerdeno-Tarraga AM, Atkins T, Crossman LC, et al. Genomic plasticity of the causative agent of melioidosis, Burkholderia pseudomallei. Proc Natl Acad Sci U S A. 2004;101(39):14240-5.

63. Tumapa S, Holden MTG, Vesaratchavest M, Wuthiekanun V, Limmathurotsakul D, Chierakul W, et al. Burkholderia pseudomallei genome plasticity associated with genomic island variation. Bmc Genomics. 2008;9.

64. Sim SH, Yu Y, Lin CH, Karuturi RKM, Wuthiekanun V, Tuanyok A, et al. The Core and Accessory Genomes of Burkholderia pseudomallei: Implications for Human Melioidosis. Plos Pathogens. 2008;4(10).

65. Nandi T, Holden MT, Didelot X, Mehershahi K, Boddey JA, Beacham I, et al. Burkholderia pseudomallei sequencing identifies genomic clades with distinct recombination, accessory, and epigenetic profiles. Genome Res. 2015;25(1):129-41.

66. Chewapreecha C, Holden MT, Vehkala M, Valimaki N, Yang Z, Harris SR, et al. Global and regional dissemination and evolution of Burkholderia pseudomallei. Nature microbiology. 2017;2:16263.

67. Godoy D, Randle G, Simpson AJ, Aanensen DM, Pitt TL, Kinoshita R, et al. Multilocus sequence typing and evolutionary relationships among the causative agents of melioidosis and glanders, Burkholderia pseudomallei and Burkholderia mallei. J Clin Microbiol. 2003;41(5):2068-79.

68. Price EP, MacHunter B, Spratt BG, Wagner DM, Currie BJ, Sarovich DS. Improved multilocus sequence typing of Burkholderia pseudomallei and closely related species. Journal of Medical Microbiology. 2016;65(9):992-7.

69. Nandi T, Ong C, Singh AP, Boddey J, Atkins T, Sarkar-Tyson M, et al. A Genomic Survey of Positive Selection in Burkholderia pseudomallei Provides Insights into the Evolution of Accidental Virulence. PLOS Pathogens. 2010;6(4):e1000845.

70. Jones AL, Beveridge TJ, Woods DE. Intracellular survival of Burkholderia pseudomallei. Infection and Immunity. 1996;64(3):782-90.

71. Pruksachartvuthi S, Aswapokee N, Thankerngpol K. Survival of Pseudomonas pseudomallei in human phagocytes. J Med Microbiol. 1990;31(2):109-14.

72. Allwood EM, Devenish RJ, Prescott M, Adler B, Boyce JD. Strategies for Intracellular Survival of Burkholderia pseudomallei. Frontiers in microbiology. 2011;2:170.

73. Moule MG, Hemsley CM, Seet Q, Guerra-Assuncao JA, Lim J, Sarkar-Tyson M, et al. Genome-wide saturation mutagenesis of Burkholderia pseudomallei K96243 predicts essential genes and novel targets for antimicrobial development. MBio. 2014;5(1):e00926-13.

74. Cuccui J, Easton A, Chu KK, Bancroft GJ, Oyston PC, Titball RW, et al. Development of signature-tagged mutagenesis in Burkholderia pseudomallei to identify genes important in survival and pathogenesis. Infect Immun. 2007;75(3):1186-95.

75. Moule MG, Spink N, Willcocks S, Lim J, Guerra-Assuncao JA, Cia F, et al. Characterization of New Virulence Factors Involved in the Intracellular Growth and Survival of Burkholderia pseudomallei. Infect Immun. 2015;84(3):701-10.

76. Heiss C, Burtnick MN, Wang Z, Azadi P, Brett PJ. Structural analysis of capsular polysaccharides expressed by Burkholderia mallei and Burkholderia pseudomallei. Carbohydrate research. 2012;349:90-4.

77. Perry MB, MacLean LL, Schollaardt T, Bryan LE, Ho M. Structural characterization of the lipopolysaccharide O antigens of Burkholderia pseudomallei. Infect Immun. 1995;63(9):3348-52.

78. Kawahara K, Dejsirilert S, Ezaki T. Characterization of three capsular polysaccharides produced by Burkholderia pseudomallei. FEMS Microbiology Letters. 1998;169(2):283-7.

79. Woodman ME, Worth RG, Wooten RM. Capsule influences the deposition of critical complement C3 levels required for the killing of Burkholderia pseudomallei via NADPH-oxidase induction by human neutrophils. PLoS One. 2012;7(12):e52276.

80. Reckseidler-Zenteno SL, DeVinney R, Woods DE. The capsular polysaccharide of Burkholderia pseudomallei contributes to survival in serum by reducing complement factor C3b deposition. Infect Immun. 2005;73(2):1106-15.

81. Atkins T, Prior R, Mack K, Russell P, Nelson M, Prior J, et al. Characterisation of an acapsular mutant of Burkholderia pseudomallei identified by signature tagged mutagenesis. J Med Microbiol. 2002;51(7):539-47.

82. Sarkar-Tyson M, Thwaite JE, Harding SV, Smither SJ, Oyston PC, Atkins TP, et al. Polysaccharides and virulence of Burkholderia pseudomallei. J Med Microbiol. 2007;56(Pt 8):1005-10.

83. Tuanyok A, Stone JK, Mayo M, Kaestli M, Gruendike J, Georgia S, et al. The Genetic and Molecular Basis of O-Antigenic Diversity in Burkholderia pseudomallei Lipopolysaccharide. PLoS Neglected Tropical Diseases. 2012;6(1):e1453.

84. Loutet SA, Valvano MA. Extreme Antimicrobial Peptide and Polymyxin B Resistance in the Genus Burkholderia. Frontiers in Microbiology. 2011;2:159.

85. DeShazer D, Brett PJ, Woods DE. The type II O-antigenic polysaccharide moiety of Burkholderia pseudomallei lipopolysaccharide is required for serum resistance and virulence. Mol Microbiol. 1998;30(5):1081-100.

86. Arjcharoen S, Wikraiphat C, Pudla M, Limposuwan K, Woods DE, Sirisinha S, et al. Fate of a Burkholderia pseudomallei Lipopolysaccharide Mutant in the Mouse Macrophage Cell Line RAW 264.7: Possible Role for the O-Antigenic Polysaccharide Moiety of Lipopolysaccharide in Internalization and Intracellular Survival. Infect Immun. 2007;75(9):4298-304.

87. Costa TRD, Felisberto-Rodrigues C, Meir A, Prevost MS, Redzej A, Trokter M, et al. Secretion systems in Gram-negative bacteria: structural and mechanistic insights. Nat Rev Micro. 2015;13(6):343-59.

88. Warawa J, DE W. Type III secretion system cluster 3 is required for maximal virulence of Burkholderia pseudomallei in a hamster infection mode. FEMS Microbiol Lett 2005;242(1):101-8.

89. Stevens MP, Haque A, Atkins T, Hill J, Wood MW, Easton A, et al. Attenuated virulence and protective efficacy of a Burkholderia pseudomallei bsa type III secretion mutant in murine models of melioidosis. Microbiology-(UK). 2004;150:2669-76.

90. Stevens MP, Wood MW, Taylor LA, Monaghan P, Hawes P, Jones PW, et al. An Inv/Mxi-Spa-like type III protein secretion system in Burkholderia pseudomallei modulates intracellular behaviour of the pathogen. Mol Microbiol 2002;46(3):649-59.

91. Treerat P, Alwis P, D'Cruze T, Cullinane M, Vadivelu J, Devenish RJ, et al. The Burkholderia pseudomallei Proteins BapA and BapC Are Secreted TTSS3 Effectors and BapB Levels Modulate Expression of BopE. PLOS ONE. 2015;10(12):e0143916.

92. Stevens MP, Stevens JM, Jeng RL, Taylor LA, Wood MW, Hawes P, et al. Identification of a bacterial factor required for actin-based motility of Burkholderia pseudomallei. Mol Microbiol 2005;56(1):40-53.

93. Stevens JM, Ulrich RL, Taylor LA, Wood MW, DeShazer D, Stevens MP, et al. Actin-binding proteins from Burkholderia mallei and Burkholderia thailandensis can functionally compensate for the actin-based motility defect of a Burkholderia pseudomallei bimA mutant. Journal of Bacteriology. 2005;187(22):7857-62.

94. Basler M, Pilhofer M, Henderson GP, Jensen GJ, Mekalanos JJ. Type VI secretion requires a dynamic contractile phage tail-like structure. Nature. 2012;483(7388):182-U78.

95. Burtnick MN, Brett PJ, Harding SV, Ngugi SA, Ribot WJ, Chantratita N, et al. The Cluster 1 Type VI Secretion System Is a Major Virulence Determinant in Burkholderia pseudomallei. Infection and Immunity. 2011;79(4):1512-25.

96. Chen YH, Wong J, Sun GW, Liu YC, Tan GYG, Gan YH. Regulation of Type VI Secretion System during Burkholderia pseudomallei Infection. Infection and Immunity. 2011;79(8):3064-73.

97. Toesca IJ, French CT, Miller JF. The Type VI Secretion System Spike Protein VgrG5 Mediates Membrane Fusion during Intercellular Spread by Pseudomallei Group Burkholderia Species. Infection and Immunity. 2014;82(4):1436-44.

98. Schwarz S, Singh P, Robertson JD, LeRoux M, Skerrett SJ, Goodlett DR, et al. VgrG-5 is a Burkholderia type VI secretion system-exported protein required for multinucleated giant cell formation and virulence. Infect Immun. 2014;82(4):1445-52.

99. DeShazer D, Brett PJ, Carlyon R, DE. W. Mutagenesis of Burkholderia pseudomallei with Tn5-OT182: isolation of motility mutants and molecular characterization of the flagellin structural gene. J Bacteriol.179(9):2116-25.

100. Chua KL, Chan YY, Gan YH. Flagella Are Virulence Determinants of Burkholderia pseudomallei. Infection and Immunity. 2003;71(4):1622-9.

101. Chuaygud T, Tungpradabkul S, Sirisinha S, Chua KL, P U. A role of Burkholderia pseudomallei flagella as a virulent factor. Trans R Soc Trop Med Hyg. 2008(102):S140-S4.

102. Ngamdee W, Tandhavanant S, Wikraiphat C, Reamtong O, Wuthiekanun V, Salje J, et al. Competition between Burkholderia pseudomallei and B. thailandensis. BMC Microbiol. 2015;15:56.

103. Pizarro-Cerda J, Cossart P. Bacterial adhesion and entry into host cells. Cell. 2006;124(4):715-27.

104. Essex-Lopresti AE, Boddey JA, Thomas R, Smith MP, Hartley MG, Atkins T, et al. A type IV pilin, PilA, Contributes To Adherence of Burkholderia pseudomallei and virulence in vivo. Infect Immun. 2005;73(2):1260-4.

105. Rutherford ST, Bassler BL. Bacterial quorum sensing: its role in virulence and possibilities for its control. Cold Spring Harbor perspectives in medicine. 2012;2(11).

106. Ulrich RL, Deshazer D, Brueggemann EE, Hines HB, Oyston PC, Jeddeloh JA. Role of quorum sensing in the pathogenicity of Burkholderia pseudomallei. J Med Microbiol. 2004;53(Pt 11):1053-64.

107. Horton RE, Grant GD, Matthews B, Batzloff M, Owen SJ, Kyan S, et al. Quorum sensing negatively regulates multinucleate cell formation during intracellular growth of Burkholderia pseudomallei in macrophage-like cells. PloS one. 2013;8(5):e63394.

108. Goo E, Majerczyk CD, An JH, Chandler JR, Seo YS, Ham H, et al. Bacterial quorum sensing, cooperativity, and anticipation of stationary-phase stress. Proc Natl Acad Sci U S A. 2012;109(48):19775-80.

109. Adler NRL, Stevens JM, Stevens MP, Galyov EE. Autotransporters and Their Role in the Virulence of Burkholderia pseudomallei and Burkholderia mallei. Frontiers in Microbiology. 2011;2:151.

110. Campos CG, Byrd MS, Cotter PA. Functional characterization of Burkholderia pseudomallei trimeric autotransporters. Infect Immun. 2013;81(8):2788-99.

111. Adler NRL, Stevens MP, Dean RE, Saint RJ, Pankhania D, Prior JL, et al. Systematic Mutagenesis of Genes Encoding Predicted Autotransported Proteins of Burkholderia

pseudomallei Identifies Factors Mediating Virulence in Mice, Net Intracellular Replication and a Novel Protein Conferring Serum Resistance. PLoS ONE 2015;10(4).

112. Sitthidet C, Korbsrisate S, Layton AN, Field TR, Stevens MP, Stevens JM. Identification of motifs of Burkholderia pseudomallei BimA required for intracellular motility, actin binding, and actin polymerization. J Bacteriol. 2011;193(8):1901-10.

113. Rhodes KA, Schweizer HP. Antibiotic resistance in Burkholderia species. Drug Resistance Updates. 2016;28:82-90.

114. Rholl DA, Papp-Wallace KM, Tomaras AP, Vasil ML, Bonomo RA, Schweizer HP. Molecular investigations of PenA-mediated beta-lactam resistance in Burkholderia pseudomallei. Frontiers in Microbiology. 2011;2.

115. Sarovich DS, Price EP, Von Schulze AT, Cook JM, Mayo M, Watson LM, et al. Characterization of Ceftazidime Resistance Mechanisms in Clinical Isolates of Burkholderia pseudomallei from Australia. Plos One. 2012;7(2).

116. Trunck LA, Propst KL, Wuthiekanun V, Tuanyok A, Beckstrom-Sternberg SM, Beckstrom-Sternberg JS, et al. Molecular Basis of Rare Aminoglycoside Susceptibility and Pathogenesis of Burkholderia pseudomallei Clinical Isolates from Thailand. PLOS Neglected Tropical Diseases. 2009;3(9):e519.

117. Mima T, Schweizer HP. The BpeAB-OprB Efflux Pump of Burkholderia pseudomallei 1026b Does Not Play a Role in Quorum Sensing, Virulence Factor Production, or Extrusion of Aminoglycosides but Is a Broad-Spectrum Drug Efflux System. Antimicrobial Agents and Chemotherapy. 2010;54(8):3113-20.

118. Chantratita N, Wuthiekanun V, Boonbumrung K, Tiyawisutsri R, Vesaratchavest M, Limmathurotsakul D, et al. Biological relevance of colony morphology and phenotypic switching by Burkholderia pseudomallei. Journal of bacteriology. 2007;189(3):807-17.

119. Tandhavanant S, Thanwisai A, Limmathurotsakul D, Korbsrisate S, Day NP, Peacock SJ, et al. Effect of colony morphology variation of Burkholderia pseudomallei on intracellular survival and resistance to antimicrobial environments in human macrophages in vitro. BMC Microbiol. 2010;10:303.

120. Austin CR, Goodyear AW, Bartek IL, Stewart A, Sutherland MD, Silva EB, et al. A Burkholderia pseudomallei colony variant necessary for gastric colonization. MBio. 2015;6(1).

121. Yang HM, Chaowagul W, Sokol PA. Siderophore production by Pseudomonas pseudomallei. Infection and Immunity. 1991;59(3):776-80.

122. Yang HM, Kooi CD, Sokol PA. Ability of Pseudomonas pseudomallei malleobactin to acquire transferrin-bound, lactoferrin-bound, and cell-derived iron. Infection and Immunity. 1993;61(2):656-62.

123. Alice AF, Lopez CS, Lowe CA, Ledesma MA, Crosa JH. Genetic and transcriptional analysis of the siderophore malleobactin biosynthesis and transport genes in the human pathogen Burkholderia pseudomallei K96243. Journal of Bacteriology. 2006;188(4):1551-66.

124. Kvitko BH, Goodyear A, Propst KL, Dow SW, Schweizer HP. Burkholderia pseudomallei Known Siderophores and Hemin Uptake Are Dispensable for Lethal Murine Melioidosis. Plos Neglected Tropical Diseases. 2012;6(6).

125. Hutchison ML, Poxton IR, Govan JRW. Burkholderia cepacia produces a hemolysin that is capable of inducing apoptosis and degranulation of mammalian phagocytes. Infection and Immunity. 1998;66(5):2033-9.

126. Thomson ELS, Dennis JJ. A Burkholderia cepacia complex non-ribosomal peptide-synthesized toxin is hemolytic and required for full virulence. Virulence. 2012;3(3):286-98.

127. Ashdown LR, Koehler JM. Production of hemolysin and other extracellular enzymes by clinical isolates of Pseudomonas-pseudomallei. Journal of Clinical Microbiology. 1990;28(10):2331-4.

128. Ahmad L, Hung TL, Akhir NAM, Mohamed R, Nathan S, Firdaus-Raih M. Characterization of Burkholderia pseudomallei protein BPSL1375 validates the Putative hemolytic activity of the COG3176 N-Acyltransferase family. Bmc Microbiology. 2015;15.

129. Nathan S, Leong YT, Sa'ariwijaya MSF. Burkholderia pseudomallei Secretes Metallo- and Serine Proteases in Culture. Malaysian Journal of Biochemistry and Molecular Biology. 2005;11:13-9.

130. Sexton MM, Jones AL, Chaowagul W, Woods DE. Purification and characterization of a protease from Pseudomonas pseudomallei. Can J Microbiol. 1994;40(11):903-10.

131. Gauthier YP, Thibault FM, Paucod JC, Vidal DR. Protease production by Burkholderia pseudomallei and virulence in mice. Acta Trop. 2000;74(2-3):215-20.

132. Chin CY, Tan SC, Nathan S. Immunogenic recombinant Burkholderia pseudomallei MprA serine protease elicits protective immunity in mice. Frontiers in Cellular and Infection Microbiology. 2012;2.

133. Cruz-Migoni A, Hautbergue GM, Artymiuk PJ, Baker PJ, Bokori-Brown M, Chang CT, et al. A Burkholderia pseudomallei toxin inhibits helicase activity of translation factor eIF4A. Science. 2011;334(6057):821-4.

134. Harley VS, Dance DA, Tovey G, McCrossan MV, Drasar BS. An ultrastructural study of the phagocytosis of Burkholderia pseudomallei. Microbios. 1998;94(377):35-45.

135. Pilatz S, Breitbach K, Hein N, Fehlhaber B, Schulze J, Brenneke B, et al. Identification of Burkholderia pseudomallei genes required for the intracellular life cycle and in vivo virulence. Infection and Immunity. 2006;74(6):3576-86.

136. Utaisincharoen P, Tangthawornchaikul N, Kespichayawattana W, Anuntagool N, Chaisuriya P, Sirisinha S. Kinetic studies of the production of nitric oxide (NO) and tumour necrosis factor-alpha (TNF-alpha) in macrophages stimulated with Burkholderia pseudomallei endotoxin. Clinical and experimental immunology. 2000;122(3):324-9.

137. Ekchariyawat P, Pudla S, Limposuwan K, Arjcharoen S, Sirisinha S, Utaisincharoen P. Burkholderia pseudomallei-induced expression of suppressor of cytokine signaling 3 and cytokine-inducible src homology 2-containing protein in mouse macrophages: a possible

mechanism for suppression of the response to gamma interferon stimulation. Infect Immun. 2005;73(11):7332-9.

138. Jitprasutwit N, Zainal-Abidin N, Broek CV, Kurian D, Korbsrisate S, Stevens MP, et al. Identification of Candidate Host Cell Factors Required for Actin-Based Motility of Burkholderia pseudomallei. J Proteome Res. 2016;15(12).

139. Harley VS, Dance DA, Drasar BS, Tovey G. Effects of Burkholderia pseudomallei and other Burkholderia species on eukaryotic cells in tissue culture. Microbios. 1998;96(384):71-93.

140. Inglis TJ, Sagripanti JL. Environmental factors that affect the survival and persistence of Burkholderia pseudomallei. Appl Environ Microbiol. 2006;72(11):6865-75.

141. West TE, Ernst RK, Jansson-Hutson MJ, Skerrett SJ. Activation of Toll-like receptors by Burkholderia pseudomallei. BMC immunology. 2008;9:46.

142. Wiersinga WJ, Wieland CW, Roelofs JJ, van der Poll T. MyD88 dependent signaling contributes to protective host defense against Burkholderia pseudomallei. PLoS One. 2008;3(10):e3494.

143. Vollmer W, Blanot D, De Pedro MA. Peptidoglycan structure and architecture. FEMS Microbiology Reviews. 2008;32(2):149-67.

144. Schleifer KH, Kandler O. Peptidoglycan types of bacterial cell walls and their taxonomic implications. Bacteriological reviews. 1972;36(4):407.

145. Dramsi S, Davison S, Magnet S, Arthur M. Surface proteins covalently attached to peptidoglycan: examples from both gram-positive and gram-negative bacteria. FEMS Microbiol Rev. 2008.

146. Typas A, Banzhaf M, Gross CA, Vollmer W. From the regulation of peptidoglycan synthesis to bacterial growth and morphology. Nature reviews Microbiology. 2011;10(2):123-36.

147. Holtje JV. Growth of the stress-bearing and shape-maintaining murein sacculus of Escherichia coli. Microbiology and molecular biology reviews : MMBR. 1998;62(1):181-203.

148. Pazos M, Peters K, Vollmer W. Robust peptidoglycan growth by dynamic and variable multi-protein complexes. Current opinion in microbiology. 2017;36:55-61.

149. Scheurwater E, Reid CW, Clarke AJ. Lytic transglycosylases: bacterial space-making autolysins. The international journal of biochemistry & cell biology. 2008;40(4):586-91.

150. Johnson JW, Fisher JF, Mobashery S. Bacterial cell-wall recycling. Annals of the New York Academy of Sciences. 2013;1277(1):54-75.

151. Paradis-Bleau C, Cloutier I, Lemieux L, Sanschagrin F, Laroche J, Auger M, et al. Peptidoglycan lytic activity of the Pseudomonas aeruginosa phage phiKZ gp144 lytic transglycosylase. FEMS Microbiol Lett. 2007;266(2):201-9.

152. Zahrl D, Wagner M, Bischof K, Bayer M, Zavecz B, Beranek A, et al. Peptidoglycan degradation by specialized lytic transglycosylases associated with type III and type IV secretion systems. Microbiology. 2005;151(Pt 11):3455-67.

153. Koraimann G. Lytic transglycosylases in macromolecular transport systems of Gram-negative bacteria. Cellular and Molecular Life Sciences (CMLS). 2003;60(11):2371-88.

154. Blackburn NT, Clarke AJ. Identification of Four Families of Peptidoglycan Lytic Transglycosylases. Journal of Molecular Evolution. 2001;52(1):78-84.

155. Scheurwater E, Reid CW, Clarke AJ. Lytic transglycosylases: Bacterial space-making autolysins. The International Journal of Biochemistry & Cell Biology. 2008;40(4):586-91.

156. Peters K, Kannan S, Rao VA, Biboy J, Vollmer D, Erickson SW, et al. The Redundancy of Peptidoglycan Carboxypeptidases Ensures Robust Cell Shape Maintenance in Escherichia coli. MBio. 2016;7(3).

157. Singh SK, SaiSree L, Amrutha RN, Reddy M. Three redundant murein endopeptidases catalyse an essential cleavage step in peptidoglycan synthesis of Escherichia coli K12. Mol Microbiol. 2012;86(5):1036-51.

158. Heidrich C, Ursinus A, Berger J, Schwarz H, Holtje JV. Effects of Multiple Deletions of Murein Hydrolases on Viability, Septum Cleavage, and Sensitivity to Large Toxic Molecules in Escherichia coli. Journal of Bacteriology. 2002;184(22):6093-9.

159. Lee M, Hesek D, Llarrull LI, Lastochkin E, Pi H, Boggess B, et al. Reactions of All Escherichia coli Lytic Transglycosylases with Bacterial Cell Wall. J Am Chem Soc. 2013;135(9):3311-4.

160. Lommatzsch J, Templin MF, Kraft AR, Vollmer W, Holtje JV. Outer membrane localization of murein hydrolases: MltA, a third lipoprotein lytic transglycosylase in Escherichia coli. Journal of Bacteriology. 1997;179(17):5465-70.

161. Ursinus A, Holtje JV. Purification and properties of a membrane-bound lytic transglycosylase from Escherichia coli. Journal of Bacteriology. 1994;176(2):338-43.

162. Powell AJ, Liu Z-J, Nicholas RA, Davies C. Crystal Structures of the Lytic Transglycosylase MltA from N.gonorrhoeae and E.coli: Insights into Interdomain Movements and Substrate Binding. Journal of Molecular Biology. 2006;359(1):122-36.

163. van Straaten KE, Dijkstra BW, Vollmer W, Thunnissen A. Crystal structure of MltA from Escherichia coli reveals a unique lytic transglycosylase fold. Journal of Molecular Biology. 2005;352(5):1068-80.

164. van Straaten KE, Barends TRM, Dijkstra BW, Thunnissen A. Structure of Escherichia coli lytic transglycosylase MltA with bound chitohexaose - Implications for peptidoglycan binding and cleavage. Journal of Biological Chemistry. 2007;282(29):21197-205.

165. Ravagnani A, Finan CL, Young M. A novel firmicute protein family related to the actinobacterial resuscitation-promoting factors by non-orthologous domain displacement. Bmc Genomics. 2005;6.

166. Quay DHX, Cole AR, Cryar A, Thalassinos K, Williams MA, Bhakta S, et al. Structure of the stationary phase survival protein YuiC from B.subtilis. BMC Structural Biology. 2015;15(1).

167. Liu W, Dong N, Zhang XH. Overexpression of mltA in Edwardsiella tarda reduces resistance to antibiotics and enhances lethality in zebra fish. Journal of Applied Microbiology. 2012;112(6):1075-85.

168. Pizza M, Scarlato V, Masignani V, Giuliani MM, Arico B, Comanducci M, et al. Identification of vaccine candidates against serogroup B meningococcus by whole-genome sequencing. Science. 2000;287(5459):1816-20.

169. Cloud KA, Dillard JP. Mutation of a Single Lytic Transglycosylase Causes Aberrant Septation and Inhibits Cell Separation of Neisseria gonorrhoeae. Journal of Bacteriology. 2004;186(22):7811-4.

170. Adu-Bobie J, Lupetti P, Brunelli B, Granoff D, Norais N, Ferrari G, et al. GNA33 of Neisseria meningitidis is a lipoprotein required for cell separation, membrane architecture, and virulence. Infection and Immunity. 2004;72(4):1914-9.

171. Dijkstra AJ, Hermann F, Keck W. Cloning and controlled overexpression of the gene encoding the 35 kDa soluble lytic transglycosylase from Escherichia coli. FEBS Lett. 1995;366(2-3):115-8.

172. Ehlert K, Holtje JV, Templin MF. Cloning and expression of a murein hydrolase lipoprotein from Escherichia coli. Molecular Microbiology. 1995;16(4):761-8.

173. van Asselt EJ, Dijkstra AJ, Kalk KH, Takacs B, Keck W, Dijkstra BW. Crystal structure of Escherichia coli lytic transglycosylase Slt35 reveals a lysozyme-like catalytic domain with an EF-hand. Structure with Folding & Design. 1999;7(10):1167-80.

174. Lamers RP, Nguyen UT, Nguyen Y, Buensuceso RNC, Burrows LL. Loss of membrane-bound lytic transglycosylases increases outer membrane permeability and β-lactam sensitivity in Pseudomonas aeruginosa. MicrobiologyOpen. 2015;4(6):879-95.

175. Artola-Recolons C, Lee M, Bernardo-Garcia N, Blazquez B, Hesek D, Bartual SG, et al. Structure and cell wall cleavage by modular lytic transglycosylase MltC of Escherichia coli. ACS chemical biology. 2014;9(9):2058-66.

176. Roure S, Bonis M, Chaput C, Ecobichon C, Mattox A, Barriere C, et al. Peptidoglycan maturation enzymes affect flagellar functionality in bacteria. Mol Microbiol. 2012;86(4):845-56.

177. Monteiro C, Fang X, Ahmad I, Gomelsky M, Romling U. Regulation of Biofilm Components in Salmonella enterica Serovar Typhimurium by Lytic Transglycosylases Involved in Cell Wall Turnover. Journal of Bacteriology. 2011;193(23):6443-51.

178. Bateman A, Bycroft M. The structure of a LysM domain from E. coli membrane-bound lytic murein transglycosylase D (MltD). J Mol Biol. 2000;299(4):1113-9.

179. Chaput C, Labigne A, Boneca IG. Characterization of Helicobacter pylori Lytic Transglycosylases Slt and MltD. Journal of Bacteriology. 2006;189(2):422-9.

180. Xu Z, Wang Y, Han Y, Chen J, Zhang XH. Mutation of a novel virulence-related gene mltD in Vibrio anguillarum enhances lethality in zebra fish. Res Microbiol. 2011;162(2):144-50.

181. Kraft AR, Templin MF, Holtje JV. Membrane-bound lytic endotransglycosylase in Escherichia coli. J Bacteriol. 1998;180(13):3441-7.

182. Fibriansah G, Gliubich FI, Thunnissen AM. On the mechanism of peptidoglycan binding and cleavage by the endo-specific lytic transglycosylase MltE from Escherichia coli. Biochemistry. 2012;51(45):9164-77.

183. Santin YG, Cascales E. Domestication of a housekeeping transglycosylase for assembly of a Type VI secretion system. EMBO reports. 2017;18(1):138-49.

184. Bingle LE, Bailey CM, Pallen MJ. Type VI secretion: a beginner's guide. Current opinion in microbiology. 2008;11(1):3-8.

185. Cavallari JF, Lamers RP, Scheurwater EM, Matos AL, Burrows LL. Changes to Its Peptidoglycan-Remodeling Enzyme Repertoire Modulate β-Lactam Resistance in Pseudomonas aeruginosa. Antimicrobial Agents and Chemotherapy. 2013;57(7):3078-84.

186. Scheurwater EM, Clarke AJ. The C-terminal domain of Escherichia coli YfhD functions as a lytic transglycosylase. Journal of Biological Chemistry. 2008;283(13):8363-73.

187. Yunck R, Cho H, Bernhardt TG. Identification of MltG as a potential terminase for peptidoglycan polymerization in bacteria. Mol Microbiol. 2016;99(4):700-18.

188. Tsui HC, Zheng JJ, Magallon AN, Ryan JD, Yunck R, Rued BE, et al. Suppression of a deletion mutation in the gene encoding essential PBP2b reveals a new lytic transglycosylase involved in peripheral peptidoglycan synthesis in Streptococcus pneumoniae D39. Mol Microbiol. 2016;100(6):1039-65.

189. Romeis T, Holtje JV. Specific interaction of penicillin-binding proteins 3 and 7/8 with soluble lytic transglycosylase in Escherichia coli. J Biol Chem. 1994;269(34):21603-7.

190. Kraft AR, Prabhu J, Ursinus A, Holtje JV. Interference with murein turnover has no effect on growth but reduces beta-lactamase induction in Escherichia coli. J Bacteriol. 1999;181(23):7192-8.

191. Koraimann G. Lytic transglycosylases in macromolecular transport systems of Gram-negative bacteria. Cellular and molecular life sciences : CMLS. 2003;60(11):2371-88.

192. Burkinshaw BJ, Deng W, Lameignere E, Wasney GA, Zhu H, Worrall LJ, et al. Structural analysis of a specialized type III secretion system peptidoglycan-cleaving enzyme. J Biol Chem. 2015;290(16):10406-17.

193. Oh HS, Kvitko BH, Morello JE, Collmer A. Pseudomonas syringae lytic transglycosylases coregulated with the type III secretion system contribute to the translocation of effector proteins into plant cells. J Bacteriol. 2007;189(22):8277-89.

194. Yoshida T, Kim S-R, Komano T. Twelve pil Genes Are Required for Biogenesis of the R64 Thin Pilus. Journal of Bacteriology. 1999;181(7):2038-43.

195. de la Mora J, Ballado T, González-Pedrajo B, Camarena L, Dreyfus G. The Flagellar Muramidase from the Photosynthetic Bacterium Rhodobacter sphaeroides. Journal of Bacteriology. 2007;189(22):7998-8004.

196. Nambu T, Minamino T, Macnab RM, Kutsukake K. Peptidoglycan-hydrolyzing activity of the FlgJ protein, essential for flagellar rod formation in Salmonella typhimurium. J Bacteriol. 1999;181(5):1555-61.

197. Herlihey FA, Osorio-Valeriano M, Dreyfus G, Clarke AJ. Modulation of the Lytic Activity of the Dedicated Autolysin for Flagellum Formation SltF by Flagellar Rod Proteins FlgB and FlgF. Journal of Bacteriology. 2016;198(13):1847-56.

198. Thunnissen AM, Isaacs NW, Dijkstra BW. The catalytic domain of a bacterial lytic transglycosylase defines a novel class of lysozymes. Proteins-Structure Function and Genetics. 1995;22(3):245-58.

199. Reid CW, Legaree BA, Clarke AJ. Role of Ser216 in the mechanism of action of membrane-bound lytic transglycosylase B: further evidence for substrate-assisted catalysis. FEBS Lett. 2007;581(25):4988-92.

200. Serruto D, Galeotti CL. The signal peptide sequence of a lytic transglycosylase of Neisseria meningitidis is involved in regulation of gene expression. Microbiology-(UK). 2004;150:1427-37.

201. Vollmer W. Structural variation in the glycan strands of bacterial peptidoglycan. Fems Microbiology Reviews. 2008;32(2):287-306.

202. Pfeffer JM, Strating H, Weadge JT, Clarke AJ. Peptidoglycan O acetylation and autolysin profile of Enterococcus faecalis in the viable but nonculturable state. Journal of Bacteriology. 2006;188(3):902-8.

203. Reid CW, Blackburn NT, Legaree BA, Auzanneaua FI, Clarke AJ. Inhibition of membrane-bound lytic transglycosylase B by NAG-thiazoline. Febs Letters. 2004;574(1-3):73-9.

204. Thunnissen A, Rozeboom HJ, Kalk KH, Dijkstra BW. Structure of the 70-kda soluble lytic transglycosylase complexed with bulgecin-a - implications for the enzymatic mechanism. Biochemistry. 1995;34(39):12729-37.

205. Williams AH, Wheeler R, Thiriau C, Haouz A, Taha MK, Boneca IG. Bulgecin A: The Key to a Broad-Spectrum Inhibitor That Targets Lytic Transglycosylases. Antibiotics-Basel. 2017;6(1).

206. Clarke CA, Scheurwater EM, Clarke AJ. The Vertebrate Lysozyme Inhibitor Ivy Functions to Inhibit the Activity of Lytic Transglycosylase. Journal of Biological Chemistry. 2010;285(20):14843-7.

207. Bentley WE, Mirjalili N, Andersen DC, Davis RH, Kompala DS. Plasmid-Encoded Protein: The Principal Factor in the "Metabolic Burden" Associated with Recombinant Bacteria. Biotechnology and Bioengineering. 2009;102(5):1284-97.

208. Dumon-Seignovert L, Cariot G, Vuillard L. The toxicity of recombinant proteins in Escherichia coli: A comparison of overexpression in BL21(DE3), C41(DE3), and C43(DE3). Protein Expression and Purification. 2004;37(1):203-6.

209. Kuhner D, Stahl M, Demircioglu oD, Bertsche U. From cells to muropeptide structures in 24 h: Peptidoglycan mapping by UPLC-MS. SCIENTIFIC REPORTS. 2014;4(7494).

210. Mukamolova GV, Murzin AG, Salina EG, Demina GR, Kell DB, Kaprelyants AS, et al. Muralytic activity of Micrococcus luteus Rpf and its relationship to physiological activity in promoting bacterial growth and resuscitation. Mol Microbiol. 2006;59(1):84-98.

211. Mukamolova GV, Murzin AG, Salina EG, Demina GR, Kell DB, Kaprelyants AS, et al. Muralytic activity of Micrococcus luteus Rpf and its relationship to physiological activity in promoting bacterial growth and resuscitation. Molecular Microbiology. 2006;59(1):84-98.

212. Engel H, Kazemier B, Keck W. Murein-metabolizing enzymes from escherichia-coli - sequence-analysis and controlled overexpression of the slt gene, which encodes the soluble lytic transglycosylase. Journal of Bacteriology. 1991;173(21):6773-82.

213. Shanklin J. Overexpression and purification of the Escherichia coli inner membrane enzyme acyl-acyl carrier protein synthase in an active form. Protein expression and purification. 2000;18(3):355-60.

214. Glauner B, Höltje JV, Schwarz U. The composition of the murein of Escherichia coli. J Biol Chem. 1988;263(21).

215. Rosano GL, Ceccarelli EA. Recombinant protein expression in Escherichia coli: advances and challenges. Frontiers in microbiology. 2014;5:172.

216. Kraft AR, Templin MF, Holtje JV. Membrane-Bound Lytic Endotransglycosylase in Escherichia coli. J Bacteriol. 1998;180(13):3441-7.

217. Dijkstra AJ, Hermann F, Keck W. Cloning and controlled overexpression of the gene encoding the 35 kda soluble lytic transglycosylase from Escherichia coli. Febs Letters. 1995;366(2-3):115-8.

218. van Asselt EJ, Dijkstra BW. Binding of calcium in the EF-hand of Escherichia coli lytic transglycosylase Slt35 is important for stability. Febs Letters. 1999;458(3):429-35.

219. Mesnage S, Dellarole M, Baxter NJ, Rouget JB, Dimitrov JD, Wang N, et al. Molecular basis for bacterial peptidoglycan recognition by LysM domains. Nat Commun. 2014;5:11.

220. Buist G, Steen A, Kok J, Kuipers OR. LysM, a widely distributed protein motif for binding to (peptido)glycans. Molecular Microbiology. 2008;68(4):838-47.

221. Wong YC, Abd El Ghany M, Naeem R, Lee KW, Tan YC, Pain A, et al. Candidate Essential Genes in Burkholderia cenocepacia J2315 Identified by Genome-Wide TraDIS. Front Microbiol. 2016;22(7).

222. Borlee GI, Plumley BA, Martin KH, Somprasong N, Mangalea MR, Islam MN, et al. Genome-scale analysis of the genes that contribute to Burkholderia pseudomallei biofilm formation identifies a crucial exopolysaccharide biosynthesis gene cluster. PLOS Neglected Tropical Diseases. 2017;11(6):e0005689.

223. Wikraiphat C, Charoensap J, Utaisincharoen P, Wongratanacheewin S, Taweechaisupapong S, Woods DE, et al. Comparative in vivo and in vitro analyses of putative

virulence factors of Burkholderia pseudomallei using lipopolysaccharide, capsule and flagellin mutants. FEMS immunology and medical microbiology. 2009;56(3):253-9.

224. Sander JD, Joung JK. CRISPR-Cas systems for editing, regulating and targeting genomes. Nature Biotechnology. 2014;32(4):347-55.

225. Schweizer HP, Peacock SJ. Antimicrobial Drug–Selection Markers forBurkholderia pseudomalleiandB. mallei. Emerging Infectious Diseases. 2008;14(11):1689-92.

226. Schweizer HP, Peacock SJ. Antimicrobial drug-selection markers for Burkholderia pseudomallei and B. mallei. Emerg Infect Dis. 2008;14(11):1689-92.

227. Miller VL, Mekalanos JJ. A novel suicide vector and its use in construction of insertion mutations: osmoregulation of outer membrane proteins and virulence determinants in Vibrio cholerae requires toxR. J Bacteriol. 1988;170(6):2575-83.

228. Hamad MA, Zajdowicz SL, Holmes RK, MI V. An allelic exchange system for compliant genetic manipulation of the select agents Burkholderia pseudomallei and Burkholderia mallei. Gene 2009;430(1-2):123-31.

229. Alexeyev MF. The pKNOCK series of broad-host-range mobilizable suicide vectors for gene knockout and targeted DNA insertion into the chromosome of gram-negative bacteria. BioTechniques. 1999;26(5):824-6, 8.

230. Moule MG, Hemsley CM, Seet Q, Guerra-Assunção JA, Lim J, Sarkar-Tyson M, et al. Genome-Wide Saturation Mutagenesis of Burkholderia pseudomallei K96243 Predicts Essential Genes and Novel Targets for Antimicrobial Development. mBio. 2014;5(1):e00926-13.

231. Kovach ME, Phillips RW, Elzer PH, Roop RM, 2nd, Peterson KM. pBBR1MCS: a broad-host-range cloning vector. BioTechniques. 1994;16(5):800-2.

232. Hamad MA, Zajdowicz SL, Holmes RK, Voskuil MI. An allelic exchange system for compliant genetic manipulation of the select agents Burkholderia pseudomallei and Burkholderia mallei. Gene. 2009;430(1-2):123-31.

233. Somprasong N, McMillan I, Karkhoff-Schweizer RR, Mongkolsuk S, Schweizer HP. Methods for genetic manipulation of Burkholderia gladioli pathovar cocovenenans. BMC research notes. 2010;3:308.

234. Chan YA, Hackett KT, Dillard JP. The lytic transglycosylases of Neisseria gonorrhoeae. Microbial drug resistance (Larchmont, NY). 2012;18(3):271-9.

235. Korsak D, Liebscher S, Vollmer W. Susceptibility to Antibiotics and -Lactamase Induction in Murein Hydrolase Mutants of Escherichia coli. Antimicrobial Agents and Chemotherapy. 2005;49(4):1404-9.

236. Cloud-Hansen KA, Hackett KT, Garcia DL, Dillard JP. Neisseria gonorrhoeae uses two lytic transglycosylases to produce cytotoxic peptidoglycan monomers. J Bacteriol 2008;190(17):5989-94.

237. Kearns DB. A field guide to bacterial swarming motility. Nat Rev Microbiol. 2010;8(9):634-44.

238. Mattick JS. Type IV pili and twitching motility. Annual review of microbiology. 2002;56:289-314.

239. Dance D. Treatment and prophylaxis of melioidosis. International Journal of Antimicrobial Agents. 2014;43(4):310-8.

240. Reed LJ, Muench H. A simple method of estimating fifty percent endpoints. American journal of epidemiology. 1938;27(3):493-7.

241. Chen K, Sun GW, Chua KL, Gan YH. Modified virulence of antibiotic-induced Burkholderia pseudomallei filaments. Antimicrobial agents and chemotherapy. 2005;49(3):1002-9.

242. Park JT, Uehara T. How bacteria consume their own exoskeletons (turnover and recycling of cell wall peptidoglycan). Microbiology and molecular biology reviews : MMBR. 2008;72(2):211-27, table of contents.

243. Chen K, Sun GW, Chua KL, Gan YH. Modified Virulence of Antibiotic-Induced Burkholderia pseudomallei Filaments. Antimicrobial Agents and Chemotherapy. 2005;49(3):1002-9.

244. Willcocks SJ, Denman CC, Atkins HS, Wren BW. Intracellular replication of the well-armed pathogen Burkholderia pseudomallei. Curr Opin Microbiol. 2016;29:94-103.

245. Toesca IJ, French CT, Miller JF. The Type VI secretion system spike protein VgrG5 mediates membrane fusion during intercellular spread by pseudomallei group Burkholderia species. Infect Immun. 2014;82(4):1436-44.

246. Carter T, Buensuceso RNC, Tammam S, Lamers RP, Harvey H, Howell PL, et al. The Type IVa Pilus Machinery Is Recruited to Sites of Future Cell Division. Mbio. 2017;8(1).

247. Flemming H-C, Wingender J, Szewzyk U, Steinberg P, Rice SA, Kjelleberg S. Biofilms: an emergent form of bacterial life. Nat Rev Micro. 2016;14(9):563-75.

248. Zeng X, Gillespie B, Lin J. Important Role of a Putative Lytic Transglycosylase Cj0843c in β-Lactam Resistance in Campylobacter jejuni. Front Microbiol. 2015;6.

249. Melly MA, McGee ZA, Rosenthal RS. Ability of monomeric peptidoglycan fragments from Neisseria gonorrhoeae to damage human fallopian-tube mucosa. The Journal of infectious diseases. 1984;149(3):378-86.

250. Fleming TJ, Wallsmith DE, Rosenthal RS. Arthropathic properties of gonococcal peptidoglycan fragments: implications for the pathogenesis of disseminated gonococcal disease. Infect Immun. 1986;52(2):600-8.

251. Bao Y, Tian M, Li P, Liu J, Ding C, Yu S. Characterization of Brucella abortus mutant strain Δ22915, a potential vaccine candidate. Veterinary Research. 2017;48(1):17.

252. Pinto D, Santos MA, Chambel L. Thirty years of viable but nonculturable state research: Unsolved molecular mechanisms. Critical reviews in microbiology. 2013.

253. Oliver JD. Recent findings on the viable but nonculturable state in pathogenic bacteria. FEMS Microbiol Rev. 2010;34(4):415-25.

254. Potgieter M, Bester J, Kell DB, Pretorius E. The dormant blood microbiome in chronic, inflammatory diseases. FEMS Microbiol Rev. 2015;39(4):567-91.

255. HS Xu NR, FL Singleton, RW Attwell. Survival and viability of nonculturable Escherichia coli and Vibrio cholerae in the estuarine and marine environment. Microbial Ecology. 1982;8:313-23.

256. Jia J, Li Z, Cao J, Jiang Y, Liang C, Liu M. Proteomic analysis of protein expression in the induction of the viable but Nonculturable State of Vibrio harveyi SF1. Current microbiology. 2013;67(4):442-7.

257. Li L, Mendis N, Trigui H, Oliver JD, Faucher SP. The importance of the viable but non-culturable state in human bacterial pathogens. Front Microbiol. 2014;5:258.

258. Oliver JD. Recent findings on the viable but nonculturable state in pathogenic bacteria. FEMS Microbiology Reviews. 2010;34(4):415-25.

259. Young DB, Gideon HP, Wilkinson RJ. Eliminating latent tuberculosis. Trends in microbiology. 2009;17(5):183-8.

260. Ramamurthy T, Ghosh A, Pazhani GP, Shinoda S. Current Perspectives on Viable but Non-Culturable (VBNC) Pathogenic Bacteria. Frontiers in Public Health. 2014;2:103.

261. Mukamolova GV, Turapov O, Malkin J, Woltmann G, Barer MR. Resuscitation-promoting factors reveal an occult population of tubercle Bacilli in Sputum. American journal of respiratory and critical care medicine. 2010;181(2):174-80.

262. Chengalroyen MD, Beukes GM, Gordhan BG, Streicher EM, Churchyard G, Hafner R, et al. Detection and Quantification of Differentially Culturable Tubercle Bacteria in Sputum from Patients with Tuberculosis. American journal of respiratory and critical care medicine. 2016;194(12):1532-40.

263. Turapov O, O'Connor BD, Sarybaeva AA, Williams C, Patel H, Kadyrov AS, et al. Phenotypically Adapted Mycobacterium tuberculosis Populations from Sputum Are Tolerant to First-Line Drugs. Antimicrob Agents Chemother. 2016;60(4):2476-83.

264. Nichols D, Cahoon N, Trakhtenberg EM, Pham L, Mehta A, Belanger A, et al. Use of ichip for high-throughput in situ cultivation of "uncultivable" microbial species. Appl Environ Microbiol. 2010;76(8):2445-50.

265. Ling LL, Schneider T, Peoples AJ, Spoering AL, Engels I, Conlon BP, et al. A new antibiotic kills pathogens without detectable resistance. Nature. 2015;517(7535):455-9.

266. Ayrapetyan M, Williams TC, Oliver JD. Interspecific quorum sensing mediates the resuscitation of viable but nonculturable vibrios. Applied and environmental microbiology. 2014;80(8):2478-83.

267. Garcia MT, Jones S, Pelaz C, Millar RD, Abu Kwaik Y. Acanthamoeba polyphaga resuscitates viable non-culturable Legionella pneumophila after disinfection. Environmental microbiology. 2007;9(5):1267-77.

268. D'Onofrio A, Crawford JM, Stewart EJ, Witt K, Gavrish E, Epstein S, et al. Siderophores from Neighboring Organisms Promote the Growth of Uncultured Bacteria. Chemistry & biology. 2010;17(3):254-64.

269. Mukamolova GV, Kaprelyants AS, Young DI, Young M, Kell DB. A bacterial cytokine. Proc Natl Acad Sci U S A. 1998;95(15):8916-21.

270. Galina V. Mukamolova OAT, Danielle I. Young, Arseny S. Kaprelyants, Douglas B. Kell and Michael Young. A family of autocrine growth factors in Mycobacterium tuberculosis. Molecular Microbiology. 2002;46(3):623-35.

271. Kana BD, Gordhan BG, Downing KJ, Sung N, Vostroktunova G, Machowski EE, et al. The resuscitation-promoting factors ofMycobacterium tuberculosisare required for virulence and resuscitation from dormancy but are collectively dispensable for growthin vitro. Molecular Microbiology. 2008;67(3):672-84.

272. Gupta RK, Srivastava R. Resuscitation Promoting Factors: a Family of Microbial Proteins in Survival and Resuscitation of Dormant Mycobacteria. Indian Journal of Microbiology. 2011;52(2):114-21.

273. Telkov MV, Demina GR, Voloshin SA, Salina EG, Dudik TV, Stekhanova TN, et al. Proteins of the Rpf (resuscitation promoting factor) family are peptidoglycan hydrolases. Biochemistry (Moscow). 2006;71(4):414-22.

274. Signoretto C, Lleo MM, Tafi MC, Canepari P. Cell wall chemical composition of Enterococcus faecalis in the viable but nonculturable state. Appl Environ Microbiol. 2000;66(5):1953-9.

275. Signoretto C, Lleo M, Canepari P. Modification of the peptidoglycan of Escherichia coli in the viable but nonculturable state. Current microbiology. 2002;44(2):125-31.

276. Kogure K, Simidu U, Taga N. A tentative direct microscopic method for counting living marine bacteria. Can J Microbiol. 1979;25(3):415-20.

277. Eiler A, Bertilsson S. Detection and quantification of Vibrio populations using denaturant gradient gel electrophoresis. Journal of Microbiological Methods. 2006;67(2):339-48.

278. Gonzalez-Escalona N, Fey A, Hofle MG, Espejo RT, C AG. Quantitative reverse transcription polymerase chain reaction analysis of Vibrio cholerae cells entering the viable but non-culturable state and starvation in response to cold shock. Environ Microbiol. 2006;8(4):658-66.

279. Yanez MA, Nocker A, Soria-Soria E, Murtula R, Martinez L, Catalan V. Quantification of viable Legionella pneumophila cells using propidium monoazide combined with quantitative PCR. J Microbiol Methods. 2011;85(2):124-30.

280. Cools I, D'Haese E, Uyttendaele M, Storms E, Nelis HJ, Debevere J. Solid phase cytometry as a tool to detect viable but non-culturable cells of Campylobacter jejuni. J Microbiol Methods. 2005;63(2):107-14.

281. Kuehl B, Marten SM, Bischoff Y, Brenner-Weiss G, Obst U. MALDI-ToF mass spectrometry-multivariate data analysis as a tool for classification of reactivation and non-culturable states of bacteria. Analytical and bioanalytical chemistry. 2011;401(5):1593-600.

282. Fernandes E, Martins VC, Nobrega C, Carvalho CM, Cardoso FA, Cardoso S, et al. A bacteriophage detection tool for viability assessment of Salmonella cells. Biosensors & bioelectronics. 2014;52:239-46.

283. Moore RA, Tuanyok A, Woods DE. Survival of Burkholderia pseudomallei in water. BMC research notes. 2008;1:11.

284. Pumpuang A, Chantratita N, Wikraiphat C, Saiprom N, Day NP, Peacock SJ, et al. Survival of Burkholderia pseudomallei in distilled water for 16 years. Trans R Soc Trop Med Hyg. 2011;105(10):598-600.

285. Pascoe B, Dams L, Wilkinson TS, Harris LG, Bodger O, Mack D, et al. Dormant cells of Staphylococcus aureus are resuscitated by spent culture supernatant. PloS one. 2014;9(2):e85998.

286. Gilbert SE, Rose LJ. Survival and persistence of nonspore-forming biothreat agents in water. Lett Appl Microbiol. 2012;55(3):189-94.

287. O'Connell HA, Rose LJ, Shams A, Bradley M, Arduino MJ, Rice EW. Variability of Burkholderia pseudomallei strain sensitivities to chlorine disinfection. Applied and environmental microbiology. 2009;75(16):5405-9.

288. Sagripanti JL, Levy A, Robertson J, Merritt A, Inglis TJ. Inactivation of virulent Burkholderia pseudomallei by sunlight. Photochem Photobiol. 2009;85(4):978-86.

289. Tong SD, Yang S, Lu ZZ, He WH. Laboratory investigation of ecological factors influencing the environmental presence of Burkholderia pseudomallei. Microbiology and Immunology. 1996;40(6):451-3.

290. Shide Tong SY, Zhenzhi Lu, and Weihai He. Laboratory investigation of ecological factors influencing the environmental presence of Burkholderia pseudomallei. Microbiol Immunol. 1996;40(6):451-3.

291. Bolton FJ, Hinchliffe PM, Coates D, Robertson L. A most probable number method for estimating small numbers of campylobacters in water. The Journal of Hygiene. 1982;89(2):185-90.

292. Shleeva MO, Bagramyan K, Telkov MV, Mukamolova GV, Young M, Kell DB, et al. Formation and resuscitation of "non-culturable" cells of Rhodococcus rhodochrous and Mycobacterium tuberculosis in prolonged stationary phase. Microbiology. 2002;148(Pt 5):1581-91.

293. Sim BMQ, Chantratita N, Ooi WF, Nandi T, Tewhey R, Wuthiekanun V, et al. Genomic acquisition of a capsular polysaccharide virulence cluster by non-pathogenic Burkholderia isolates. Genome Biology. 2010;11(8):R89.

294. Postgate JR, Hunter JR. Acceleration of bacterial death by grown substrates. Nature. 1963;198:273.

295. Heeb S, Itoh Y, Nishijyo T, Schnider U, Keel C, Wade J, et al. Small, stable shuttle vectors based on the minimal pVS1 replicon for use in gram-negative, plant-associated bacteria. Mol Plant Microbe Interact. 2000;12(2):232-7.

296. Xu HS, Roberts N, Singleton FL, Attwell RW, Grimes DJ, Colwell RR. Survival and viability of nonculturableEscherichia coli andVibrio cholerae in the estuarine and marine environment. Microbial ecology. 1982;8(4):313-23.

297. Ducret A, Chabalier M, Dukan S. Characterization and resuscitation of 'non-culturable' cells of Legionella pneumophila. BMC Microbiol. 2014;14:3.

298. Calabrese JP, Bissonnette GK. Improved detection of acid mine water stressed coliform bacteria on media containing catalase and sodium pyruvate. Can J Microbiol. 1990;36(8):544-50.

299. Bang W, Drake MA, Jaykus LA. Recovery and detection of Vibrio vulnificus during cold storage. Food microbiology. 2007;24(6):664-70.

300. Sun F, Chen J, Zhong L, Zhang XH, Wang R, Guo Q, et al. Characterization and virulence retention of viable but nonculturable Vibrio harveyi. FEMS Microbiol Ecol. 2008;64(1):37-44.

301. Oliver JD, Bockian R. In vivo resuscitation, and virulence towards mice, of viable but nonculturable cells of Vibrio vulnificus. Appl Environ Microbiol. 1995;61(7):2620-23.

302. Lewis K. Multidrug tolerance of biofilms and persister cells. Current topics in microbiology and immunology. 2008;322:107-31.

303. Totsika M. Benefits and Challenges of Antivirulence Antimicrobials at the Dawn of the Post-Antibiotic Era. Current Medicinal Chemistry. 2016;6(1):30-7.

304. Cusumano CK, Pinkner JS, Han Z, Greene SE, Ford BA, Crowley JR, et al. Treatment and Prevention of Urinary Tract Infection with Orally Active FimH Inhibitors. Science translational medicine. 2011;3(109):109ra15-ra15.

305. Brument S, Sivignon A, Dumych TI, Moreau N, Roos G, Guerardel Y, et al. Thiazolylaminomannosides as potent antiadhesives of type 1 piliated Escherichia coli isolated from Crohn's disease patients. Journal of medicinal chemistry. 2013;56(13):5395-406.

306. Muh U, Schuster M, Heim R, Singh A, Olson ER, Greenberg EP. Novel Pseudomonas aeruginosa quorum-sensing inhibitors identified in an ultra-high-throughput screen. Antimicrob Agents Chemother. 2006;50(11):3674-9.

307. Kauppi AM, Nordfelth R, Uvell H, Wolf-Watz H, Elofsson M. Targeting Bacterial Virulence: Inhibitors of Type III Secretion in Yersinia. Chemistry & Biology. 2003;10(3):241-9.